

# Sheffield Hallam University

*The rheology of liquid crystal polymer blends.*

HAWKSWORTH, M.

Available from the Sheffield Hallam University Research Archive (SHURA) at:

<http://shura.shu.ac.uk/19773/>

## A Sheffield Hallam University thesis

This thesis is protected by copyright which belongs to the author.

The content must not be changed in any way or sold commercially in any format or medium without the formal permission of the author.

When referring to this work, full bibliographic details including the author, title, awarding institution and date of the thesis must be given.

Please visit <http://shura.shu.ac.uk/19773/> and <http://shura.shu.ac.uk/information.html> for further details about copyright and re-use permissions.

Sheffield Hallam University

**REFERENCE ONLY**

101 381 2387

ProQuest Number: 10697075

All rights reserved

INFORMATION TO ALL USERS

The quality of this reproduction is dependent upon the quality of the copy submitted.

In the unlikely event that the author did not send a complete manuscript and there are missing pages, these will be noted. Also, if material had to be removed, a note will indicate the deletion.



ProQuest 10697075

Published by ProQuest LLC (2017). Copyright of the Dissertation is held by the Author.

All rights reserved.

This work is protected against unauthorized copying under Title 17, United States Code  
Microform Edition © ProQuest LLC.

ProQuest LLC.  
789 East Eisenhower Parkway  
P.O. Box 1346  
Ann Arbor, MI 48106 – 1346

THE RHEOLOGY OF LIQUID CRYSTAL  
POLYMER BLENDS

by

M. Hawsworth BSc(Hons)

This thesis is submitted to  
Sheffield Hallam University  
in partial fulfilment for  
the degree of

Doctor of Philosophy

APRIL 1993

Sponsoring Establishment : School of Engineering  
Sheffield Hallam University  
Sheffield

Collaborating Establishment : ICI Advanced Materials  
Wilton  
Middlesborough  
Cleveland

## PREFACE

The work reported in this thesis was carried out at Sheffield Hallam University between October 1987 and September 1991 whilst the candidate was registered for a higher degree.

The candidate has not during the above period of registration for the degree of Ph.D been registered for any other award or University degree. The results presented here are, as far as can be certain, original except where reference has been made to previous work.

In accordance with the regulations covering the Total Technology Ph.D. in Industrial Metallurgy, a course in Metallurgical Process Management was successfully completed.

The performance of the candidate during this course was assessed by means of written examination and continuous assessment.

The details of the course are given below :-

### MODULE 1

- a) Process Metallurgy
- b) Mechanical Metallurgy
- c) Advanced Thermodynamics

## MODULE 2

- a) Accountancy
- b) Micro-Economics and Financial Control
- c) Computational Methods and Operational Research
- d) Operational Research

## MODULE 3

- a) Quality Assurance
- b) Metals and Competitive Materials
- c) Atmospheric and Pollution Control
- d) Solidification of Alloys
- e) Stainless Steels
- f) Automatic and Computer Aided Control of Metallurgical Operations

## MODULE 4

Three industrial case studies, one of which is related to the current work, is presented in this thesis in Appendix II.

In addition, two conferences were attended :-

- a) Flow Processes in Composite Materials, 17 - 18th May, at Brunel University, 1988
- b) Golden Jubilee Meeting of the British Society of Rheology and the Third European Rheology Conference, at Edinburgh University 2 - 7th September, 1990

## ACKNOWLEDGEMENTS

The author would like to express his sincere gratitude to the following :-

Dr A. A. Collyer, Director of Studies for his assistance, advice and useful discussion, without whose help and guidance this work would not have been completed.

Dr J. B. Hull for help throughout the project to date.

Special thanks goes to members of Sheffield City Polytechnic technical and Library staff who have helped in a variety of ways, especially :-

Miss R. A. Collington, Mr P. Slingsby, Mr S. Creasy, Mr G. France and Mr M. Jackson.

The author is indebted to ICI Advanced Materials for finance for the project and materials.

Special thanks to my parents for their support to date and helping with the proof reading.

# THE RHEOLOGY OF LIQUID CRYSTAL POLYMER BLENDS

SUBMITTED FOR THE DEGREE OF DOCTOR OF PHILOSOPHY

BY

M. HAWKSWORTH

## ABSTRACT

The present studies are concerned with the observation and explanation of the interaction between liquid crystal and isotropic polymers. An investigation of the rheological behaviour has been carried out on blends containing small additions of a main chain thermotropic liquid crystal polymers using capillary rheometry. Samples of these blends were moulded and tested using a Hounsfield tensometer and a Hounsfield swinging arm impact rig. The addition of a small amount of liquid crystal polymer was found to have a major effect upon both the rheological and morphological properties of the base material. This indicates the liquid crystal polymer can be used as a processing aid. A reduction of viscosity was noticed in all of the tests carried out and is attributed to the change in morphology induced by the addition of liquid crystal polymer. It would be of great benefit to the polymer processor if an understanding of the mechanisms involved could be highlighted. It is felt that the large interfacial area created between the binodal and spinodal has a bearing on the viscosity reduction. The morphology was different for material in the centre and the skin regions. The characteristic skin/core morphology was seen in all samples produced above a critical amount of liquid crystal polymer and temperature. The interaction between the liquid crystal polymer and the base material was explained using a model which predicted the velocity profiles given the shear rate, consistency constant and shear thinning index of the blends. The interface position is important because on one side of the interface the material is subject to elongational forces and compressive forces on the other. The elongational forces extend the LCP domains inducing an imposed morphology on the isotropic matrix. This could be seen in extruded and injection moulded samples, in the form of highly orientated surface skin layers. The orientation in the skin layers improved the barrier properties of the resultant blends, by allowing molecules in the surface layers to pack more closely together.

## NOMENCLATURE

A = AREA,  $m^2$

B = INTERACTION ENERGY DENSITY,  $J/m^3$

$\Delta G_m$  = GIBBS FREE ENERGY OF MIXING, J

$\Delta H_m$  = ENTHALPY OF MIXING, J

$\Delta L$  = LENGTH OF ELEMENT IN DIE, m

L = LENGTH, m

Q = VOLUMETRIC FLOW RATE,  $m^3/s$

$R_o$  = DIE RADIUS, m

K = CONSISTENCY CONSTANT  $Ns/m^2$

$n_i$  = MOLES OF SPECIES i

n = SHEAR THINNING INDEX

P = PRESSURE AT POINT OF MEASUREMENT, Pa

$\Delta P$  = PRESSURE DROP ACROSS DIE, Pa

R = GAS CONSTANT  $J \text{ mole}^{-1} K^{-1}$

$\Delta S_m$  = ENTROPY OF MIXING,  $J K^{-1}$

T = ABSOLUTE TEMPERATURE, K

V = VELOCITY,  $m^2/s$

$\dot{\gamma}$  = SHEAR RATE,  $s^{-1}$

$\dot{\gamma}_w$  = WALL SHEAR RATE,  $s^{-1}$

$\eta$  = APPARENT SHEAR VISCOSITY, Pa s

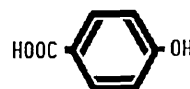
$\tau$  = SHEAR STRESS, Pa

$\tau_w$  = WALL SHEAR STRESS, Pa

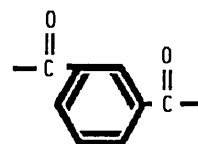
$\phi_i$  = VOLUME FRACTION OF SPECIES, i

## ABBREVIATIONS

Hydroxybenzoic acid - HBA



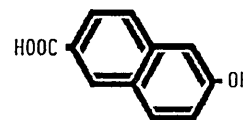
Isophthalic acid - IA



Terephthalic acid - TA



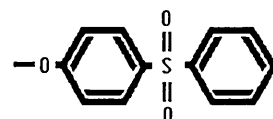
Hydroxynaphthoic acid - HNA



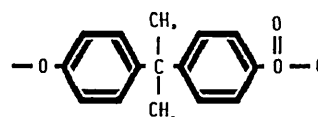
Hydroquinone - HQ



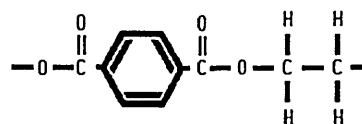
Polyethersulphone - PES



Polycarbonate - PC



Polyethyleneterephthalate - PET



## ABSTRACT

1:	INTRODUCTION . . . . .	1
1.1	History and background of liquid crystal polymers . . . . .	1
1.2	Crystallinity . . . . .	4
1.3	Liquid crystallinity or mesomorphism . . . . .	6
1.4	Lyotropic liquid crystal polymers . . . . .	9
1.5	Thermotropic liquid crystal polymers . . . . .	9
1.6	Side chain liquid crystal polymers . . . . .	10
1.7	Main chain liquid crystal polymers . . . . .	11
2:	MOLECULAR ARCHITECTURE OF THERMOTROPIC LIQUID CRYSTAL POLYMERS . . . . .	14
2.1	Structure of liquid crystal polymers . . . . .	14
2.2	Tailoring of the molecule . . . . .	14
2.3	Discontinuities within the backbone chain . . . . .	15
2.4	Frustrated chain packing . . . . .	15
2.4.1	Crankshaft monomer . . . . .	16
2.4.2	Ring substituted groups . . . . .	17
2.5	Flexible spacer units . . . . .	18
2.5.1	Regularly spaced flexible linkages . . . . .	20
2.5.2	Randomly arranged flexible spacer units . . . . .	21
2.6	Kinked units . . . . .	21

3:	PHASE BEHAVIOUR OF LIQUID CRYSTAL POLYMERS . . .	23
	3.1 Nematic phase . . . . .	23
	3.2 Cholesteric phase . . . . .	25
	3.3 Smectic phase . . . . .	26
	3.4 Morphology of liquid crystal polymers . . .	28
4:	RHEOLOGY . . . . .	33
	4.1 Background to rheology . . . . .	33
	4.2 Viscosity . . . . .	34
	4.3 Types of fluid flow . . . . .	36
	4.3.1 Time independent fluids . . . . .	37
	4.3.2 Time dependent fluids . . . . .	42
	4.4 Viscoelastic materials . . . . .	42
	4.5 Measurement of flow properties . . . . .	43
	4.6 Rotational rheometers . . . . .	43
	4.7 Capillary rheometer . . . . .	44
	4.8 Entrance effects . . . . .	45
	4.8.1 Bagley correction . . . . .	46
	4.8.2 Orifice die method . . . . .	47
	4.8.3 Couette-Hagenbach method . . . . .	47
	4.9 Modes of rheological deformation . . . . .	49
	4.9.1 Bulk deformation . . . . .	49
	4.9.2 Elongational flow . . . . .	50
	4.9.3 Shearing flow . . . . .	53
	4.10 Rheological properties in capillary flow	53
	4.11 Rheology of liquid crystal polymers . . .	59
	4.11.1 Region I . . . . .	59
	4.11.2 Region II . . . . .	62
	4.11.3 Region III . . . . .	62

4.12	Rheology of blends . . . . .	67
5:	BLEND . . . . .	71
5.1	Motivation for blending . . . . .	71
5.2	Method of blending . . . . .	72
5.3	Properties of blends . . . . .	72
5.3.1	Thermodynamics . . . . .	73
5.3.2	Phase behaviour . . . . .	74
5.3.2.1	Spinodal decomposition . . . . .	81
5.3.3	Phase behaviour of liquid crystal polymers blended with engineering polymers . . . . .	81
5.4	Crystallisation . . . . .	82
5.5	Blend morphology . . . . .	82
5.5.1	Droplet/fibril morphology . . . . .	83
5.6	Log additive rule . . . . .	84
6:	EXPERIMENTAL PROCEDURES . . . . .	87
6.1	Component polymers . . . . .	87
6.2	Blend preparation . . . . .	88
6.2.1	Blends prepared at Sheffield Hallam University . . . . .	89
6.2.2	Blends prepared at I.C.I Wilton . . . . .	91
6.3	Davenport Capillary Rheometer . . . . .	92
6.4	Rosand Capillary Rheometer . . . . .	94
6.5	Collection of capillary extrudates . . . . .	94
6.6	Scanning electron microscopy . . . . .	96

6.6.1	Sample loading . . . . .	96
6.6.2	Edax scanning . . . . .	96
6.7	Optical microscopy . . . . .	97
6.7.1	Transmitted light microscopy . . . . .	98
6.7.2	Reflected light microscopy . . . . .	98
6.8	Differential scanning calorimetry . . . . .	99
6.9	Injection moulding of polymer blends . . . . .	100
6.10	Tensile testing of polymer blends . . . . .	101
6.11	Impact testing of polymer blends . . . . .	102
6.12	Water absorbtion tests . . . . .	102
7:	RESULTS . . . . .	104
7.1	Rheological properties of the blends . . . . .	104
7.1.1	Davenport Capillary data . . . . .	104
7.1.2	Rosand Capillary data . . . . .	119
7.2	Tensile testing of PES/LCP blends . . . . .	123
7.3	Impact data . . . . .	133
7.4	Water absorbtion tests . . . . .	137
7.5	Differential scanning calorimetry . . . . .	137
7.6	Microscopy . . . . .	141
7.6.1	Transmission light microscopy . . . . .	143
7.6.2	EDAX - Electron microscopy . . . . .	146
7.7	Modelling the flow profiles . . . . .	146
8:	DISCUSSION . . . . .	156
8.1	Introduction . . . . .	156
8.2	Rheological testing . . . . .	157
8.2.1	Rheology of liquid crystal polymers . . . . .	158

8.2.2 Rheology of liquid crystal	
polymer blends . . . . .	159
8.3 Die swell . . . . .	167
8.4 Shear heating . . . . .	167
8.5 Flow behaviour of liquid crystal polymers	169
8.6 Skin/core morphology . . . . .	175
8.6.1 Skin macrolayer . . . . .	179
8.6.2 Core macrolayer . . . . .	184
8.7 Migration . . . . .	187
8.8 Phase equilibria . . . . .	190
8.9 Miscibility . . . . .	191
8.10 Binodal/Spinodal decomposition . . . . .	193
8.11 Mechanical properties . . . . .	194
8.12 Modelling of velocity profile . . . . .	198
8.13 General discussion . . . . .	204
9: CONCLUSIONS . . . . .	206
10: FURTHER WORK . . . . .	209
11: REFERENCES . . . . .	211

APPENDICES

- A: MODEL FOR PREDICTING THE VELOCITY PROFILE
- B: MSc CASE STUDY
- C: PUBLISHED PAPERS

## CHAPTER 1: INTRODUCTION

### 1.1 HISTORY AND BACKGROUND OF LIQUID CRYSTAL POLYMERS

The use of LCP's as processing aids when added to engineering polymers has been known for some time<sup>1</sup>. This work is concerned with gaining a better understanding of the mechanisms involved. Firstly a basic understanding of LCP's is necessary.

Reinitzer<sup>2</sup>, an Austrian botanist, was the first person to show the existence of a liquid crystalline state in 1888. His work showed that certain cholesteryl esters exhibited two apparent melting points, between which the material was cloudy, but fully liquid. The first completely synthetic compound to exhibit such characteristics was p-azoxyanisole<sup>3,4</sup>. The discovery of these unusual new materials led to the nomenclature of flowing crystals (1889), crystalline liquids (1890) and liquid crystals (1900). By the early 1900's research on liquid crystalline materials had begun in earnest with several German scientists working in the field, Lehmann<sup>5</sup>, Schenk<sup>6</sup> and Vorländer<sup>7</sup>. The last of these realised that liquid crystalline materials existed, in 1923:-

'What happens to the molecules when one makes them longer and longer? Will the liquid crystalline state disappear? From my experience there is no limit to that state by chain elongation unless the substances

could not melt any more without decomposition and could not be seen under a microscope. Starting from the p-oxybenzoic acid, Klepl and later Emil Fischer and his collaborators had already obtained long chains, but did not realise their liquid crystalline character'.

Friedel<sup>8</sup> was the next German scientist to research the area of liquid crystalline materials further and subsequently devised the classifications used to the present day. The 1930's saw the development of polyamides at DuPont. They proved difficult to synthesise and it was not until the 1950's that it was discovered that diacid chlorides and diamines could be prepared using interfacial polymerisation.

Work by Flory in 1956 predicted lyotropic behaviour<sup>9</sup> and this theoretical prediction was well demonstrated in the synthetic polymer area with the work of Kwolek at Du Pont, leading to the later patents issued by ICI<sup>1</sup> and Carborundum<sup>10</sup>. These patents, however, made no reference to liquid crystalline behaviour. Throughout the 1960's, high molecular weight fully aromatic polyamides were developed by workers at DuPont<sup>11-19</sup>. The development and investigation of p-linked aromatic polyamides led to the discovery of liquid crystalline solutions characterised by Kwolek<sup>17</sup>. Continuation of this work by Kwolek at the DuPont laboratories led to the development of Kevlar, a lyotropic

dry jet wet spun aromatic polyamide fibre. Further work carried out at the DuPont laboratories concentrated on copolymers containing ring substituted monomers such as chloro, methyl or phenyl substituted hydroquinone<sup>20,25</sup>. Apart from these wholly aromatic polyesters, an LCP was developed by Eastman-Kodak (XG7) with a flexible spacer in which poly (p-hydroxybenzoic acid) HBA is modified with flexible poly(ethylene terephthalate) PET. The polymer exhibited the phenomenon of opaque melts, low viscosities and anisotropic properties. This gave early indications that some polyesters possessed liquid crystalline behaviour, and was cited by Jackson and co-workers<sup>21-24</sup>. There was subsequent work on a series of copolyesters prepared by the acidolysis of PET with p-acetoxybenzoic acid. The next generation of liquid crystalline materials was patented by Schaeffgen, Kleinschuster and Pletcher<sup>25-28</sup>, with a final third generation which were developed by Calundann and co-workers<sup>29-33</sup> at Celanese, who issued patents in 1978. PET itself although partly-crystalline has been available commercially since the early 1950's and played an important role as a synthetic fibre for over 25 years<sup>34,35</sup>. Overviews of this area through the 1980's have been given by Jackson<sup>36</sup> and Jin<sup>37</sup>.

The 1980's saw brand new polymers on the market, Kevlar fibres from DuPont, Vectra from Celanese, Xydar from Dartco (now from Amoco) and the SRP range from ICI (now withdrawn from the market place).

The structure of SRP1 consists of units of hydroxybenzoic acid (HBA), terephthalic acid (TA), isothalic acid (IA), and small amounts of hydroxynapthoic acid (HNA). The bent rigid unit IA provides the necessary disruption to give the liquid crystalline behaviour. The VECTRA polymer, manufactured by Celanese is produced using more expensive constituents namely HBA and HNA (in this case the HNA crankshaft unit is used to disrupt the linearity of the molecule).

In Japan under joint development programs with Nippon Telegraph and Telephone Corporation (NTT), Unitika Ltd. developed a liquid crystal polyester. Mitsubishi Chemicals, also under joint development with NTT, achieved similar results<sup>38</sup>. At the present time, there is the capability of manufacturing several different varieties of LCP. Recent studies using macromolecules with rigid rod and flexible segments gave promising results, although more work is needed to explain the phase formations. In recent years, many academic research groups have worked on the synthesis and characterisation of liquid crystalline polyesters.

## 1.2 CRYSTALLINITY

Simple science texts explain that matter exists in three states; solid, liquid and gas. A solid can be defined as any substance that responds elastically to a shear stress. On the other hand liquids and gases can be categorised as fluids, substances which do not deform

elastically to shear. Certain organic materials do not show a single transition from a solid to liquid phase, but a series of transitions involving new phases. A phase is defined as follows :-

'A region within which all the chemical and physical properties are uniformly the same<sup>39</sup>'.

Crystalline materials have atoms in a three-dimensional pattern which repeats over a long range<sup>40</sup>. Non-crystalline 'solids' such as glass, pitch and many amorphous (from the Greek meaning 'without form') polymers can be considered as extremely viscous liquids in terms of their physical and mechanical properties, having atoms that are irregularly and randomly arranged.

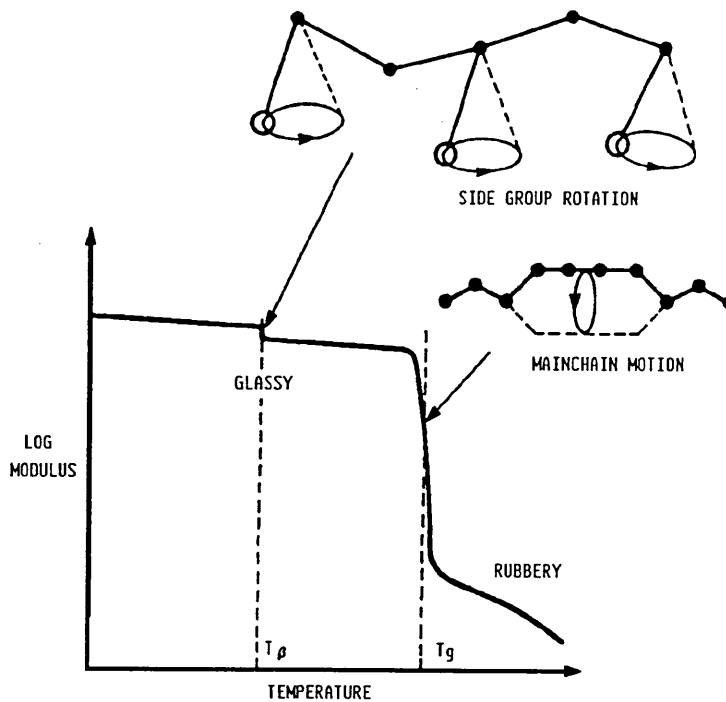


FIGURE 1.1 - Transitions in amorphous polymers

If an amorphous polymer is sufficiently cold, no chains or parts of the molecule can move: the polymer is frozen in a rigid glassy state. On slow heating the  $\beta$  transition temperature  $T_{\beta}$  is reached, at which the side groups have sufficient energy to rotate. There is an associated reduction in modulus (see figure 1.1). On further heating the glass transition temperature,  $T_g$ , is reached accompanied by a drop in the modulus of several orders of magnitude and by thermal expansion. The closer the temperature to the  $T_g$  the more pronounced is the main chain movement, and the more time dependent is the stiffness of the polymer.

Many so called non-crystalline polymers do possess some highly ordered regions known as fringed micelles (similar to crystalline polymers). These are often linked together by long chain molecules, which extend from one micelle (region of crystallinity) to another (see figure 1.2). Since intermolecular bonding is weak (Van der Waals forces), these regions tend to be both small and imperfect, especially over long range (bearing in mind the cumbersome chain molecules).

### 1.3 LIQUID CRYSTALLINITY OR MESOMORPHISM

The attributes of liquid crystals are intermediate between those of a liquid and a crystal, (a substance which has an ordered and regular internal atomic

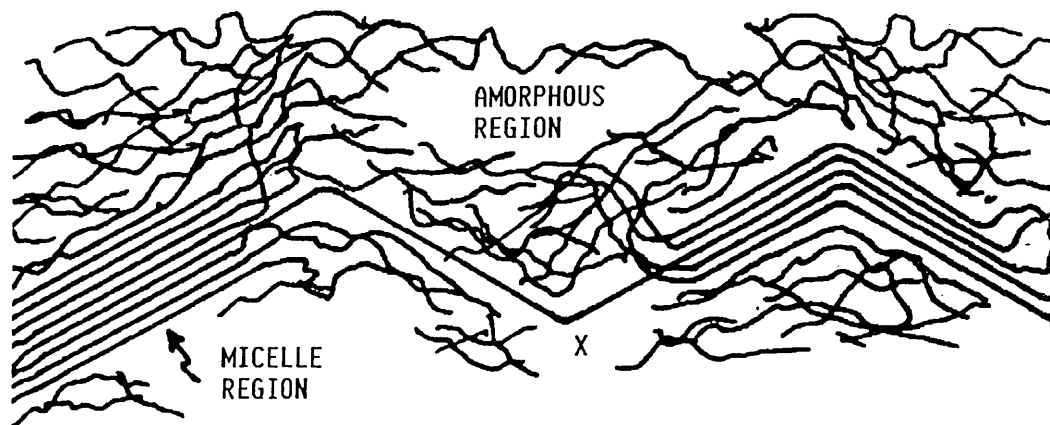


FIGURE 1.2 - Fringed micelles in polyethylene showing one molecule (X) extending between two micelles.

arrangement), hence the term liquid crystallinity, expressing this dualism of physical properties. Many small molecules and some polymers exhibit liquid crystalline behaviour. The common molecular feature is an elongated rod-like or lath-like structure usually based on a highly aromatic intransigent backbone, with flexible end groups. All of these individual molecules within the backbone chain orientate approximately parallel to a particular direction (director). The degree of alignment between the director and the molecular axes is defined by the order parameter as follows :-

$$s = 0.5 (3 \cos^2 \bar{\theta} - 1) \quad (1.1)$$

where :-

$s$  = order parameter

$\bar{\theta}$  = angle between molecular axis and the director

The value of 's' denotes the degree of order within the system for values of (s=0) in isotropic systems to (s=1) for a perfectly aligned system. If this orientation is present as a long range order then a nematic, smectic or cholesteric liquid crystalline material is formed. The various classifications of thermotropic liquid crystal polymers will be defined in a later section. There are two rules that can be established about the structure of LCP's from the data published to date :-

- i) the polymer backbone should contain a high level of aromatic moiety, which is essential for the formation of liquid crystalline domains as well as for the chemical stability of the macromolecules; and
- ii) the two atom polar groups linking the aromatic rings play only a minor role as far as the liquid crystalline behaviour is concerned. The linkage determines both the chemical and optical stability.

Liquid crystal polymers may be sub-divided into two broad categories :-

- i) lyotropic, in which the phenomenon occurs in solutions and depends upon the concentration<sup>41</sup> of the liquid crystal additive or mesogen; and
- ii) thermotropic, in which the phenomenon occurs in the melt phase and is dependent upon the temperature<sup>42</sup>.

#### 1.4 LYOTROPIC LIQUID CRYSTAL POLYMERS

Lyotropic liquid crystalline materials are formed in solution. Aromatic polyamides constitute the most important class. Such solutions exist in the nematic phase within certain limits. Some criteria for the formation of a nematic phase instead of an isotropic phase are :-

- i) polymer concentrations above a critical value;
- ii) polymer molecular weight above a critical value; and
- iii) temperature below a critical value.

Lyotropic polymers are processed in solution to form fibres such as Kevlar. The solvent is then flashed off and the remaining fibre is heat treated. The solvent production method is necessary because the bonds in the backbone chain are so intransigent they decompose before softening sufficiently to flow. These inflexible molecules decompose if processing is attempted using a conventional melt processing route.

The transition from the isotropic to the nematic phase was predicted by Flory<sup>9</sup>, as previously mentioned. The research carried out in the present study was solely on thermotropic liquid crystalline materials and so the remainder of the review will concentrate on them.

#### 1.5 THERMOTROPIC LIQUID CRYSTAL POLYMERS

In contrast to the lyotropic systems, thermotropic

polymers do not require solvents for the formation of a liquid-crystalline phase, which is created over a definite temperature range.

Brostow<sup>43</sup> has written a full review on the classifications of liquid crystal polymers and split them into 13 major classes and sub-classes. These are described as longitudinal, orthogonal, cross, soft or rigid discs, one-comb, palisade comb, disc comb, parallel, inverse comb, biaxial, double and network.

The LCP's in the current study fall into the first class, an example of which is the rigid polyester connected at either end by another rigid or flexible spacer unit. The author will not discuss the many different types of LCP known, but will instead review the two main types of thermotropic polymers: main chain LCP's and side chain LCP's<sup>44</sup>.

## 1.6 SIDE CHAIN LIQUID CRYSTAL POLYMERS

In side chain or 'comb' LCP's the mesogenic moieties link to the polymer backbone is by flexible spacer groups (CH<sub>2</sub>) as pendants. These groups act to de-couple the movement of the backbone and side chains. This allows the unfettered mesogens to move and align free of the backbone.

( It is known that the length of the spacer units has a significant effect on the liquid crystalline behaviour. )

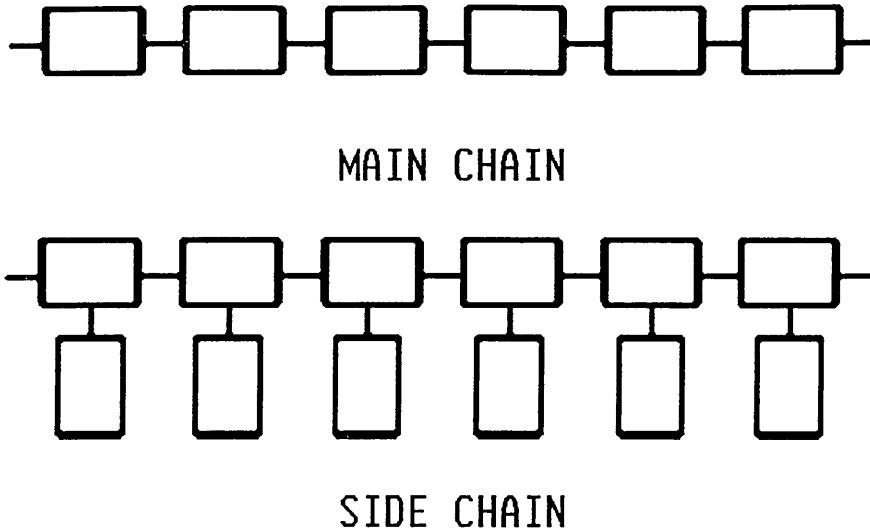


FIGURE 1.3 - The two different types of thermotropic liquid crystal polymers

(Side chain LCP's are used because of their optical properties (especially opto-electrical)). They are not used for engineering applications and as such will not be reviewed further.

### 1.7 MAIN CHAIN LIQUID CRYSTAL POLYMERS

In main chain thermotropic LCP's the mesogenic moiety is situated within the backbone itself. The LCP can be built up of just these units, or flexible spacer units (similar to the ones mentioned previously), can also be incorporated into the backbone. The molecular architecture can be tailored using flexible spacer units so that the nematic transition of the polymer can be reduced. This enables the polymer to be processed at a low enough temperature to be melt processable but high enough to retain molecular organisation. Experience has shown that

melt processing is possible only if the decomposition temperature ( $T_d$ ) is greater than the melting temperature plus  $30^\circ\text{C}$  ( $T_m+30^\circ\text{C}$ )<sup>45</sup> for partly crystalline polymers and ( $T_g+100^\circ\text{C}$ ) for amorphous polymers. Polymers possessing a stiff intransigent backbone are able to establish a domain structure of high order and microscopic dimension, within the domain itself. The overall orientation may differ from domain to domain (similar to grains within cast metal) and is signified by a director. It is well documented that this quiescent texture can subsequently be altered by the application of elongational forces, resulting in a unidirectional macroscopic morphology. The terms macro and micro describe the following morphology :-

- i) macro - features visible with the naked eye, for instance the wood grain texture visible in fracture facets of LCP mouldings; and
- ii) micro - features visible with the use of optical or scanning electron microscopy, for instance the highly ordered layers in the skin of injection mouldings.

The morphology conferred by LCP gives rise to several interesting properties, which are as follows :-

- i) outstanding physical properties, namely high modulus and tensile strengths and good impact resistance;
- ii) a low coefficient of thermal expansion; and

iii) a high thermal conductivity in the flow direction.

The coefficient of thermal expansion of LCP is comparable to steel. This makes LCP ideal for applications where polymer and metal surfaces come into contact (an example being the hot dipping of polymer circuit boards in molten solder). The use of LCP's becomes desirable if the previous properties could be tailored to meet customer requirements.

## CHAPTER 2: MOLECULAR ARCHITECTURE OF THERMOTROPIC LIQUID CRYSTAL POLYMERS

### 2.1 STRUCTURE OF LIQUID CRYSTAL POLYMERS

A main chain thermotropic LCP should have:-

- i) a high level of aromatic moiety in the backbone chain; and
- ii) two polar groups linking the aromatic rings to improve the chemical stability.

Certain groups have classically been incorporated into LCP architecture which include ester, amide, azomethine groups and C-C double and tripe<sup>l</sup> bonds.

### 2.2 TAILORING OF THE MOLECULE

A long linear inflexible molecule exhibits a high degree of liquid crystalline behaviour. The major drawback to such molecular architecture is that the highly intransigent molecule will decompose before it softens sufficiently to flow. Examples of such molecules are poly(4-oxybenzoyl), poly(p-phenyleneterephthalamide), (Kevlar) and also the homo-polymer<sup>of</sup> p-hydroxybenzoic acid.

The design of the molecules is therefore of the utmost importance, if liquid crystal polymers are to be melt processable. The uniform nature of the backbone chain must

be disrupted to a sufficient level that mesomorphism can occur below the decomposition temperature ( $T_d$ ). The accomplishment of this gives a polymer that can be processed in the fluid state, (thus using conventional processing techniques), but giving the high orientation observed in LCP's. The technique of disruption can be accomplished in two ways:-

- i) incorporation of discontinuities into the backbone;  
and
- ii) incorporation of ring substituents onto the backbone.

### 2.3 DISCONTINUITIES WITHIN THE BACKBONE CHAIN

The backbone chain can be disrupted using the following techniques:-

- i) frustrated chain packing;
- ii) flexible spacers; and
- iii) kinked linkages<sup>46</sup>.

With all of these techniques, it must be borne in mind that excessive use of disruption will cause the molecule to lose its 'rod-like' nature, leading to the formation of an isotropic fluid with a higher viscosity and no order.

### 2.4 FRUSTRATED CHAIN PACKING

This is a mechanism that maintains the essential linearity and stiffness of the backbone chain, but makes close and regular correlation into a three dimensional

lattice difficult. Unsymmetrically substituted nuclei are randomly sequenced and increase chain separation using different classes of disrupter, which fall into two main classes:-

- i) crankshaft monomer; and
- ii) ring substituted groups.

#### 2.4.1 CRANKSHAFT MONOMER

A crankshaft monomer is an aromatic molecule in which the linkages are parallel but offset. Molecules such as the 2,6 functionally disubstituted naphthalene unit, examples being 2,6-Naphthalene dicarboxylic acid, 2,6-Naphthalene diol and 6-Hydroxy-2-Naphthoic acid (see figure 2.1).

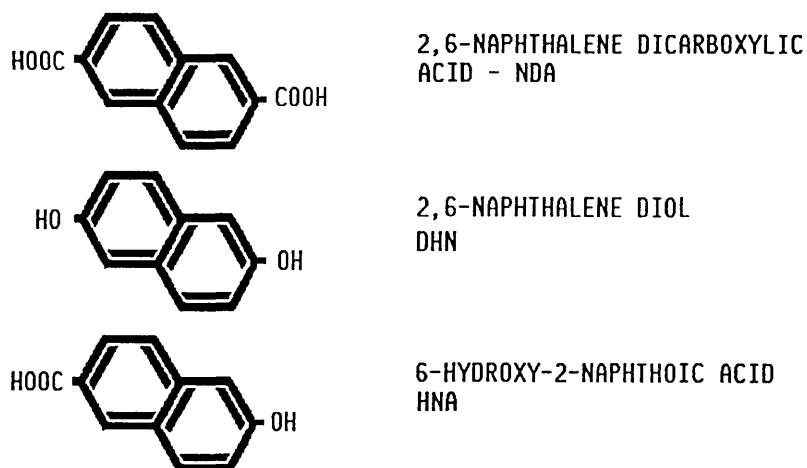


FIGURE 2.1 - Parallel offset molecules

All of these molecules are effective at reducing the  $T_n$  to within the industrially convenient melt temperature zone of 250-310°C, to allow the resultant material to be

melt processable. Figure 2.2 taken from a book by Calundann et al,<sup>47</sup> demonstrates that the addition of HNA to HBA causes a decrease in the melting point: there is an increase in the free volume associated with the disruption caused. Additions of HNA also cause a reduction in the linearity of the molecule, as reported by Chivers et al<sup>48</sup>.

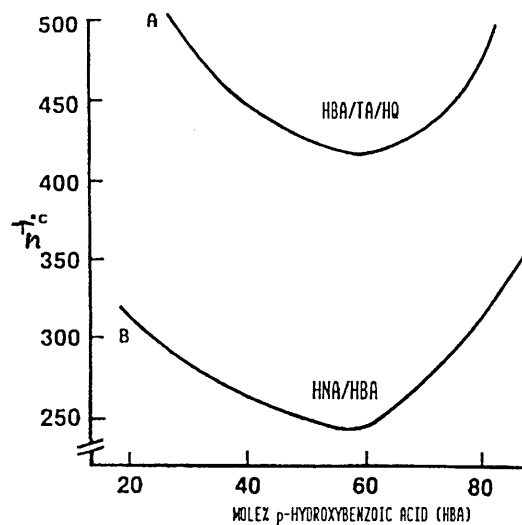


FIGURE 2.2 - Graph to demonstrate the variation of  $T_M$  with composition for two random copolyesters A: without crankshaft unit B: with crankshaft unit

#### 2.4.2 RING SUBSTITUTED GROUPS

Morgan et al were the pioneers who developed this approach at Du Pont<sup>13</sup>. They showed that substituents strongly affected the mechanical properties of heat treated fibres. Jackson<sup>24</sup> reported that the presence of a phenyl substituent group on the aromatic ring had a significant effect on the time for fibre heat treatment. The disruption of symmetry is affected by ring substituted monomers such as chloro, methyl or phenyl rings. Larger substituents such as methoxy and bromo reduce the nematic mesophase

stability, but the phenyl substituent reduces the nematic transition to give a stable nematic mesophase. The chain packing is disrupted by both the random occurrence of the units and also by a steric effect which increase the chain separation as mentioned earlier. Ring substitution alone does not lower the  $T_n$  sufficiently to permit melt processability, large phenyl-like groups are also required. Ring substitution can have an adverse effect on the thermal stability of the polymer when groups such as chloro or methyl are used (see figure 2.3).



X=Cl, CH<sub>3</sub>, Phenyl

FIGURE 2.3 - Substitution by chloro, methyl and phenyl groups

## 2.5 FLEXIBLE SPACER UNITS

If a discontinuity is inserted into the backbone chain of a thermotropic LCP three things happen :-

- i) there is a decrease in the polymer transition temperature;
- ii) an even-odd zig-zag effect occurs on the nematic/isotropic temperature (see figure 2.4) which is related to the length of the flexible spacer<sup>42</sup>; and
- iii) there is a change in the molecular packing structure.

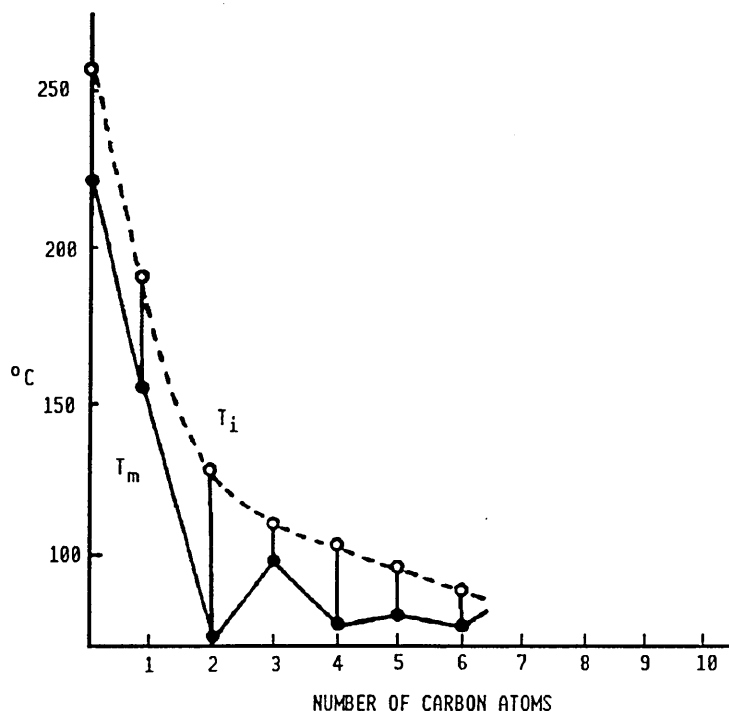


FIGURE 2.4 - Dependence of transition temperatures on substituent group length,  $T_i$  - Isotropic temperature,  $T_m$  - Melting temperature

Flexible spacer units are built up of methyl/ethyl groups and allow a degree of movement between adjacent rigid segments. Another type of flexible unit is a 'swivel' unit containing an oxy group which also allows a degree of flexibility. Examples of swivel or linked ring molecules are 3,4 or 4,4 hydroxy/carboxy disubstituted diphenyl ether, sulphide or ketone monomers (see figure 2.5). As their name suggests they allow a degree of rotation and tractability between the rigid sections lowering the  $T_n$  in a similar fashion to methyl units.

The spacers can either be regularly or randomly distributed. Thermotropic materials showing nematic,

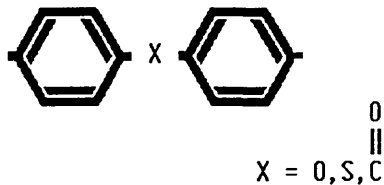


FIGURE 2.5 - Diagram to show a swivel or linked ring molecule.

smectic and cholesteric behaviour occur in many polyesters containing regularly dispersed flexible spacer units (see figure 2.6).

### 2.5.1 REGULARLY SPACED FLEXIBLE LINKAGES

Thermotropic behaviour is observed in many polymers that contain rigid-rod type units alternating periodically with flexible spacer units.

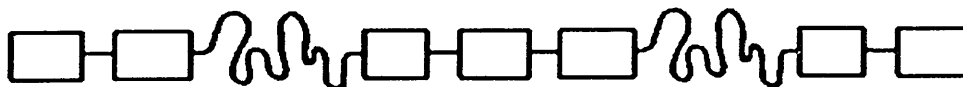


FIGURE 2.6 - Main chain thermotropic LCP, with regular flexible spacers.

The two main criteria are :-

- i) the rigid rod length must be greater than a critical length; and
- ii) the flexible spacer unit should be less than a critical length dependent on the structure of both units.

The nematic phase becomes more stable as the length:diameter ratio of the rigid-unit increases, and the flexible unit length decreases. The spacer unit can also be angular and relatively inflexible. Polymer produced from mono-substituted p-phenylenedioxy groups and diphenyl ether 4,4-dicarbonyl groups are angular (120°) and give stable nematics by suppressing the tendency to crystallise. The nematic is the most stable, with a higher length:diameter ratio for the rigid rod and a shorter flexible unit.

#### 2.5.2 RANDOMLY ARRANGED FLEXIBLE SPACER UNITS

In molecules containing randomly distributed flexible spacer units (see figure 2.7) there is a wider spread in the nematic temperature range than for a similar regularly distributed molecule. The inclusion of angular flexible or rigid spacers can be included as non-mesogenic components of thermotropic random copolymers. In these cases, the length of both the mesogenic and spacer units are irregular and the upper limit of nematic phase stability is not reached, which leads to a reduction in strength and modulus.



FIGURE 2.7 - Main chain thermotropic LCP with randomly distributed spacer units.

## 2.6 KINKED UNIT

Kinks can be incorporated into the backbone by using meta-aromatic or ortho-aromatic isomers. These units are usually ortho and meta diacids or dihydric phenols, due to the relatively low cost of these molecules (see figure 2.8):-

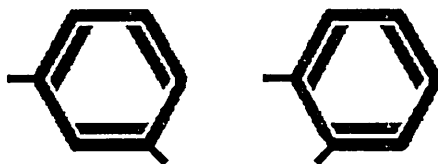


FIGURE 2.8 - To show how a meta and ortho benzene ring can be used as a kink unit.

Nomex or poly(m-phenylene isophthalamide) is an example of a commercial flame resistant fibre produced by using a kink approach. Structures using this type of disruption have less rigidity in the mesogenic structure than for other systems, such as the ring substituted types. This method was used by Cottis<sup>49</sup> over a decade ago to lower the softening point of poly(p-oxybenzoyl) homopolyester. The initial work on the meta-isomer approach was carried out by Jackson<sup>36</sup> at Easton Kodak and Griffin and Cox at ICI<sup>46</sup>. It was discovered that a low melting point polymer could be produced by replacing HBA, HQ and TA by meta-HBA and IA. This method would seem to be an effective way of reducing the melting point of an LCP. Other work at Celanese has shown that the resultant polymer is more likely to lose its oxidation resistance and hydrolytic stability. All current commercial LCP's are of this type.

### 3.1 NEMATIC PHASE

Friedel<sup>8</sup> carried out much of the early work on liquid crystal polymers and it was he who named the nematic system. The term is from the greek  $\eta\nu\mu\alpha$  (thread) and refers to the thread-like defects that are commonly observed in these materials.

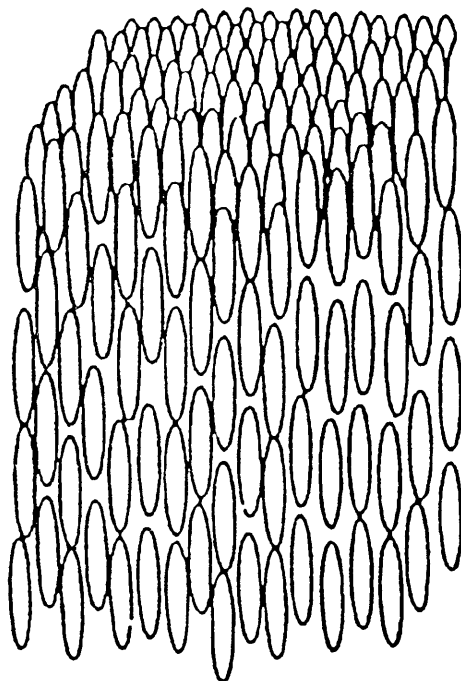


FIGURE 3.1 - Structure of Nematic phase

The main features of nematic liquid crystals are listed below :-

- i) the centres of gravity of the molecules have no long range order, and as such, there is no Bragg peak in the X-ray diffraction pattern. There is a preferred direction along which the molecules

tend to align. As such, nematics flow like liquids;

- ii) there is a general order in the alignment direction, caused by either flow or stress, which can be seen optically. A nematic is a uniaxial medium with the optical axis along the alignment direction. (There is also complete rotational symmetry around the alignment axis (see figure 3.1); and
- iii) nematic mesophases occur only with materials that do not distinguish between right and left. Either each constituent molecule must be identical to its mirror image (chiral<sup>50</sup>) or the system must have equal amounts of right and left handed species (racemic). The dual aspect of the nematic phase (i.e. liquid-like properties but uniaxial alignment; albeit no long range order) is shown in their nuclear magnetic resonance (NMR) spectra. The uniaxial symmetry causes certain line splittings, which are absent in the isotropic liquid phase (caused by a random orientation). Nematics are anisotropic liquids that show a low temperature phase, where the molecules are aligned preferentially along one direction; there are no layers present and the nematic state is typically less viscous than the smectic, which is often less viscous than the isotropic liquid phase.

The molecules although ordered are not perfectly aligned. There is a distribution of angles with respect to an overall director, as defined previously (see equation 1.1). The value for  $S$  ranges from zero (for random systems) to unity (for perfectly aligned systems).

### 3.2 CHOLESTERIC PHASE

The cholesteric family is so named because it was noticed that the helical distortion found in these materials could also be found in pure cholesterol esters. The distortion occurs if a chiral molecule is dissolved in a nematic liquid.

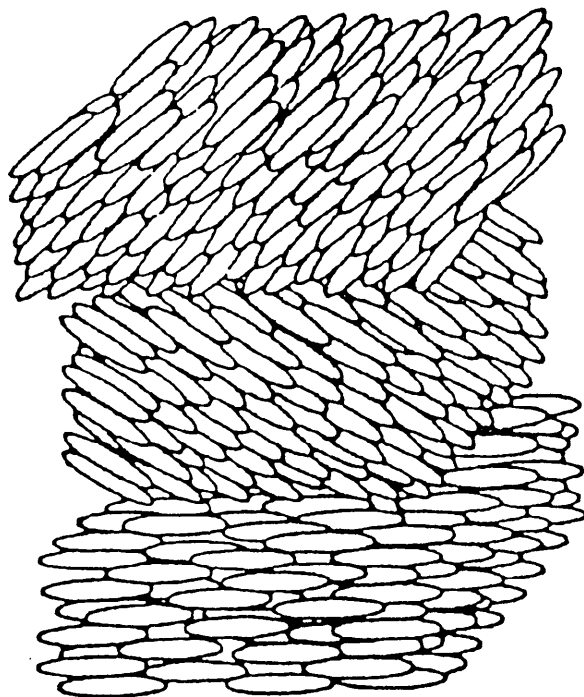


FIGURE 3.2 - Structure of Cholesteric phase

Cholesterics are similar to nematics having no long range positional order and a preferred direction of molecular orientation. The structure consists of a series

of stacked layers. Within each layer, the molecules are packed with their long axes in the plane of the layer. The molecular axes in adjacent layers are not parallel, but point in slightly different directions. The progressive twist of the molecular axes takes about 1500 layers for the top and bottom layers to be aligned; the pitch of the helix is of a size comparable to the wavelength of light. This gives rise to interesting optical effects (vivid iridescent colours) which change under the influence of variables such as, temperature, pressure, and magnetic or electrical fields.

### 3.3 SMECTIC PHASE

It was also from Friedel's<sup>8</sup> work that smectics received their name; it comes from the greek σμῆμα (soap). This arises because certain smectic mesophases have soap-like properties. There are three main types of smectic - A, B and C, but many other sub-types, as mentioned previously. Even though the types are different, they are all layered structures. As a general rule, smectics :-

- i) are a layered structure where the layer thickness is the length of one unit molecule;
- ii) each layer is a two-dimensional sheet, although within each layer the rod-like molecules are packed irregularly; and
- iii) have a structure that is optically uniaxial with the axis being perpendicular to the layers. The structure

is made up of rod-like molecules which pack together in layers, which in turn stack on top of one another (see figure 3.3).

The structure is thus organised in two dimensions, although within each layer the rod - like molecules are packed irregularly. Smectic liquid crystals are the most solid, being turbid and quite viscous.

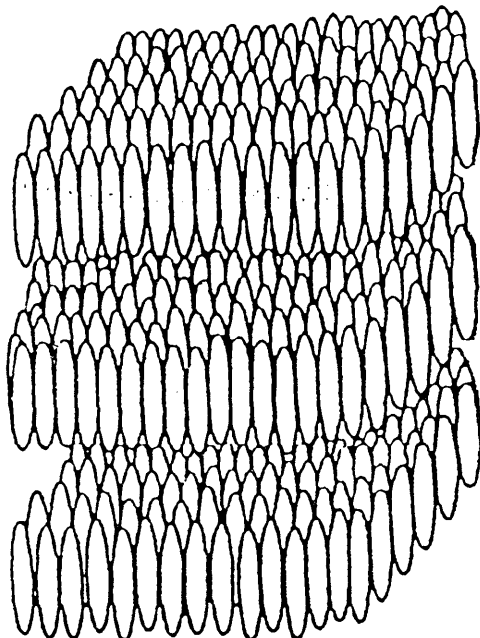


FIGURE 3.3 - Structure of Smectic phase

Similar to conventional polymers, LCP's have phase transformations. Polymeric crystals may form either smectic or nematic structures on melting, a further temperature rise will give an isotropic melt phase. If the temperature at which the isotropic melt is formed is higher than the decomposition temperature of the polymer, then the polymer will decompose before it will flow. By disrupting the

linearity of the backbone chain by adding kinked or bent units, the nematic transition temperature ( $T_n$ ) can be reduced sufficiently so that the isotropic melt temperature falls below the decomposition temperature. The nematic transition temperature is reduced and the range over which the nematic mesophase occurs can be altered. The level of disruption is important; too much disruption and the material will no longer be liquid crystalline.

### 3.4 MORPHOLOGY OF LIQUID CRYSTAL POLYMERS

It is well referenced that LCP behaviour is based around domains, as previously mentioned. The way that these domains interact determine the flow characteristics of the polymer. Injection moulding of LCP's gives complex flow regimes, which give rise to three distinct regions across the moulding, two skins, with a core sandwiched in between (see figure 3.4).

On further examination of these three regimes it can be seen that they split into separate smaller components<sup>51-53</sup>. The skin region has a distinct morphology, with highly ordered/orientated layers at the surface of the moulding, becoming less ordered towards the centre of the moulding. The orientation effect in LCP is caused when the liquid crystalline material is subjected to elongational flow.

When filling a mould or flowing through a die, the LCP moves in a fountain flow fashion<sup>54,55</sup> (see figure 3.5).

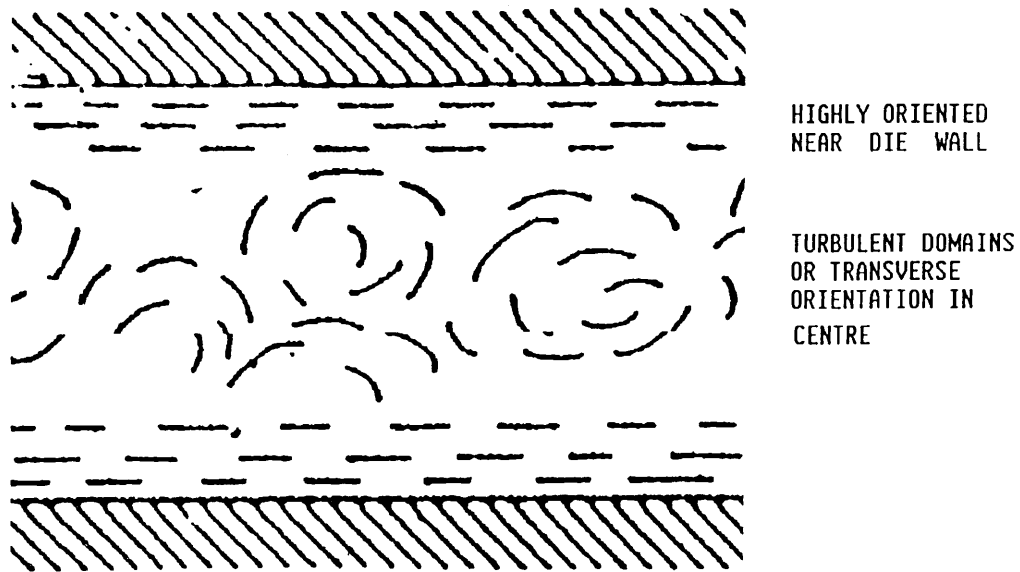


FIGURE 3.4 - Figure to show high degree of orientation at wall, with turbulent or transverse orientation in centre

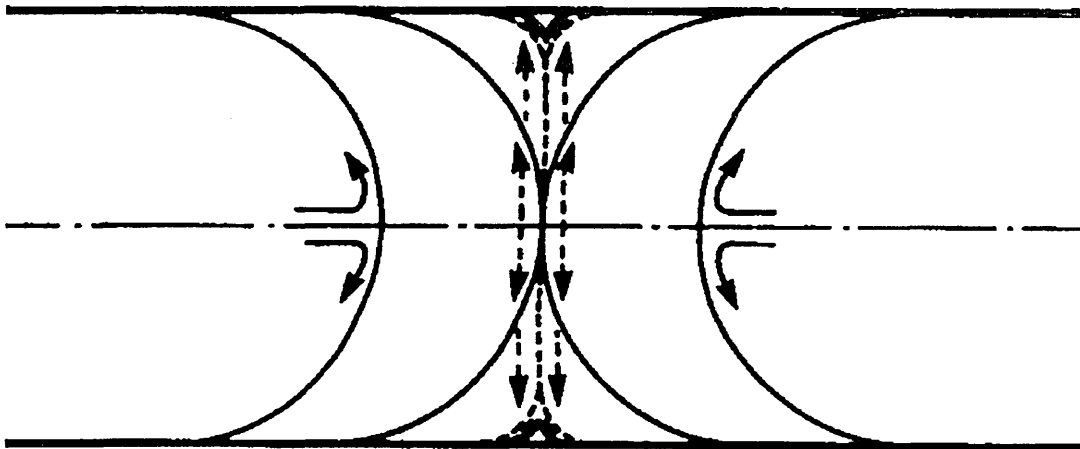


FIGURE 3.5 - Figure to show two advancing fountain flow fronts

This causes high levels of molecular orientation at the flow front. This material is then pushed to the side and eventually forms the surface skin. Ensuing material is

not as highly ordered, hence a structural gradient is set up within the skin layers.

The core, on the other hand, is far less ordered, because it is subject to virtually no elongation forces, only shear. The core is formed by later material to enter the die/mould, which flows through the channel created between the skin regions. It has been cited that the orientation in the core may even be perpendicular to the flow direction due to the deceleration and subsequent compression of the core region. The orientation of the LCP chain is affected by the vector of the flow profile at that point<sup>56</sup> across the cross section. This forms the basis for the mathematical model which is discussed in a subsequent section.

The skin and core region can be further subdivided again and again until the layers or fibrils are on a molecular level (see figures 3.5 and 3.6). From various studies in this area, the layers/sub-layers can be divided into three categories:-

- i) micro layers -  $\approx 0.005\mu\text{m}$ ;
- ii) sub-layers -  $\approx 0.5\mu\text{m}$ ; and
- iii) macro layers -  $\approx 5\mu\text{m}$ .

The thickness of these layers appears to be inversely proportional to the distance from the core, that is samples

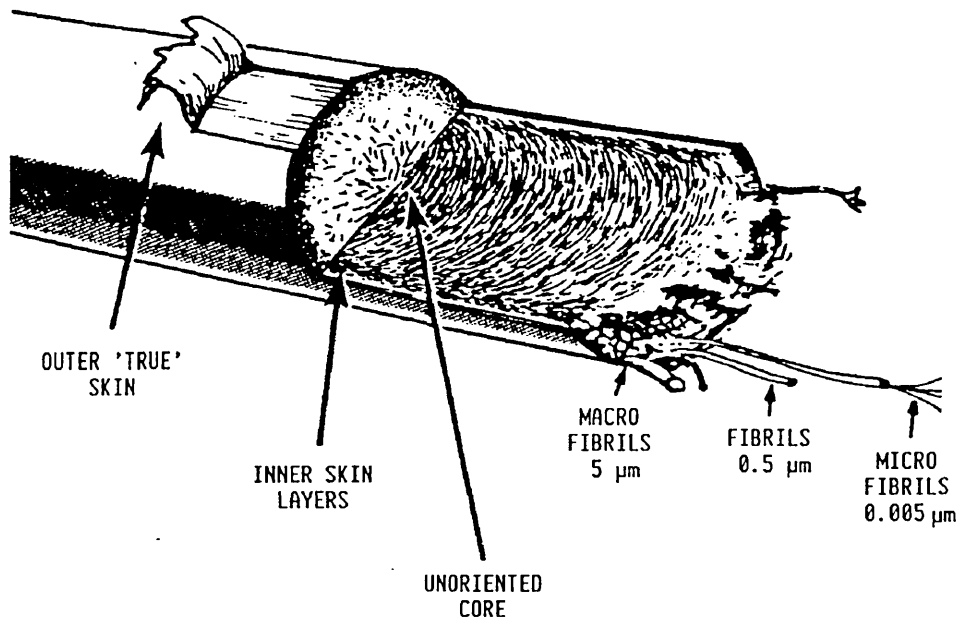


FIGURE 3.6 - Figure to show the macro/micro morphology of an extruded section of liquid crystal polymer

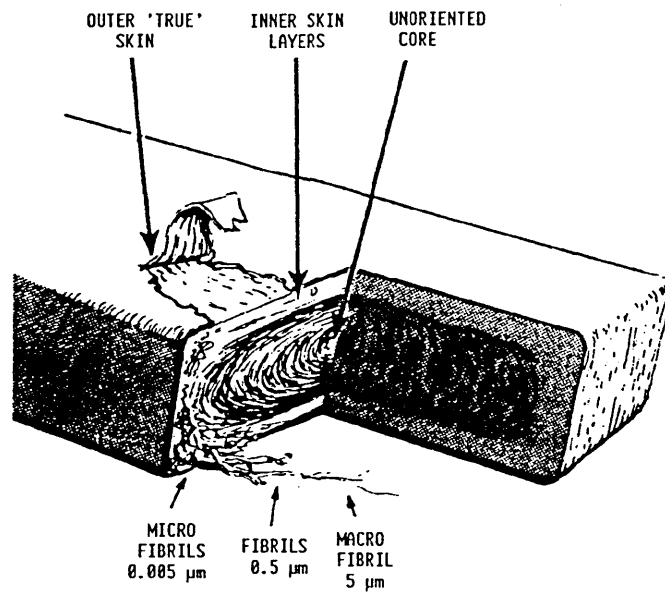


FIGURE 3.7 - Figure to show the macro/micro morphology of an injection moulded bar

taken in the outermost layers are found to be very thin and highly aligned. It is hoped that the LCP will confer a degree of orientation to the blend, although the author is unsure how large this effect will be.

## CHAPTER 4: RHEOLOGY

### 4.1 BACKGROUND TO RHEOLOGY

The term rheology originates from the Greek, 'rheol' - meaning flow or deformation of matter and 'ology' - meaning science. Rheology is the science of flow and deformation of matter and received its present name from Professor E. C. Bingham of Lafayette College, Pennsylvania, in 1929. In the pioneering work of the early rheologists, the deformation of matter was divided into two simple categories :-

- i) reversible deformation, called elasticity (Hookean behaviour) and;
- ii) irreversible deformation, called flow (Newtonian behaviour).

It is now known that many materials can experience both reversible and irreversible deformation. If the basic properties are liquid-like, the materials are called elastic or elastico-viscous liquids; the more solid-like materials are called viscoelastic solids. The definitions of liquid and solid are as follows :-

'A liquid is defined as a material that will change its shape continually (it will flow) when subjected to stresses, irrespective of how small these stresses may be.'

A solid is defined as a material that will not continually change its shape when subjected to stresses; for a given stress field there will be a fixed deformation, which may or may not be relaxed instantaneously<sup>57</sup>.

#### 4.2 VISCOSITY

The most widely used flow parameter is the shear viscosity. The shear viscosity is only defined for a certain class of simple flows called viscometric flows, i.e. flows where the viscosity can be measured. Viscometric flows are essentially uniform flows where the particles of the material undergo steady shear flow independent of time. The concept of using viscosity to measure rheological properties was conceived by Isaac Newton<sup>58</sup>. He published the following hypothesis:-

'The resistance which arises from the lack of slipperiness of the parts of the liquid, other things being equal, is proportional to the velocity with which the parts of the liquid are separated from one another.'

The viscosity of a fluid refers to its lack of slipperiness or resistance to flow and is synonymous with internal friction. If a shearing force ( $F$ ) is applied to the top and bottom surfaces of a liquid (see figure 4.1) each of which has an area of ( $A$ ) the shearing stress

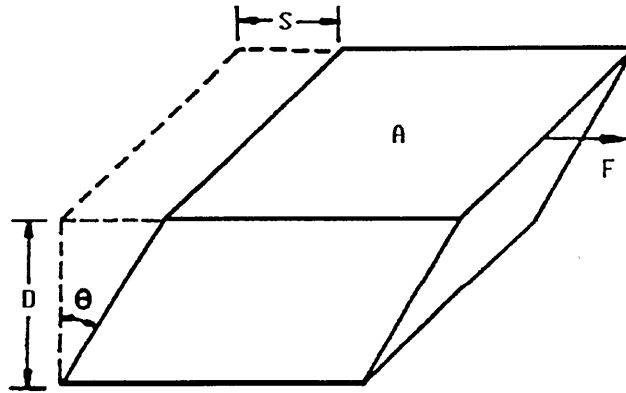


FIGURE 4.1 - Diagram to show simple shear

applied to the fluid is defined as :-

$$\text{Shear stress } (\tau) = \frac{\text{Shear Force } (F)}{\text{Area } (A) \text{ of Shear Face}} \quad (4.1)$$

The shear strain and thus viscosity can also be calculated, by the following equations :-

$$\text{Shear strain } (\gamma) = \frac{\text{Shear displacement } (S)}{\text{Distance separating surfaces } (D)}$$

$$\text{Hence } \gamma = \tan \theta \approx \theta = S/D \quad (4.2)$$

$$\text{Shear Viscosity } (\eta) = \frac{\text{Shear Stress}}{\text{Rate of shear strain}} = \frac{\tau}{\frac{\partial \gamma}{\partial t}}$$

$$\eta = \frac{\tau}{\dot{\gamma}} \quad (4.3)$$

If the viscosity ( $\eta$ ) is dependent on shear rate and there are no time dependent or visco-elastic effects, the liquid is said to be Newtonian. In such liquids the ratio

of the applied shear stress to the rate of shear is constant for a given temperature and pressure. This type of fluid is not to be confused with the idealistic Pascallian fluids :-

'The pressure applied to a fluid at a point is transmitted to all other points of the fluid without loss<sup>59</sup>.'

The slope of the curve is equal to the shear modulus. If the viscosity as calculated by equation (4.3) is not found to be constant but a function of shear rate :-

$$\eta = f(\dot{\gamma}) \quad (4.4)$$

The liquid is said to be non-Newtonian. In such cases, viscoelastic effects may or may not be in evidence.

#### 4.3 TYPES OF FLUID FLOW

This class of fluids does not obey Newton's equation, because the dissipation of energy is either by impact between large molecules or a dispersed second phase. In general, polymer melts fall into this category. They do not obey equation (4.3) and a single measurement of viscosity is insufficient to characterise the fluid. The viscosity of these materials is not a constant but varies with some external influence, for example shear rate: the viscosity is commonly referred to as the apparent viscosity ( $\eta_a$ ). Three main classes of fluid flow behaviour are recognised

and are categorised below :-

- i) time independent fluids - the shear viscosity is a single valued function of the shear stress. Newtonian fluids fall into this class;
- ii) time dependent fluids - the shear viscosity depends on the shear stress and the duration of the shear; and
- iii) elasticoviscous fluids - which are viscous liquids but possess elastic-like solids. Viscoelastic materials are solids that exhibit limited flow, undergoing elastic deformation below their  $T_g$ .

#### 4.3.1 TIME INDEPENDENT FLUIDS

A Newtonian fluid is one in which the viscosity is constant, because it does not depend upon the dynamic independent variable ( $\dot{\gamma}$ ). The 'constitutive equation' for Newtonian fluids is:-

$$\tau = \eta \dot{\gamma} = \eta \frac{dv}{dr} \quad (4.5)$$

where  $\frac{dv}{dr}$  = shear rate.

The constitutive equations can be used to construct differential equations, which can then predict the deformation arising from any type of external strains or stresses. The viscosity of the fluid is given by the slope of the line from the origin to the point of reference on the curve. Once the viscosity is measured a complete

rheological characterisation is obtained for the material at a particular temperature and pressure. Although single phase low molecular weight liquids behave experimentally as Newtonian fluids in laminar flow, polymer solutions and melts approximate to Newtonian behaviour only at very low shear rates or stresses. If the viscosity alters, when there is a change in the shear rate, the fluid is either shear thickening or shear thinning. A shear thinning fluid is one where the viscosity decreases as the shear rate increases. A shear thickening fluid is one where the viscosity increases as the shear rate increases.

If the fluid needs a finite shear stress before any flow occurs, the fluid is classed as a Bingham plastic fluid. The constitutive equation is as follows :-

$$\tau - \tau_y = \eta \dot{\gamma} \quad (4.6)$$

$$\tau_y = \text{yield stress}$$

If the viscosity changes with time under stress at a certain shear rate, the material is either thixotropic or negative thixotropic. The viscosity decreases with time for thixotropic fluids, as opposed to negative thixotropic fluids in which the viscosity increases with time. In thixotropic and negative thixotropic materials, the structure depends upon the previous shearing history; similarly viscoelastic materials, have a partial memory of past deformations. A material is inelastic if it is subject to steady shear, which subsequently stops giving an instantaneous stress relaxation. The material is

viscoelastic, if the stress does not return to zero instantaneously, but follows an exponential decay curve. Another effect is elastic recoil, which is due to long chain molecules taking up orientation conformation on application of stress, but on release of stress bond rotations cause the molecules to take up random form. This leads to contraction, in usually one direction and expansion in the perpendicular direction. Die swell (see figure 4.12). Figure 4.2 shows the rheological characteristics for 4 different fluids by plotting the shear stress vs shear rate curve.

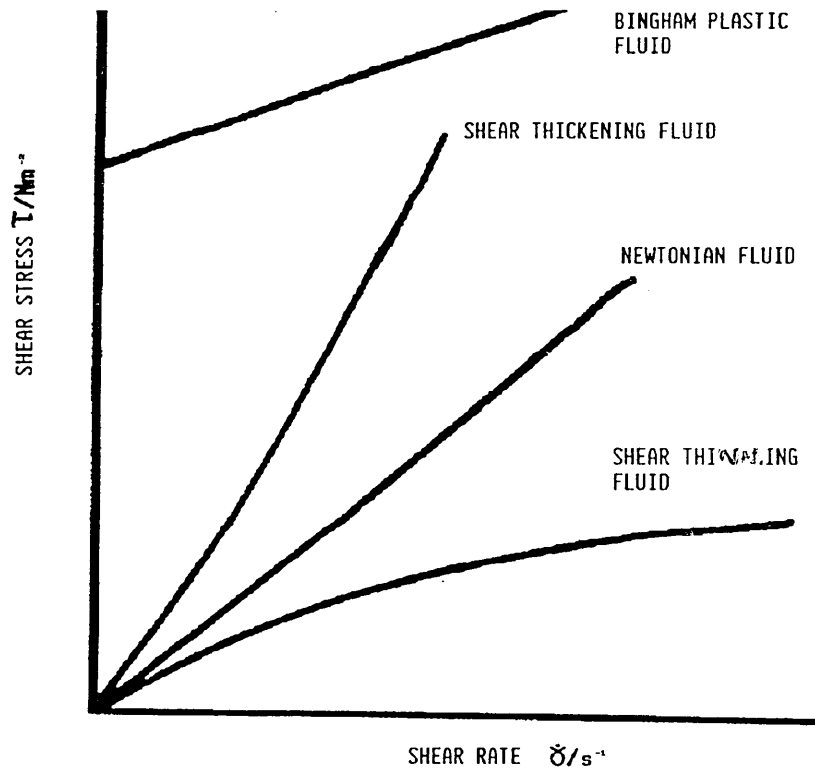


FIGURE 4.2 - Graph to demonstrate the behaviour of Bingham plastic, Shear thinning, Shear thickening and Newtonian fluids.

A variety of rheological models have been proposed to describe the flow characteristic of non-Newtonian fluids. The power law model is generally adopted to describe the

flow properties of polymer melts :-

$$\tau = K\dot{\gamma}^n = K\left(\frac{dv}{dr}\right)^n \quad (4.7)$$

where :-

$\tau$  = shear stress (N/m<sup>2</sup>)

K = consistency constant (Ns<sup>n</sup>/m<sup>2</sup>)

$\dot{\gamma}$  = shear rate (s<sup>-1</sup>)

n = shear thinning index

The consistency constant and the shear thinning index are sufficient to characterise the shear flow of many polymers. The symmetry of the flow dictates that shear stress and shear rate are zero at the centre of the pipe or capillary and increase monotonically to maximum values at the wall. The velocity profile, which is the integral of the shear rate profile, is determined by the form of the influence of shear rate on the shear stress. For Newtonian fluids, the velocity profile is parabolic; shear thinning fluids have less resistance to flow at high shear rates than for Newtonian fluids. The velocity profile will be steeper at the wall and flatter in the centre of the flow. The lower the value of (n) the further the profile deviates from a parabola and the more plug-like the flow becomes (see figure 4.3).

Equation (4.7) can also be written in a logarithmic form :-

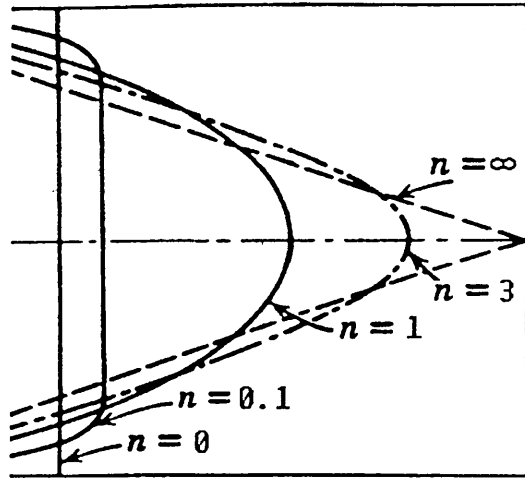


FIGURE 4.3 - Graph of die diameter (ordinate) vs velocity (abscissa) for shear thinning indexes varying between 0 and  $\infty$ .

$$\log \tau = \log K + n \log \dot{\gamma} \quad (4.8)$$

A log - log plot of shear stress ( $\tau$ ) vs shear rate ( $\dot{\gamma}$ ) will yield a straight line. Reasonably straight lines can be drawn over 1 or 2 decades of shear. At higher decades of shear, real materials do not give straight line <sup>rate</sup>  $\frac{5}{\lambda}$  as do ideal materials but give a curved response. The rate of shear has an alignment effect upon the polymer chains: as the rate of shear increases the degree of alignment increases. The higher level of orientation at high shear rates allows adjacent chains to pass more easily over one another. This effect causes an associated lowering of viscosity. There is a relationship between the apparent viscosity ( $\eta$ ) and the power law constants ( $K$ ) and ( $n$ ). The combination of equations 4.5 and 4.7 gives :-

$$\eta = K\dot{\gamma}^{(n-1)} \quad (4.9)$$

#### 4.3.2 TIME DEPENDENT FLUIDS

For these fluids, the apparent shear viscosity on the shear stress and the duration of the shear fluids have a memory. There are two types, thixotropic and negative thixotropic fluids. A thixotropic material demonstrates a reversible, isothermal gel-sol-gel transformation. It can be regarded as a time-dependent shear-thinning fluid. A negative thixotropic fluid demonstrates the opposite behaviour, a reversible, isothermal sol-gel-sol transformation. It can be regarded as a time-dependent shear thickening fluid. This type of behaviour is not important in polymer processing: it occurs sometimes in polymer melts, but this is generally due to degradation or crosslinking of the polymer, and is not reversible.

#### 4.4 VISCOELASTIC MATERIALS

The materials in this section exhibit the properties of viscosity and elasticity. Many commonplace fluids have elastic properties. The elasticity of a material can be measured by observing the recoil in the material once the applied force has been removed.

In polymer melts, the elasticity arises from the deformation of the long chains in the melt. Once the applied force has been removed, melts attempt to return to their original partially coiled configuration. This accounts for the phenomenon of die swell or the Barus

effect, extrudate distortion and draw resonance.

#### 4.5 MEASUREMENT OF FLOW PROPERTIES

There are many methods of studying the flow properties of liquids. For the study of the rheological properties of polymers there are two main types of instrument, rotational and capillary rheometers.

#### 4.6 ROTATIONAL RHEOMETERS

The rheometer works on the principle that every element of the material is subjected to an identical and well-defined shear history. In a rotational rheometer, there is a pressure profile across the faces of the instrument and a normal action forcing the faces apart (see figure 4.4).

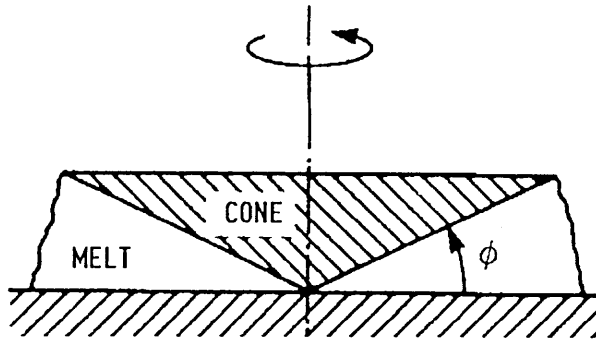


FIGURE 4.4 - Diagram to demonstrate how a rotational (cone and plate) rheometer works

Rotational rheometers can be used to determine the elastic response of melts. Several measurements can be taken; stress, strain, normal stresses and strain recovery.

There are several advantages of rotational rheometers :-

- i) they give a precisely defined flow at low shear stresses;
- ii) they can provide data on both elasticity and viscosity in a variety of experiments; and
- iii) they are sensitive to the structural characteristics of the melt, if the structure breaks down when highly stressed.

There are limitations using this type of instrument:-

- i) there is a large ratio of surface area to volume;
- ii) there are problems with slip and a high rate of heat generation between the metal-polymer interface; and
- iii) measurements are usually taken at atmospheric pressure, whereas polymers are processed at high pressures.

This type of rheometer was not used in the current investigation and will not be discussed further.

#### 4.7 CAPILLARY RHEOMETER

The standard type of capillary rheometer consists of a heated barrel, with a capillary die fitted into the bottom. There are two basic designs :-

- i) the plunger is forced down into the barrel at a

- constant rate and the associated pressure for that rate is measured; and
- ii) a load is applied to the top of the melt and the output rate for that load is measured (commonly used for melt flow index units).

The Davenport capillary rheometer uses the first principle (see figure 4.5).

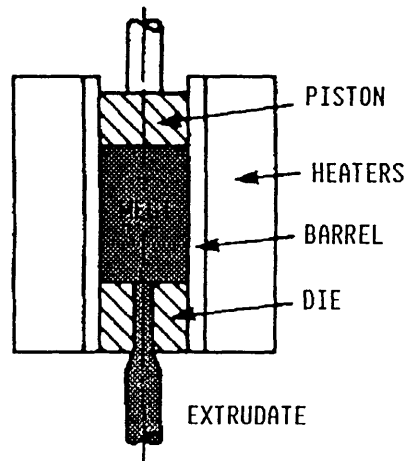


FIGURE 4.5 - Diagram to demonstrate how a capillary rheometer works

In the practical measurement of flow properties it is necessary to make corrections for entrance effects.

#### 4.8 ENTRANCE EFFECTS

The effect occurs because of the convergent flow of the polymer as it enters the die region. Once the polymer enters the capillary there is a large amount of extensional flow. The pressure in the barrel should be measured as close to the capillary die as possible, in order to eliminate the change in pressure drop along the barrel.

There should also be a full development of a velocity profile in the die region.

In practice there are three methods of correcting the entrance pressure:-

- i) Bagley correction;
- ii) Orifice die method; and
- iii) Couette-Hagenbach method.

#### 4.8.1 BAGLEY CORRECTION

The Bagley correction assumes that a die of length (L), has an effective length of (L+eR), where (e) is a 'extra length' and (R) is the radius of the capillary. The true shear stress becomes :-

$$\tau_t = \frac{\Delta PR}{2(L+eR)} \quad (4.10)$$

Dies of the same radius (R) and different (L/R) ratios are used in the measurement. The total pressure drop across each die is measured as a function of the uncorrected shear rate. A graph is then drawn for several shear rates of pressure drops versus (L/R) ratios. This is known as a Bagley plot and the value of (e) can be read off the negative intercept (see figure 4.6).

#### 4.8.2 ORIFICE DIE METHOD

This theory assumes that two dies exist. A metal die

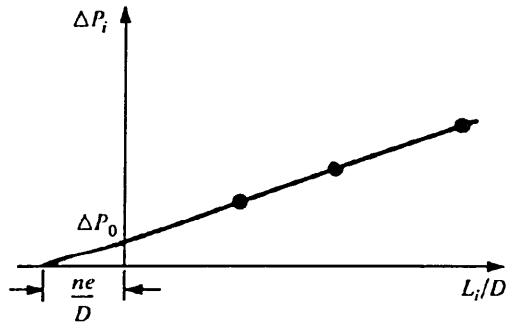


FIGURE 4.6 - Graph of pressure drop vs L/D ratio for various dies of the same diameter but different lengths.

in series with an imaginary polymer die. Extrusions are carried out in two dies of the same radius but a die of length (L) and the other is of zero length. The pressure ( $P_0$ ) obtained with the orifice die is assumed to combine both entrance and exit corrections. It is assumed that the pressure obtained for the orifice can be subtracted from the total pressure drop obtained with the long die to give the true wall stress :-

$$\tau_t = \frac{(P_L - P_0) R}{2L} \quad (4.11)$$

Where  $P_L$  and  $P_0$  are the pressure drop across the long and orifice dies respectively.

#### 4.8.3 COUETTE-HAGENBACH METHOD

This method uses two dies of length  $L_1$  and  $L_2$ , for each of which the output (Q) and the pressure drop value (P) are obtained. It is common practice to use the same

shear rate in both tests, to allow the same pressure drop in the die entry region along with the development of a similar velocity profile. At a given shear rate, the entrance pressure is the same for each die and a simple subtraction of the pressures for the two dies will give the wall shear stress as follows :-

$$\tau_t = \frac{(P_1 - P_2) R}{2 (L_1 - L_2)} \quad (4.12)$$

Where the subscripts  $_1$  and  $_2$  refer to the longer and the shorter dies respectively. This method gives no indication of the magnitude of the entrance and exit corrections and has no indication of the recoverable tensile strain.

In conclusion, the fully developed flow problem is common for all the techniques. The Bagley approach<sup>60</sup> offers the most accurate result. The pressure effect and the viscous heating of the modelling system render this method rather more complicated to use. The Couette-Hagenbach method is used in the present study in conjunction with the Davenport Capillary rheometer. Two separate runs are performed one with a long die and the other with a short die at the same shear rate, and the system is more simple to use. The rheological data obtained is generated with *fewer* runs than would be used by the Bagley method.

#### 4.9 MODES OF RHEOLOGICAL DEFORMATION

There are three definite ways that a polymer melt can be deformed :-

- i) bulk deformation;
- ii) elongational flow; and
- iii) shearing flow.

##### 4.9.1 BULK DEFORMATION

When the polymer is subjected to hydrostatic tension or compression there is an associated volume change. The bulk modulus decreases as the temperature increases and as the hydrostatic pressure decreases. The modulus is independent of the average molecular weight and weight distribution.

The bulk deformation changes at different stages of processing. The melting stage allows up to a 30% increase in the specific volume while flow through small channels can cause volume changes of  $\approx 10\%$ . In the final stages of processing, where the molten polymer is squirted into a metal mould, the change in density of the polymer can be up to 30%. One final important point to note is that solidification occurs from the outside; an outer shell is formed and the stresses generated by this process may lead to warping. Deformation of this kind can be seen in the form of sink marks, frozen in stress or cavitation.

#### 4.9.2 ELONGATIONAL FLOW

The study of elongational flow has advanced rapidly over the past ten years. Direct elongational flow measurements have a particular advantage over shear, because shear measurements do not involve an interface with the wall of the instrument, so that slip is not a problem.

Simple liquids are isotropic; their properties are the same in all directions. Polymers contain long molecules, which may become orientated on deformation. In a stretching flow the stress acts normal to the cross-section (see figure 4.7).

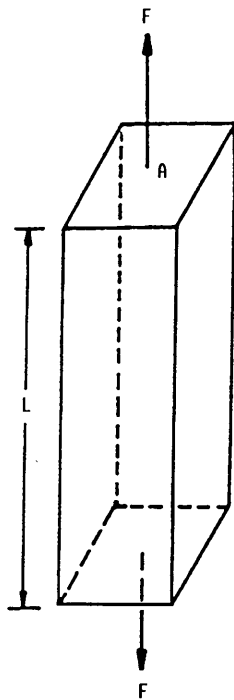


FIGURE 4.7 - Diagram to shows an extensional force acting upon Area (A)

For simple materials Trouton derived the following expression for Newtonian fluids and polymer melts at low

shear stress where the shear behaviour is Newtonian :-

$$\bar{\eta} = 3\eta_0 \quad (4.13)$$

where :-

$\bar{\eta}$  = Tensile viscosity

$\eta_0$  = Shear viscosity

Polymer melts do not behave in such a fashion. The rheological response combines three determinants, viscosity, elasticity and fracture. It has previously been shown that the viscosity of all polymer melts decreases with increasing stress. As a first approximation, as shown by equation 4.13, the tensile viscosity is independent of stress and equal to three times the zero shear viscosity. At higher elongation rates three types of behaviour can be seen :-

- i) Troutonian behaviour at all measurable elongation rates; this occurs with linear polymers of a low degree of polymerisation e.g. polymethyl methacrylate;
- ii) the material is Troutonian over a range of elongation rates, but at a critical elongation rate the material becomes shear thinning or pseudoplastic, this occurs in systems with linear polymers having a high degree of polymerisation, e.g polypropylene; and
- iii) the material becomes non-Troutonian with

increasing viscosity as the stress increases, the material is tension stiffening, this occurs in branched polymers, e.g low density polyethylene.

Measurement of steady state extensional viscosity at high extension rates presents serious problems. There is the difficulty of maintaining a constant rate of extension for the times required for a steady state to develop. Extensional flow occurs in extrusion, where the material is forced from a reservoir with a large diameter into a small die. Since the fluid is assumed to be incompressible, the decrease in cross-sectional area imposed on the fluid can only be accommodated by an increase in length in the flow direction, i.e. uniaxial extension. The extension in the flow direction matches the increase in linear velocity required to maintain a constant volumetric flow rate. Near the die walls, the flow is predominantly shear, as the velocity increases rapidly from zero with distance from the wall. In the centre of the flow, the shear is zero by symmetry and the velocity profile is flat. It can be seen that the fluid in the centre undergoes pure extension. If the walls of the die could be perfectly lubricated, the flow would be totally extensional and an extensional viscosity could be determined from the pressure drop along the die. A true steady-state viscosity could not be measured because of the length of the die required for true steady flow to develop.

### 4.9.3 SHEARING FLOW

In a shearing flow, the force acts tangentially, as shown previously (see figure 4.1). The shear stress is defined as force over area of surface acted upon. The viscosity of simple shear can be seen in equation 4.1.

In practice there are two classes of shearing flow, flow between moving laminar surfaces and flow induced by a pressure gradient (as in capillary rheometry). There are two main differences between such flows. Firstly there is the question of the interface: in flows between moving surfaces there is a possibility of a lack of adhesion between the melt and the constraining surface. Secondly the adhesion is greater because of the driving force. The flow for moving surfaces is found in screw type processes and the pressure driven type flow is found in dies and moulds.

The resistance to stretching flow may be more than a hundred times greater than the resistance to shearing flow. The implication is that the stretching flow component need be only 1% of the total deformation to be significant, even dominant in its effect. The stretching flow component should never be ignored.

### 4.10 RHEOLOGICAL PROPERTIES IN CAPILLARY FLOW

Capillary rheometers are very useful for the determination of rheological properties of polymer melts at the normally high shear rates used in polymer

processing. The output flow rate ( $Q$ ) is proportional to the driving pressure force ( $\Delta P$ ). In the analysis of flow in capillaries the following assumptions are made :-

- i) there is no slip at the wall;
- ii) the melt is incompressible;
- iii) the flow is steady, laminar and time independent;
- iv) the fluid viscosity is not affected by pressure changes along the barrel; and
- v) isothermal conditions prevail throughout.

The pressure-induced force  $\Delta P * \pi R_0^2$  moves along the column in the section of flow and is balanced by the viscous force  $\tau * 2\pi R_0 l$  resisting the column of fluid.

Equating the two we have :-

$$\tau 2\pi R_0 L = \Delta P \pi R_0^2 \quad (4.14)$$

Thus we have :-

$$\tau_w = \left( \frac{R_0 \Delta P}{2L} \right) \quad (4.15)$$

where:-

$r$  = radial position within die

$R_0$  = radius of the capillary

$L$  = length of the capillary

$\Delta P$  = pressure drop across the capillary

$\tau_w$  = wall shear stress

Consider an element ABCD (see figure 4.8) the flow in the die region is assumed to be steady state.

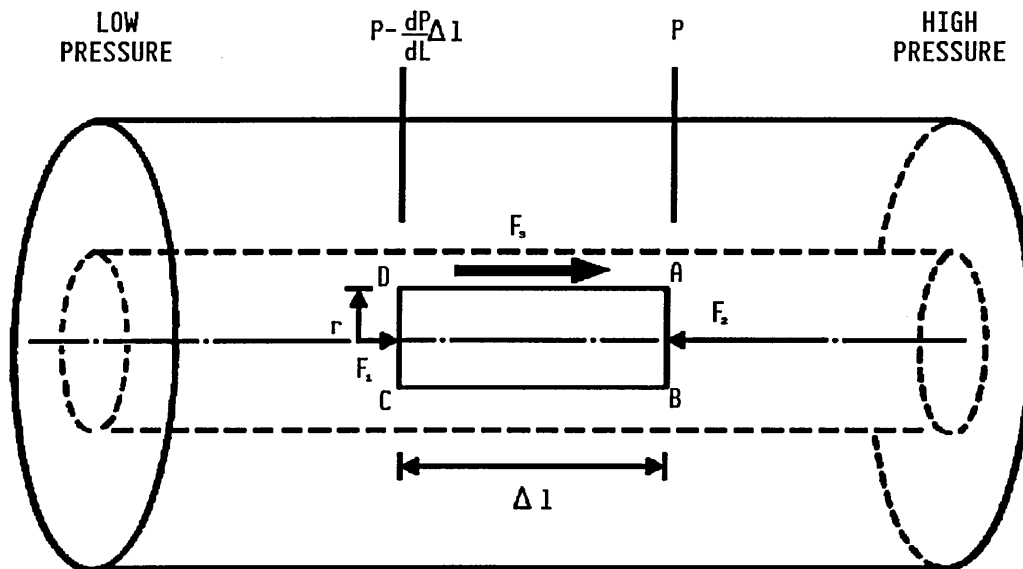


Figure 4.8 - Force vector for an element of fluid inside a capillary

The laws of motion, the sum of all the forces acting upon the cylinder must be zero, i.e :-

$$\sum F = 0 = F_1 + F_2 + F_3 \quad (4.16)$$

The three forces which act upon the cylinder are as follows :-

$$F_1 = \pi r^2 (P - \xi \Delta L) \quad (4.17)$$

$$F_2 = \pi r^2 P \quad (4.18)$$

$$F_3 = 2\pi r^2 \Delta L \tau \quad (4.19)$$

$$F_3 = F_2 - F_1 \quad (4.20)$$

$$\tau = \frac{r}{2} \xi \quad (4.21)$$

where :-

$$\xi = \frac{\partial P}{\partial L} \quad (4.22)$$

The equation for the wall shear stress has previously been derived in equation 4.15, combining equation 4.21 and expanding we have :-

$$\tau = \frac{r}{R_o} \tau_w \quad (4.23)$$

The previous control volume ABCD flows in the die region at a distance (r) from the centre at a velocity of ( $v_z$ ). The shear rate at any point will be ( $dv_z/dr$ ). The volumetric flow rate (Q) can be calculated as follows :-

$$VOLUME\ OF\ SHELL = 2\pi v_z r \delta r \quad (4.24)$$

Integrating between the limits of (0 → R) will give  
Q:-

Integrating by parts we have :-

$$Q = \int_{r=0}^{r=R_0} 2\pi v_z dr = 2\pi \int_{r=0}^{r=R_0} v_z r dr \quad )$$

$$Q = 2\pi \int_{r=0}^{r=R_0} v_z r dr = 2\pi \left[ \left[ \frac{r^2}{2} v_z \right]_{r=0}^{r=R_0} - \int_{r=0}^{r=R_0} \left[ \frac{r^2}{2} \right] dv_z \right]$$

When  $(r = R_0, v_z = 0)$  the first term is zero, and so hence:-

$$Q = -\pi \int_{r=0}^{r=R_0} r^2 dv_z = -\pi \int_{r=0}^{r=R_0} r^2 \left( \frac{\partial v_z}{\partial r} \right) dr \quad (4.26)$$

Substituting equation 4.23, into equation 4.26 and substituting  $\dot{\gamma}$  for  $dv_z/dr$  we have :-

$$Q = -\frac{\pi R_0^3}{\tau_w^3} \int_0^{\tau_w} \dot{\gamma} \tau^2 d\tau \quad (4.27)$$

Rearranging gives :-

$$\frac{\tau_w^3 Q}{\pi R_0^3} = -\int_0^{\tau_w} \dot{\gamma} \tau^2 d\tau \quad (4.28)$$

Differentiating both sides with respect to  $\tau_w$  (and using the Leibnitz rule for differentiation of a definite integral), we have :-

$$\frac{1}{\pi R_0^3} \left[ \tau_w^3 \frac{dQ}{d\tau_w} + 3\tau_w^2 Q \right] = -\dot{\gamma}_w \tau_w^2 \quad (4.29)$$

Since ( $\tau_w = R_o \Delta P / 2L$ ), substituting and re-arranging gives :-

$$-\dot{\gamma}_w = \frac{1}{\pi R_o^3} \left[ 3Q + \Delta P \frac{dQ}{d\Delta P} \right] \quad (4.30)$$

This is known as the Rabinowitsch equation and enables the wall shear rate to be calculated from three measurable quantities ( $R_o$ ,  $Q$ , and  $\Delta P$ ).

The equation now allows the shear stress and rate to be found at one point, i.e. the wall at several different temperatures and pressures. A series of different pressures readings at one temperature, allow a series of flow curves to be constructed of ( $\tau_w$ ) vs ( $\dot{\gamma}_w$ ) and ( $\tau$ ) vs ( $\dot{\gamma}$ ).

In proof of the Rabinowitsch equation an integral between the limits ( $0 \rightarrow R_o$ ) was used to give the total volumetric flow rate ( $Q$ ), (see appendix I).

It has been mentioned previously that the direction of the vector of the flow profile dictates the orientation of the LCP chains at that point<sup>56</sup>. The flow profile will give the orientation vector for the skin and the core regions, when the physical constraints of the system are entered into the model. It is hoped that the relative ratios of the skin and core are the same as in the experimental data, and that the flow profile gives some insight into the difference in orientation in the regions.

Hobbs and Pratt<sup>61</sup> refer to a skin/core morphology in their paper, and explain how the characteristic skin/core morphology can occur.

#### 4.11 RHEOLOGY OF LIQUID CRYSTAL POLYMERS

The rheological behaviour of thermotropic liquid crystal polymers is complex and not fully understood, with some disagreement between observers. A review written by Wissbrun<sup>62</sup> in 1981 cites the rheological behaviour of thermotropic liquid crystal polymers and looked at the framework proposed by Onogi and Asada<sup>63</sup>, similar to the interpretation of Pochan<sup>64</sup> for cholesteric mesophases. This type of three zone flow curve is cited by other authors, Cogswell<sup>65</sup>, Chapoy et al.<sup>66</sup> and Parasadarao, Pearce and Han<sup>67</sup>. The rheological characteristics of LCP's fall into three distinct sections (see figure 4.9), which are :-

- i) Region I - a shear thinning region;
- ii) Region II - a Newtonian flattening; and
- iii) Region III - a second shear thinning region.

##### 4.11.1 REGION I

This zone is the low shear rate shear thinning region, which is not always clearly visible. The shear thinning would appear to have many possible causes and determination is fraught with experimental difficulties. Cogswell<sup>65</sup> mentions a three zone flow curve, but went on to say that he preferred to use the term two zone (presumable zone I

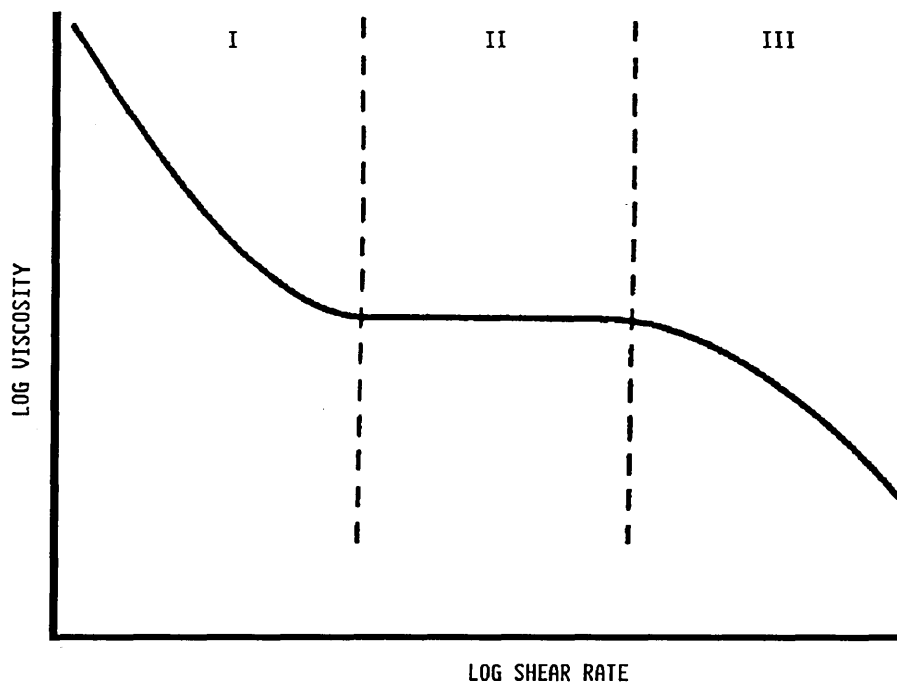


FIGURE 4.9 - Plot of log viscosity vs log shear rate showing regions I,II and III.

was difficult to determine). It is known that region I is associated with a yield stress with the polymer exhibiting Bingham-plastic behaviour at the onset of flow as observed by Cogswell<sup>65</sup> and Han et al<sup>67</sup>. There have been three separate mechanisms postulated to describe the behaviour for region I :-

- i) shear rate dependency due to the competition between orientation of the molecules at a boundary and in a shear field;
- ii) plastic flow of piled domains; and
- iii) phase separation synonymous with dispersed systems.

The author is in agreement with the second mechanism

as detailed by Onagi and Asada<sup>63</sup>. A piled domain isotropic texture is present in the quiescent LCP (see figure 4.10A) which on the application of stress transforms into a dispersed polydomain system (see figure 4.10B). This would account for the shear thinning (Region I) behaviour of the curve. After the initial yield stress to induce flow due to the nature of the LCP, it requires a smaller amount of energy to maintain flow. As the shear rate increases, the energy needed to maintain flow reduces and shear thinning behaviour results. If the system is subject to further stress, the polydomain texture breaks down into a monodomain continuous phase (see figure 4.10C), leading to a flattening of the flow curve or Region II.

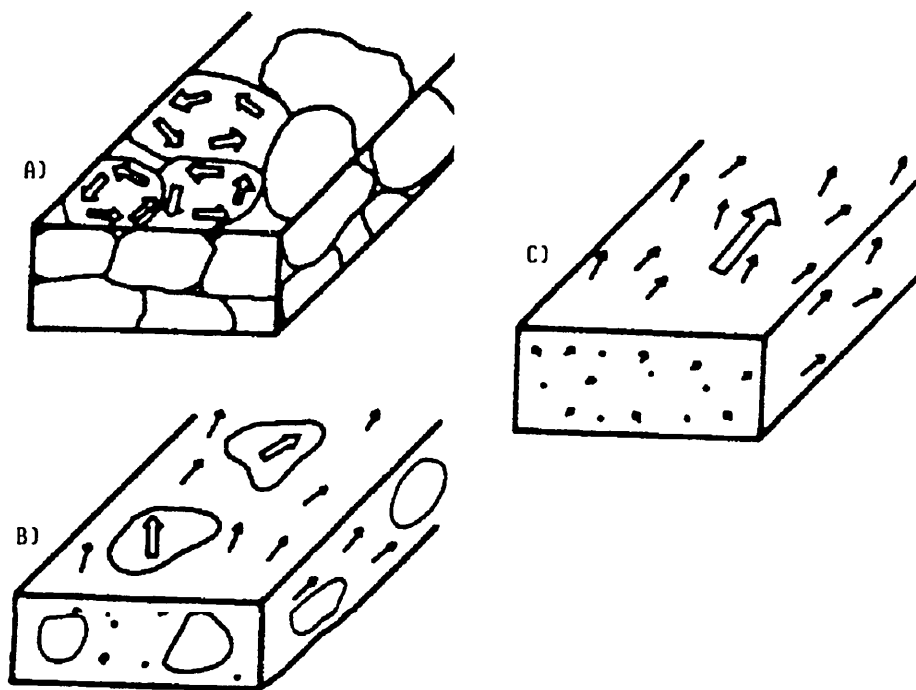


FIGURE 4.10 - Change in domain texture at the onset of flow for A→B→C.

#### 4.11.2 REGION II

This region is unusual in that the viscosity does not change monotonically with increasing shear rate, but instead has a virtually constant value over the entire region. Onogi and Asada<sup>63</sup> did state in their paper that there was no obvious reason for this constant value, because as the shear rate increases the size of the domains decreases (see figure 4.10A→C). It is possible that as the domain texture breaks down so the increase in surface area acts to oppose the driving force. This is dissimilar to standard polymers: on the application of force, polymers tend to align, leading to a drop in subsequent energy to induce flow. This is normally shown in the form of a stress overshoot when measurements are taken from the quiescent state. The modelling of this region is difficult when taking the texture of the material into account. It has been stated that a monodomain texture is achieved at high shear rates, although the order parameter is not necessarily high. Measurements taken of birefringence have shown that there is little change in texture between region I and II. This could account for the results of Cogswell<sup>65</sup>, and the difficulties in determining the change from region I to region II behaviour.

#### 4.11.3 REGION III

This is the final region described by Onogi and Asada<sup>63</sup>, in which the onset of shear thinning behaviour begins. Region III is essentially preceded by a flat

Newtonian region. At the onset of region III the fluid begins to shear thin, which results in a concave downward shape on a log-log plot (see figure 4.11).

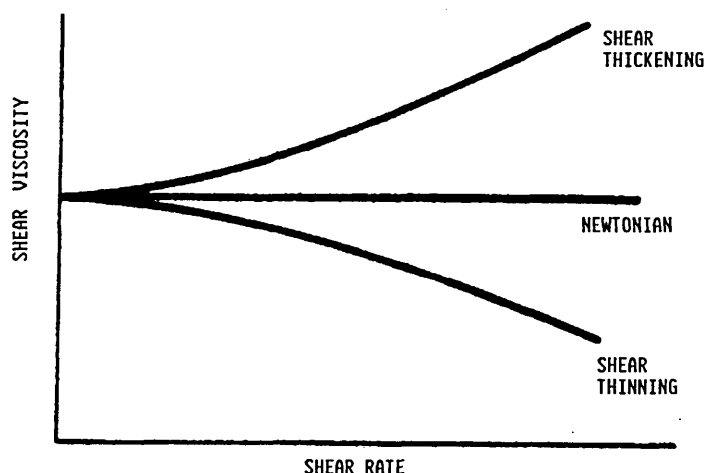


FIGURE 4.11 - Graph of shear viscosity vs shear rate showing the deviation from Newtonian behaviour for shear thinning/thickening fluids.

Generally the shear thinning begins at several decades of shear rates lower than for anisotropic solutions, as seen from the work of Jackson and Kuhfuss<sup>24</sup>. They discovered that the LCP used in the study had a lower Newtonian flattening viscosity and was also shear thinning at much lower shear rates.

The most extensive investigations in this area have involved the study of the shear viscosity of aromatic polyesters. From the work published by Wissbrun<sup>62</sup>, Han et al,<sup>67</sup>, Cogswell<sup>68</sup>, and Sugiyama et al<sup>69</sup>, it can be said that the viscosity increases indefinitely at low shear stresses, and yield values are observed. Wissbrun and Cogswell reported that the shear viscosity ( $\eta$ ) increased

with increasing shear rate ( $\dot{\gamma}$ ) over limited shear rate ranges for certain materials. Generally, the shear viscosity is found to decrease uniformly with increasing temperature. A paper by Gotsis and Baird<sup>70</sup> reviews the work by Wissbrun<sup>62</sup>

Yevseyev et al,<sup>71</sup> found that the dependencies of shear viscosity tend to level out in regions of high shear rate. Work has also been carried out on cellulose esters by Shimamura, White and Fellers<sup>72</sup>, with very similar results to those from the aromatic polyesters. Joseph et al,<sup>73</sup> looked at the same area as Wissbrun, but used wide angle X-ray scattering (WAXS) to investigate the differences in the orientation of the skin and core regions.

The shear viscosities are lower for the liquid crystal polymer in the nematic phase than in the isotropic phase. The fall in viscosity due to the onset of nematic behaviour has been estimated in one case by comparing polymers of similar molecular weight but different chemical composition<sup>74</sup>. Most high molecular weight polymers exhibit die swell on extrusion (see figure 4.12).

Thermotropic polymers display very little or no die swell at all<sup>75,76</sup>. It is known that die swell is associated with viscoelasticity in the melt. Even so, in the isotropic phase, there is little or no elastic behaviour observed. It may be associated with the inherent stiffness

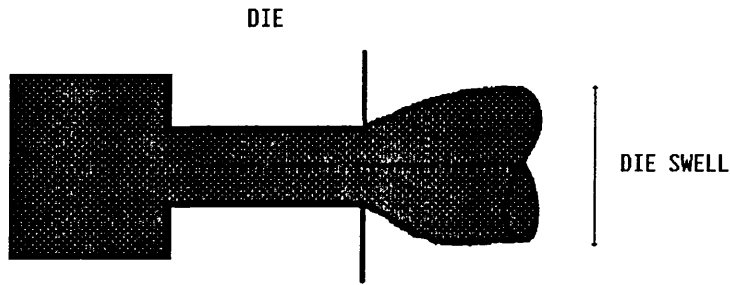


FIGURE 4.12 - Diagram to show how an amorphous polymer increases in cross section upon exit from the die region.

of the liquid crystalline molecules, which remain aligned after leaving the die, hence there is little or no elastic recoil.

Practically, the low melt viscosity of LCP's at high shear rates, when compared to conventional polymers of the same molecular weight, gives them superior properties in the following areas<sup>77</sup> :-

- i) the ability to injection mould components with long or complex flow paths with thin cross sections;
- ii) moulding with very high filler loadings (up to 70%);  
and
- iii) as a processing aid at low additions (10%) of LCP to conventional polymers as covered by ICI's patent<sup>1</sup>.

In recent years, thermotropic liquid crystal polymers

have entered the polymer market<sup>44,78,79</sup>. The main advantages of these polymers, being they process at lower melt viscosities than conventional polymers of a comparable molecular weight, and are capable of forming highly orientated crystalline structures. At the transition to nematic state, the melt viscosity is of three decades less order of magnitude than that of a non mesogenic polymer. They attain high modulus and strength, when subject to shear above their melting point. The rod-like molecular conformation and stiffness of their back-bone chains cause liquid crystal polymers to form fibrous chains in the final product with fracture surfaces similar to that of wood. The mechanical properties of liquid crystal polymer products are close to those of fibre reinforced composites. Owing to high molecular orientation in the flow direction, their ultimate properties in the direction transverse to flow are usually weak<sup>80</sup>. It is also important to note that if weld lines are formed during production (see figure 3.5) by the meeting of two advancing flow front, the resultant boundary will always be a weak point and act as a stress raiser.

The rheology of liquid crystal polymers is complicated in some cases by smectic phase formation and differences in thermal history, since both shear and thermal history affect viscosity, and usually, neither is adequately defined. As a result of this, comparison of work from different sources is at present hazardous, unless the experimental conditions are well defined.

#### 4.12 RHEOLOGY OF BLENDS

The effect of reinforcing fibres and fillers on the mechanical properties of polymers is well documented<sup>81,82</sup>. In general, fibres and solid fillers increase the elastic modulus, while the effect on strength can be positive or negative depending upon the aspect ratio of the reinforcing body<sup>83</sup>. Associated with their effect on stiffness, reinforcing fillers tend to lower the coefficient of thermal expansion. In this regard, stiff fibres can be added to a polymer in order to minimise the shrinkage normally encountered upon cooling the material from the melt in common polymer processing operations. The addition of a small amount of chopped glass filaments to a thermoplastic such as polystyrene can result in a significant reduction of film shrinkage during extrusion<sup>84</sup>.

Although the addition of fibres to a polymer can improve the mechanical properties, it can also have a deleterious effect on the processability of the resulting composite material. For the same reasons that account for the increase in the modulus and the decrease in the coefficient of thermal expansion, the presence of fibres in a polymer melt increases the viscosity; this has been well documented by Han and White<sup>85-89</sup>. The associated increase in the melt viscosity increases the power consumption of the plastic processing equipment, and in some instances the viscosity could be too high to be practical. The rheological properties of more standard

polyblends are governed by the :-

- i) particle size;
- ii) particle shape;
- iii) volume fraction;
- iv) deformability of dispersed phase; and
- v) state of dispersion.

Han<sup>83</sup> stated that flow instabilities were encountered when breakup of the droplets occurred, as the droplets began to elongate, followed by breakup. He also stated that the formation of long thread-like liquid cylinders was an unstable flow phenomenon for normal polymer-polymer dispersions. Liquid crystal polymers, by their very nature, formed long thin fibres under the right conditions. Composites of polymers and inorganic/metallic fillers are commonplace in the plastics industry. In fibre reinforcement, there is never a perfect transfer of stress from the matrix to the fibre because of the variability of surface adhesion. By using liquid crystal polymer blends it is hoped that the degree of adhesion between fibre and matrix is higher than would be the case for normal fibre reinforcement. Seigmann et al,<sup>90</sup> found good fusion between the liquid crystal polymer dispersed phase and an amorphous polyamide (PA) matrix. Using scanning electron microscopy (SEM) the fibrillar/elliptical liquid crystal polymer particles could be seen in the etched PA surface.

Work carried out by Jung and Kim<sup>91</sup> used polycarbonate (PC) as the matrix. Again SEM and wide angle X-ray diffraction (WAXS) were used as analysis tools. They carried out work on the stress - elongation relationship of the blends to show how the pure PC is amorphous giving ductile behaviour. This changes as the liquid crystal polymer content increases, owing to a high degree of anisotropy in the polymer crystallites, causing an overall increased level of orientation. There was an associated change in the mechanical properties, and the blend begins to exhibit brittle properties at about 10 to 20% LCP. Some micrographs in this paper show liquid crystal polymer fibres protruding from the PC matrix at various compositions. The liquid crystal polymer particles were reported to be elongated into rod-like fibrils. Good interfacial adhesion was also reported between the two polymers, with no particle pull-out.

Similar work carried out using a PC matrix was reported by Isayev and Modic<sup>92</sup> and Nishimura and Sakai<sup>93</sup>. Isayev and Modic reported the formation of high strength fibres within the blend at low concentrations and high shear rates. SEM work carried out revealed these fibres to have a diameter of 2 - 5  $\mu\text{m}$ . They found no fibre formation at higher liquid crystal polymer contents. Instead large spherical domains of liquid crystal polymer were found. They show the stress - strain relationships for various blend compositions, unusually giving the 90/10 PC/LCP

composition superior strength than the pure LCP. It was also stated in several sources that liquid crystal polymers can be added to melt processable polymers, not only to affect both morphology and rheology of the resulting blend, but also to act as a processing aid<sup>1,92</sup>. Nishimura looked at the correlation between phase structure and mechanical properties, showing that these types of binary systems do not obey a logarithmic rule. Instead he preferred to classify them into three groups as described by Utracki<sup>94</sup>. A good rheological paper on LCP blend rheology has been written by Blizard and Baird<sup>95</sup>. In it they attempted to correlate the structure of the blends using SEM in conjunction with rheological measurements. A review by Brostow et al<sup>96</sup> explained that liquid crystal polymers provide very useful thermophysical, rheological and mechanical properties in their blends. They showed good dimensional stability, chemical resistance and low flammability. The properties of ordinary engineering polymers can be largely improved by blending with thermotropic liquid crystal polymers. The costs of the resultant blends are lower than the pure liquid crystal polymer. These types of blends should find applications in electrical, electronic, chemical, aircraft, aerospace and automotive industries.

## CHAPTER 5: BLENDS

### 5.1 MOTIVATION FOR BLENDING

The driving factor behind the blending of polymers is cost. If a material having properties of an expensive resin, but only containing a fraction of that resin, can be produced then manufacturers will use the blend to remain competitive. This was the main thrust behind the current study, to see if a small addition of LCP to an engineering resin could render properties similar to or even better than the matrix polymer (as cited by Isayev and Modic<sup>92</sup>). The accepted rules for blending are as follows :-

- i) extending engineering polymers performance by diluting it with a low cost polymer;
- ii) developing 'new' materials in which the properties can be tailored to suit customers' needs;
- iii) forming a high performance blend from polymers that interact on a molecular level; and
- iv) recycling plastic scrap.

The above reasons are the driving force for blending, as the reserves of organic materials become depleted so the importance of blending will increase. The principal cost of the price of the resultant blend depends on the cost of the principal polymeric component, and the modifier if one is used. The use of blends is therefore geared to the more expensive engineering resins; the bulk of blend production

is to improve or modify existing mechanical properties of these engineering resins.

## 5.2 METHODS OF BLENDING

Polymer blends can be created in a variety of ways. The following are the ones most commonly used today :-

- i) mechanical mixing;
- ii) dissolution in a solvent followed by casting or spraying;
- iii) latex blending;
- iv) fine powder mixing; and
- v) use of a monomer solvent for IPN/HIPS manufacture.

In the current study the components of the blend were mechanically mixed together. The two polymers were mixed in their granular form and then processed twice through a single screw extruder.

## 5.3 PROPERTIES OF BLENDS

The properties of blends are indeed multifarious due to the interaction of many different factors namely :-

- i) thermodynamics;
- ii) phase behaviour;
- iii) morphology; and
- iv) rheology.

The close association of the above elements means the

final properties of the blend are difficult to model with any accuracy. The effects of processing on the blend result in deformation under many types of stress/strain fields.

### 5.3.1 THERMODYNAMICS

The first law of thermodynamics deals with energy conservation, and states that the total energy within any isolated system remains constant. It follows that if a quantity of heat ( $Q$ ) is absorbed by a body then part of the heat will do work ( $W$ ) and part will be connected with the rise in internal energy ( $\Delta E$ ). The expression governing this is as follows :-

$$Q = \Delta E + W \quad (5.1)$$

If the system is also at constant temperature and pressure the rise in enthalpy (heat content) due to the rise in internal energy and work done by expansion can be defined as follows :-

$$\Delta H = \Delta E + P\Delta V \quad (5.2)$$

where :-

$\Delta V$  = change in volume

$\Delta H$  = change in enthalpy

$\Delta S$  = change in entropy

$P$  = pressure

Combining the two an expression for the free energy

( $\Delta F$ ) is obtained where :-

$$\Delta F = \Delta H - T\Delta S \quad (5.3)$$

The Gibbs free energy is important as it tells us the following information :-

- i) increasing the temperature (T) increases the degree of mixing;
- ii) increasing the entropy increases the degree of mixing; and
- iii) the less the change in enthalpy ( $\Delta H$ ), the greater is the degree of mixing.

All of the above statements are linked with the variable factors in equation 5.3.

### 5.3.2 PHASE BEHAVIOUR

The low diffusion rates of polymer macromolecules makes a thermodynamic equilibrium difficult to achieve. In spite of research in this area the majority of polymer pairs are not miscible to any degree. The main factors important to immiscible blends are the spatial arrangements of the phases and the nature of the phases between them. There are four main categories of polymer-polymer blends, which are as follows<sup>97</sup> :-

- i) Homogeneous - where the components are completely miscible, e.g. polyphenylene oxide - polystyrene. The

properties of these blends are usually additive and complement one another. The interaction between molecules is on a molecular level and polymers will have similar values for solubility parameters<sup>98</sup> and also a common glass transition temperature.

- ii) Polymer-polymer dispersions - where one of the components is dispersed as very small particles, often about one micron or less, in the other (matrix). Interaction takes place at the particle-particle surface and thus surfactants (compatibilisers) are usually added. The properties of these systems are usually intermediate between the parent materials and are dependent on the concentration and hence the properties of the resultant blend can be tailored.
- iii) Interpenetrating polymer networks - where the two component polymers are in the form of two interconnecting networks (see figure 5.1). The blends are usually prepared by the polymerisation of two monomers using different reactions of a monomer, in the presence of another polymer. An alternative method of preparation is by the combination of the two polymers followed by selective crosslinking.
- iv) Laminar blends - where the blend is prepared by the control of morphology and distribution of the dispersed phase. The dispersed phase is distributed as large two dimensional thin sheets having controlled interfacial adhesion.

The materials in the current study form immiscible blends, which makes the modelling of blend behaviour difficult, to say the least. There are also complications due to the concentration of local stress fields and also obtaining an average response for the blend. Within the same concentration range, different proportions of rods and droplets will co-exist<sup>52</sup>, depending on the flow conditions and associated thermodynamics. Bearing in mind all of the variables, no one model/system can determine the phase equilibrium of polymer blends. Modifications of blend components afford a degree of adaptability for manufacturers. However altering the composition can significantly affect the compatibility of the components.

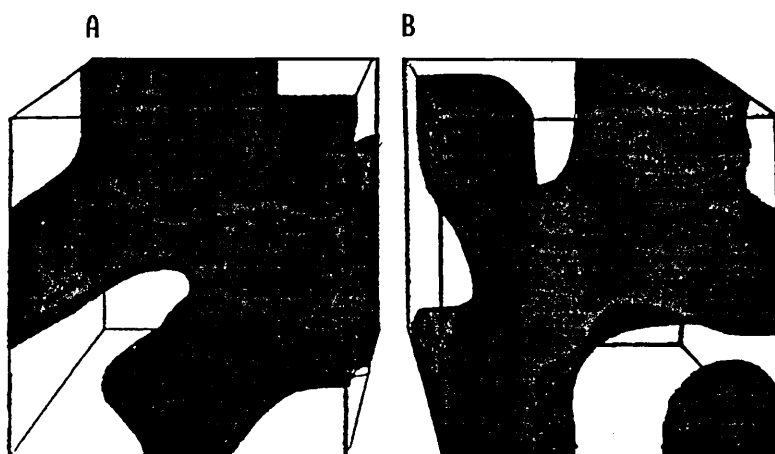


FIGURE 5.1 - Diagram to show two interpenetrating networks, where A and B are the two component polymers.

Prior to 1975 three key papers formed the basis for polymer blend literature<sup>99-101</sup>. All of these papers covered compatibility and all state that most systems are incompatible, and that compatibility is the exception to

the rule. Compatibility is the term used to describe the formation of a single phase mixture on the blending of two polymers. True mutual compatibility of two polymers is rare, due to the small entropy gain on mixing, which often involve optical clarity and a sharp glass transition temperature.

The initial prediction of polymer-polymer miscibility was outline in a paper by Dobry and Boyer-Kawenoki<sup>99</sup>, who used a lattice theory which was followed by subsequent papers by Scott<sup>102</sup>, Flory<sup>103</sup>, and Huggins<sup>104</sup>. The Flory-Huggins theory as it came to be known obtained a value for the heat of mixing as follows<sup>101</sup> :-

$$\Delta G = \frac{RTV}{V_r} \left[ \frac{V_A}{x_A} \ln v_A + \frac{V_B}{x_B} \ln v_B + \chi_{AB} v_A v_B \right] \quad (5.4)$$

where :-

- V = total volume of the mixture
- V<sub>r</sub> = reference volume
- v<sub>A,B</sub> = volume fractions of A and B
- x<sub>A,B</sub> = volume fractions of A and B
- R = gas constant
- T = absolute temperature
- χ<sub>AB</sub> = interaction parameter

The interaction parameter can be calculated as follows:-

$$\chi_{AB} = \frac{V_I}{RT} (\delta_A - \delta_B)^2 \quad (5.5)$$

where :-

$\delta_A$  = Hildebrand solubility parameter for A

$\delta_B$  = Hildebrand solubility parameter for B

It was discovered that no matter how compatible two polymers may be, it is always possible to make a very dilute solution containing both polymers, as long as there is a common solvent. Polymer molecules are large and therefore the entropy of mixing is small.

It was also stated by Krause<sup>101</sup> that the region between the binodal and spinodal formed a metastable region within which the phases can coexist. Within the region bound by the spinodal unstable mixtures are formed, whereas the region above the binodal stable mixtures are formed.

Figure 5.2 demonstrates the variation of the Gibbs free energy with concentration. Figure 5.3 shows the equivalent phase diagram at  $P=P_1$  showing both the spinodal and binodal curves.

For a given binary system, the free energy may vary with composition at a constant temperature  $T_1$  (see figure 5.2). Between the points A and B both of the phases can coexist; that is the boundary of the two phase region in the

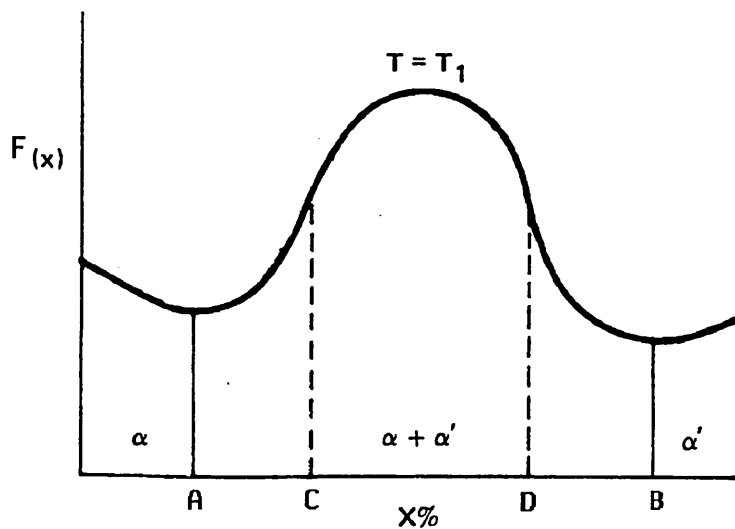


FIGURE 5.2 - Graph of concentration vs free energy at temperature  $T = T_1$

phase diagram is the locus of the points on the free energy curve where  $dF(x)/dx = 0$  defines the maximum solubility (solid line) of the polymers in the homogeneous solution, (see figure 5.3).

In the phase diagram (see figure 5.3), points C and D are inflection points on the free energy curve where  $d^2F(x)/dx^2 = 0$ . The locus of these points the dotted line defines the spinodal region.

Starting at a low concentration and following the straight line  $T_1$  it can be seen that the line cuts the phase diagram at a corresponding point of inflection on the Gibbs free energy curve. Moving further along the line a spinodal point is next followed by the upper critical solution temperature (UCST) at the positive inflection in the free energy curve. Carrying on along the line, another spinodal point is reached, followed by a second binodal

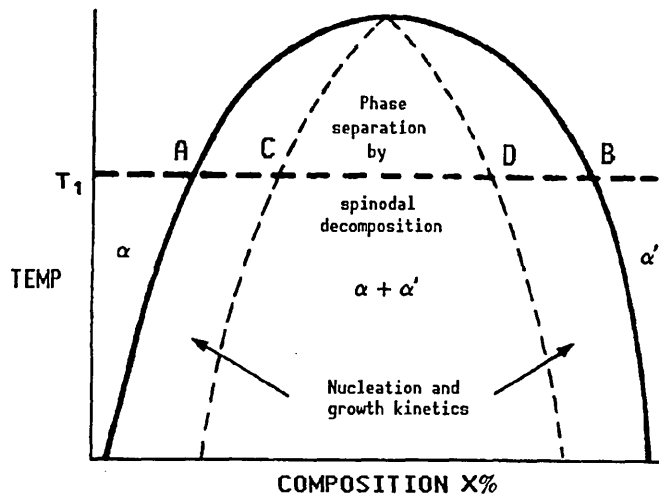


FIGURE 5.3 - Graph of temperature vs composition showing the miscibility gap between the binodal and spinodal.

point at the other negative inflection in the free energy curve. There is a meta-stable region between the binodal and spinodal curves within which a large area is created, which enhances interfacial slip between the two phases, without the two phases spontaneously separating. Work by Aharoni<sup>105</sup> attempted to describe the viscosity vs concentration curve. He studied the compositions over which the LCP went from an isotropic phase to a biphasic region containing isotropic and anisotropic phases (see figure 5.3,  $\alpha$  and  $\alpha'$  phases respectively). Theories put forward for the modelling of rheological behaviour attempt to predict the isotropic and anisotropic phases, but as yet cannot explain the more complicated spinodal biphasic region of the temperature-composition graph. This is discussed more fully in the next section.

### 5.3.2.1 SPINODAL DECOMPOSITION

Work by Lipatov<sup>106</sup> on polyoxymethylene (POM) in cellulose acetate butyrate (CAB) demonstrated the connection between the Gibbs free energy function and the viscosity, with respect to the POM concentration. Lipatov discovered at low concentrations of POM in CAB the heat of mixing decreased demonstrating compatibility between the two species and a binodal composition. Subsequent addition of POM to CAB gave rise to an increase in the heat of mixing as the concentration of POM moved into the meta-stable region between the binodal and spinodal. Lipatov also discovered that the blend viscosity had a degree of correlation to the log additive rule.

It can be seen that for the LCP to be aligned into fibrils it is not necessary for the two polymers to be compatible. The optimum composition for processing is the region between the binodal and spinodal, where a large interfacial area is created over which slip can occur.

### 5.3.3 PHASE BEHAVIOUR OF LIQUID CRYSTAL POLYMERS BLENDED WITH ENGINEERING POLYMERS.

Noel and Billard<sup>107</sup> looked at the phase behaviour of nematic TLCP's, as did Ballauff<sup>108</sup>. From his work<sup>108</sup> he discovered that low concentrations of the LC phase gave a two phase region on the phase diagram (nematic and isotropic) when the mixture was cooled from a single phase. At higher concentrations of LC, cooling led to phase

existence of a polymer rich isotropic phase and a polymer denuded nematic phase.

Achard et al<sup>109</sup> discovered a 'biphasic' region in mixtures containing low molecular mass nematic solvents and liquid crystalline polymethacrylates or polyacrylates. The author stated that similarities between the polymer and monomer mesogen promoted miscibility.

#### 5.4 CRYSTALLISATION

Joseph et al<sup>73</sup> studied the thermal behaviour of PET and a LCP based on 60% PHB and 40% PET. The rate of crystallisation was found to increase with increasing LCP content, which was attributed to the nucleation of PET by the LCP. This effect was also noted in work by Sharma et al<sup>110</sup> and Takayanagi et al<sup>111</sup>. In the previous papers the authors postulated that the LCP acted as a nucleating agent for the crystallisation of the matrix polymer.

#### 5.5 BLEND MORPHOLOGY

Morphology is the science of structure, which is strongly dependent on the size and form of the dispersed phase, miscibility, character and size of the interphase domains and the distribution of residual stresses, all discussed previously. The resultant morphology of the blend and thus post-processing properties are dependent on the initial preparation. In the process of mechanical blending, the blend is subject to both shearing and elongational

forces, which help to provide a good dispersion of one polymer within the other. It is expected that if the polymers have a low miscibility, there will be large differences in morphology within the specimen. If the polymers are miscible then this difference will be less pronounced. The morphology is not just dependent on the miscibility, other factors include:- polydispersity, chemical reaction during processing, crystallisation and degradation. Degradation is especially important when considering the processing of PC, where exposure to elevated temperatures for long periods of time will result in the breakdown of the PC architecture. The breakdown of the structure results in an increase of the viscosity of the PC affecting the viscosity ratio of the blend :-

$$\lambda = \frac{\eta(PC)}{\eta(LCP)} \quad (5.6)$$

If the viscosity ratio was altered sufficiently, a fibrous texture could be altered to a droplet texture. The change in droplet/fibre morphology will be discussed more fully in the following section.

#### 5.5.1 DROPLET/FIBRIL MORPHOLOGY

Starita<sup>112</sup> interpreted the changes in morphology and related this to the change in the viscosity ratio (see equation 5.5). Starita stated that in systems where the ratio was less than or equal to 1, the resultant system was

a fine dispersion of one polymer in another. As the ratio increased to greater than one, the system became coarse with larger coalesced sections of the dispersed phase clearly visible. Starita also stated that when the viscosity ratio was approximately equal to one and the normal stress ratio was greater than 1, a fibrillar texture was produced. Conversely, when the viscosity ratio was approximately equal to 1 and the normal stress ratio was less than 1, a droplet morphology was produced. It is known that blends containing LCP's are susceptible to flow orientation and it is possible that the blends in this study will behave in a different fashion.

Han<sup>83</sup> looked at both the viscosity and normal stress ratios, and noticed that the less viscous polymer was forced to migrate towards the metal/polymer interface. This effect caused a skin/core morphology in the resultant extrudates/mouldings. Other authors in this field have stated that this effect is by no means the rule White<sup>88</sup> did not observe this effect for polymers in which the viscosity ratio was approximately equal to one, but the normal stress ratio was greater than one.

## 5.6 LOG ADDITIVE RULE

The rule of mixing or log additive rule was cited in the paper by Utracki<sup>94</sup>, however Nishimura et al.<sup>93</sup> expressed the rule as follows :-

$$\ln \eta = \phi_1 \ln \eta_1 + \phi_2 \ln \eta_2 \quad (5.7)$$

where :-

$\phi_{1,2}$  = weight fraction of components 1 and 2

$\eta_{1,2}$  = viscosity of component 1 and 2

The above relationship assumes that both the polymers deform elastically and their Poisson's ratios are equal. For binary blends there are three distinct groups<sup>94</sup>, as stated previously:-

- i) Positive deviation blends;
- ii) Negative deviation blends; and
- iii) Positive-Negative deviation blends.

For polymer blends showing negative deviation from equation 5.1, both separation and limited miscibility at low concentrations would be expected. Immiscible blends usually have properties less than predicted by equation 5.1 due to the poor interphase adhesion, whereas partly miscible blends have been shown to exhibit mechanical properties close to equation 5.1.

Utracki stated in his paper<sup>94</sup> that a low concentration of one polymer in another resulted in the coil volume of the matrix polymer decreasing, which in turn lowers the frequency of entanglements and the viscosity of the blend. The change in free volume (below the additivity line) is

one method of explaining the lowering of viscosity. However from literature studied by the author there is no tangible evidence to suggest the validity of the mixing rules for even miscible systems. Data for immiscible systems are at best sparse, due to the inability to predict the blend morphology essential to derive a constitutive equation.

Blends showing positive deviation behaviour are either heterogeneous or emulsion-like immiscible blends. The blends in this study do not fall into either of these categories and so positive deviation behaviour will not be discussed.

To summarise, for blends in which there is a potential degree of compatibility at low concentrations (in the metastable region of the phase diagram), there is a correlation between thermodynamics and flow. As the phase behaviour, rheology and morphology are closely linked, the control of flow should give a tailor-made morphology. It is hoped to show how processing variables can lead to a desired morphology. The author will attempt to model the behaviour in a later section to show how the velocity flow profile in the die affects the resultant morphology. The results of this modelling can be seen in a later section.

### 6.1 COMPONENT POLYMERS

The materials used in the current study consisted of two conventional thermoplastic polymers, polyethersulphone (PES) and polycarbonate (PC). The monomer units for both of these polymers can be seen in the key at the beginning of the thesis. Both the PES (3600G grade) and PC (LEXAN) were provided in a granular form. The PES was supplied by I.C.I. and the PC was purchased from G.E.C.

PES is a transparent yellow polymer with good long term thermal ageing resistance and low smoke emission. It also has reasonable resistance to ionizing radiation and aliphatic hydrocarbons, with a high continuous use temperature (180°C). PES has the disadvantage that it is expensive, requires high processing temperatures (320-380°C) and mouldings may contain higher levels of residual stress than more easily processed materials. Applications for PES include electrical components e.g. circuit boards, bobbins, lamp holders and lenses. PES is also used in medical and agricultural components requiring repeated sterilisation.

PC is a transparent polymer with high impact resistance at room temperature down to -40°C. PC has a reasonably high continuous use temperature (115°C), an intermediate temperature processing range (280-320°C) with

low creep and mould shrinkage. PC has the disadvantage that it has poor barrier properties and it is susceptible to attack from organic solvents, acids and alkalis. PC suffers from hydrolysis at temperatures above 70°C, with low fatigue properties, wear resistance and a high melt viscosity. Applications for PC include safety shields, goggles, lenses, and glazing panels (including bullet proof glazing). Other applications include kitchenware, tableware and medical components (sterilisable).

The LCP's used were VICTREX SRP1500G provided by I.C.I. and VECTRA B900 purchased from Celanese. VECTRA B900 is based on hydroxybenzoic acid (HBA) and hydroxynaphthoic acid (HNA). VICTREX SRP1500G is based on HBA, HNA, isophthalic acid (IA) and terephthalic acid (TA). All of these monomer units can be seen at the beginning of the thesis.

## 6.2 BLEND PREPARATION

Blends were produced with a range of liquid crystal polymer compositions 0%, 2%, 4%, 6%, 8%, 10%, 15%, 20%, 25% (by mass) mixed with PC and PES, giving four blend combinations. A primary consideration when producing polymer blends is that the materials should have overlapping processing temperatures. At the temperature used for testing, both of the materials should be fluid. The temperature must also be lower than the degradation temperature of the polymer, otherwise a major change in the

rheological properties will result.

#### 6.2.1 BLENDS PREPARED AT SHEFFIELD HALLAM UNIVERSITY

The blends were produced by adding the two component polymers together in a granular form. Relative amounts of the two polymers were weighed out using an electric pan balance and the mix was then physically agitated until a good mix was achieved. The blends were mixed on the basis of weight with a 5% blend containing 5mass% LCP within 95mass% PES/PC with each blend mix weighing approximately 1kg. These figures can be seen below (see table 6.1). This table shows the standard test percentages compared with the actual blend composition.

% LCP	PES/SRP	PES/VECTRA	PC/SRP	PC/VECTRA
2	1.97	2.00	2.01	2.03
4	3.99	4.04	4.01	3.98
6	6.01	6.03	6.02	5.98
8	8.00	8.01	8.03	8.03
10	9.99	10.03	9.97	10.01
15	14.98	14.97	14.96	14.99
20	20.02	19.96	20.00	20.01
25	24.96	24.99	24.97	25.05

TABLE 6.1 - To show the difference between stated % composition used in the thesis and the actual % tested for PES/PC blends.

The pre-mixed blends were then placed on steel trays of dimension 40mm x 30mm x 2mm and spread evenly to a depth of 1.5mm. The trays were placed in a Baird and Tatlock air circulating oven and dried overnight at 130°C. The

following morning the trays were removed from the oven and the mixed granules were placed in the hopper of a single screw extruder, with the heating zones set to appropriate temperatures for the matrix material (see tables 6.2 and 6.3).

HOPPER	REAR	CENTRE	FRONT	DIE
-	310°C	320°C	320°C	330°C

TABLE 6.2 - Temperature settings for the four heating zones of the single screw extruder used in the processing of PES/LCP blends.

HOPPER	REAR	CENTRE	FRONT	DIE
-	260°C	260°C	280°C	290°C

TABLE 6.3 - Temperature settings for the four heating zones of the single screw extruder used in the processing of PC/LCP blends.

Prior to the loading of the hopper pure PC (for the PC blends) and PES (for the PES blends) were fed through the extruder for a period of approximately 5 minutes, to purge the barrel in an attempt to remove any unwanted contaminants. After the barrel had been purged the 2% LCP blend was added and after 2 minutes (to allow the barrel to clear of the initial cleansing polymer) samples of the resultant extrudate were cut into 30 mm strips and collected on a metal tray in an attempt to reduce contamination. Once all of the material had been passed through the barrel, the extrudate was processed in a rotary granulator. The resultant 'chips' were collected and placed

back into the hopper of the single screw extruder. The blends were processed twice through the single screw extruder because of poor mixing within the barrel as mentioned previously in the review (the author is aware that the dual processing operation could lead to different rheological properties compared to the blends prepared using a twin screw extruder. This procedure was carried out over the range of compositions starting with the 2% composition and finishing with the 25% composition (so that a pocket of high composition material possibly held within a dead zone within the barrel could not drastically change the composition of a lower composition blend). A period of approximately five minutes was allowed between consecutive runs to allow the new composition to percolate the barrel. Once the blend had been processed twice through the extruder and granulator, the chips were placed in a bag and sealed ready for testing. The author is aware that VICTREX SRP grades absorb up to 0.2 % w/w of atmospheric moisture even under sealed storage<sup>77</sup>. The four 'pure' standards were also processed in this manner so that they had the same thermal history as the blends.

#### 6.2.2 BLENDS PRODUCED AT I.C.I. WILTON

The PES/Glass fibre/SRP1 blends were produced at I.C.I Wilton. The component granules were mixed together as described previously in the following compositions 80% PES, 72% PES, 68% PES and 64% PES with 20% glass fibres, the balance being SRP1500G. Once mixed the blends were dried

overnight at 120°C. Before moulding the blends were pre-dried for 3-4 hours at 150°C and then fed into a ZSK-30 type co-rotating twin screw extruder. Once processed the resultant blends were chipped and bagged ready for rheological testing in a Rosand Capillary Rheometer.

### 6.3 DAVENPORT CAPILLARY RHEOMETER

The Davenport Capillary Rheometer incorporates a heated barrel (21.92mm -internal bore) and a piston, which was used to compress the blend through a die (1mm - diameter by 20mm - long). The die was held in place at the end of the barrel by a threaded nut. Both the pressure transducer (10,000 p.s.i. situated just above the die in the barrel) and the piston motor (via an analogue/digital convertor) were connected to a BBC microcomputer. The computer controlled the shear rate and also measured the pressure at the entrance to the die by means of a 10,000 p.s.i mercury transducer. The program then took a burst of 100 readings over a second, when two sets of consecutive data correlated within a set tolerance the data was accepted and the program increased the speed of the piston in a series of steps until all of the data sets had been recorded. The piston speed settings varied from 2.4 - 24 cm/minute and was controlled by the software. The shear rate ( $\dot{\gamma}$ ) was then be calculated using the following equation :-

$$\dot{\gamma} = \frac{4Q}{\pi R_0^3} \quad (6.1)$$

where :-

$Q$  = volumetric flow rate ( $\text{m}^3\text{s}^{-1}$ )

$R_0$  = capillary radius (m)

At the lower speed of 2.4 cm/minute the volumetric flow rate was  $1.5 \times 10^{-7}$  ( $\text{m}^3\text{s}^{-1}$ ) with the shear rate ( $\dot{\gamma}$ ) being approximately 1500 ( $\text{s}^{-1}$ ). At the higher shear rate of 24 cm/minute the volumetric flow rate was  $1.5 \times 10^{-6}$  ( $\text{m}^3\text{s}^{-1}$ ) with the shear rate ( $\dot{\gamma}$ ) being approximately 15000 ( $\text{s}^{-1}$ ). It was not possible to obtain readings at the maximum speed as the barrel emptied very quickly, hence the maximum speed used was 12 cm/minute.

The dual processed chips were dried as previously stated (overnight at  $130^\circ\text{C}$ ) and then placed in the capillary barrel. The piston (see figure 4.5) was used to compact the chips after which more chips were added to give sufficient material in the barrel to obtain a full set of data points over the entire range of piston speeds. The compacted material was then allowed to soak for a pre-set period of time (10 minutes) to allow the polymer in the barrel to achieve a uniform temperature across its section (to within  $\pm 0.5^\circ\text{C}$ ). The soak time was controlled by the computer program making the whole testing process automatic. After the polymer was at temperature the piston was brought down, with the speed increasing in a stepped fashion, forcing the polymer through the long die.

After the run was completed the barrel was emptied and cleaned out. The cleaned barrel was then refilled in a manner as described previously and allowed to soak, after which time the procedure was repeated using a zero length die. Subtraction of the zero length from the long die data two runs allowed the pressure difference (equation 4.12) and the wall shear stress to be calculated.

#### 6.4 ROSAND CAPILLARY RHEOMETER

The Rosand Capillary Rheometer incorporated two heated barrels (15mm -internal bore) with two dies (long die 1mm x 16mm and a zero length die). A 10,000 p.s.i. transducer was situated above the long die and a 1500 p.s.i transducer was situated above the zero length die. The piston speed settings were varied from 0.2 - 30 cm/minute automatically controlled by the rheometer. The two barrels allow the readings to be taken simultaneously and only required one run to calculate the pressure difference.

At the lower speed of 0.2 cm/minute the volumetric flow rate was  $8 \times 10^{-9}$  ( $\text{m}^3\text{s}^{-1}$ ) with the shear rate ( $\dot{\gamma}$ ) being 80 ( $\text{s}^{-1}$ ), at the higher shear rate of 30 cm/minute the volumetric flow rate was  $1.2 \times 10^{-6}$  ( $\text{m}^3\text{s}^{-1}$ ) with the shear rate ( $\dot{\gamma}$ ) being 12000 ( $\text{s}^{-1}$ ). The results were plotted in a similar fashion to the Davenport capillary data.

#### 6.5 COLLECTION AND STUDY OF CAPILLARY EXTRUDATES

Extrudates of the four blends were collected for

further investigation. The Davenport Capillary Rheometer was run at various temperatures and shear rates. The extrudates from each run were collected on a sheet of card to minimise extensional effects due to gravity, left to air cool and then set in a low temperature mount. The mounts were ground and polished down to a 0.25 $\mu$ m finish. The polished samples were then studied using both optical and electron microscopy. Additional work was carried out on the PC/LCP blends; the extrudates were collected by the previous method and placed in phials containing 1,1,1-trichloroethane for 24 hours at room temperature. The trichloroethane softened the PC matrix sufficiently, that if a small tensile force was applied to either end of the extrudate, the extrudate split revealing the internal cross section containing whole LCP fibres. The softened extrudates were placed on aluminium stubs (1cm in diameter) using a conductive quick drying silver paint (silver dag). After the dag had dried the extrudate samples were placed in a Polaron SEM 5100 platinum coating unit where the surface was made conductive. The coating cell was evacuated to 0.02 torr and argon was then bled into the cell until a constant voltage of 25 mv was achieved across the cell. The unit ran for 1.5 minutes and coated the sample with approximately 0.1 to 0.2 nm of platinum.

The sample preparation was exactly the same for the injection moulded test bars fractured on the tensometer. It was felt that the ability of the electron microscope to

detail topographical effects would render a superior image.

## 6.6 SCANNING ELECTRON MICROSCOPY

A Joel JXA-840A and a Philips P500 were used for the electron microscopy. Both units use a link analytical system (EDAX) which can detect the elements from nitrogen to uranium, using either windowless or a thin beryllium window.

### 6.6.1 SAMPLE LOADING

Before the specimen could be added to the viewing chamber the filament current was reduced to a minimum (to prevent damage to the filament). The high tension control in the optic control unit was switched off at this point and air could then be admitted to the chamber. The platform upon which the sample was held could be removed and the aluminium stub containing the sample was fixed in place. Once the sample was firmly secured the chamber was closed, the air release mechanism was closed and the chamber was evacuated. The electron optic control unit was turned on and the filament current was increased until an image was obtained on the visual display unit.

### 6.6.2 EDAX SCANNING

PES contains sulphur, which is not present in any of the LCP monomer units. Three injection moulded bars were produced in the manner described earlier; one bar was of pure PES; one bar was pure VICTREX SRP1 and the third was

composed of 25 mass% VICTREX SRP1 in 75 mass% PES. The PES and LCP bars were forced together and mounted in a low temperature curing resin. The mount was polished to a 25 $\mu$ m finish, coated in platinum (as described earlier) and placed in the electron microscope. The EDAX unit was then set to scan the boundary between the two mouldings using a sulphur fingerprint (calibrated on a pure sulphur standard). The electron microscope was used to scan for sulphur in both the pure polymer standards and the 25/75% (LCP/PES) samples. Two positions across the 25%/75% VECTRA/PES and one position on the 25%/75% SRP1/PES sections were used. The first location was in the outer skin layers of the VECTRA/PES sample. The second was in the core region of the VECTRA/PES sample. The final sample was taken in the centre of the SRP1/PES moulding.

## 6.7 OPTICAL MICROSCOPY

It was necessary to use both optical and transmission microscopy to obtain images from all of the samples. The transmission microscope gave good results and showed the immiscibility of the two polymers well, when used in conjunction with polarising techniques. The reflection microscopy gave good results on a macroscopic examination of skin/core effects using very highly polished samples. To obtain good images it was necessary to polish the samples to a 0.25  $\mu$ m finish. This presented problems with the relief of the LCP phase leading to particle fallout. This was particularly the case with the longitudinal

sections (see figures 8.1 and 8.2)<sup>136</sup>.

#### 6.7.1 TRANSMITTED LIGHT MICROSCOPY

Two tensile bars were taken, one 25 mass% VECTRA in 75 mass% PES, the other 25 mass% VICTREX SRP1 in 75 mass% PES. The bars were cut at right angles to the flow direction and placed in a micro-tome. A pre-used glass knife was used to trim the surface of the specimen level. Once a flat surface finish was obtained the old knife was changed for a fresh glass knife with a new edge. This knife was then used to shave 3  $\mu\text{m}$  slivers from the surface. One of these slivers was placed on a slide (pre-washed and dusted). A cover slide was also dusted and cleaned with a sharp blade to remove any surface particles. A drop of oil (hydrogenated terphenyl 1-bromo naphthalene) with a refractive index of 1.648, similar to PES, was then placed on top of the sliver. The sliver was then cut to size using a scalpel and the cover slide was carefully lowered one edge first (in an attempt to avoid the entrapment of air bubbles) until it sandwiched the sample. The cover slide was then sealed air tight on to the slide using arabic gum. Once both of the samples had been prepared they were placed in an Olympus Vanox transmission microscope between cross polars.

#### 6.7.2 REFLECTED LIGHT MICROSCOPY

An Olympus Vanox-T microscope was used for the reflected light microscopy. The extrudates were collected

and cut to size and placed in a low temperature setting resin, (to keep any thermal distortions or relaxation to a minimum) and allowed to cure. The mount containing the extrudate was initially polished using a 240 carbide paper down through 320, 400 to a 600 grade, rotating through 90° at each stage so that the scratches made by the previous paper were removed. Once the sample only contained 600 grade surface scores, the mount was washed in acetone and transferred to polishing wheels covered in different grades of diamond polish from 6µm through to 0.25µm. The mount was washed and cleaned between each polishing operation before it was placed on the next wheel to avoid cross contamination. Once the process had been completed the mount was placed on a glass slide levelled using a mounting press. The samples were photographed using a 35mm camera mounted on the microscope. A selection of pictures taken using this technique can be seen in the results section (see figures 8.1-8.3, 8.7, 8.8, 8.10 and 8.11).

#### 6.8 DIFFERENTIAL SCANNING CALORIMETRY

A Mettler TA3000 controller was used in conjunction with a Mettler DSC 30 cell. All analysis runs were carried out from room temperature to 350°C using a heating rate of 10°C minute<sup>-1</sup>.

Small pieces of the four base polymers were placed in small pre-weighed aluminium crucibles. The lid was placed on top and crimped using the Mettler tool. The crucible was

then again weighed to determine the weight of polymer within the crucible. The crucible was placed in the DSC cell along with a reference crucible and the material was heated from room temperature to 320°C (PC) and 350°C (PES), at a rate increase of 10°C per minute, to dry the samples fully. Once at temperature the samples were then cooled at 10°C minute<sup>-1</sup> to room temperature before the sample run was started. This allowed good thermal contact between the polymer and the pan. All of the analysis runs were carried out at 10°C per minute . The DSC unit was equipped with an electronic device which used an integrator method to calculate the number of calories or joules, corresponding to a particular transition. The output from the unit came in the form of a printout and using the data it was possible to identify the nematic transition points of the liquid crystal polymers and the glass transition of the PES/PC.

#### 6.9 INJECTION MOULDING OF POLYMER BLENDS

The blends were pre-dried as mentioned above before processing and then injection moulded into tensile and impact bars. The processing temperatures used were (see Tables 6.4 and 6.5).

HOPPER	REAR	CENTRE	FRONT	DIE
-	310°C	330°C	330°C	340°C

TABLE 6.4 - Processing temperatures used to produce the PES/LCP blend samples for tensile and impact testing.

HOPPER	REAR	CENTRE	FRONT	DIE
-	280°C	300°C	310°C	310°C

TABLE 6.5 - Processing temperatures used to produce the PC/LCP blend samples for tensile and impact testing.

A Betol 1" single screw injection moulding machine was used to process the blend samples. As in the preparation of the blends, the barrel was initially purged using either PC or PES and after a period of 5 minutes, the blends were fed into the hopper using the above temperature setting (see tables 6.4 and 6.5). Production started with the pure standards followed by the low composition blends and onto the higher compositions until finally the 25% LCP blends were processed. The samples were produced using a mould press force was 2000 p.s.i. and the samples were processed at 8000 p.s.i., with a holding pressure of 1200 p.s.i, using a screw speed of 150 r.p.m. If holding pressures of above 1200 p.s.i. were used the bars produced had excessive flash. Short cycle times were used with an injection pressure time of 3 seconds, holding pressure time of 10 seconds and a cooling time of 10 seconds into a mould held at 40°C. A small amount of mould release was required periodically to allow easy removal of the samples.

#### 6.10 TENSILE TESTING OF POLYMER BLENDS

The 'dumbbell' shaped mouldings of dimension 19 cm x 12 mm x 3 mm were produced by injection moulding the

blends. They were subsequently tested on a JJ Tensile Testing Machine No T20K. An 8kN load was used as a full scale deflection for the samples. The samples were placed between two sets of friction gripping jaws and the speed was set at 50 mm/minute (to minimise any creep effects). It was assumed that the ratio of the extension of the equipment to the extension of the polymer sample was negligible. The data *were* graphically represented in the form of a load vs extension plot.

#### 6.11 IMPACT TESTING OF POLYMER BLENDS

The blends containing 4%, 8%, 15% and 25% SRP1/VECTRA in PC were injection moulded into impact bars of dimension 6.4 mm x 6.4 mm x 5 cm, using the temperature settings stated (see table 6.5). The bars were removed from the mould and a 2mm notch was then cut into the moulding, using a triangular section blade (apex 15°). The samples were fractured by impact with a swinging arm (0.25 lb), using a portable Hounsfield impact testing rig. The data *were* displayed in a graph of notched impact strength vs blend composition.

#### 6.12 WATER ABSORPTION TESTS

Injection moulded samples produced as previously stated were measured shortly after production using a top pan electronic balance. The weights were noted and the samples were then placed in a water bath at room temperature and left. At periodic intervals (which increased as the

experiment proceeded), the samples were removed from the bath, quickly dried using a warm air drier and re-weighed. This process was repeated over a number of weeks and the sample weights obtained were plotted against number of days.

## CHAPTER 7: RESULTS

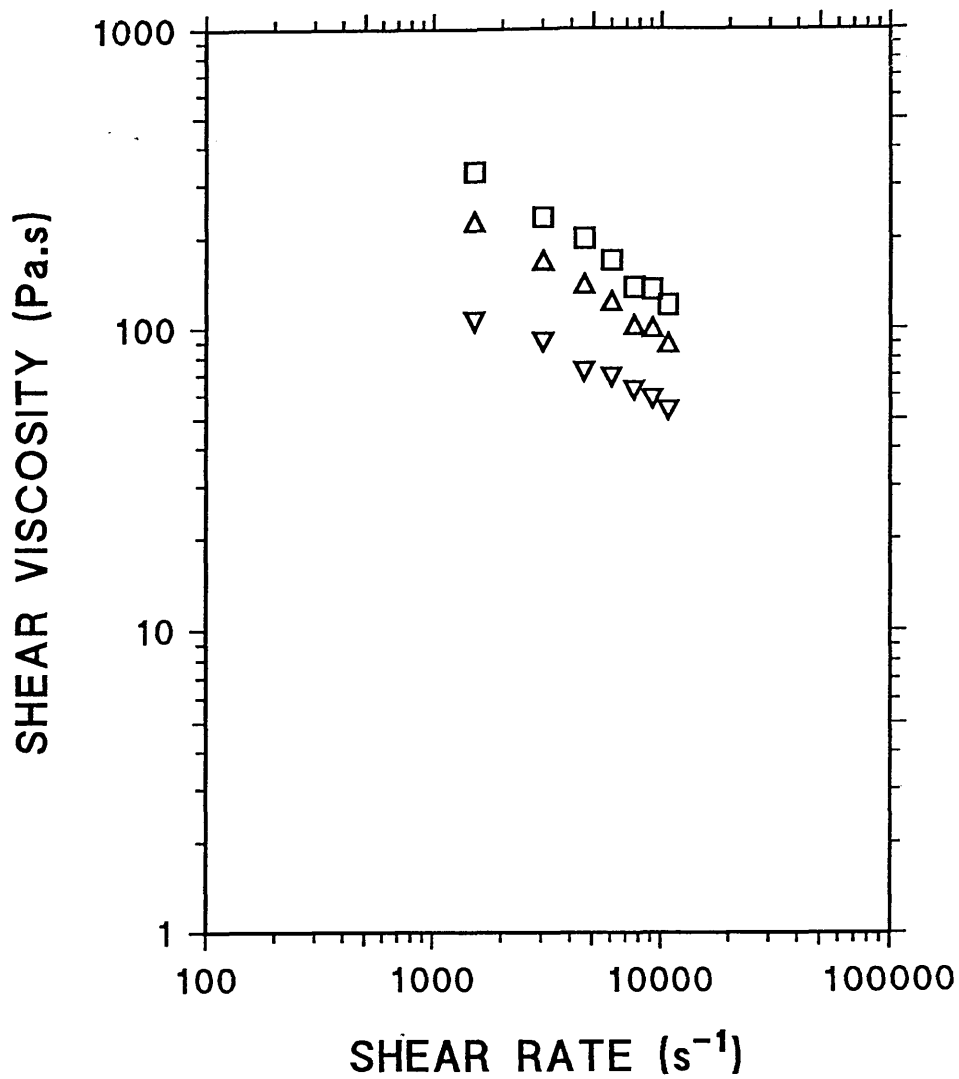
### 7.1 RHEOLOGICAL PROPERTIES OF THE BLENDS

The results split into two main sections, one giving the data obtained from the Davenport Capillary Rheometer and the other being the results obtained from the Rosand Capillary Rheometer.

#### 7.1.1 DAVENPORT CAPILLARY DATA

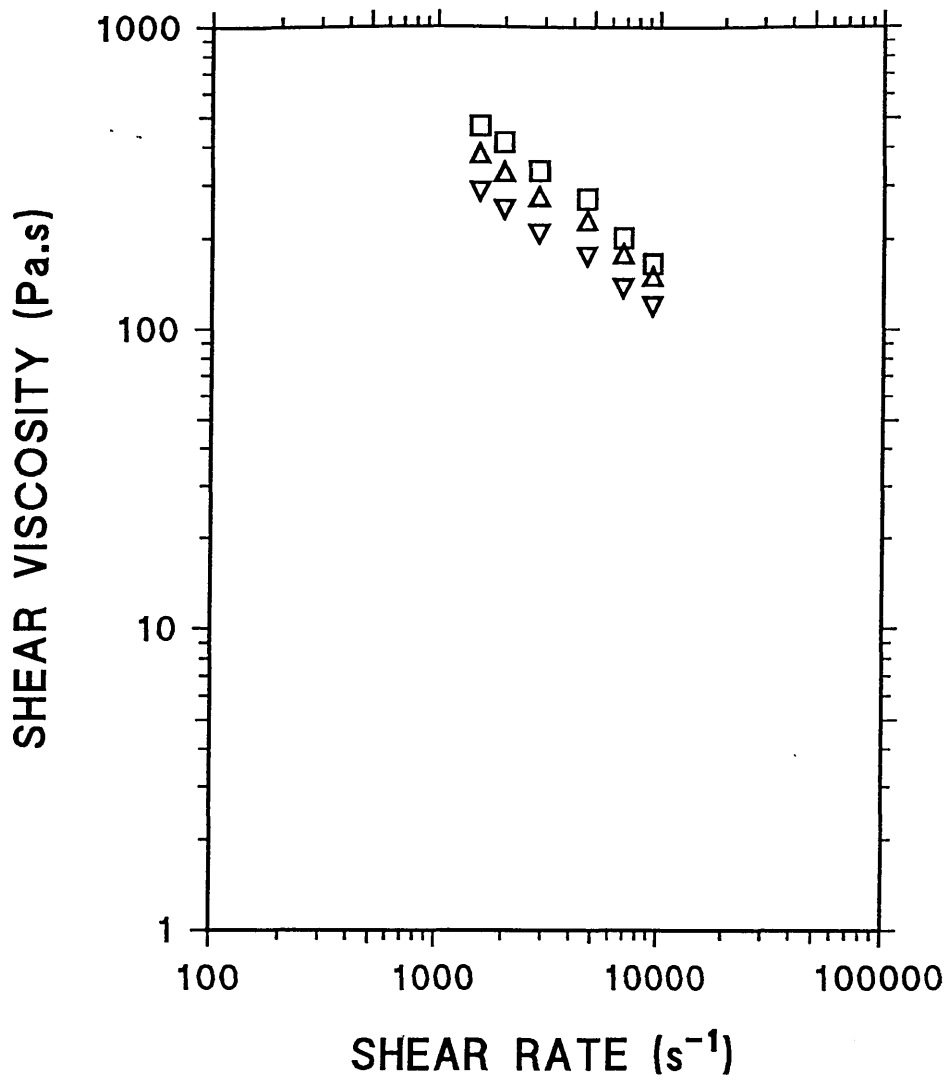
The standard flow curves were obtained over the following temperature ranges:- PC (280°C-320°C), PES (330°C-350°C), SRP1 (300°C-340°C) and VECTRA (280°C-320°C). The tests were carried out on the dual processed standards and the shear rate was calculated using the Rabinowitsch equation (see equation 4.30). The results (see figures 7.1-7.4) are shown in a graph of viscosity plotted against shear rate. Table 7.1 below shows the piston speed of the Davenport Capillary Rheometer with the corresponding extrudate speed and average shear rate.

All of the graphs clearly demonstrate that an increase in temperature reduces the viscosity, as does an increase in the shear rate at a constant temperature. A rise in temperature increases the mobility of the polymer chain, whereas an increase in shear rate induces alignment (even in the amorphous polymers).



KEY -  
 □ - PC AT 280°C  
 △ - PC AT 300°C  
 ▽ - PC AT 320°C

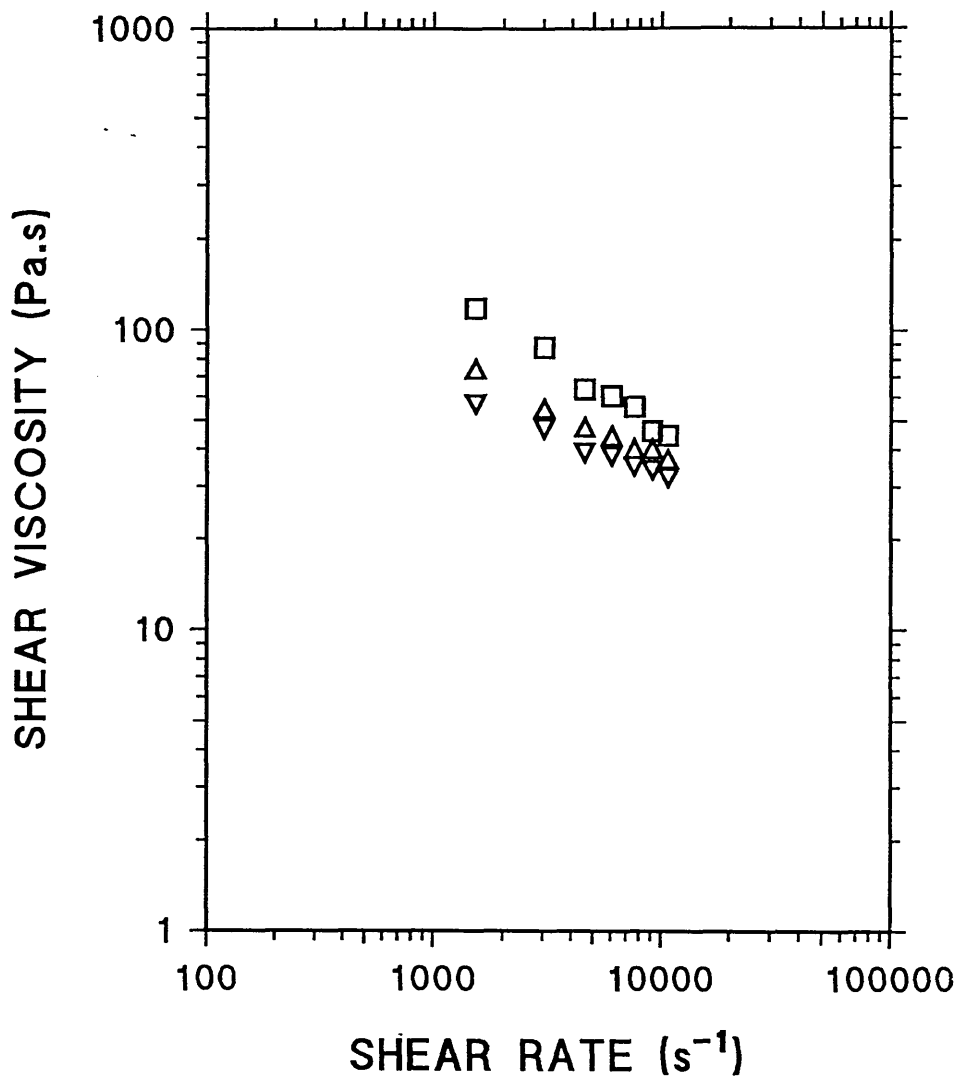
FIGURE 7.1 - Graph of shear viscosity vs shear rate for PC, processed at 280°C, 300°C and 320°C.



KEY -

- - PES AT 330°C
- △ - PES AT 340°C
- ▽ - PES AT 350°C

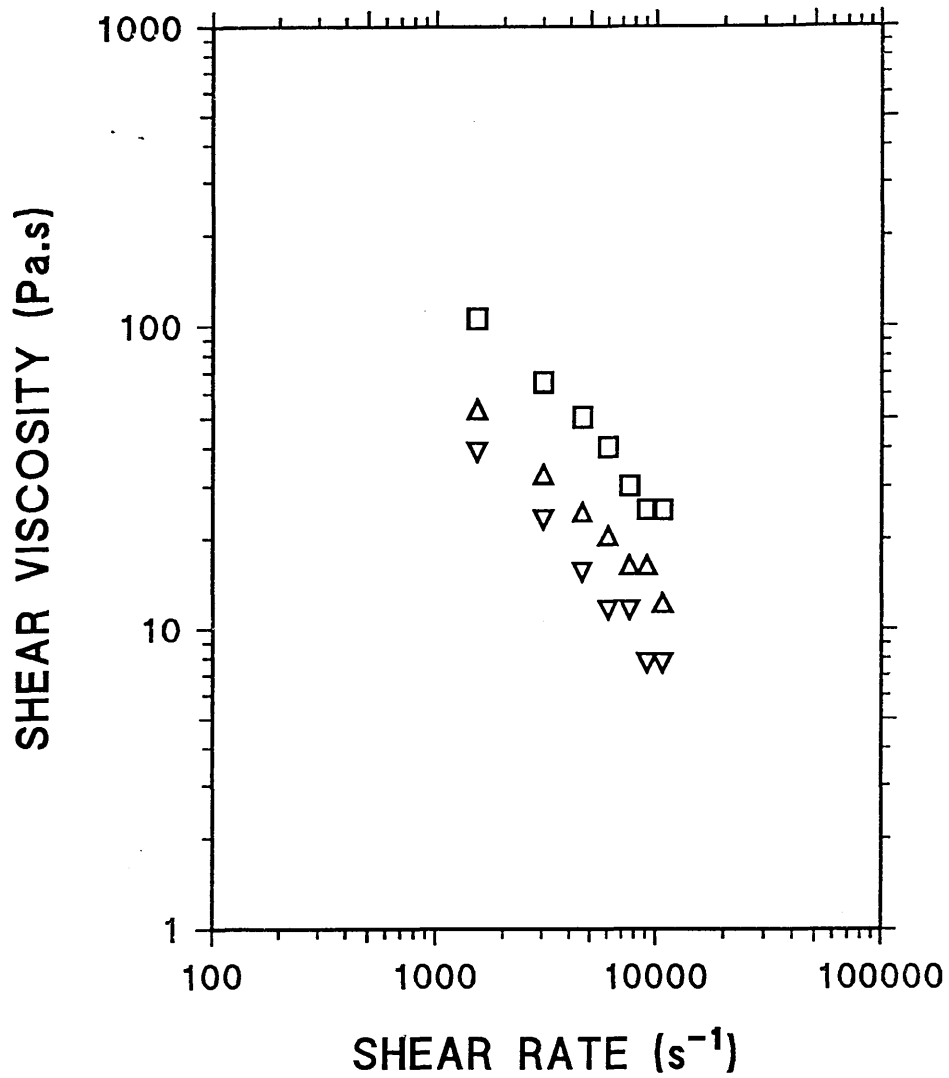
FIGURE 7.2 - Graph of shear viscosity vs shear rate for PES, processed at 330°C, 340°C and 350°C.



KEY -

- - VECTRA AT 280°C
- Δ - VECTRA AT 300°C
- ▽ - VECTRA AT 320°C

FIGURE 7.3 - Graph of shear viscosity vs shear rate for VECTRA, processed at 280°C, 300°C and 320°C.



KEY -

- - SRP1 AT 300°C
- △ - SRP1 AT 320°C
- ▽ - SRP1 AT 340°C

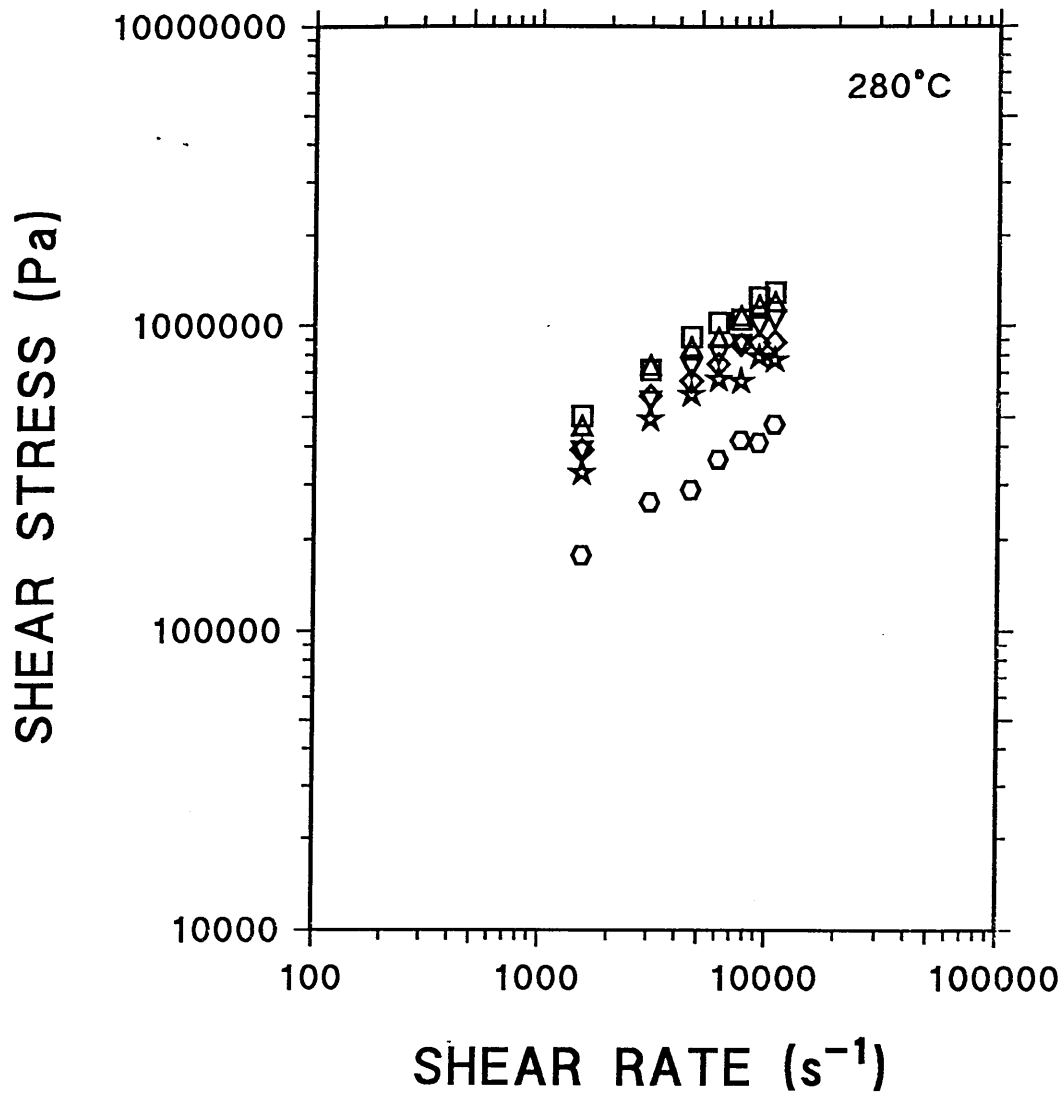
FIGURE 7.4 - Graph of shear viscosity vs shear rate for SRP1, processed at 300°C, 320°C and 340°C.

PISTON SPEED (cm min <sup>-1</sup> )	EXTRUDATE SPEED (ms <sup>-1</sup> )	SHEAR RATE (s <sup>-1</sup> )
2.4	0.1922	1500
4.8	0.3844	3000
7.2	0.5766	4500
9.6	0.7688	6000
12.0	0.9610	7500
14.4	1.1532	9000

TABLE 7.1 - Table to show the various piston speeds used and the corresponding average extrudate speed and shear rate, for the Davenport capillary rheometer.

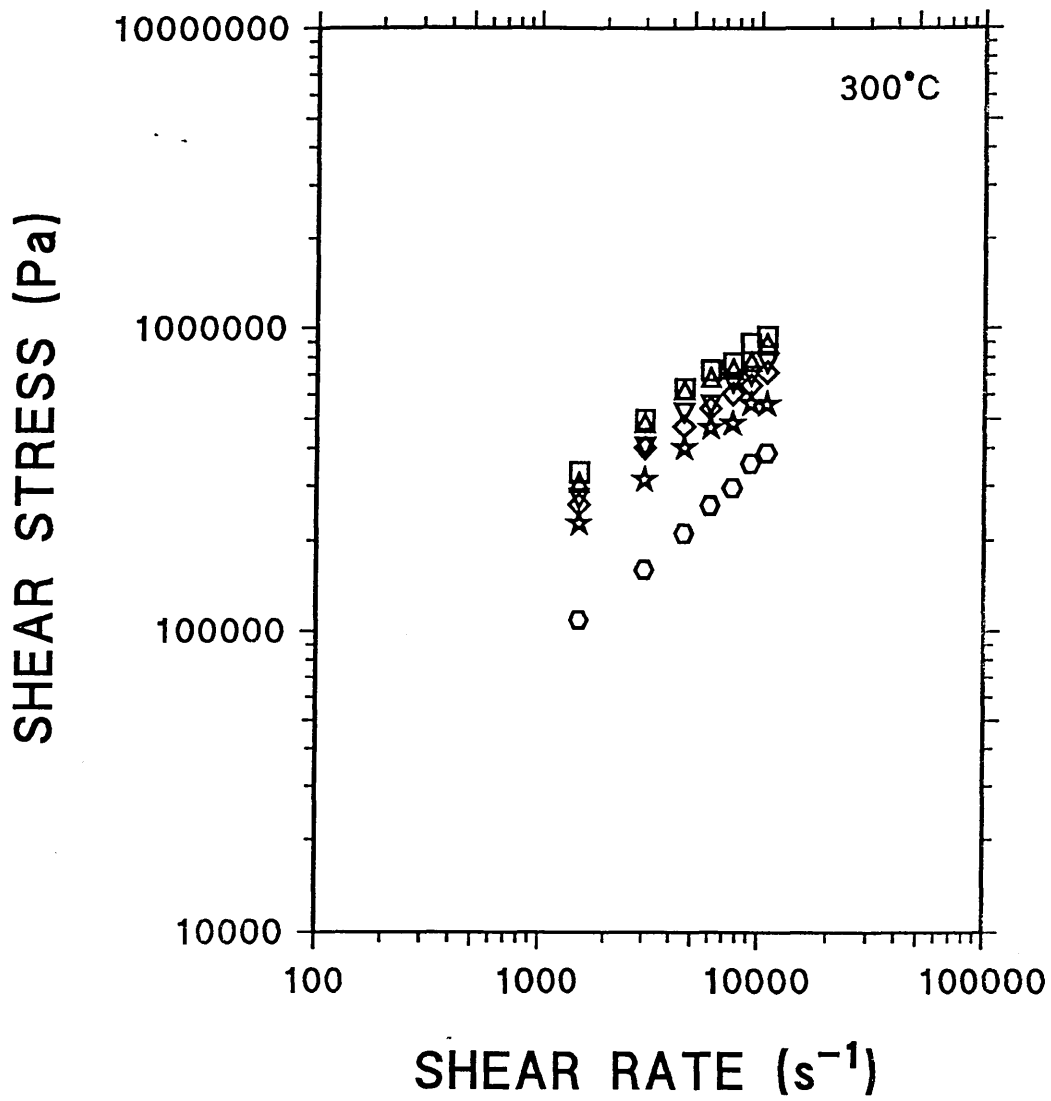
The next graphs (see figures 7.5-7.7) are of shear stress vs shear rate at 280°C, 300°C and 320°C for blends containing 4%, 10%, 15%, 25%, 100% VECTRA in PC. These graphs demonstrate that a small addition of VECTRA can cause a large reduction in viscosity for the resultant PC/VECTRA blend. The reduction of viscosity appears to be proportional to the amount of VECTRA within the blend. There were, however, no signs of a viscosity minimum and the blends behaved in a fairly linear fashion over the entire range of shear rates studied.

The other distinctive feature of these graphs was that the reduction in viscosity for VECTRA 280°C → 300°C was much larger than the corresponding difference for VECTRA 300°C → 320°C. This is due to the nematic transition temperature of the VECTRA ( $T_n$ ). The resultant extrudates of these tests were collected and prepared for optical microscopy as previously detailed. It was interesting to



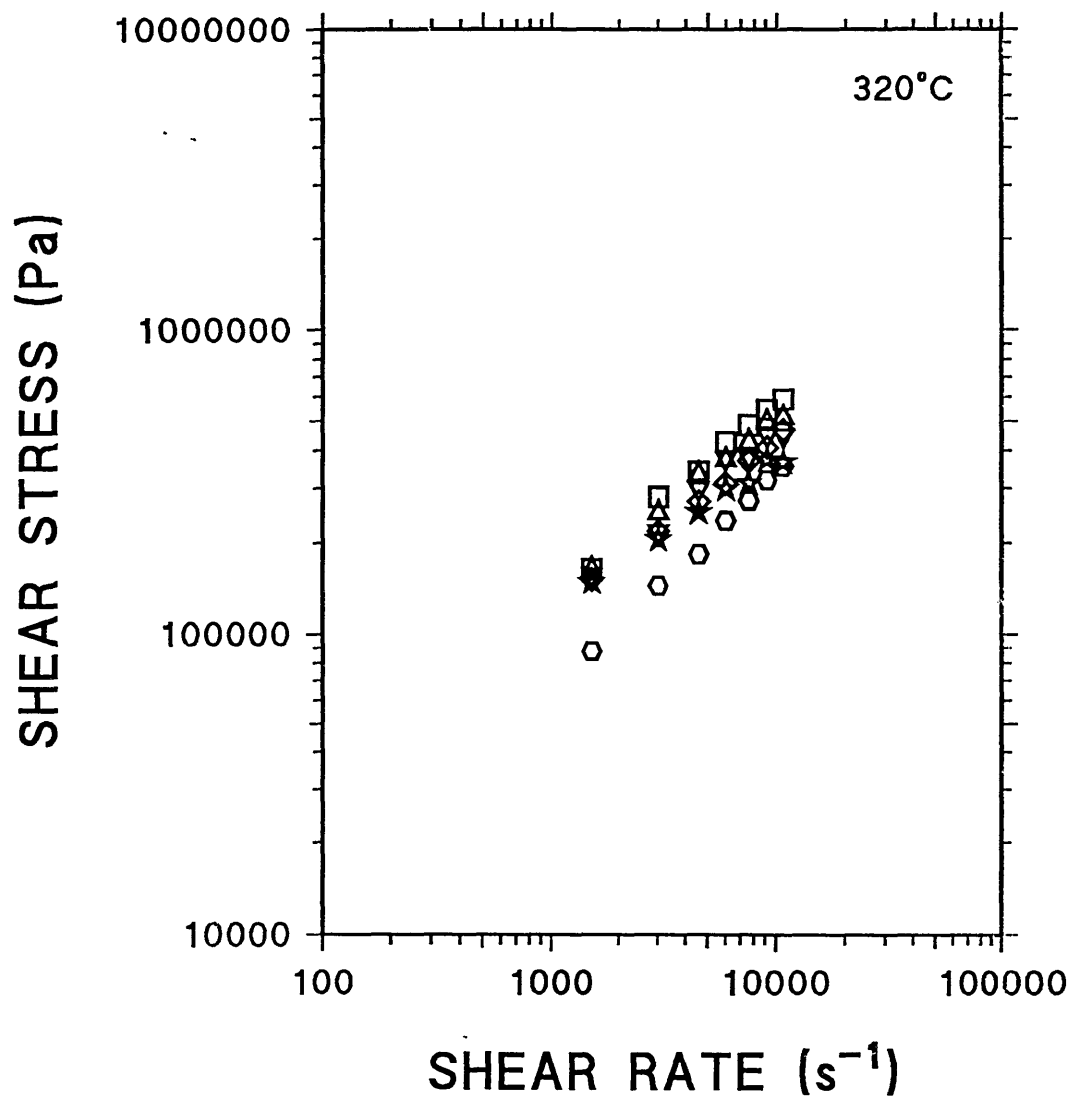
- KEY —
- - PC
  - △ - 4% VECTRA
  - ▽ - 10% VECTRA
  - ◇ - 15% VECTRA
  - ★ - 25% VECTRA
  - - VECTRA

FIGURE 7.5 - Graph of shear stress vs shear rate for PC and blends containing 4%, 10%, 15% and 25% VECTRA processed at 280°C.



- KEY -
- - PC
  - △ - 4% VECTRA
  - ▽ - 10% VECTRA
  - ◇ - 15% VECTRA
  - ★ - 25% VECTRA
  - - VECTRA

FIGURE 7.6 - Graph of shear stress vs shear rate for PC and blends containing 4%, 10%, 15% and 25% VECTRA processed at 300°C.



KEY -

- - PC
- △ - 4% VECTRA
- ▽ - 10% VECTRA
- ◇ - 15% VECTRA
- ★ - 25% VECTRA
- - VECTRA

FIGURE 7.7 - Graph of shear stress vs shear rate for PC and blends containing 4%, 10%, 15% and 25% VECTRA processed at 320°C.

note that the VECTRA/PC blends processed at 280°C (below the nematic transition temperature of the VECTRA), resulted in a dispersion of VECTRA throughout the section of the extrudate. Figure 7.8 is a micrograph of a 20% VECTRA/PC blend in which the VECTRA appeared to form a coarse sub-structure with particles varying in size from  $6.5 \times 10^{-3}$  mm to  $2.5 \times 10^{-2}$  mm in diameter. Samples taken from the same composition (20% VECTRA in PC) but at temperatures 290°C, 300°C and 310°C (see figures 7.9-7.11) samples had more order. At 290°C the onset of a skin/core morphology was noticed which was also visible in the samples taken at 300°C and 310°C. This morphology will be discussed more fully later. These figures clearly show that processing must be above the nematic transition temperature ( $T_n$ ) for the LCP to confer order to the matrix.

The results for SRP1/PC blends are slightly different, (see figures 7.12 and 7.13). The graphs of shear stress vs shear rate show the flow curves of SRP1 in PC at 300°C and 320°C at the compositions mentioned. At 300°C (see figure 7.12) and low shear rates ( $1500 \text{ s}^{-1}$ ) the addition of SRP1 resulted in a small reduction of the blend viscosity. At higher shear rates ( $7500 \text{ s}^{-1}$ ) the reduction was more pronounced, as seen previously; the shear rate at which the blend is processed is an important factor. The second graph (figure 7.13) shows the results at 320°C, which also demonstrate that increasing additions of SRP1 results in a reduction of blend viscosity in an almost linear fashion.

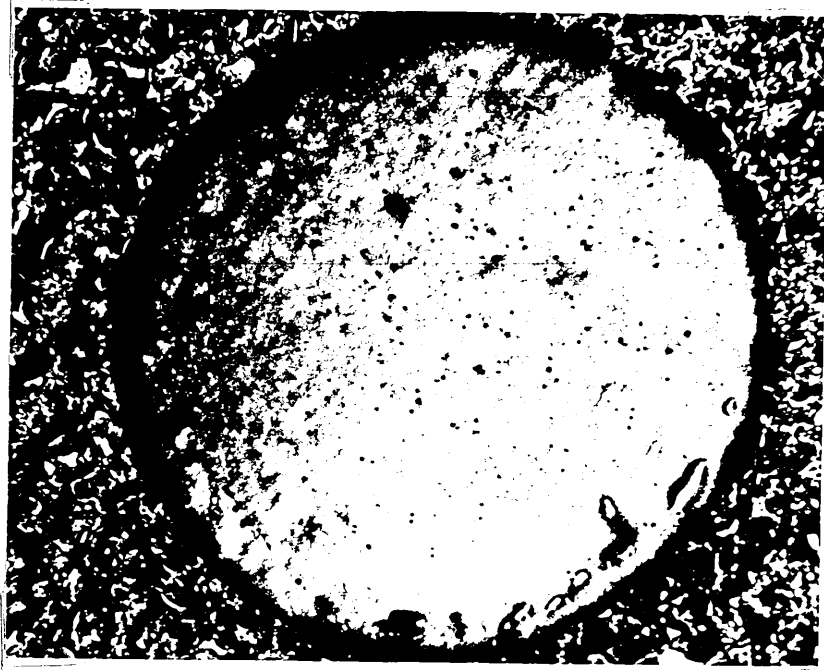


FIGURE 7.8 - Extrudate cross section of a 20% VECTRA/PC processed at 280°C and a shear rate of  $\approx 3200 \text{ s}^{-1}$   
MAGNIFICATION x 75

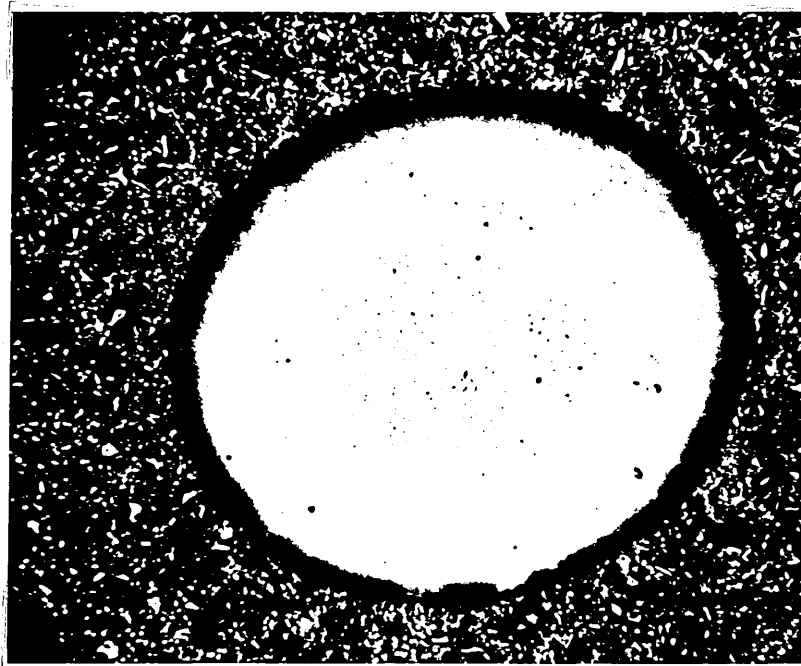


FIGURE 7.9 - Extrudate cross section of a 20% VECTRA/PC processed at 290°C and a shear rate of  $\approx 3200 \text{ s}^{-1}$   
MAGNIFICATION x 75



FIGURE 7.10 - Extrudate cross section of a 20% VECTRA/PC processed at 300°C and a shear rate of  $\approx 3200 \text{ s}^{-1}$   
MAGNIFICATION x 75

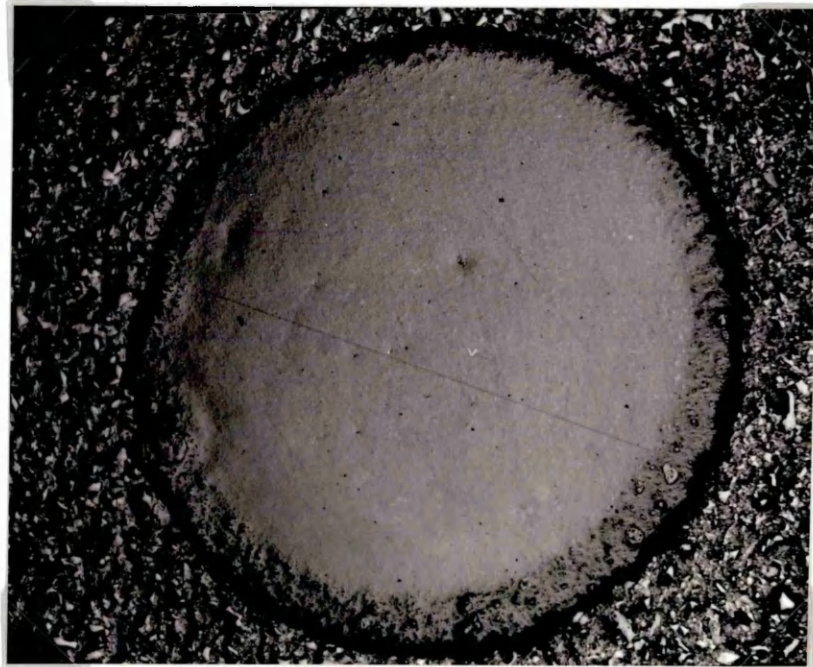
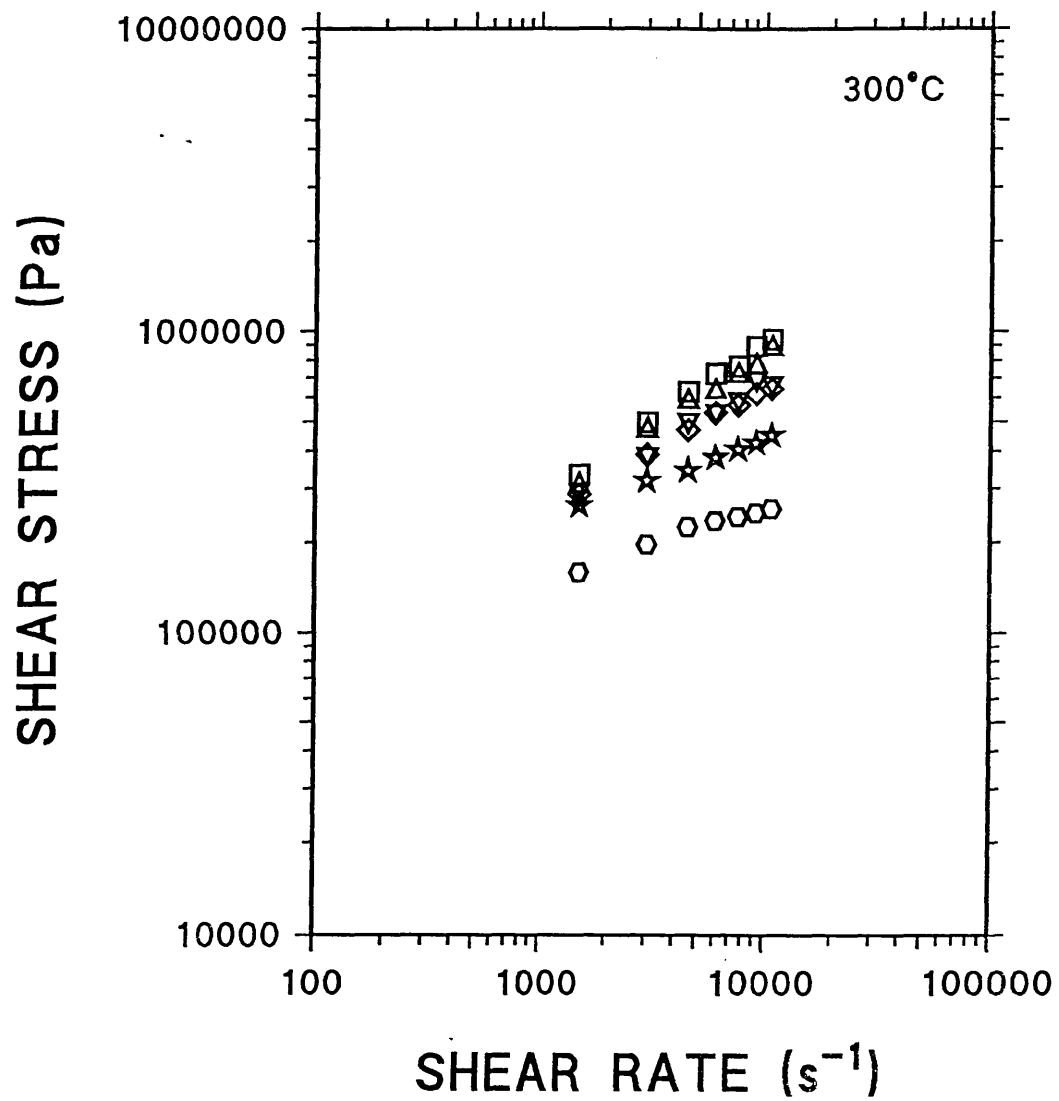


FIGURE 7.11 - Extrudate cross section of a 20% VECTRA/PC processed at 310°C and a shear rate of  $\approx 3200 \text{ s}^{-1}$   
MAGNIFICATION x 75

There is a large drop in the viscosity of SRP1 between 300°C and 320°C. This is attributable to the nematic transition temperature of the SRP1 ( $T_n$ ) and will be discussed more fully later. The rheological data for SRP1 behaved in a linear manner over the entire range of shear rates tested. Processing the SRP1/PC blends above a critical shear rate and temperature resulted in the SRP1 significantly reducing the blend viscosity.

The results obtained for the PES/LCP blends (see figures 7.14-7.16) are shown in graphs of shear stress vs shear rate. The compositions were the same and a temperature range of 330°C - 350°C was used. The curves were again fairly linear: increasing additions of LCP resulted in a viscosity reduction. No viscosity minima were found in any of the previous tests, as cited by other authors in the field<sup>75,76</sup>. The reasons for this and implications will be discussed later. The results obtained are similar to other workers in the field namely Mehta and Isayev<sup>113</sup>, Acierno, Nobile and Marino<sup>114</sup> and Nishimura and Sakai<sup>115</sup>.

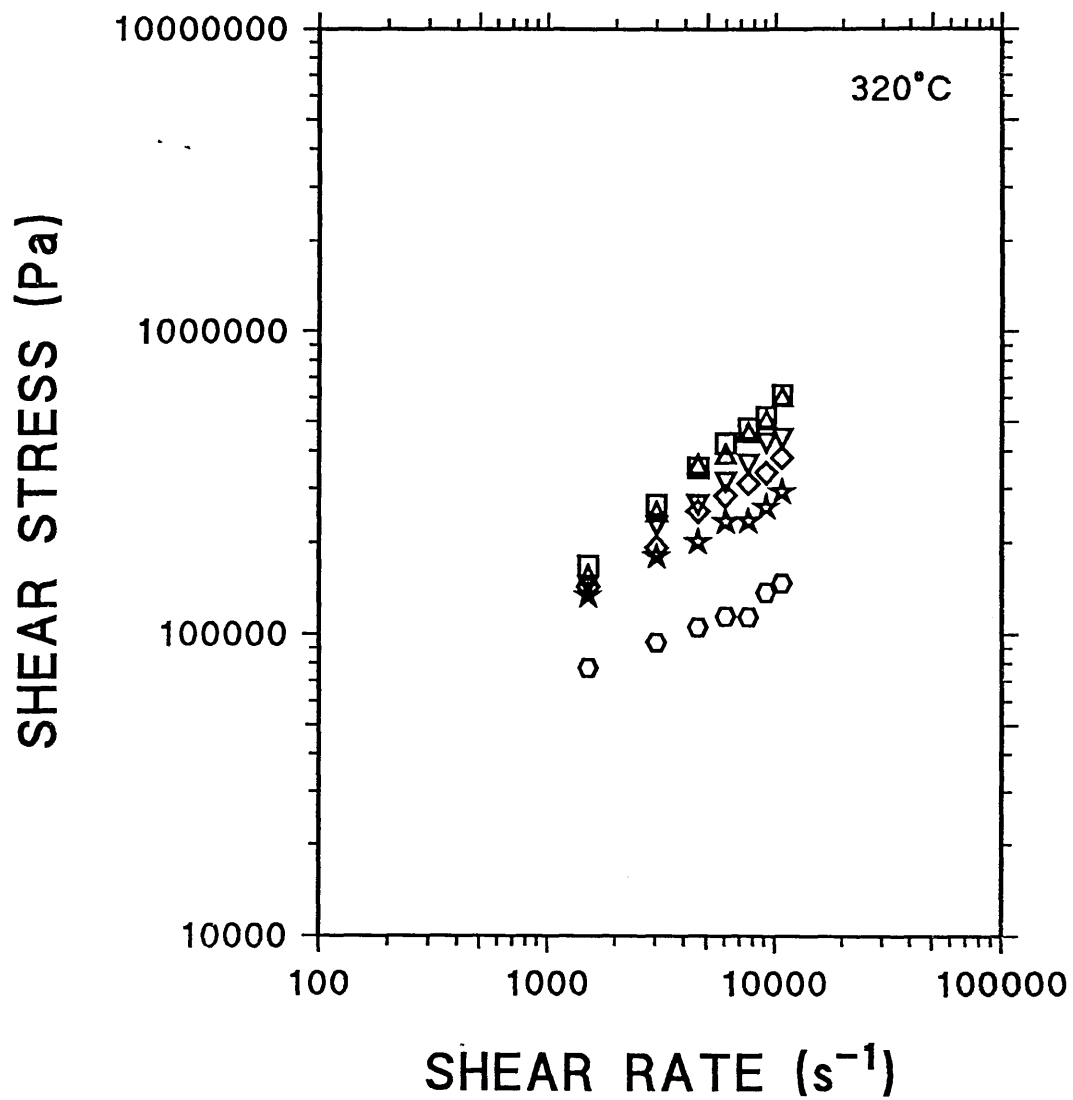
The shear viscosities were taken for all compositions at a mid shear rate (6000/6500 s<sup>-1</sup>) and plotted against composition. These graphs (see figures 7.17-7.20) show negative deviation in all cases. The negative deviation was more pronounced for the PC blends when compared to the PES. The deviation was smaller at low shear rates and increased



KEY -

- - PC
- △ - 4% SRP1
- ▽ - 10% SRP1
- ◇ - 15% SRP1
- ★ - 25% SRP1
- - SRP1

FIGURE 7.12 - Graph of shear stress vs shear rate for PC and blends containing 4%, 10%, 15% and 25% SRP1 processed at 300°C.



KEY -

- - PC
- △ - 4% SRP1
- ▽ - 10% SRP1
- ◇ - 15% SRP1
- ★ - 25% SRP1
- - SRP1

FIGURE 7.13 - Graph of shear stress vs shear rate for PC and blends containing 4%, 10%, 15% and 25% SRP1 processed at 320°C.

with increasing composition. The negative deviation of PC/LCP blends (see figure 7.17) correlates with the results obtained by Nishimura and Sakai<sup>115</sup> for similar processing conditions.

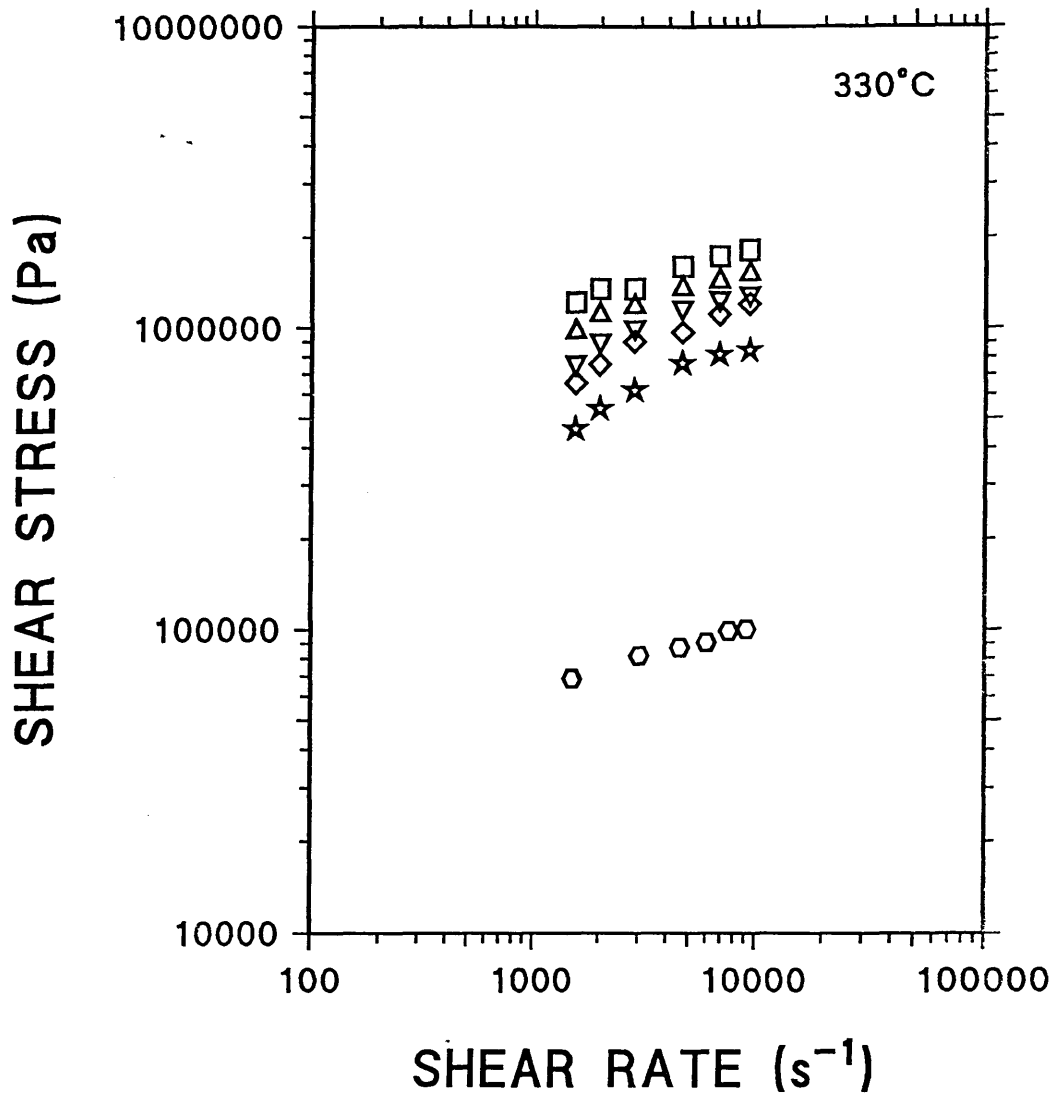
#### 7.1.2 ROSAND CAPILLARY DATA

The blends prepared at I.C.I. Wilton were processed at 350°C and 370°C. The blend composition always contained 20% glass fibres (mass%), with SRP1 making up the difference. The data were plotted in graphs of shear stress vs shear rate (see figures 7.21-7.24). Table 7.2 below shows the piston speeds of the Rosand capillary rheometer and the corresponding extrudate speed and average shear rate.

PISTON SPEED (cm/min)	EXTRUDATE SPEED (m/s)	SHEAR RATE (s <sup>-1</sup> )
0.2	0.0075	80
0.5	0.0187	200
1.0	0.0375	400
2.0	0.0750	800
5.0	0.1875	2000
10.0	0.3750	4000
20.0	0.7500	8000
30.0	1.1250	12000

TABLE 7.2 - Table to show the various piston speeds used and the corresponding average extrudate speed and shear rate, for the Rosand capillary rheometer.

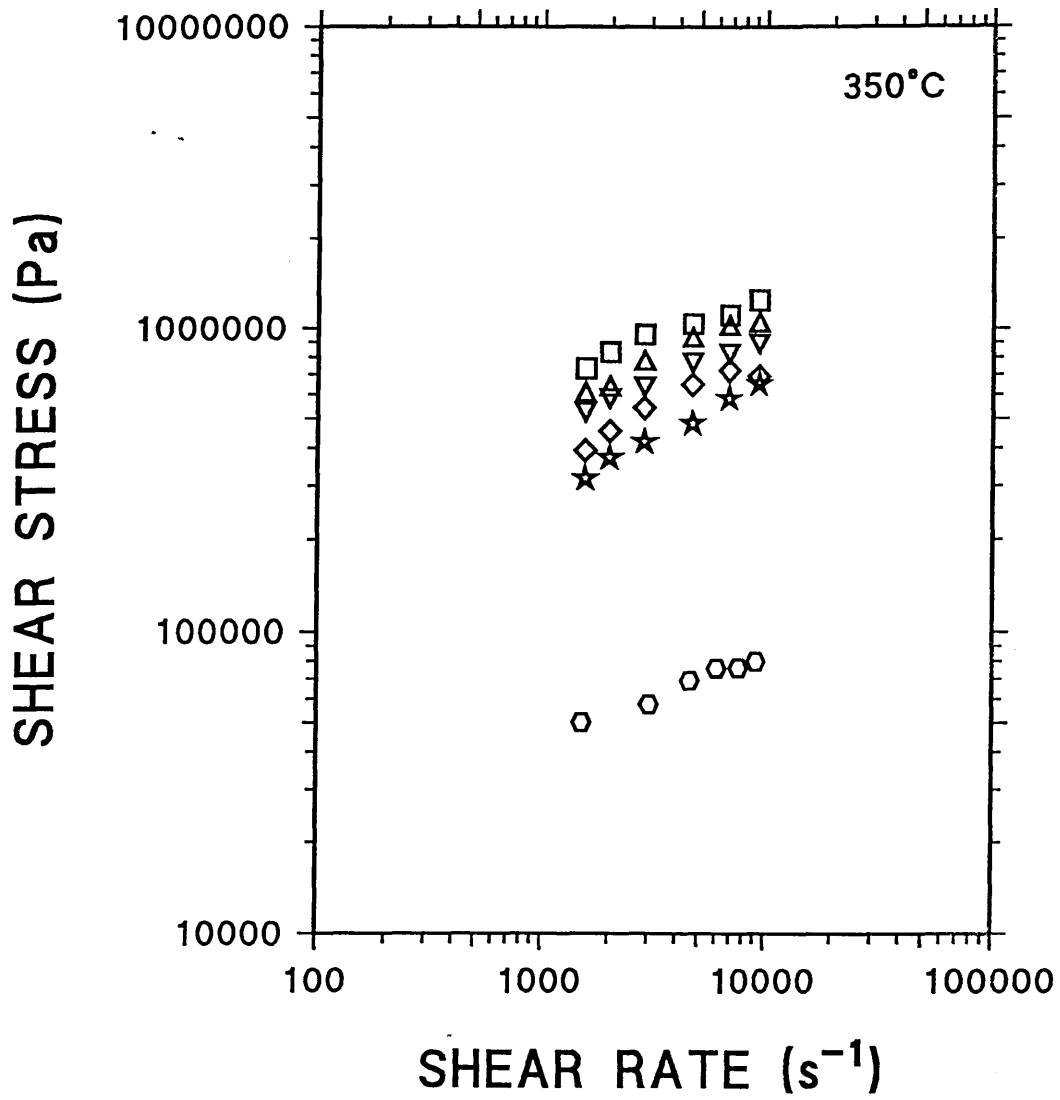
The plots of shear stress vs shear rate and



KEY -

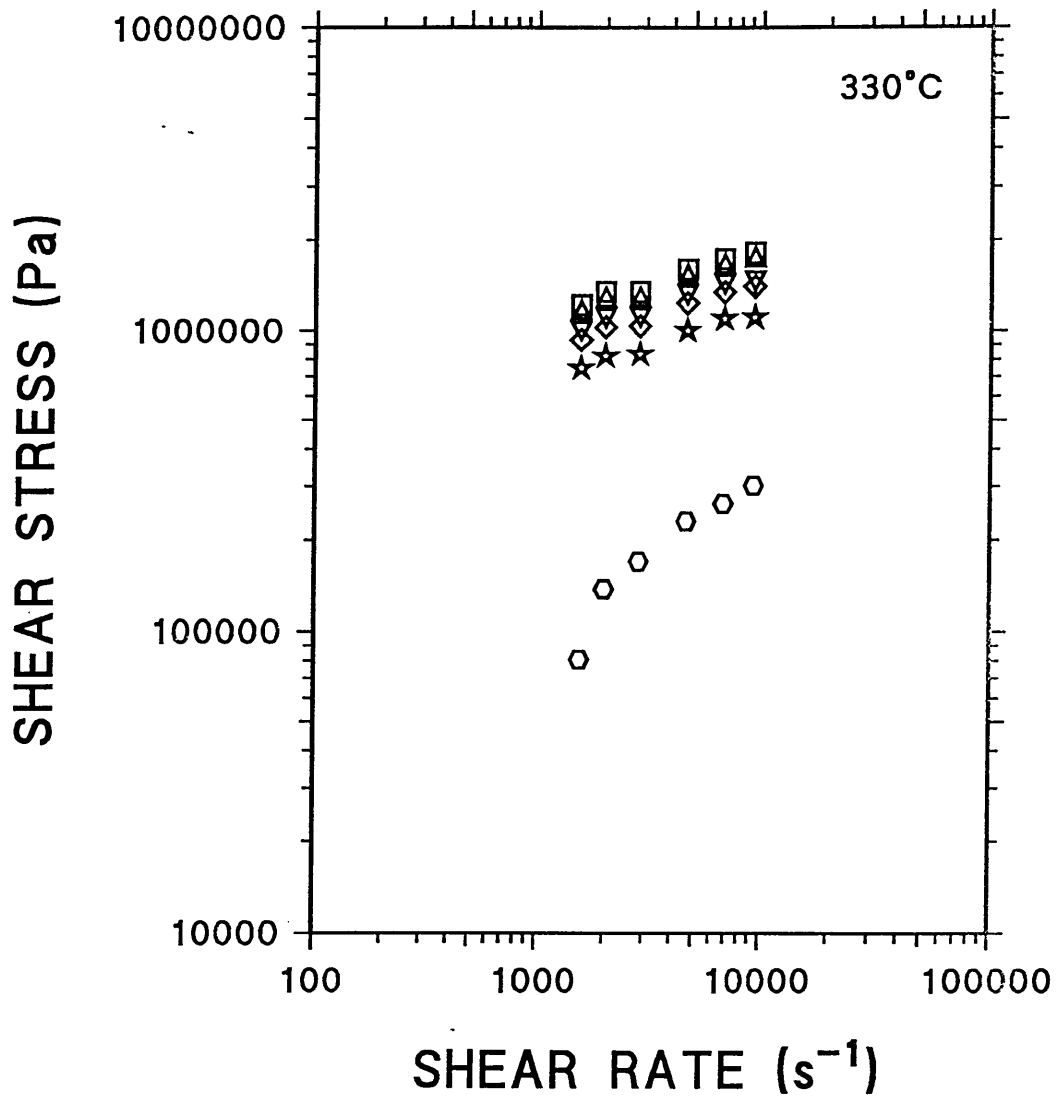
- - PES
- △ - 4% SRP1
- ▽ - 10% SRP1
- ◇ - 15% SRP1
- ★ - 25% SRP1
- - SRP1

FIGURE 7.14 - Graph of shear stress vs shear rate for PES and blends containing 4%, 10%, 15% and 25% SRP1 processed at 330°C.



- KEY -
- - PES
  - △ - 4% SRP1
  - ▽ - 10% SRP1
  - ◇ - 15% SRP1
  - ★ - 25% SRP1
  - - SRP1

FIGURE 7.15 - Graph of shear stress vs shear rate for PES and blends containing 4%, 10%, 15% and 25% SRP1 processed at 350°C.



- KEY -
- - PES
  - △ - 4% VECTRA
  - ▽ - 10% VECTRA
  - ◇ - 15% VECTRA
  - ★ - 25% VECTRA
  - - VECTRA

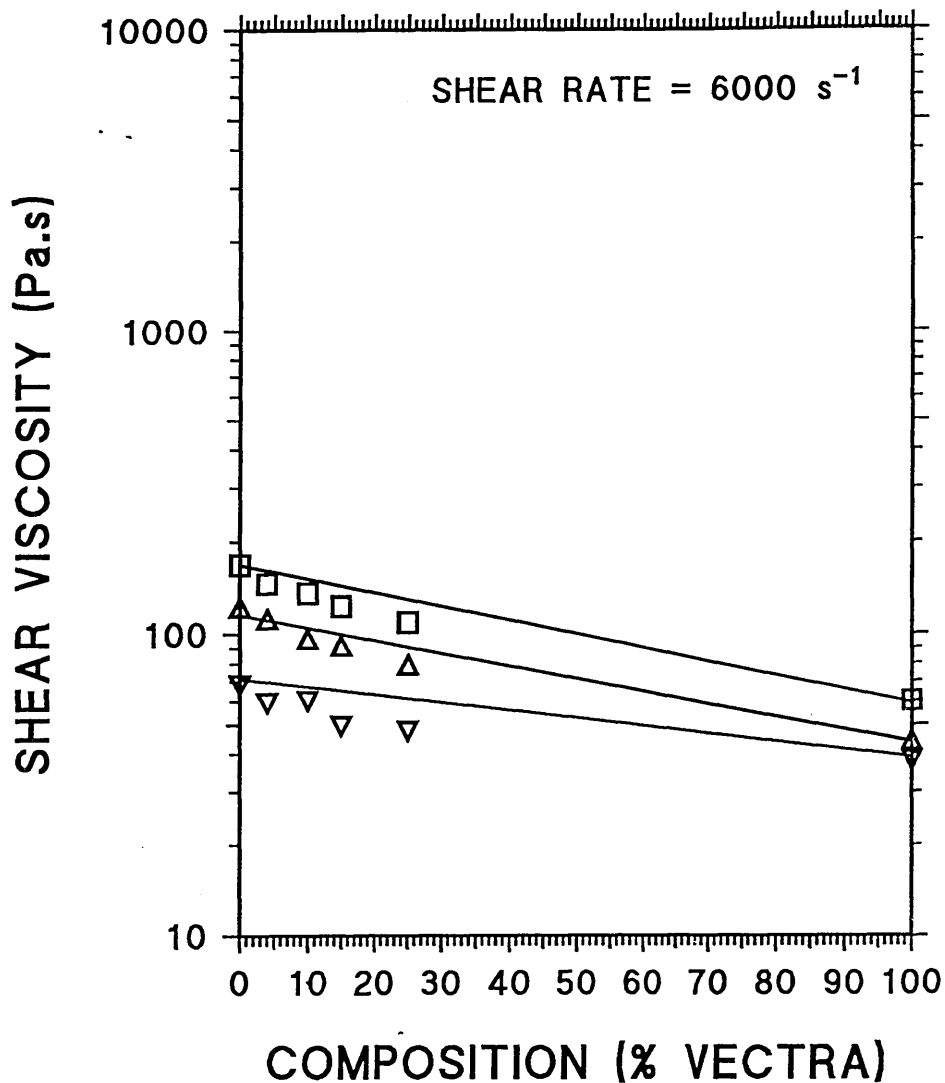
FIGURE 7.16 - Graph of shear stress vs shear rate for PES and blends containing 4%, 10%, 15% and 25% VECTRA processed at 330°C.

demonstrate several points namely the glass filled blends have a higher viscosity than the unfilled blends. Also as the amount of SRP1 within the blend increases so the resultant blend becomes more shear thinning. The viscosities of pure PES (Davenport Rheometer) are comparable with the 72/20/8 PES/GLASS FIBRES/SRP1 results (Rosand Rheometer). This indicated that the LCP was useful in countering the viscosity increase caused by the addition of glass fibres.

## 7.2 TENSILE TESTING OF PES/LCP BLENDS

The tensile bars produced were fractured and the data from these tests were plotted as load vs extension, (see figures 7.25-7.27). The curve for PES clearly demonstrates an elastic region, followed by the onset of necking, with a final fracture point. An addition of 4% LCP changed the mechanical properties of tensile specimens quite markedly (see figure 7.25). The addition of SRP1 (4%) increased the modulus of the blend (the LCP had a reinforcing effect). The sample still 'necked' and fractured at the same point (the blends was still partially ductile).

The fracture facets of PES (figure 7.28) showed both a 'necked' region (seen by the reduction in cross sectional area) and demonstrated that the fracture mode was initiated at several points in the sample which then spread rapidly. The fracture facets of 4% SRP1 in PES (figure 7.29) were quite different. Along the top left half, the left side and



KEY -

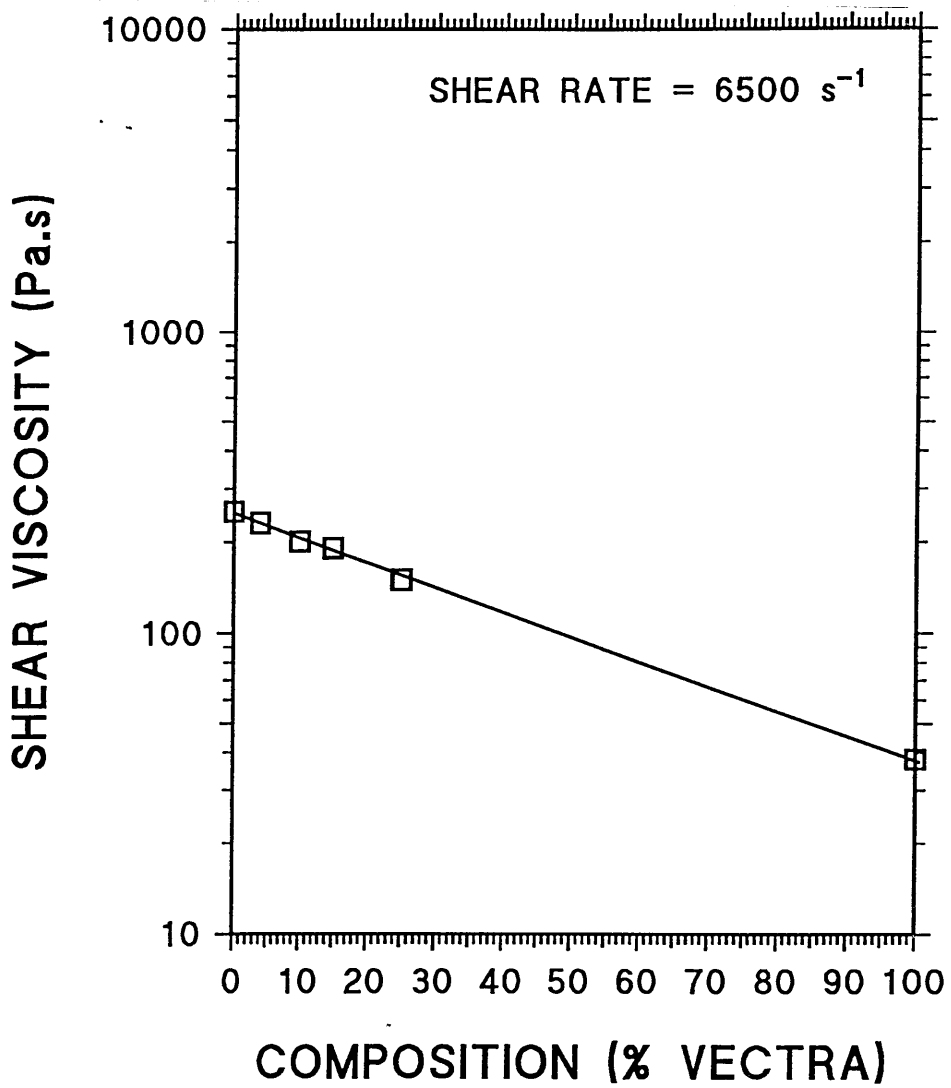
□ - PC/VECTRA AT 280°C

△ - PC/VECTRA AT 300°C

▽ - PC/VECTRA AT 320°C

— LOG ADDITIVE LINE

FIGURE 7.17 - Graph of shear viscosity vs composition for PC/VECTRA blends processed at 280°C, 300°C and 320°C.

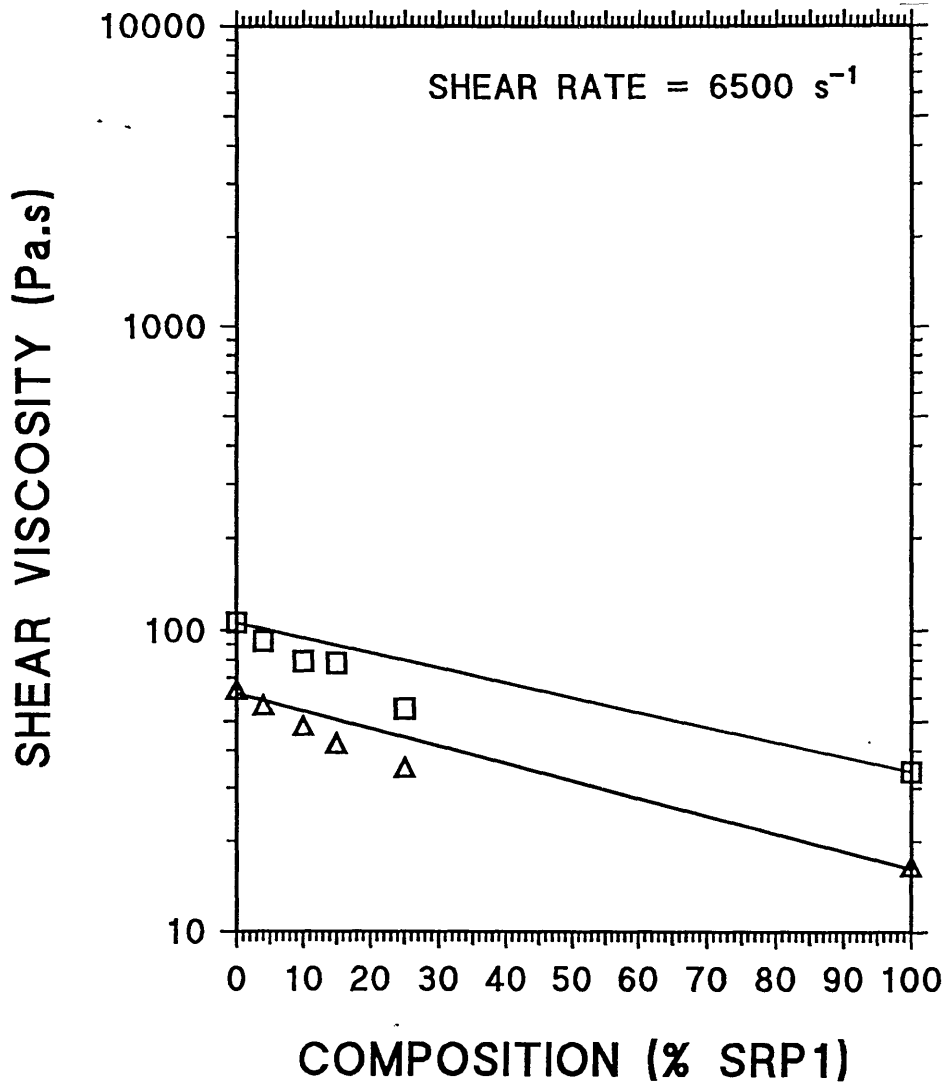


KEY -

□ - PES/VECTRA AT 330°C

— LOG ADDITIVE LINE

FIGURE 7.18 - Graph of shear viscosity vs composition for PES/VECTRA blends processed at 330°C.



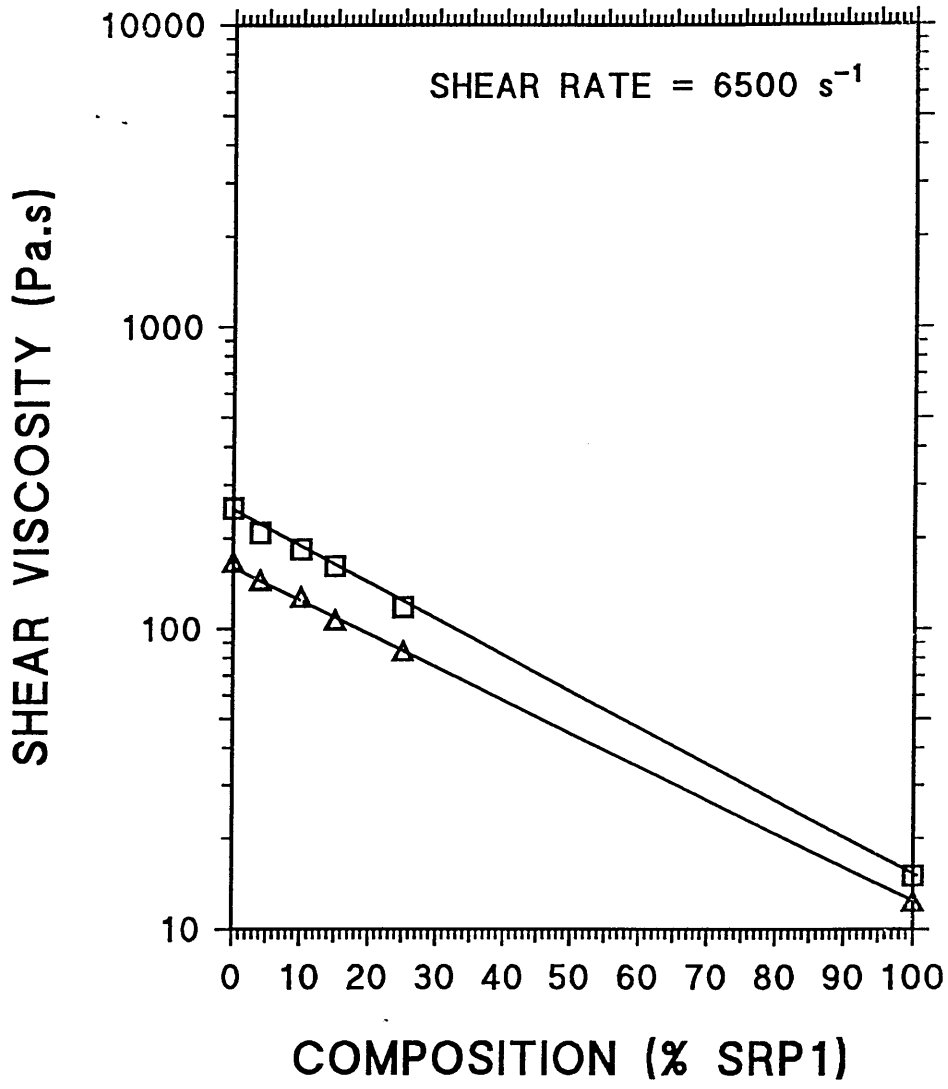
KEY -

□ - PC/SRP1 AT 300°C

△ - PC/SRP1 AT 320°C

— LOG ADDITIVE LINE

FIGURE 7.19 - Graph of shear viscosity vs composition for PC/SRP1 blends processed at 300°C and 320°C.



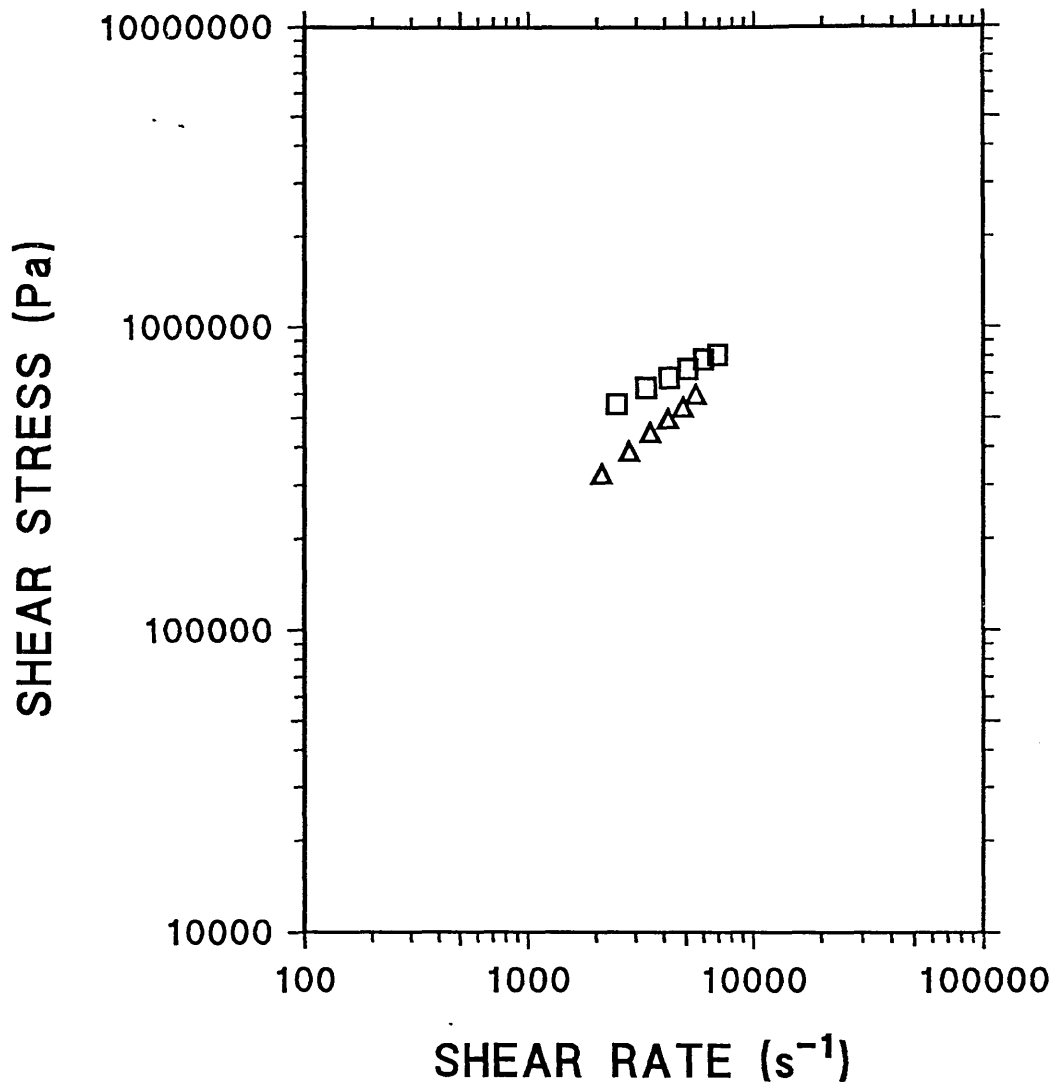
KEY -

- - PES/SRP1 AT 330°C
- △ - PES/SRP1 AT 350°C

— LOG ADDITIVE LINE

FIGURE 7.20 - Graph of shear viscosity vs composition for PES/SRP1 blends processed at 330°C and 350°C.

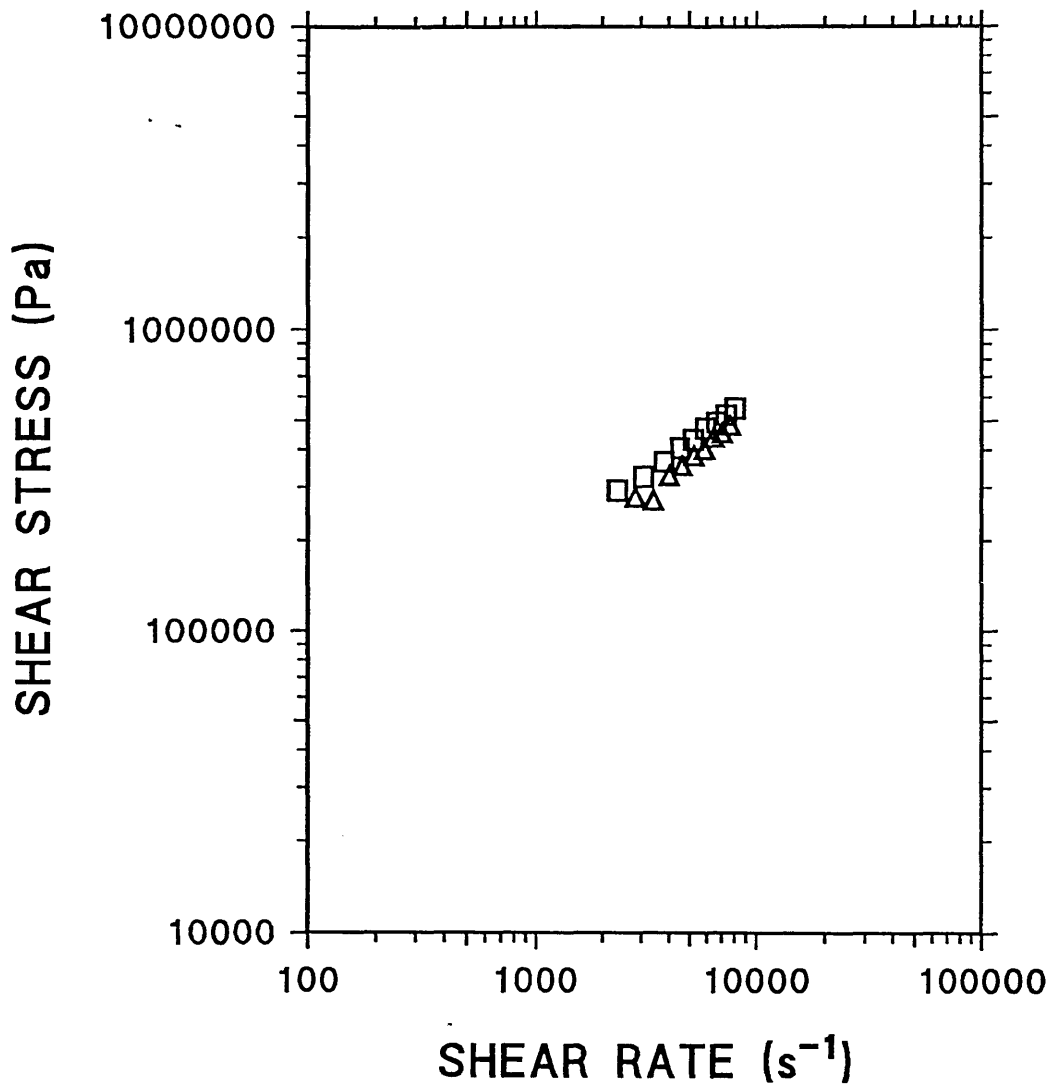
the bottom edge of the sample there was a lip which was  $\approx$  0.1mm thick. It is unknown whether this lip was drawn out during the testing process or if it was present because of the initial moulding operation. The lip would explain, however, why the tensile bar was still ductile (the necked region can clearly be seen in figure 7.29) but could withstand a higher loading. The other interesting point to note in this micrograph is that at the top right edge of the tensile bar something (possibly a particle of SRP1 in the skin region) had acted as a stress concentrator, evident by the semi-circular area around a central point (located  $\approx$ 17mm from the right edge of the facet). The flat appearance around this point indicates that the crack started at a central point and spread rapidly in all directions, hence the semi-circle. Once the crack was initiated it spread towards the opposite side, leading to fracture of the specimen as found by Kiss in PES/LCP blends<sup>131</sup>. The 4% VECTRA sample did not neck (seen graphically in figure 7.25). Fracture occurred in a more brittle fashion than for the SRP1 blend. Samples containing 8% LCP in PES (see figure 7.26) did not neck, *In* this case the 8% SRP1 samples fractured in a brittle manner and at this composition the author began to notice the onset of a skin/core effect (see figures 7.30 and 7.31). The VECTRA affected the blend to a greater extent than the SRP1; the 8% VECTRA/PES samples were more brittle than the SRP1 blend and showed signs of internal layering. Samples containing 15% LCP in PES were both brittle and showed a high degree



**KEY -**

- - 80% PES  
20% GLASS FIBRES AT 350°C
- △ - 80% PES  
20% GLASS FIBRES AT 370°C

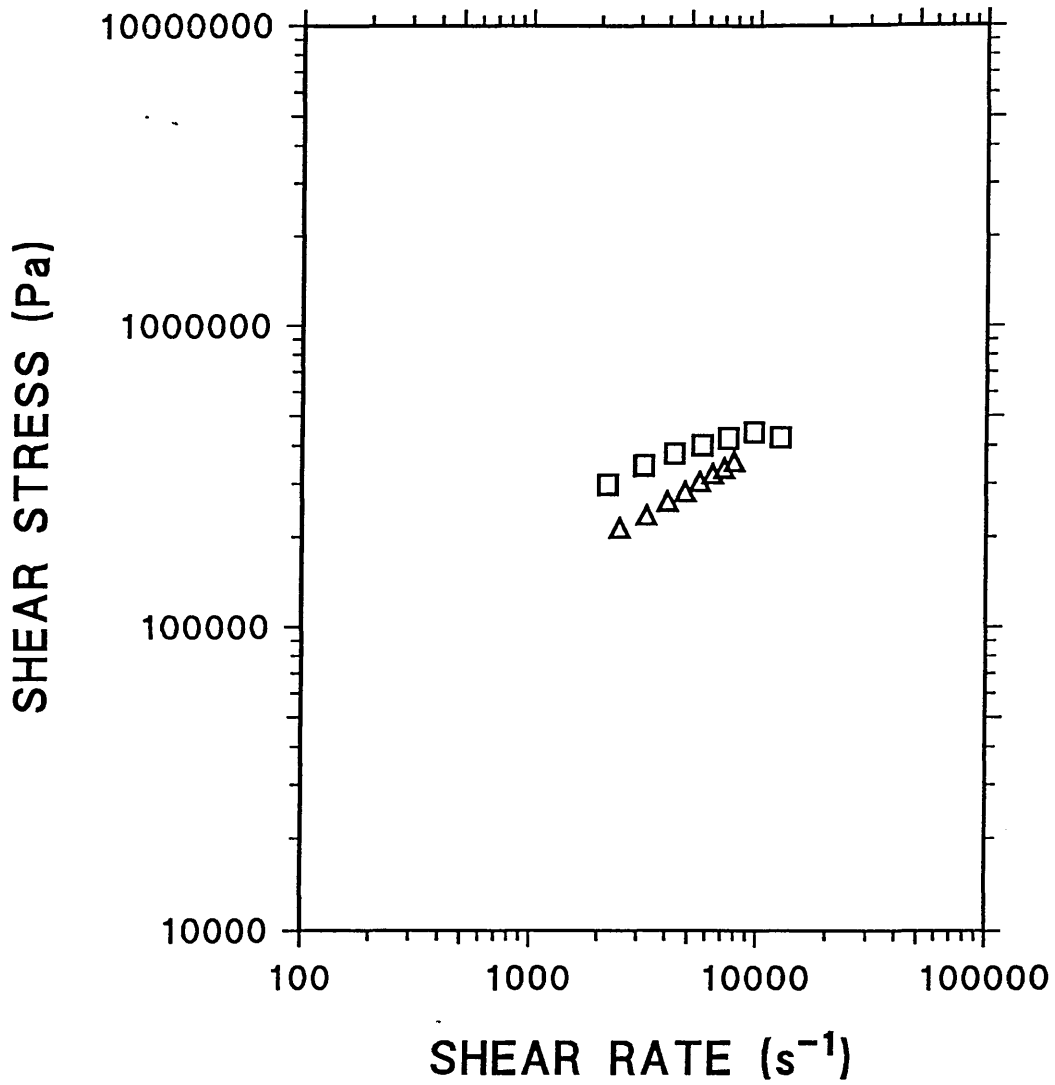
FIGURE 7.21 - Graph of shear stress vs shear rate for 80% PES/20% GF blend processed at 350°C and 370°C.



**KEY -**

- - 72% PES  
20% GLASS FIBRES  
8% SRP1 AT 350°C
- △ - 72% PES  
20% GLASS FIBRES  
8% SRP1 AT 370°C

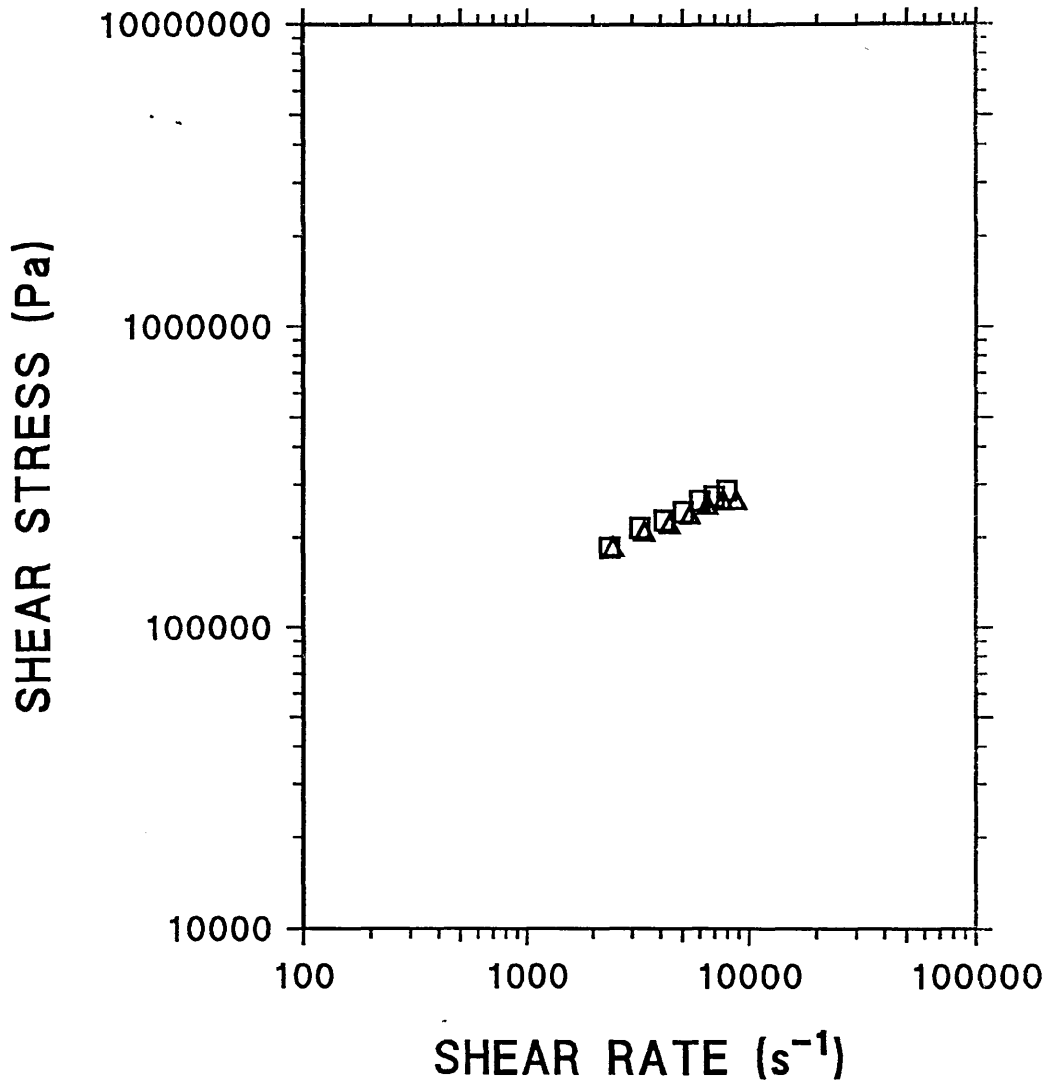
FIGURE 7.22 - Graph of shear stress vs shear rate for 72% PES/20% GF/8% SRP1 blend processed at 350°C and 370°C.



KEY -

- - 68% PES  
20% GLASS FIBRES  
12% SRP1 AT 350°C
- △ - 68% PES  
20% GLASS FIBRES  
12% SRP1 AT 370°C

FIGURE 7.23 - Graph of shear stress vs shear rate for 68% PES/20% GF/12% SRP1 blend processed at 350°C and 370°C.



**KEY -**

- - 64% PES  
20% GLASS FIBRES  
16% SRP1 AT 350°C
- △ - 64% PES  
20% GLASS FIBRES  
16% SRP1 AT 370°C

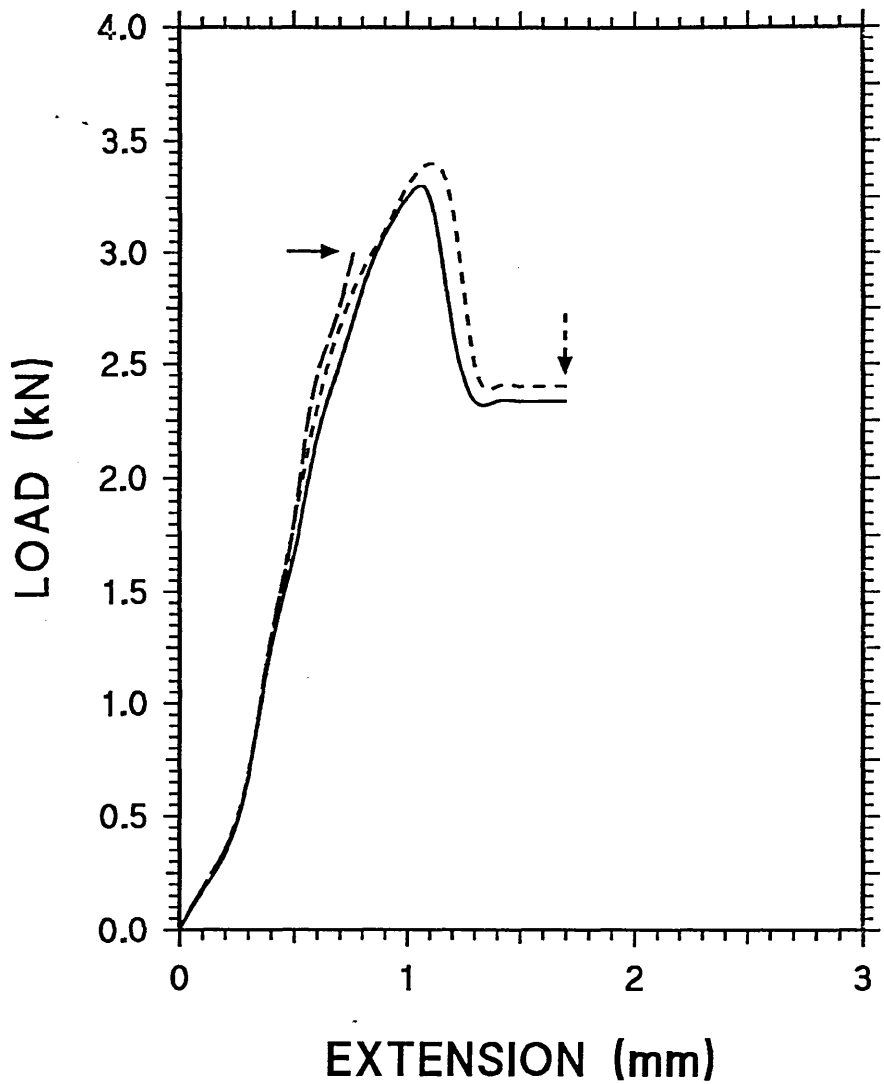
FIGURE 7.24 - Graph of shear stress vs shear rate for 64% PES/20% GF/16% SRP1 blend processed at 350°C and 370°C.

of internal layering with fracture facets having the appearance of 'wood' (see figure 7.32). The degree of order increased as the amount of LCP increased (see figure 7.33). This figure shows a 25% SRP1/PES blend after fracture with a highly ordered internal arrangement.

### 7.3 IMPACT DATA

The PC/LCP blends were injection moulded into bars, which were then notched as described earlier. The notched bars were then placed in the Hounsfield Impact Tester. The pure PC standard had impact strengths of around  $600 \text{ Jm}^{-1}$ ; an addition of 4% VECTRA caused a drastic reduction in the impact strength to around half of this value. The SRP1 blends had slightly higher impact strengths than the corresponding VECTRA blends. As the amount of LCP within the blend increased so the impact strength decreased.

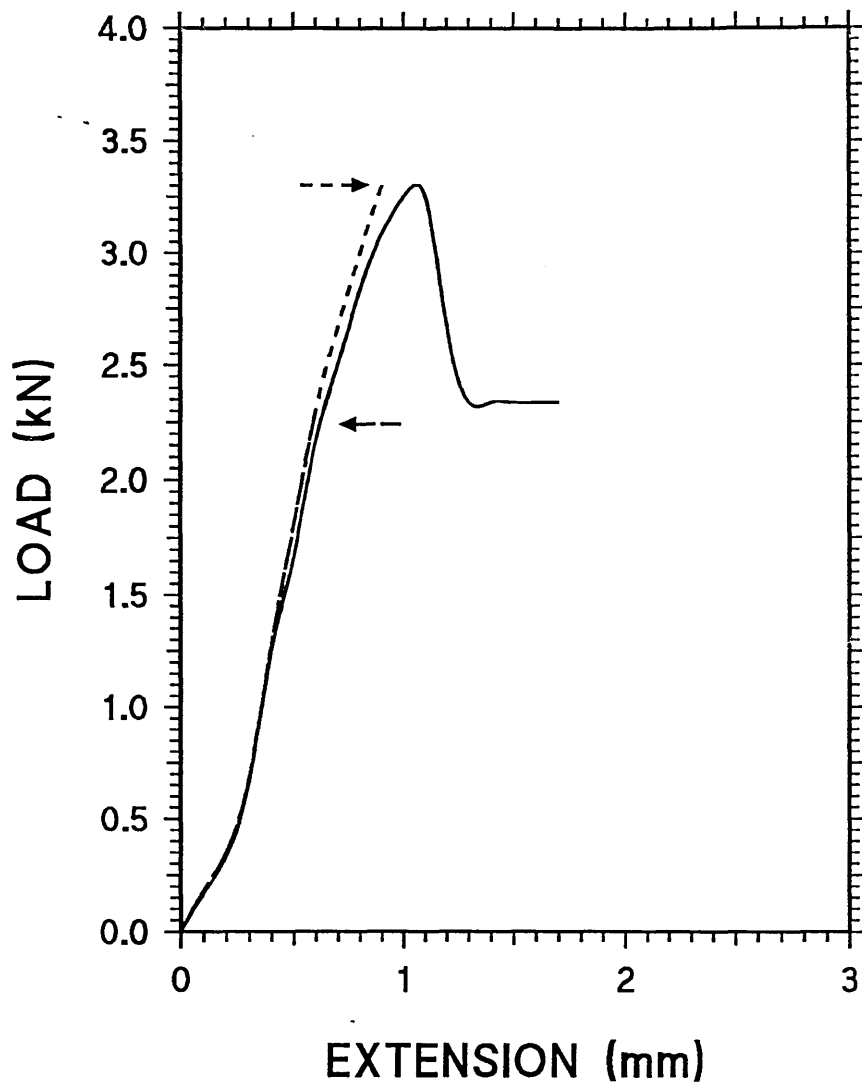
These results show that relatively low additions of LCP to PC/PES had a major effect on the mechanical properties. It was apparent that the LCP acted to induce orientation in the flow direction, reinforcing the properties in the flow direction, but decreasing the properties perpendicular to the flow direction. This is immediately apparent if the sample is stressed at right angles to the flow direction. The critical composition was found to be around 6% VECTRA or 8% SRP1. At these compositions, the PC/LCP samples lost their amorphous characteristics and became brittle.



KEY -

- PES
- - - 4% VECTRA IN PES
- · - · 4% SPR1 IN PES
- ← - FRACTURE POINT OF VECTRA
- ← - - FRACTURE POINT OF SPR1

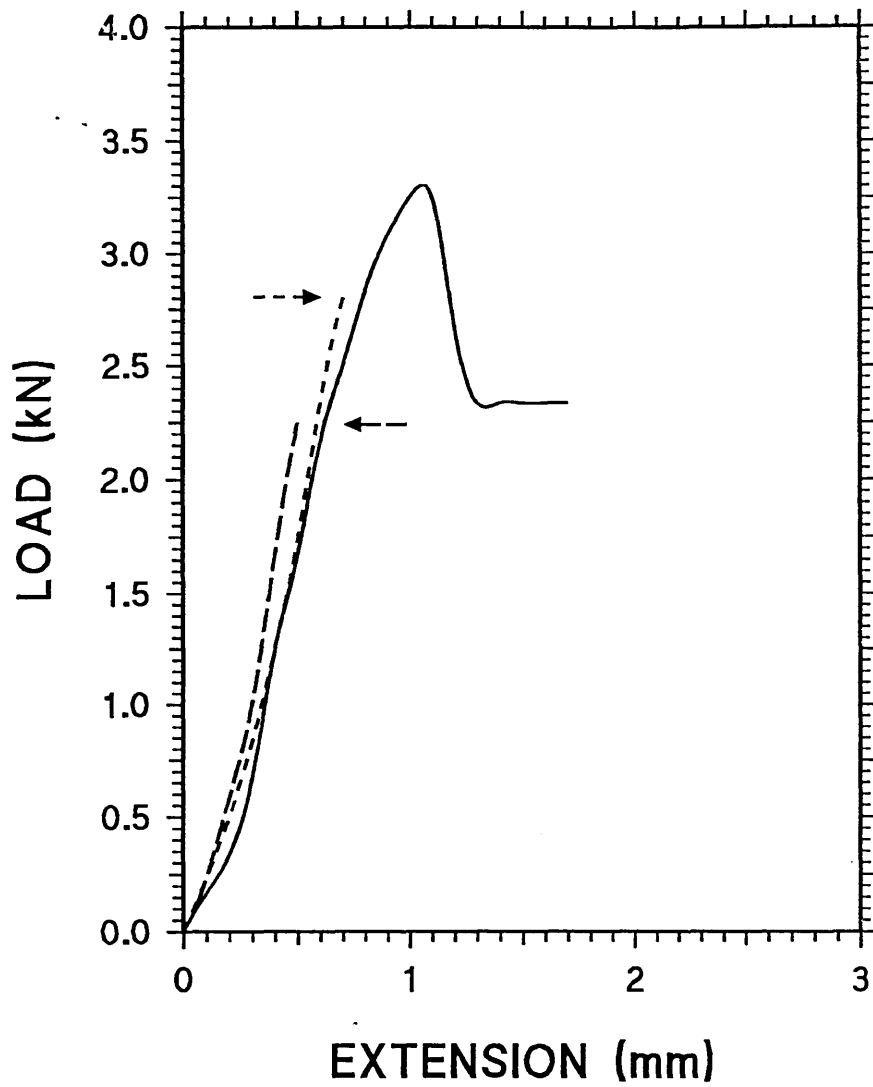
FIGURE 7.25 - Graph of load vs extension for PES/4% LCP tensile specimens processed at 340°C and a shear rate of  $\approx 5000s^{-1}$ .



KEY —

- PES
- - - 8% VECTRA IN PES
- · - · 8% SPR1 IN PES
- ← - - FRACTURE POINT OF VECTRA
- ← - · - FRACTURE POINT OF SPR1

FIGURE 7.26 - Graph of load vs extension for PES/8% LCP tensile specimens processed at 340°C and a shear rate of  $\approx 5000\text{s}^{-1}$ .



KEY —

— PES

- - - 15% VECTRA IN PES

- · - · 15% SPR1 IN PES

← - - FRACTURE POINT OF VECTRA

← · · FRACTURE POINT OF SPR1

FIGURE 7.27 - Graph of load vs extension for PES/15% LCP tensile specimens processed at 340°C and a shear rate of  $\approx 5000\text{s}^{-1}$ .

#### 7.4 WATER ABSORPTION TESTS

This experiment was carried out to see if subsequent additions of LCP to PC would increase the barrier properties of the resultant blend. Figures 7.35-7.36 represent the data graphically, with the best fit lines for samples containing 0%, 4%, 8%, 15% and 25% LCP in PC. The results of these tests clearly show that as the amount of LCP within the sample increased so the ability of the blend to resist the absorption of water also increased. The author feels that this ability is closely related to the skin/core effect, which will be discussed fully later. It can also clearly be seen that both samples containing 4% LCP absorb virtually the same amount of water (behaviour close to pure PES). The 8% VECTRA sample appears to have better resistance than the 8% SRP1 blend, in keeping with previous results. The 25% SRP1 appeared to have superior barrier properties, but over a period of time the amount of water absorbed was much greater, making the VECTRA blends superior.

#### 7.5 DIFFERENTIAL SCANNING CALORIMETRY

The DSC traces allowed the nematic transition point of the LCP's to be determined along with the glass transition temperatures of the matrix polymers. The glass transitions of the PES and PC were found to be  $\approx 222^{\circ}\text{C}$  and  $\approx 149^{\circ}\text{C}$  respectively. The reason for obtaining the glass transition temperatures was to check the equipment against standard known data as a means of calibration. The nematic

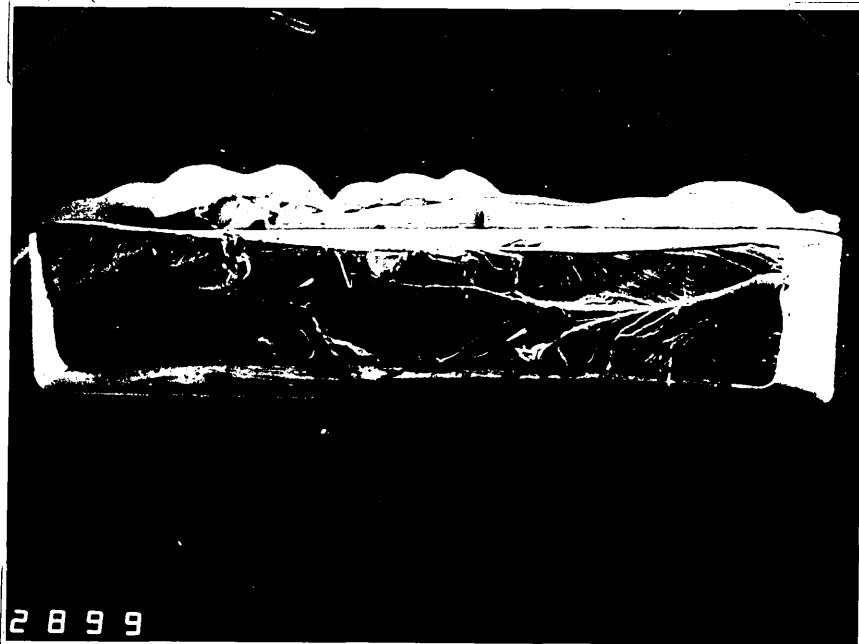


FIGURE 7.28 - Fracture facet of PES tensile bar moulded at 340°C and shear rate of  $\approx 5000\text{s}^{-1}$   
MAGNIFICATION x 9

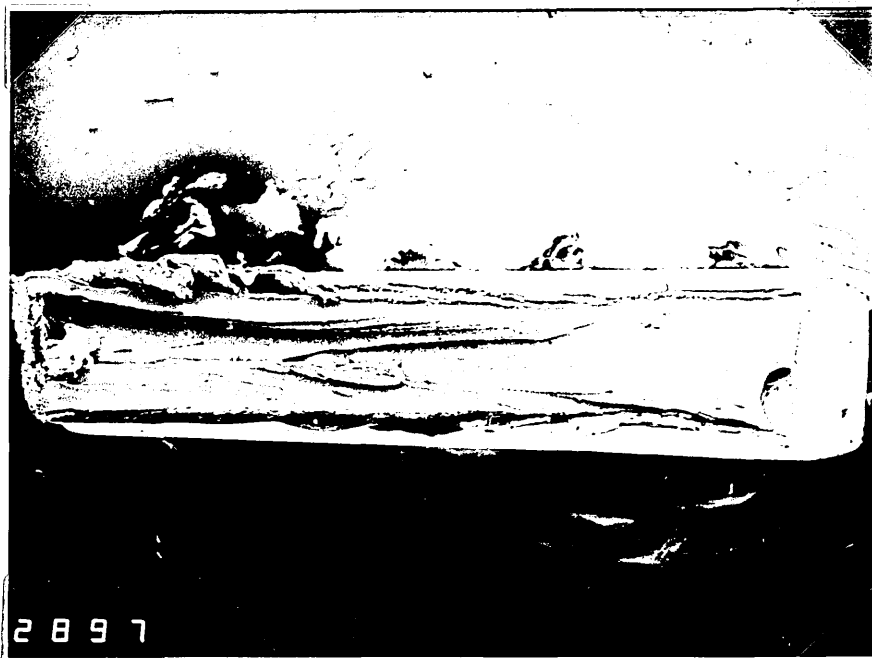


FIGURE 7.29 - Fracture facet of 4% SRP1/PES tensile bar moulded at 340°C and shear rate of  $\approx 5000\text{s}^{-1}$   
MAGNIFICATION x 9

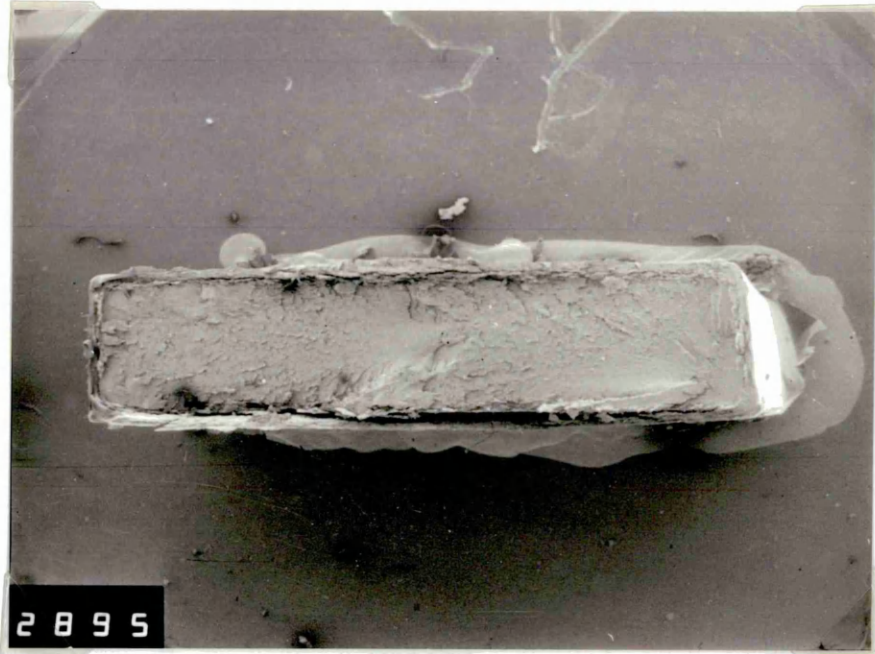


FIGURE 7.30 - Fracture facet of 8% SRP1/PES tensile bar moulded at 340°C and shear rate of  $\approx 5000\text{s}^{-1}$  MAGNIFICATION x 9

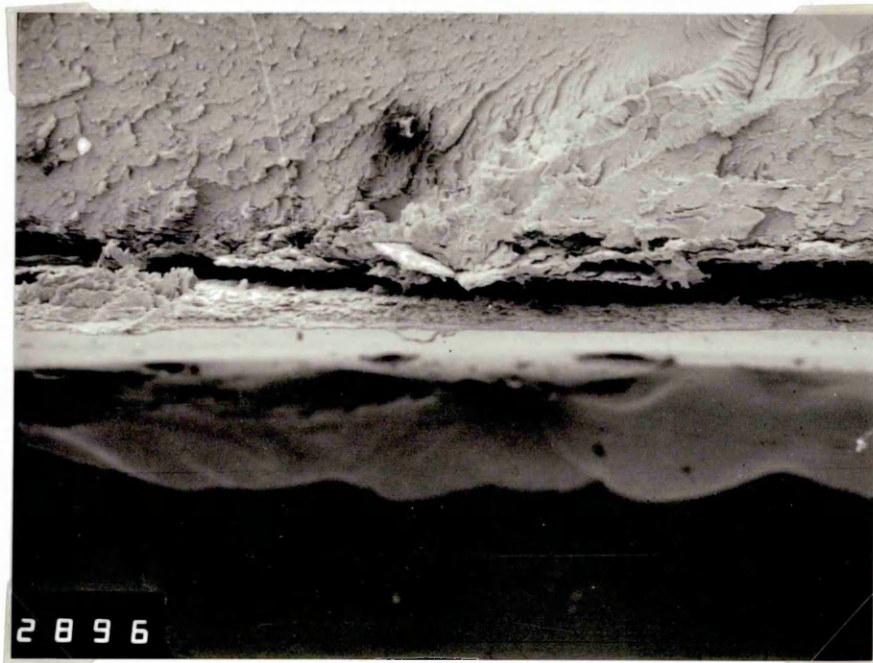


FIGURE 7.31 - Fracture facet of 8% SRP1/PES tensile bar moulded at 340°C and shear rate of  $\approx 5000\text{s}^{-1}$  MAGNIFICATION x 9

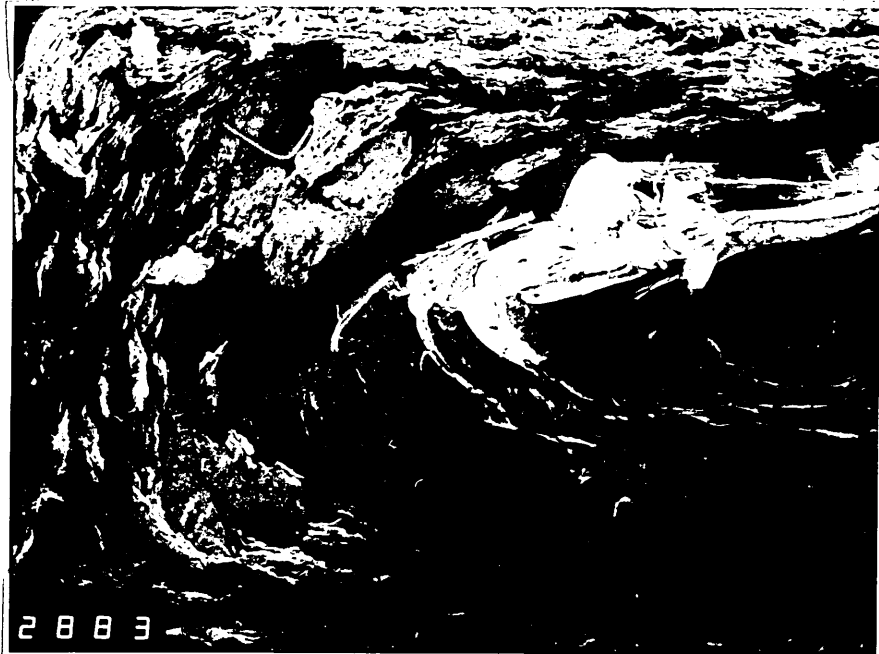


FIGURE 7.32 - Fracture facet of 15% VECTRA/PES tensile bar moulded at 340°C and shear rate of  $\approx 5000\text{s}^{-1}$   
MAGNIFICATION x 26

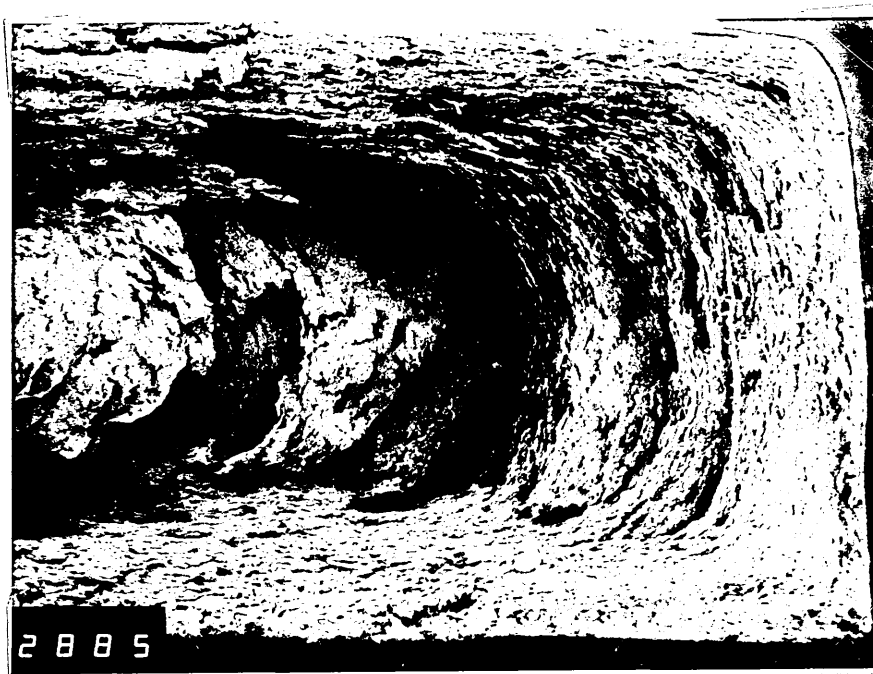


FIGURE 7.33 - Fracture facet of 25% SRP1/PES tensile bar moulded at 340°C and shear rate of  $\approx 5000\text{s}^{-1}$   
MAGNIFICATION x 24

transition temperatures of SRP1 and VECTRA were found to be  $\approx 304^{\circ}\text{C}$  and  $\approx 275^{\circ}\text{C}$  respectively. The exact temperatures could not be determined because there was a degree of variation between consecutive runs ( $\pm 3^{\circ}\text{C}$ ).

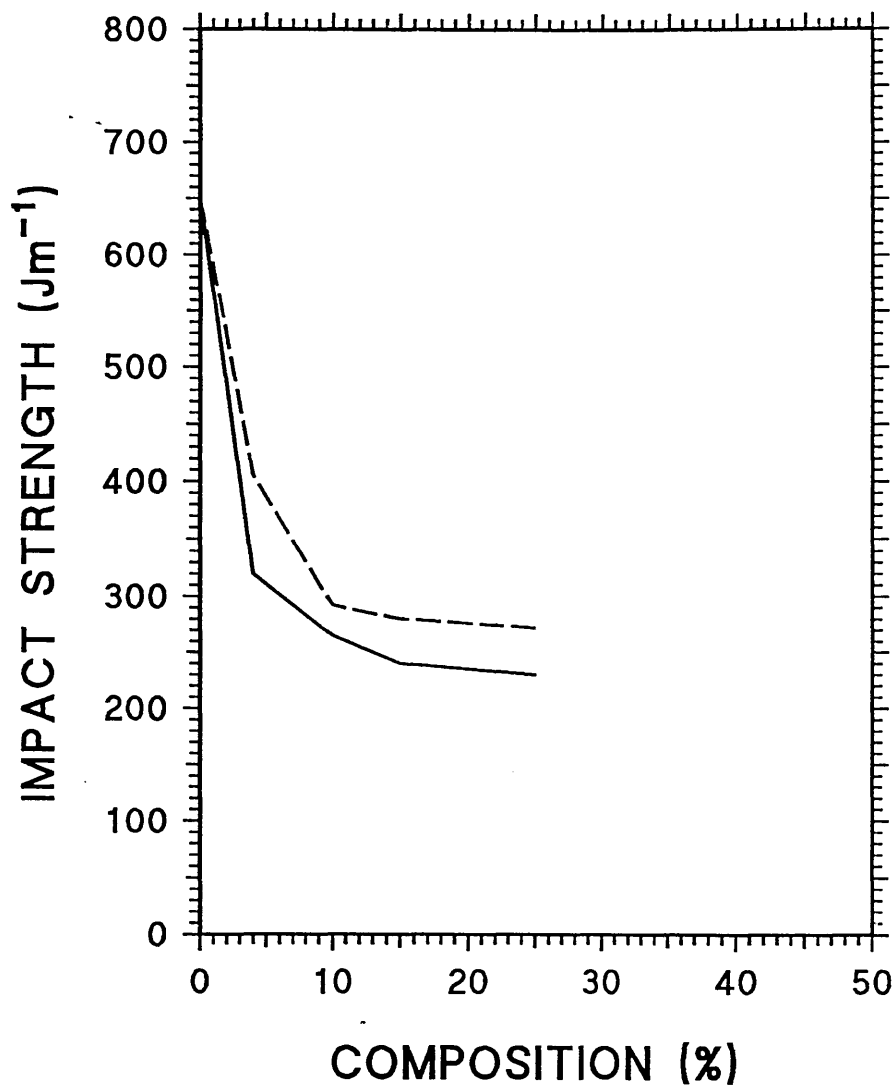
It was necessary to determine the nematic transition temperatures of the LCP's in order to show that they needed to be fluid at the processing temperature to confer favourable properties to the blend. The data obtained from the DSC runs are shown below (see table 7.3).

MATERIAL	WEIGHT (mg)	NEMATIC TRANSITION TEMPERATURE
SRP 1500G	28.16	303°C
SRP 1500G	27.89	307°C
SRP 1500G	31.12	302°C
SRP 1500G	30.49	305°C
VECTRA	32.45	275°C
VECTRA	31.23	277°C
VECTRA	17.89	274°C
VECTRA	29.06	276°C

TABLE 7.3 - Table of nematic transition temperatures obtained for SRP1 and VECTRA for four separate runs carried out at a cooling rate of  $10^{\circ}\text{C minute}^{-1}$ .

## 7.6 MICROSCOPY

The micrographs obtained can be seen throughout the results and discussion section, however the main points will now be highlighted.



KEY —

—————	PC/VECTRA
- - - - -	PC/SRP1

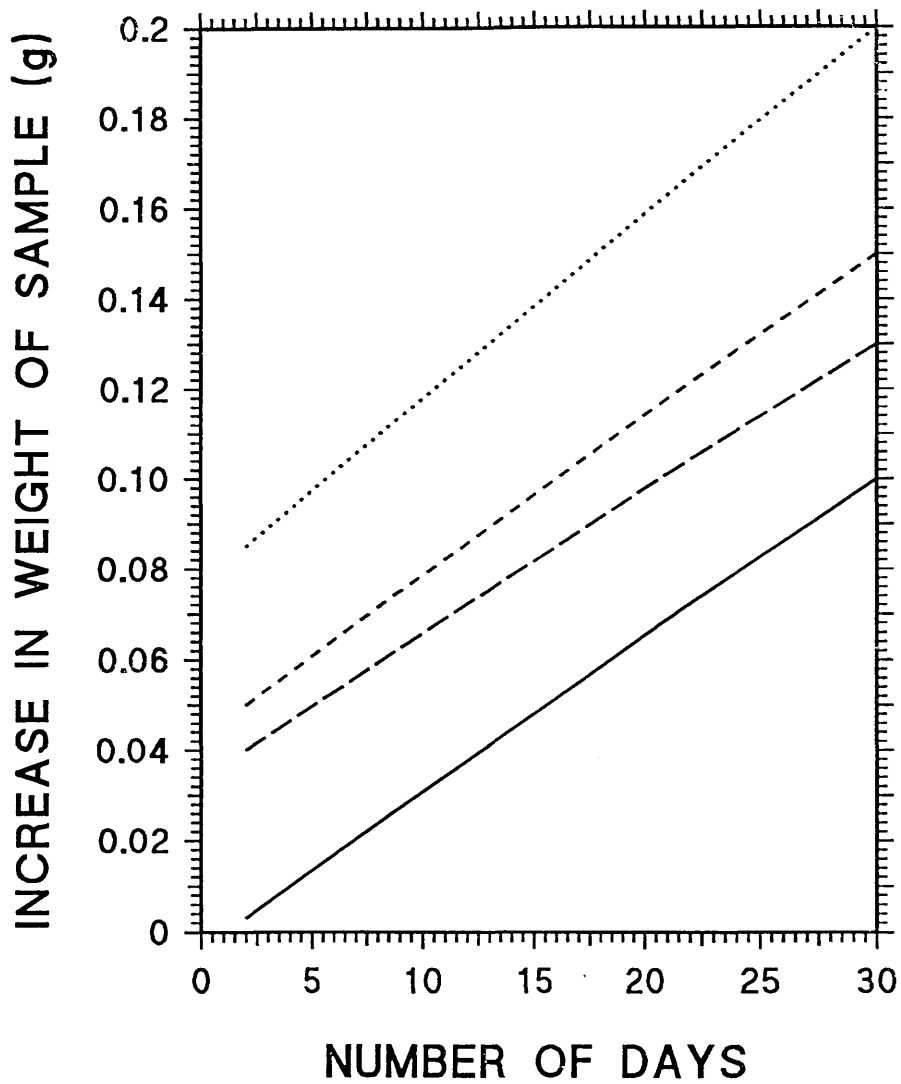
FIGURE 7.34 - Graph of impact strength vs composition for PC/LCP impact specimens processed at 300°C and a shear rate of  $\approx 5000\text{s}^{-1}$ .

### 7.6.1 TRANSMISSION LIGHT MICROSCOPY

The samples prepared at I.C.I Wilton were observed through a transmission light microscope. Positions within the skin and core regions were selected and micrographs were taken of the 25% LCP/PES blends. There were two main features observed, firstly the VECTRA/PES blends (see figures 7.37 and 7.38) appeared to have a more granular structure. It was also noticed in the micrograph taken from the core section (figure 7.37) the VECTRA phase was more spherical in appearance. The micrograph taken in the skin region showed the VECTRA to be more acicular (see figure 7.38) suggesting that the VECTRA in the 'skin' region was subjected to extensional forces (possibly at the outlet).

The PES appeared to be more compatible with SRP1 which adopted a finer acicular dispersion throughout the matrix. The core region was made up of a series of wavy lines between which the SRP1 formed smaller spheroid fragments. In the skin region a series of bands were observed, one such band could be seen in figure 7.38 towards the top of the micrograph.

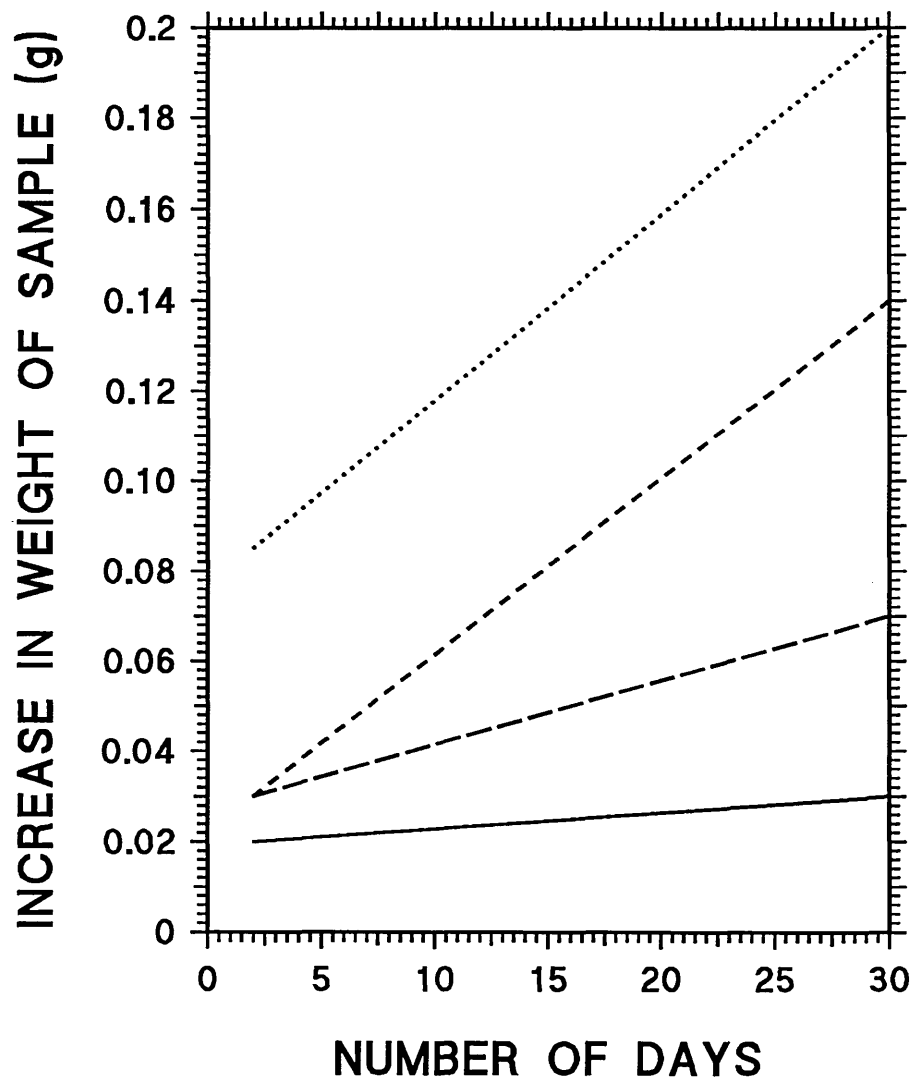
From these figures it can be seen that the VECTRA is less compatible than the SRP1 and forms a macro aggregate within the PES matrix. The SRP1 is not compatible (but it is more compatible than the VECTRA) and gives a finer dispersion throughout the whole section.



KEY -

- ..... 4% SRP1 IN PES
- 8% SRP1 IN PES
- - - - 15% SRP1 IN PES
- 25% SRP1 IN PES

FIGURE 7.35 - Graph of increase of weight vs period PES/SRP1 samples processed at 340°C and a shear rate of  $\approx 5000\text{s}^{-1}$ .



KEY —

- ..... 4% VECTRA IN PES
- 8% VECTRA IN PES
- 15% VECTRA IN PES
- 25% VECTRA IN PES

FIGURE 7.36 - Graph of increase of weight vs period PES/VECTRA samples processed at 340°C and a shear rate of  $\approx 5000\text{s}^{-1}$ .

## 7.6.2 EDAX - ELECTRON MICROSCOPY

The Joel JX40A electron microscope was calibrated using a sulphur standard and the pure PES and SRP1 mouldings were scanned for sulphur. A sulphur ( $S_K$ ) map and line scan were carried out on the two samples, along with a secondary electron image (see figure 7.41). The equipment was used to show any sulphur denuded areas (LCP). The morphology of the LCP was different in the two regions (see figure 7.41 A,B and C). The 25% SRP1/PES core image (figure 7.41 C) shows that the SRP1 adopted a ball-like morphology. Spherical particles could also be seen in the 25% VECTRA/PES core image (figure 7.41 A). The skin region (figure 7.41 B) had a higher aspect ratio due to being elongated in the flow direction.

## 7.7 MODELLING THE FLOW PROFILES

Values of the shear thinning index and the consistency constant ( $Ns^n/m^2$ ) were calculated from the graphs of shear stress vs shear rate (see figures 7.5-7.7 and 7.12-7.16) using the gradient and the intercept of the line. Table 7.4 contains the relevant data for the PC/VECTRA blend.

	VECTRA		PC	
TEMPERATURE	n	K	n	K
280°C	0.49	4897	0.47	15488
320°C	0.71	467	0.65	1445

TABLE 7.4 - The above table demonstrates the change in both the values of (n) and (K) for VECTRA/PC for temperatures (280°C - 320°C).



FIGURE 7.37 - Micrograph from core region of 25% VECTRA/PES blend moulded at 340°C and shear rate of  $\approx 5000\text{s}^{-1}$  MAGNIFICATION x 2500

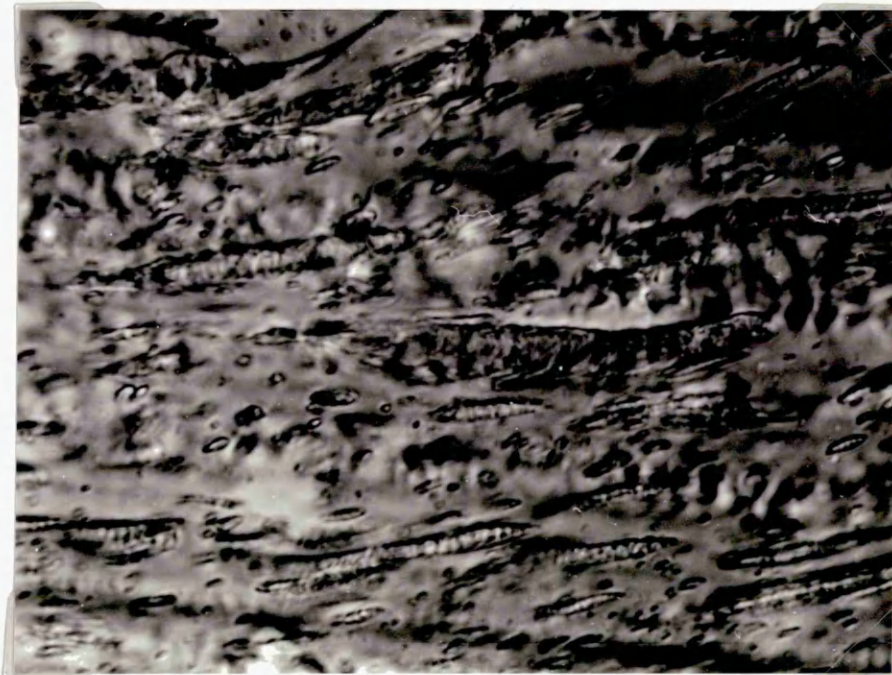


FIGURE 7.38 - Micrograph from skin region of 25% VECTRA/PES blend moulded at 340°C and shear rate of  $\approx 5000\text{s}^{-1}$  MAGNIFICATION x 2500

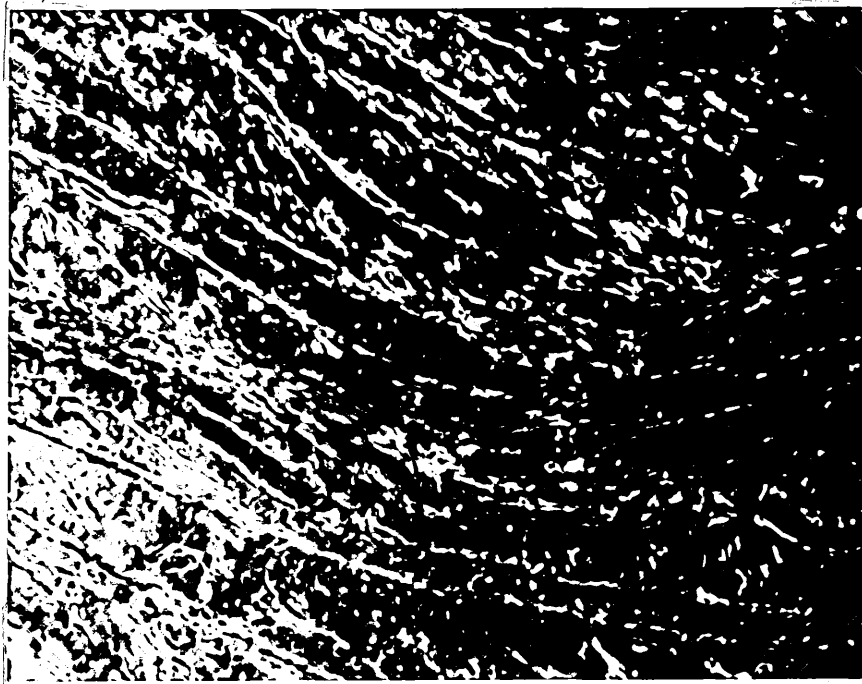


FIGURE 7.39 - Micrograph from core region of 25% SRP1/PES blend moulded at 340°C and shear rate of  $\approx 5000\text{s}^{-1}$   
MAGNIFICATION x 2500

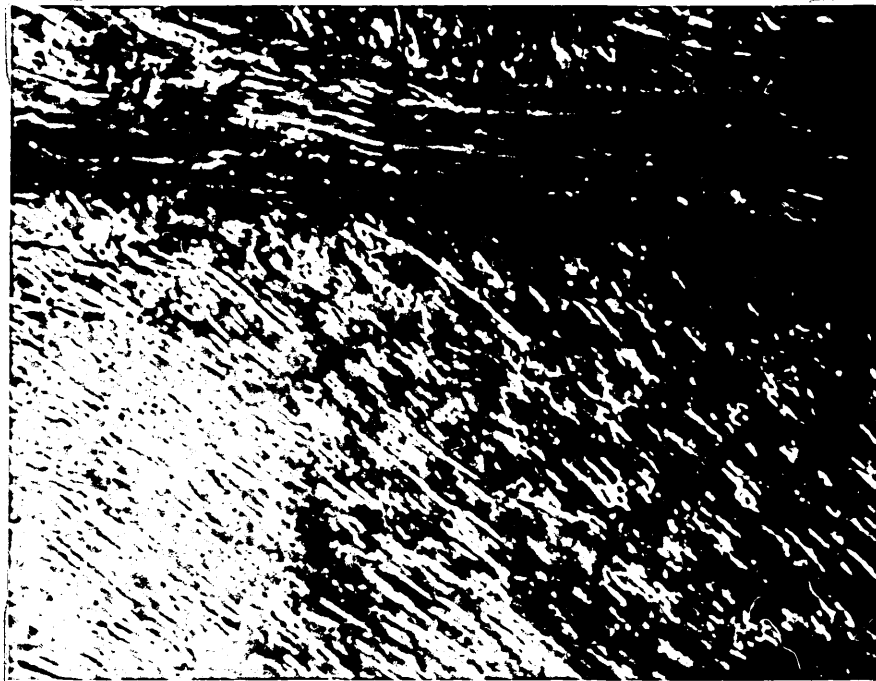


FIGURE 7.40 - Micrograph from skin region of 25% SRP1/PES blend moulded at 340°C and shear rate of  $\approx 5000\text{s}^{-1}$   
MAGNIFICATION x 2500

The above data were used in conjunction with information from the experiment as follows :-

$$v_r = \left( \frac{\partial P}{\partial l} \right)^{\frac{1}{n}} \frac{n}{2K} \left( R_o^{\frac{n+1}{n}} - r^{\frac{n+1}{n}} \right) \quad (7.1)$$

where :-

$v_r$  = velocity at radial position 'r' within the die ( $\text{ms}^{-1}$ )

$\partial P/\partial l$  = pressure gradient in the die ( $\text{Pam}^{-1}$ )

$r$  = radial position within the die (m)

$R_o$  = radius of the die (mm)

$n$  = shear thinning index

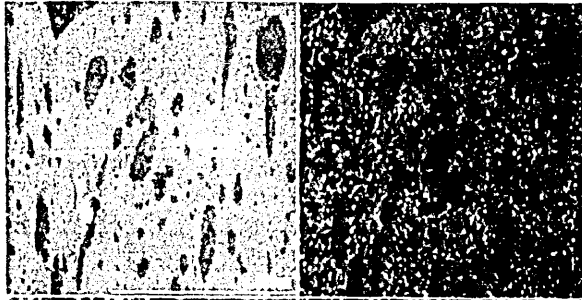
$K$  = consistency constant ( $\text{Ns}^n\text{m}^{-2}$ )

The mean velocity within the die region is given by ' $\bar{v}$ ' which occurs at  $R_o/2$  and is calculated as follows :-

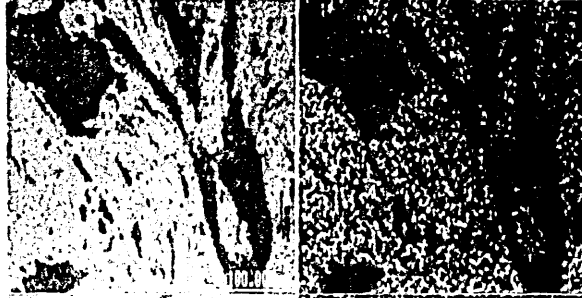
$$\bar{v} = \left( \frac{\partial P}{\partial l} \right)^{\frac{1}{n}} \frac{n}{3n+1} R_o^{\frac{n+1}{n}} \quad (7.2)$$

The derivation of these equations can be seen in appendix A. Using equation (7.2) the velocity can be calculated at any point across the section of the die. If all of these loci are plotted a profile results (see figure 4.3). An interface occurs where the velocity profile equals the mean velocity<sup>160</sup>. The polymer sandwiched between the die and the mean velocity is subject to longitudinal

A



25% VECTRA/PES  
CORE



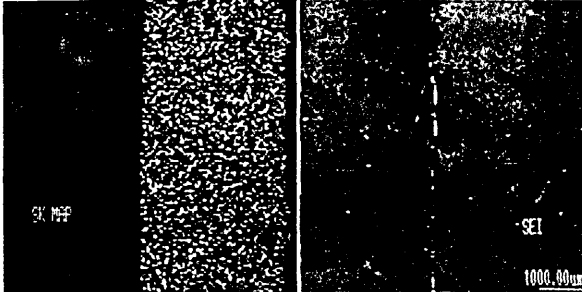
25% VECTRA/PES  
SKIN

B



25% SRP1/PES  
CORE

C



STANDARDS :-  
PES AND SRP1

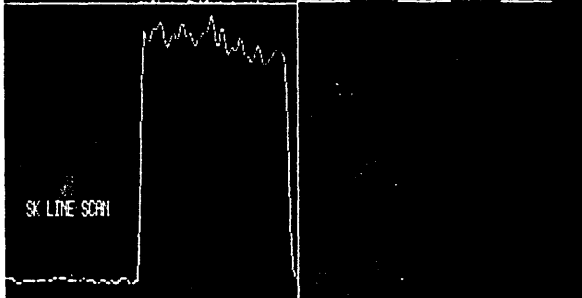
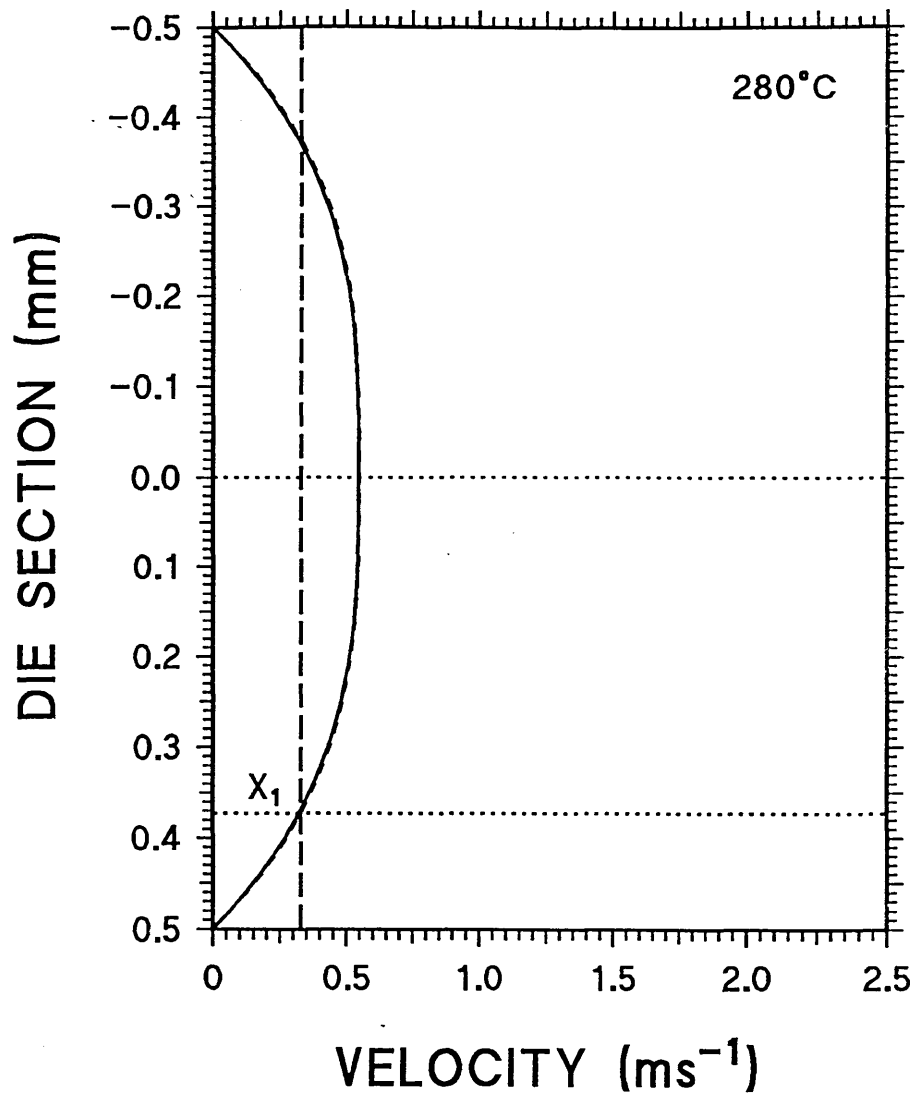


FIGURE 7.41 - EDAX micrographs showing sulphur scans for both VECTRA and SRP1 samples demonstrating morphology and immiscibility of PES and the liquid crystal polymers.

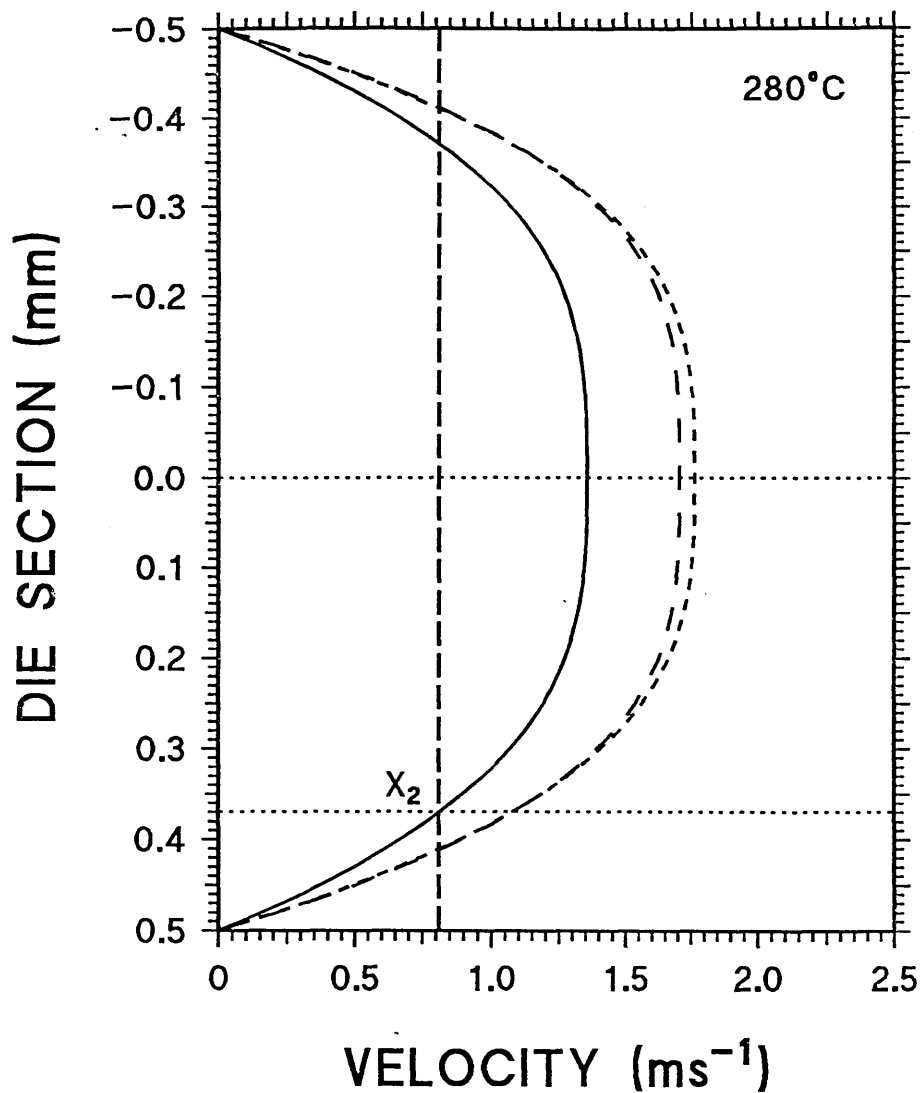
acceleration, whereas the polymer between the mean velocity and the centre line is subject to axial compression. Remembering what was said earlier about LCP's under elongational forces, it can be seen that at the point where the mean velocity cuts the velocity profile a macro-interface results. This interface can clearly be seen in figures 8. 7 and 8. 8. The effect becomes more pronounced at higher shear rates: in samples which are injection moulded, the interface becomes more pronounced and moves closer to the die wall (as  $n \rightarrow 1$ ). Figures 7.42 - 7.45 show the velocity profiles for VECTRA and PC at 280°C - 320°C along with the mean velocities of the extrudate. The point where the mean velocity and the velocity profile of the LCP intersect was found to be in close proximity to the interface position. This would indicate that the LCP induces orientation, without necessarily moving radially in the die region. The extensional forces in the outer section of the die act to orientate the LCP molecules, whilst the axial deceleration in the core acts to compress the LCP molecules rather like closely packed logs in a river. This accounts for the region in between where the accelerating region meets the decelerating region forming a crack (see figures 7.30, 7.31 and 8.7).



KEY —

- VELOCITY PROFILE OF PC
- VELOCITY PROFILE OF VECTRA
- MEAN VELOCITY OF VECTRA
- ..... CENTRE LINE AND INTERFACE POSITION

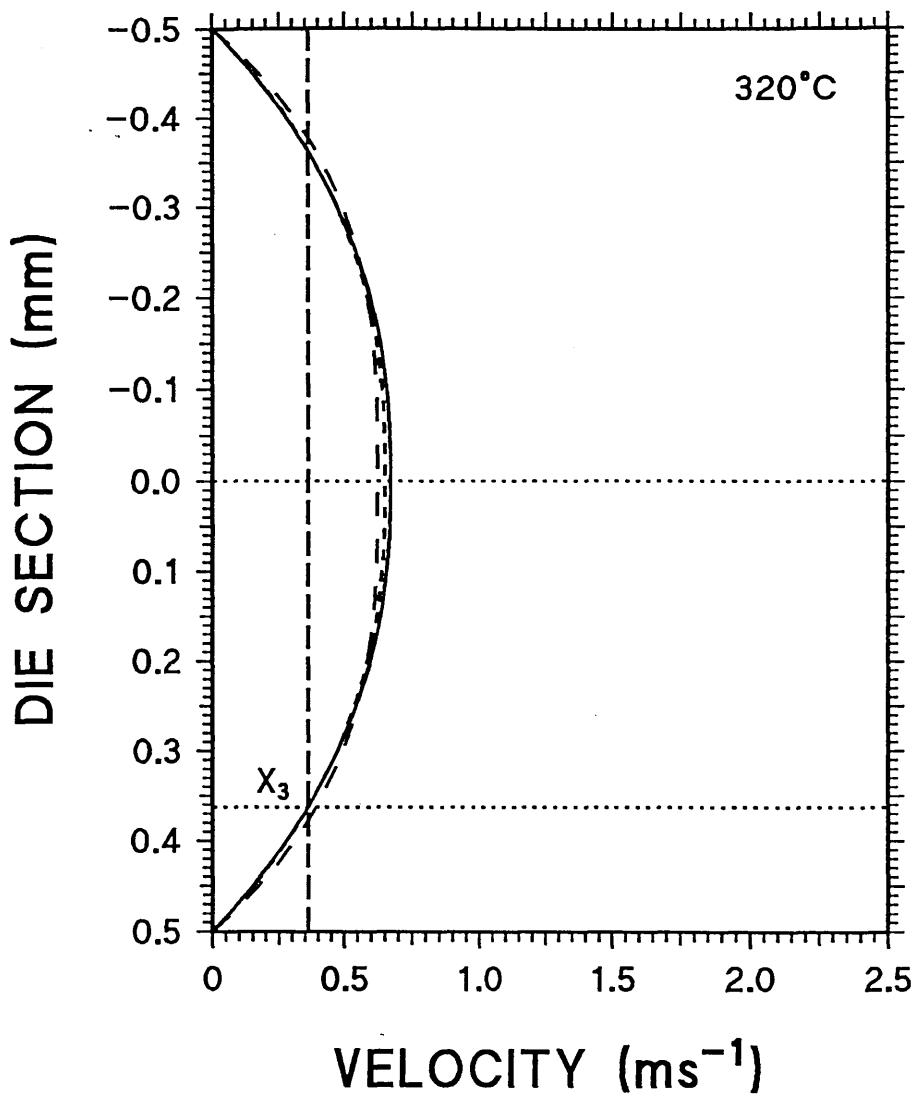
FIGURE 7.42 - Flow profiles for PC and VECTRA processed at 280°C and a shear rate of  $3000\text{s}^{-1}$ , showing the predicted interface position ( $X_1$ ).



KEY —

- — VELOCITY PROFILE 25% VECTRA/PC
- VELOCITY PROFILE OF PC
- VELOCITY PROFILE OF VECTRA
- — MEAN VELOCITY OF VECTRA
- ..... CENTRE LINE AND INTERFACE POSITION

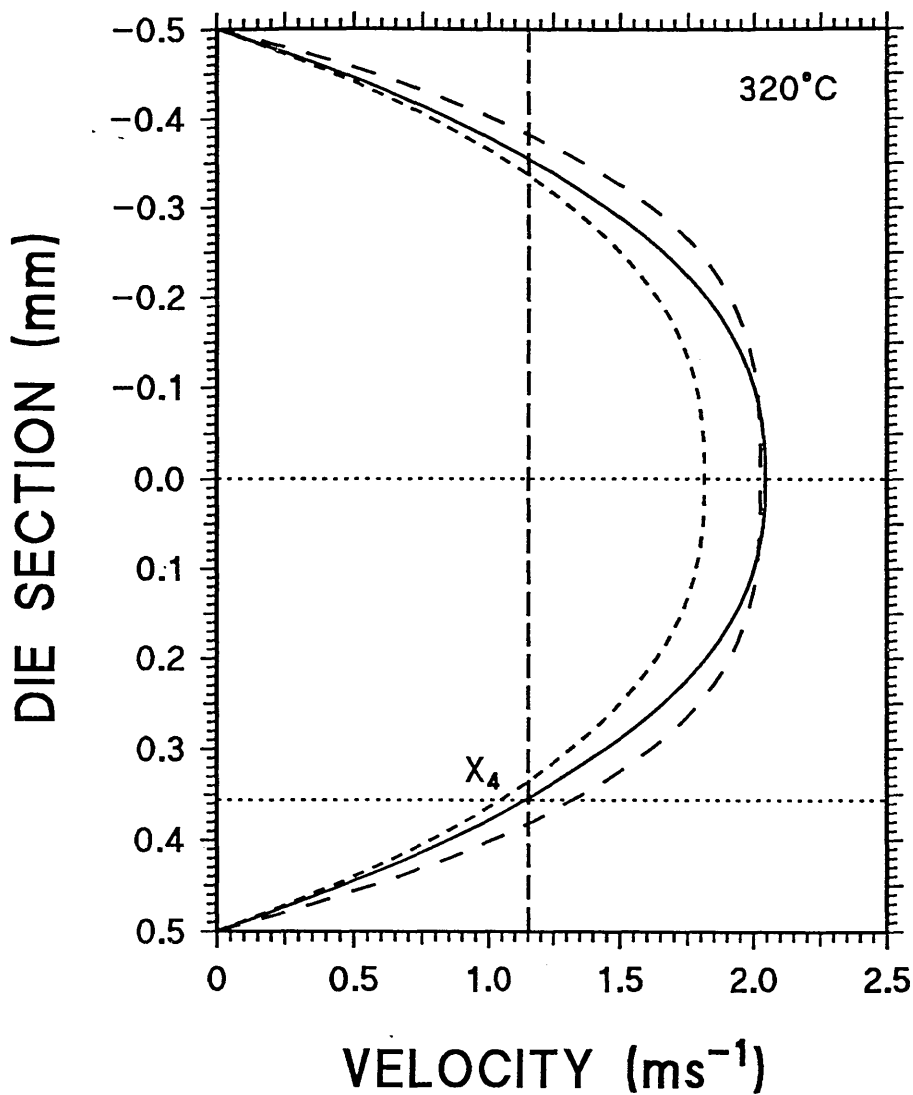
FIGURE 7.43 - Flow profiles for PC, 25% VECTRA in PC and VECTRA processed at 280°C and a shear rate of  $9000\text{s}^{-1}$ , showing the predicted interface position ( $X_2$ ).



KEY —

- — VELOCITY PROFILE OF 25% VECTRA/PC
- VELOCITY PROFILE OF PC
- VELOCITY PROFILE OF VECTRA
- — MEAN VELOCITY OF VECTRA
- ..... CENTRE LINE AND INTERFACE POSITION

FIGURE 7.44 - Flow profiles for PC, 25% VECTRA in PC and VECTRA processed at 320°C and a shear rate of  $3000\text{s}^{-1}$ , showing the predicted interface position ( $X_3$ ).



- KEY —
- — VELOCITY PROFILE OF 25% VECTRA/PC
  - VELOCITY PROFILE OF PC
  - VELOCITY PROFILE OF VECTRA
  - — MEAN VELOCITY OF VECTRA
  - ..... CENTRE LINE AND INTERFACE POSITION

FIGURE 7.45 - Flow profiles for PC, 25% VECTRA in PC and VECTRA processed at 320°C and a shear rate of  $9000\text{s}^{-1}$ , showing the predicted interface position ( $X_4$ ).

8.1 INTRODUCTION

The results showed that blending LCP's with the engineering matrix polymers selected gave blends with different rheological, physical and morphological properties. To aid research in this field a range of experimental tests were carried out to determine the characteristics of the base materials<sup>115,116</sup>, their blends and the subsequent change in properties, which are important in understanding what mechanisms occur during processing. Processing above the nematic transition temperature of the LCP and a critical composition ( $\approx 8\%$  LCP) the author noticed the formation of a definite skin/core effect in both extrudate and moulded samples (see figures 8.16 and 7.30). In an attempt to explain this a mathematical model was developed to predict the flow behaviour using processing conditions along with the shear thinning index and consistency constant. The author believes that as the blend passes through the die/gate region the extensional force causes the material to adopt its characteristic morphology (this effect would be enhanced by the acceleration of the outer skin region as the extrudate exits from the die). The ability to predict the final morphology using the flow behaviour would be invaluable in tailoring the resultant structure to one desired by the polymer processor. The data obtained from this model show the effect that processing variables have

on the interface position. The prediction was not as accurate as hoped (due to shear heating). The experimental result will now be discussed with reference to the current flurry of research activity in this area. The author will then attempt to bring together the separate sections as a whole and finally discuss the future development work which needs to be carried out.

## 8.2 RHEOLOGICAL TESTING

From the papers reviewed by the author it was noted that there were two methods of testing rheological characteristics. They give different morphologies and thus different rheological results. Rotational rheometers use shear rates which are several decades of shear rate lower than capillary rheometers; the same material is continually subject to shearing forces which induce the molecular architecture of the LCP to 'ball up'. Capillary rheometers use a testing process where new material is continually forced through a die (giving rise to both tensile and shear stresses). This leads to poor overlap<sup>117</sup> of the viscosity data between the two methods of testing. In capillary rheometers the extensional (tensile) forces align the backbone chains of the LCP. The orientated domains glide smoothly over one another lubricating the melt and causing an overall viscosity reduction. This allows polymers sensitive to thermal degradation to be processed at lower temperatures or confers polymers with the ability to fill larger or more complex moulds at the same temperature.

### 8.2.1 RHEOLOGY OF LIQUID CRYSTAL POLYMERS

The framework for the discussion of LCP rheology was initially postulated by Onogi and Asada<sup>63</sup>. A plot of  $\log \eta$  vs  $\log \dot{\gamma}$  gave a curve with three distinct regions I, II and III (see figure 4.9). In Region I the LCP exhibited shear thinning behaviour followed by Newtonian behaviour (Region II - a plateauing of the flow curve). In the final region (III) the LCP exhibited further shear thinning behaviour.

The  $\log \eta$  vs  $\log \dot{\gamma}$  plots for pure LCP's (see figures 7.3 and 7.4) demonstrate that the behaviour is not Newtonian. The downward slope indicates shear thinning behaviour. The three region flow curve is cited by many authors; Cogswell<sup>65</sup>, Chapoy et al.<sup>66</sup>, Prasadarao, Pearce and Han<sup>67</sup>. Cogswell mentions a 'three-zone' flow curve (referred to by Wissbrun<sup>76</sup>) but stated in this paper that he preferred to use the term two region (presumably region I was difficult to determine). Both Cogswell<sup>65</sup> and Prasadarao et al.<sup>67</sup> observed a yield stress (implying Bingham plastic behaviour) along with a 'pseudo-Newtonain' *behaviour* followed by a shear thinning region. Wissbrun<sup>76</sup> reported that PET modified with p-hydroxybenzoic acid had an observable yield stress which decreased and finally disappeared altogether as the processing temperature was increased.

Prasadarao et al.<sup>67</sup> carried out their research on copolyesters of PET and (PAB + HQTM). Plots of viscosity vs

shear rate showed Newtonian behaviour up to shear rate of  $100\text{s}^{-1}$ . Shear thinning behaviour became prevalent as the amount of (PAB + HQTm) was increased to 46% or greater. Similar behaviour was observed by Jackson and Kuhfuss<sup>24</sup> for PET modified with p-hydroxybenzoic acid.

Chapoy et al.<sup>66</sup> used the same nomenclature as Onogi and Asada<sup>63</sup> and stated that the director was aligned with the flow field above a critical yield stress  $\dot{\gamma}_c$  leading to a non-Newtonian regime, as in the model postulated by Currie<sup>118</sup>, which relates the capillary diameter and shear rate to the overall flow characteristics. Chapoy et al.<sup>66</sup> found that the rheological response of LCP's was irreproducible at very low shear rates in consecutive experiments. The behaviour was highly dependent on the previous thermomechanical history. Overall factors affecting the rheology were found to be temperature, previous thermal and shear history and the negative normal force values, as outlined by Gochanour and Weinberg<sup>119</sup>. They discovered that completely different results could be obtained for the same experimental conditions. This is due to the unpredictable behaviour of mono/poly-domain morphology.

### 8.2.2 RHEOLOGY OF LIQUID CRYSTAL POLYMER BLENDS

Work by Lee<sup>120</sup> showed that at low concentration of LCP there was an increase in the spiral mould flow and a decrease in die swell. Kohli et al.<sup>117</sup> looked at blends of PC

and an LCP based on HNA/HBA/TA/HQ (similar to the LCP's used in this study) and noticed that an addition of  $\approx 5\%$  LCP resulted in a 68% drop in viscosity. They found that the drop in viscosity was proportional to the amount of LCP in the blend over the range of shear rates studied (results which correlate to those of the current study). Tables 8.1-8.4 show the relative % reduction in viscosity for various compositions of PC blends (both SRP1 and VECTRA).

	SHEAR RATE $s^{-1}$	
	3000 $s^{-1}$	9000 $s^{-1}$
PC	100 %	100 %
4%	65 %	54 %
10%	59 %	48 %
25%	54 %	48 %
SRP1	28 %	29 %

TABLE 8.1 - Table to show the relative change in viscosity for PC/SRP1 blends at 300°C and shear rates of 3000  $s^{-1}$  and 9000  $s^{-1}$ .

	SHEAR RATE $s^{-1}$	
	3000 $s^{-1}$	9000 $s^{-1}$
PC	100 %	100 %
4%	96 %	93 %
10%	87 %	86 %
25%	81 %	80 %
SRP1	43 %	48 %

TABLE 8.2 - Table to show the relative change in viscosity for PC/SRP1 blends at 320°C and shear rates of 3000  $s^{-1}$  and 9000  $s^{-1}$ .

The reduction in viscosity in the current study was not as pronounced as that found by Isayev and Modic<sup>92</sup>. The LCP nematic transition temperature ( $T_n$ ), is 304°C for SRP1 processing at 300°C, means that the SRP1 is still partially unfused and should act as a particulate filler increasing the viscosity ignoring any shear heating effects.

	SHEAR RATE $s^{-1}$	
	3000 $s^{-1}$	9000 $s^{-1}$
PC	100 %	100 %
4%	61 %	47 %
10%	58 %	44 %
25%	54 %	41 %
VECTRA	20 %	20 %

TABLE 8.3 - Table to show the relative change in viscosity for PC/VECTRA blends at 300°C and shear rates of 3000  $s^{-1}$  and 9000  $s^{-1}$ .

	SHEAR RATE $s^{-1}$	
	3000 $s^{-1}$	9000 $s^{-1}$
PC	100 %	100 %
4%	96 %	91 %
10%	87 %	80 %
25%	81 %	76 %
VECTRA	30 %	25 %

TABLE 8.4 - Table to show the relative change in viscosity for PC/VECTRA blends at 320°C and shear rates of 3000  $s^{-1}$  and 9000  $s^{-1}$ .

Nishimura and Sakai<sup>93</sup> stated that if the blend was processed below  $T_n$  (LCP) the rheological characteristic of

the blend would be similar to the matrix. The need for an overlap of the processing temperature of the matrix polymer and the  $T_n$  is also cited by Lorenzo<sup>121</sup> and La Mantia et al<sup>122</sup>. The consequence of processing below  $T_n$  is a higher processing viscosity than the pure base matrix with no associated increase in mechanical properties, as seen in the current study.

The work by Nishimura and Sakai<sup>93</sup> involved blends of PC/PA and Vectra A950, the viscosity of the blend decreased linearly with increasing shear rate at any temperature. They found the melting temperature  $T_n$  of the VECTRA A950 was 275°C and demonstrated that the power law index 'n' varied with temperature. The index increased with increasing temperature and a large increase occurred at the melting temperature ( $T_n$ ) of the LCP. Table 8.5 below demonstrates the variation of the power law index for PC VECTRA and SRP1.

	PC	SRP1	VECTRA
300°C	0.52	0.31	0.71
320°C	0.65	0.24	0.64

TABLE 8.5 - Table to demonstrate the variation of shear thinning index with temperature for PC, VECTRA AND SRP1.

Nishimura and Sakai<sup>93</sup> noticed that if the LCP was processed below  $T_n$  the index was suppressed to a low value. When the processing temperature reached  $T_n$  'n' increased dramatically in value and eventually approximated to 1<sup>93</sup>.

The values for 'n' increase with increasing temperature for the PC and decrease for the LCP's. The author feels that this demonstrates the difference in molecular structure of the two polymers. Malik et al<sup>123</sup> carried out work on PC/LCP blend and also discussed the different molecular architecture. They postulated that because of the amorphous nature of PC it has a rapid decrease in modulus as the temperature reaches the glass transition temperature ( $T_g$ ). This was due to the nature of the polymer chains fixed in a 'quasi-lattice' with segments vibrating about fixed positions (see figure 1.1). As the temperature approaches the  $T_g$  the vibrational motions become more important leading to a decrease in modulus. The converse is found to be true for the LCP's contained within the blend whose relaxation modulus decreased slowly with time without passing through a real transition.

Siegmann et al<sup>90</sup> demonstrated that small additions of LCP (based on HNA/HBA - VECTRA/SRP1) to an amorphous polyamide resulted in a large reduction of viscosity from that of the pure polyamide. They observed that all melts exhibited non-Newtonian behaviour over the shear rates tested using capillary rheometry. James et al<sup>124</sup> observed that an addition of up to 20% of LCP to PES gave a four fold decrease in viscosity. The behaviour was Newtonian up to  $16s^{-1}$  tested on a rotational rheometer.

Isayev and Modic<sup>92</sup> and Nobile et al<sup>125</sup> noticed that over

all of the temperatures and shear rates investigated the viscosities of the blends at intermediate compositions were found to lie between those of the parent polymers. They stated that at high shear rate the blend curves lay between the curves for the pure PC and LCP curves for blends containing up to 25% LCP. This is in accordance with the work carried out in this study (see figures 7.5-7.7 and figures 7.12-7.16) of shear stress vs shear rate. The flow curves for 4-25% LCP lie between the parent curves and there was convergence at lower shear rates (see figures 7.12 and 7.13). Over all the shear rates studied the blend curves exhibited fairly linear behaviour ( $n \neq 1$ ) which could be approximated by the power law equation.

Isayev and Modic<sup>92,126</sup> found that the viscosities of blends of PC and LCP (HBA/HNA) had a range of viscosity curves which lay between the parent curves for all compositions of 25% and less, as in this study. They used scanning electron microscopy and determined at low shear rates that the LCP formed small spherical particles within the parent PC matrix. A yield stress was observed for the pure LCP's at low shear rates; it was not surprising that a yield stress was also apparent in blends containing LCP's. Isayev and Modic discovered that the yield stress and viscosity decreased with additions of LCP up to 5% and monotonically increased above this value in agreement with patent literature<sup>1</sup>.

Nobile et al<sup>125</sup> explained the phenomenon of intermediate viscosities by observing extruded samples using electron microscopy. They found that at concentrations of 5-10% the LCP domains were of the order of a few microns in diameter with little elongational deformation. The work also indicated that above a critical concentration and temperature a fine fibrous network (LCP) was set up within the matrix.

Chung<sup>127</sup> noticed there was a minimum viscosity ( $\approx 10\%$  LCP) and a maximum viscosity ( $\approx 20\%$  LCP) for blends of HNA/HBA and Nylon-12. Below 10% Chung discovered that the LCP domains were well dispersed with the Nylon 12 matrix and acted as a lubricant. The LCP formed an interpenetrating network (see figure 5.1) which led to a sharp increase in viscosity at  $\approx 20\%$ . It was theorised that VECTRA/PC blends (A950 VECTRA) formed miscible blends at concentrations less than 10% and partly miscible blends above this concentration<sup>123</sup>.

The authors found no viscosity minima as cited in several texts<sup>90,128</sup> and proposed that the elongation was insufficient to give an acceptable surface area for slip to occur. The graphs of viscosity vs concentration (figures 7.17-7.20) show how addition of LCP to the blend lead to a reduction in viscosity. This was true for all the blends tested<sup>117</sup>.

Malik et al<sup>123</sup> stated that a blend containing only 10% LCP had behaviour intermediate between the LCP and PC. Small additions of LCP significantly influenced the relaxation behaviour of PC over several decades of shear (see ICI patent<sup>1</sup>). The author is in agreement with the results of Malik et al<sup>123</sup>, although the results from the current study did not exhibit the same magnitude. The difference in experimental results are possibly due to the different blending processes. Malik et al, pre-blended the polymers for 15 minutes in a Plasticorder, whereas the blends in this study were processed twice allowing the blend to cool in between processes. It is evident from the work carried out that the previous thermal history has a direct bearing on the resultant rheological characteristics. The author was unaware at commencement of the study of the effect of pre-blending history on subsequent testing (an attempt was made to minimise this affect by treating all of the base materials in a similar manner).

The LCP/PES blends containing 20% glass fibres and tested on a Rosand capillary rheometer were found to have higher viscosities than the corresponding unfilled blends. The LCP was effective in reducing the viscosity of the glass filled blends as in the unfilled blends. It is useful to note that the increase in viscosity encountered by the addition of traditional filler could be countered by the addition of LCP. The LCP also increases the orientation in

the flow direction (in the outer skin regions). The only major drawbacks foreseen are that the weld line and transverse strength of finished mouldings may be less than the base material.

### 8.3 DIE SWELL

Metzner and Prilutski<sup>129</sup> stated in their paper that LCP's do not exhibit the strain hardening found in Newtonian fluids (where the Trouton ratio = 3). The materials were so inelastic that they exhibited die swell less than that observed for Newtonian fluids. It is known that die swell is related to both the elastic properties of the melt and the velocity profile within the die. At concentrations above 10% there was evidence of this phenomenon<sup>75,76</sup>. Minimal die swell was seen in the majority of samples and is attributed to the long relaxation times of the LCP's coupled with their ability to resist elastic recoil and elongation. The stiff elongated LCP domains act against the natural recoil of the matrix reducing the die swell. The addition of LCP's to engineering polymers can therefore produce blends with less shrinkage, warpage and higher dimensional accuracy.

### 8.4 SHEAR HEATING

The pressure forces on a fluid as it is forced through a capillary causes a change in the internal energy. This results in an increase of the ambient temperature of the fluid. The amount by which the fluid increases in

temperature is seen below in equation 8.1:-

$$\Delta T = \left( \frac{\Delta P}{\rho C_p} \right) \quad (8.1)$$

where :-

$\Delta P$  - is the pressure drop across the die (MPa)

$C_p$  - is the heat capacity at constant volume  
(J kg<sup>-1</sup> K<sup>-1</sup>)

$\rho$  - is the density (kg m<sup>-3</sup>)

$$\tau = \frac{\Delta P}{4 \left( \frac{l}{d} \right)} \quad (8.2)$$

combining the two we have :-

$$\Delta T = \frac{4\tau \left( \frac{l}{d} \right)}{\rho C_p} \quad (8.3)$$

where :-

$l$  - is the length of the die (m)

$d$  - is the diameter of the die (m)

Equation 8.3 is a simplified equation and can only be used as an estimate (i.e. it assumes no heat is lost through the wall). Heat is not generated uniformly across the extrudate, the amount of heating is directly proportional to the local shear rate and shear stress. The temperature rise is greater at the die wall (where the

shear rate and shear heating are higher) than at the core. This localised heating effect causes the LCP close to the die wall to have a lower viscosity leading to a local slip/stick effect giving a further apparent reduction in viscosity. The local increase in temperature could also be responsible for the different morphology of the LCP at the surface (see figure 7.41A→C), for extrusion temperatures close to  $T_n$ .

## 8.5 FLOW BEHAVIOUR OF LIQUID CRYSTAL POLYMERS

The results showed that the domain texture of the LCP had a significant effect on the rheology and morphology of the final blend. The previous processing history had a bearing on the domain texture and it has become apparent that the pre-testing history is as important as the subsequent testing.

LCP's have long relaxation times<sup>71,76</sup> when compared with conventional polymers. Tensile flow aligns the LCP; the long relaxation times involved do not allow the LCP to relax. The flow process is not sufficiently strong to compete with previous thermal history which has a direct bearing on subsequent testing. Standard polymers with shorter relaxation times are affected by the shear rate to a greater degree. The interplay between the director and velocity gradient gives rise to viscous and elastic stresses modelled by both Frank<sup>129</sup> and Ericksen<sup>130</sup>. Papers by Cogswell<sup>65</sup> and Wissbrun<sup>76</sup> demonstrate quite clearly the

difference in morphology/texture for the LCP in the quiescent and post stressed states. At the onset of flow adjacent domains (LCP) have a similar overall orientation: Kiss<sup>131</sup> uses an analogy whereby the structure of the LCP is represented by uncooked spaghetti and the engineering based polymers are represented by cooked spaghetti. It shows that the domains must move together co-operatively since the transformation from a poly-domain to mono-domain material involves the removal of the 'grain boundaries' or disclinations<sup>66</sup>.

The resistance to subsequent flow becomes smaller as the domains are broken down, leading to an increase in interfacial area. This process continues until finally the poly-domain morphology breaks down completely<sup>65,76</sup>. The tensile forces at the entry region to the die cause the constituent intransigent rods within the domains to line up almost parallel with one another (in the flow direction) leading to an elongated LCP morphology. Shearing forces (rotational component) lead to many smaller domains or nemata to be produced<sup>65</sup>. In the shear region of the capillary the elongated phase can either relax back into a spherical morphology or break up into smaller spherical droplets (see figures 8.1-8.3) as a consequence of competition between viscous and interfacial forces<sup>117</sup>. High extrusion rates and very short dies<sup>117</sup> (high capillary aspect ratios) develop and maintain a dispersed LCP morphology with little or no orientation. Low capillary



FIGURE 8.1 - Micrograph of 20% VECTRA/PES  
processed at 310°C and a shear  
rate of  $\approx 9500\text{s}^{-1}$   
MAGNIFICATION x 40

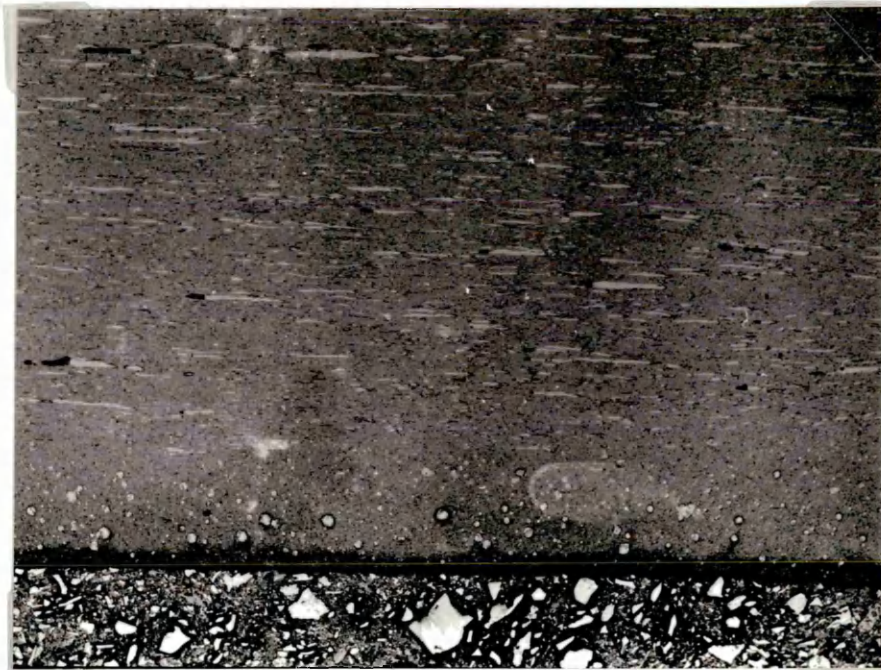


FIGURE 8.2 - Micrograph of 20% VECTRA/PC  
processed at 310°C and a shear  
rate of  $\approx 9500\text{s}^{-1}$   
MAGNIFICATION x 150

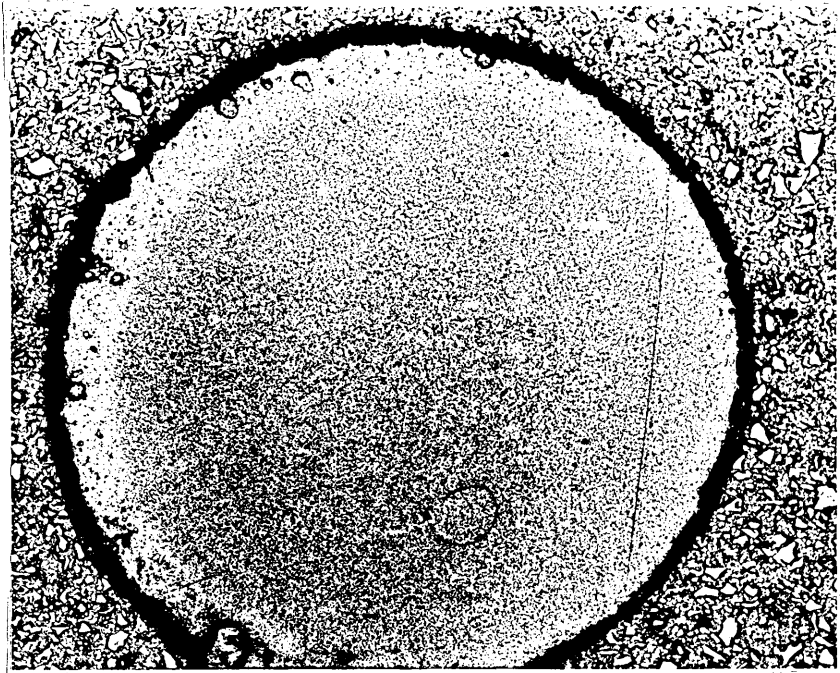


FIGURE 8.3 - Micrograph of 20% VECTRA/PC processed at 310°C and a shear rate of  $\approx 9500\text{s}^{-1}$   
MAGNIFICATION x 40

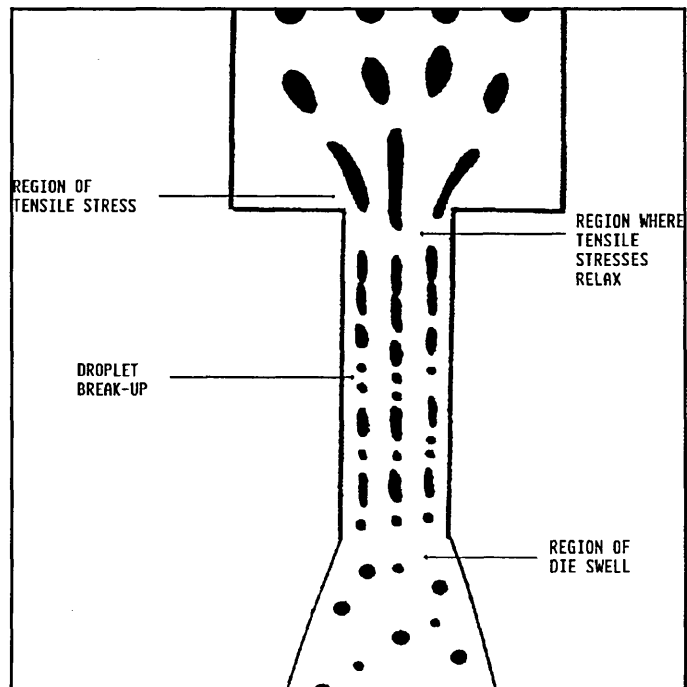


FIGURE 8.4 - Die swell figure showing LCP domain break-up.

aspect ratios lead to the LCP domains becoming more elongated (see figure 8.4).

Weiss et al<sup>132</sup> stated in their paper that additions of LCP to PS gave rise to an increase in viscosity. The authors postulated that the increase was due to rotation and tumbling of phase separated LCP regions at low shear rates as stated by Marrucci<sup>133</sup>. At higher shear rates the viscosity decreased with increasing LCP content because the LCP does not have time to relax and is drawn into the blend in the form of fibres by the tensile forces in the entrance to the die region<sup>92</sup> (see figure 8.4). Tensile forces coupled with lack of time to rotate lead to extensional deformation, which lubricates the flow and gives an overall reduction of viscosity.

This type of behaviour is also cited by Acierno et al<sup>134</sup> in their work blending LCP's with PS, PC and Nylon-6. They noticed that two different dies of L/D=7.8 and L/D=21 gave a change from a fibrillar to a droplet morphology; for dies with a high L/D ratio and low shear rates the LCP domains were spherical. If the L/D ratios were increased the LCP domains became more elongated. The viscosities of all of the PS/LCP blends were higher than the pure PS at low shear rates. They justified this behaviour in terms of morphological observations. The authors found that the LCP existed as spherical domains which were not deformed by the shear field at low shear rates. An increase in viscosity

was therefore due to the additional energy needed, because of the rotation and tumbling of the domains<sup>133</sup>. The converse was found at high shear rates; the viscosity of the blend decreased with increasing LCP concentration. The viscosity drop was attributed to the fact that at higher shear rates the LCP domains were deformed and orientated in the entrance region of the die<sup>134</sup>.

Min, White and Feller<sup>135</sup> stated in their paper that blend morphology was strongly dependent on the differences in polarity of the constituents in terms of interfacial and viscous forces. A droplet to fibre transformation occurred in Newtonian fluids. The major parameter was the viscosity ratio; close to unity many thin fibrils were formed throughout the cross-section that did not break up as the tensile forces relaxed. Work using PE/PS blends showed that droplets were formed when the viscosity ratio ( $\lambda$ ) was greater than 2.2 (i.e too high to elongate). When the dispersed phase was less viscous than the continuous phase the droplets were elongated into long fibrils running parallel to the flow direction (which did not break up provided  $\lambda < 1$ ). Deformation only occurred at very large applied stresses when the dispersed phase was more viscous than the matrix. This makes LCP ideal for fibril formation although it must have a sufficient modulus at the processing temperature and pressure to overcome fibre breakup.

Work by Perkins et al<sup>136</sup> stated that fibrillation would occur if the viscosity ratio  $\lambda$  of the two polymers was greater than or equal to 1. More recent papers by Isayev and Modic<sup>92,126</sup> stated that the fibrillation of the LCP within the matrix became a maximum where the ratio of the viscosities approached unity, in accordance with the results of Seigmann et al<sup>90</sup>. Other workers in the field have been more specific, Tsebrenko et al<sup>137</sup> observed an optimum viscosity ratio range of  $0.76 \leq \lambda \leq 0.91$ . Fibres were formed for  $\lambda < 1$  but they broke up into smaller segments. If  $\lambda \approx 1$  then break-up was minimised.

The current study showed that the viscosity ratio approached unity at low shear rates. Figure 8.5 is a micrograph of 20% SRP1 in PC processed at 280°C processed using a shear rate of  $9500\text{s}^{-1}$ , which shows lack of fibres in the core region. Figure 8.6 shows the same composition processed at the lower shear rate of  $3200\text{s}^{-1}$  and a higher temperature of 310°C. The two figures clearly demonstrate that the blend must be processed above the melting temperature of the LCP and the formation of fibres is not necessarily a function of shear rate.

## 8.6 SKIN-CORE MORPHOLOGY

The existence of a skin-core morphology in injection mouldings is not a new concept. It has been reported for many different polymers under a range of different processing conditions. Clark<sup>138</sup> demonstrated that



FIGURE 8.5 - Micrograph of 20% SRP1/PC processed at 280°C and a shear rate of  $\approx 9500\text{s}^{-1}$   
MAGNIFICATION x 2500

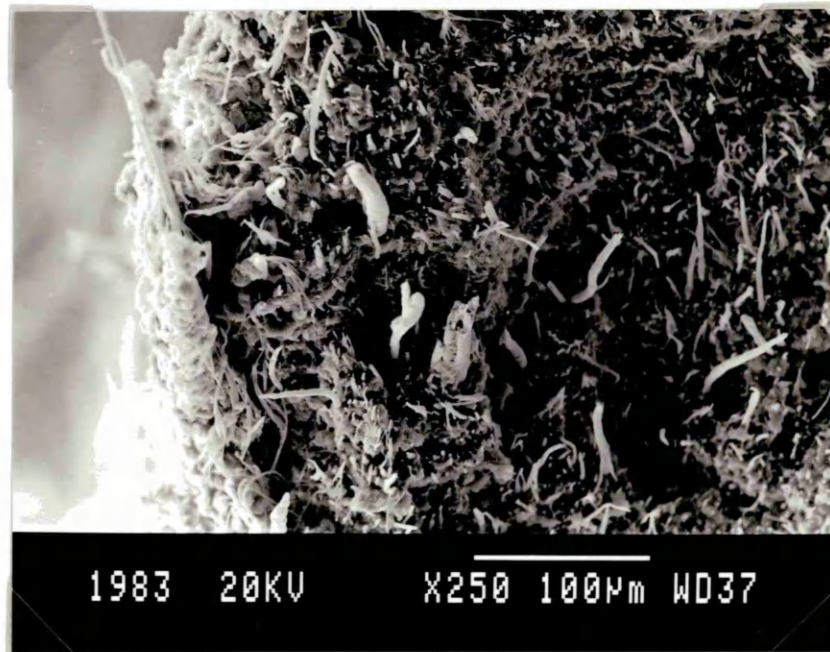


FIGURE 8.6 - Micrograph of 20% SRP1/PC processed at 310°C and a shear rate of  $\approx 3200\text{s}^{-1}$   
MAGNIFICATION x 250

crystallisation coupled with quench kinetics was responsible for a skin-core morphology in polyoxymethylene. McNally<sup>139</sup> stated that the orientation distribution of short glass fibres in a Nylon injection moulding were highly complex and gave rise to a layered structure with up to six separate distinct macro-layers. Callear and Shortall<sup>140</sup> studied the macro-morphology of injection moulded (PTMT) a semi-crystalline thermoplastic. They discovered four distinct macro-layers each with a distinct character even though the material in question was not fully liquid crystalline. Several authors have reported three distinct layers, two skin regions and one core region. Work by Weng et al.<sup>53</sup> involved studies of thermotropic liquid crystalline material and found three distinct regions, two skin\$which sandwiched a core, each representing approximately one third of the total thickness. Their work also demonstrated that the transition between the skin and core can be sharp, with a definite border as found in this study (see figures 8.1-8.3 and 8.7-8.8)<sup>141</sup>. Research by Ophir and Ide<sup>80</sup> into the injection moulding of thermotropic liquid crystalline material found four distinct regions, a light skin layer, a dark skin layer, a layer in which flow traces or 'arcs' were observed and a final unorientated core region.

The work cited shows that other authors in the field have observed similar macro-morphologies to the ones obtained in this study. The author found a characteristic skin/core morphology in all samples produced as discovered

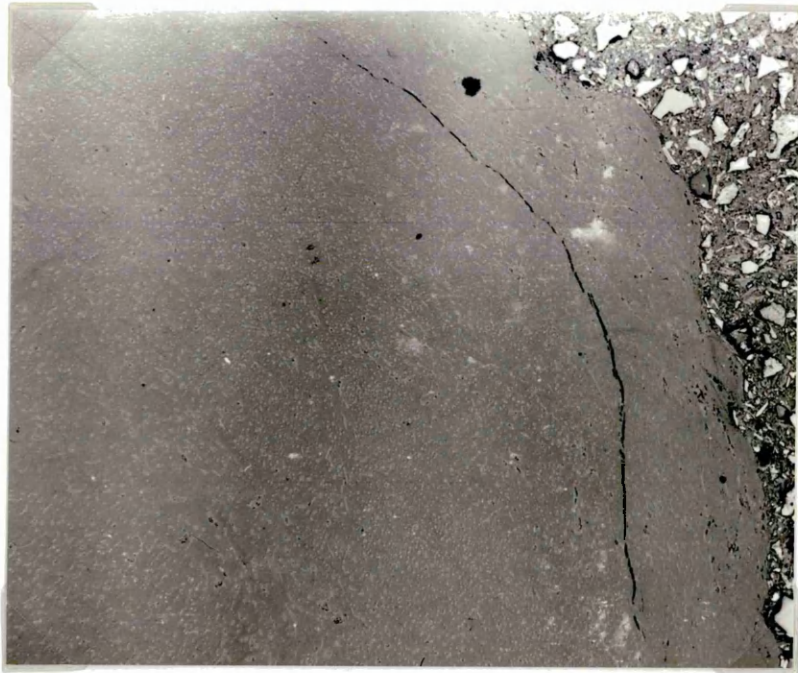


FIGURE 8.7 - Micrograph of 20% VECTRA/PES  
processed at 300°C and a shear  
rate of  $\approx 3200\text{s}^{-1}$   
MAGNIFICATION x 150



FIGURE 8.8 - Micrograph of 20% VECTRA/PES  
processed at 340°C and a shear  
rate of  $\approx 3200\text{s}^{-1}$   
MAGNIFICATION x 150

by Heino and Seppälä<sup>142</sup>.

#### 8.6.1 SKIN MACROLAYER

It was Tadmor<sup>143</sup> in 1974 who postulated that the fluid particles which hit the cold mould wall/die will immediately solidify, freezing in the orientation induced by the elongation of the flow they have experienced. The magnitude of the orientation depends on the rate of elongation (once unstressed this orientation is rapidly lost). The 'outer' skin region made up of the first material into the mould will retain a higher degree of orientation than the core (which fills in a plug flow type manner). Kantz<sup>144</sup> worked with Polypropylene and discovered that the skin region of extruded samples containing LCP with a high aspect ratio and a less orientated 'spherulitic core'. Liquid crystal polymers are aligned easily in extensional flows and retain this alignment; there is a high degree of extension force at the flow front. This is due to the 'fountain flow'<sup>73,80</sup> phenomenon (see figure 3.5). The extensional forces at the flow front extend the LCP backbone chain giving a micro-morphology in which there is a high degree of molecular orientation. This in turn allows adjacent chains to pack very closely.

From the research it was possible to see the high degree of orientation in the surface layers of injection mouldings (see figure 8.9). In samples which contained amounts of liquid crystal polymer between 8%-25% it was

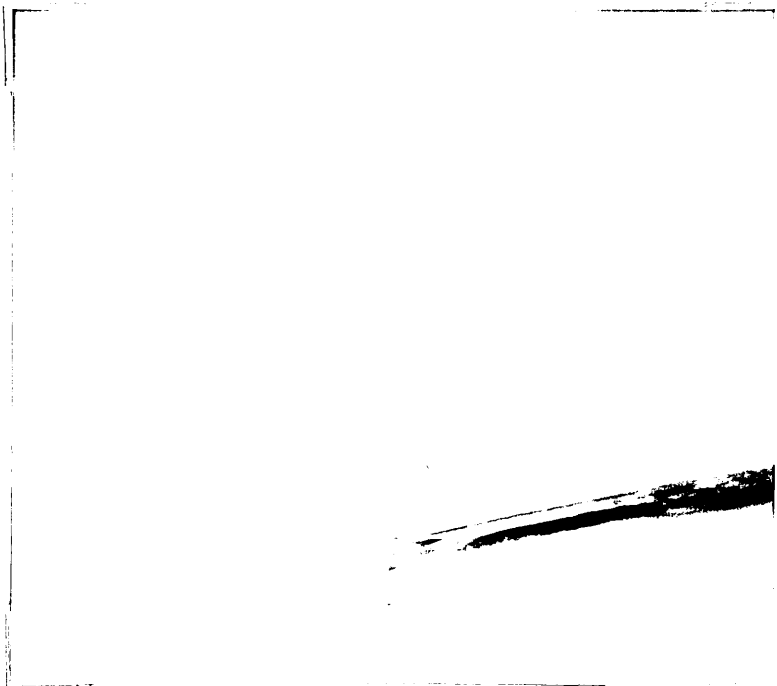


FIGURE 8.9 - Photograph of fracture tensile specimen of 25% SRP1/PES processed at 330°C and a shear rate of  $\approx 9000\text{s}^{-1}$   
MAGNIFICATION x 0.6

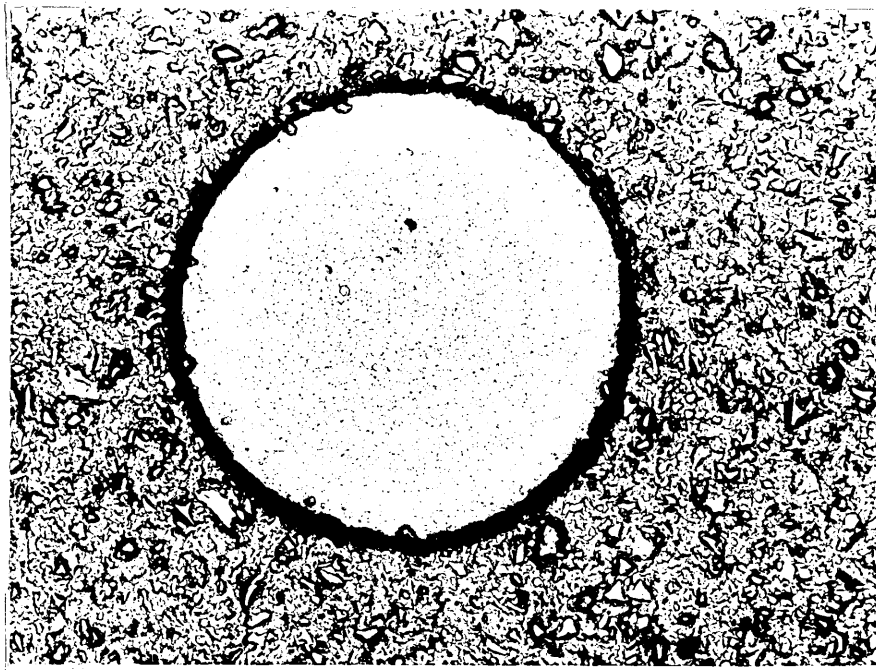


FIGURE 8.10 - Micrograph of 25% VECTRA/PES processed at 340°C and a shear rate of  $\approx 9500\text{s}^{-1}$   
MAGNIFICATION x 30

possible to separate the 'outer' skin layers (by exfoliation) using tweezers (indicating a high degree of orientation). The 'outer skin' region or Band I was in the order of 10-20 $\mu$ m. The peeling back of layers was repeated for several successive layers until the next region was reached described by Callear and Shortall<sup>140</sup> as Band II. Samples peeled off the surface were examined and found to have excellent mechanical properties in the flow direction with very poor mechanical properties in other directions. Individual fibres had been drawn out forming a number of 'pleated sheets'<sup>145</sup>. The sheets differed in average orientation with respect to one another with the orientation becoming less pronounced nearer to the core.

The degree of bonding from skin to core progressively improved, indicating that the orientation within the 'sheets' became less pronounced the closer to the core samples were taken. This was different for the capillary produced samples. The material next to the die wall was not subject to the same degree of extensional force as the shear rates were lower. The forces on the polymer in the outer surface were more rotational (at low shear rates) as opposed to elongational. This gave rise to spherical LCP morphology in the outer layers as cited by Marrucci<sup>133</sup>. It was also noted that for the same blend composition, an increase in temperature did not cause an associated increase in the size of the outer band. There was a sample which did not follow this rule (see figure 8.11), the

reason for this is not fully understood by the author.

The close proximity to which the molecules are aligned in the outer most skin region reduces the ability of solvents (water) to enter the moulding. This in turn gives the finished component increased solvent resistance. Work by Kantz, Newman and Stigale<sup>146</sup> found that polymers containing units with a high aspect ratio had better chemical resistance to oxidising agents and solvents. If the architecture was such that the molecules were acicular (had a high aspect ratio) they could pack very closely together preventing the absorption of solvents and giving excellent barrier properties. It may be possible for solvents to enter through the less well packed skin region if the backbone chain is disrupted using a mechanism such as kinks or crankshaft monomers (discussed earlier). The ability of the liquid crystalline polymer/PES blend to resist absorption of water (see figures 7.35 and 7.36) becomes superior as the amount of liquid crystalline material in the blend is increased.

The next region was found to contain a series of layers which were thicker and more fibrillar in nature. The layers became more difficult to separate and on stressing they tended to 'break-up' into fragmented pieces. The thickness of these sheets were in the order of 50 $\mu$ m. The total thickness of the skin layers was found to be approximately  $\approx 0.04$ mm for injection mouldings (see figure

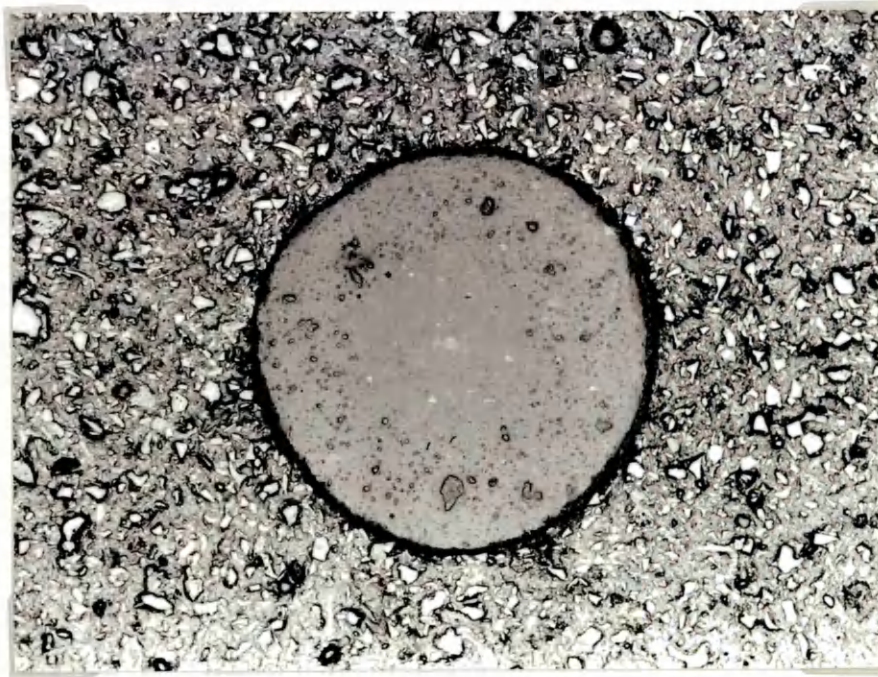


FIGURE 8.11 - Micrograph of 25% VECTRA/PES processed at 340°C and a shear rate of  $\approx 9500\text{s}^{-1}$   
MAGNIFICATION x 30

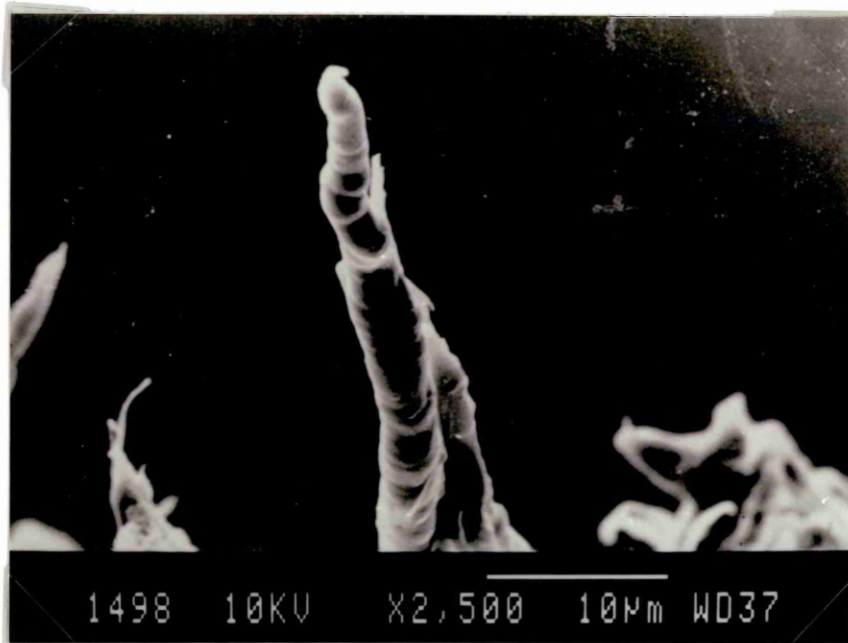


FIGURE 8.12 - Micrograph of 20% VECTRA/PC processed at 280°C and a shear rate of  $\approx 5200\text{s}^{-1}$   
MAGNIFICATION x 2500

7.31). In samples taken from capillary rheometry the outer skin region was found to be in the order of 150 $\mu\text{m}$  in thickness. This indicated that as rate of processing increased (shear rate) so the thickness of the skin region decreased in thickness, but increased in modulus giving superior mechanical properties in the flow direction.

The layers can be sub-divided further and further until finally fibres of diameter  $\approx 0.5\mu\text{m}$  are observed<sup>53,131,145</sup> (see figure 3.6 and 3.7). A fibre of this diameter was observed in a sample obtained in a capillary processes sample of a 20% VECTRA/PC blend processed at 280°C and 5200  $\text{s}^{-1}$  (see figure 8.12). Other capillary samples of blends containing 20% SRP1/PC blend processed at 310°C/280°C and 3200/9500  $\text{s}^{-1}$  showed many fibres of diameter  $\approx 0.5\mu\text{m}$  (see figure 8.13 and 8.14). It is reported that the micro-morphology goes even further than the results observed in this study. Chivers et al,<sup>48</sup> observed order down to a molecular level which goes beyond the scope of the work carried out in this study.

#### 8.6.2 CORE MACROLAYER

The core section is made up of the material which passed through the gating region/die after the skin region had formed. The skin region is subject to a large elongational force; the core region is subject to shearing forces which produces little if any orientation in liquid crystalline material. The core region represents the



FIGURE 8.13 - Micrograph of 20% SRP1/PC processed at 310°C and a shear rate of  $\approx 3200\text{s}^{-1}$   
MAGNIFICATION x 1000

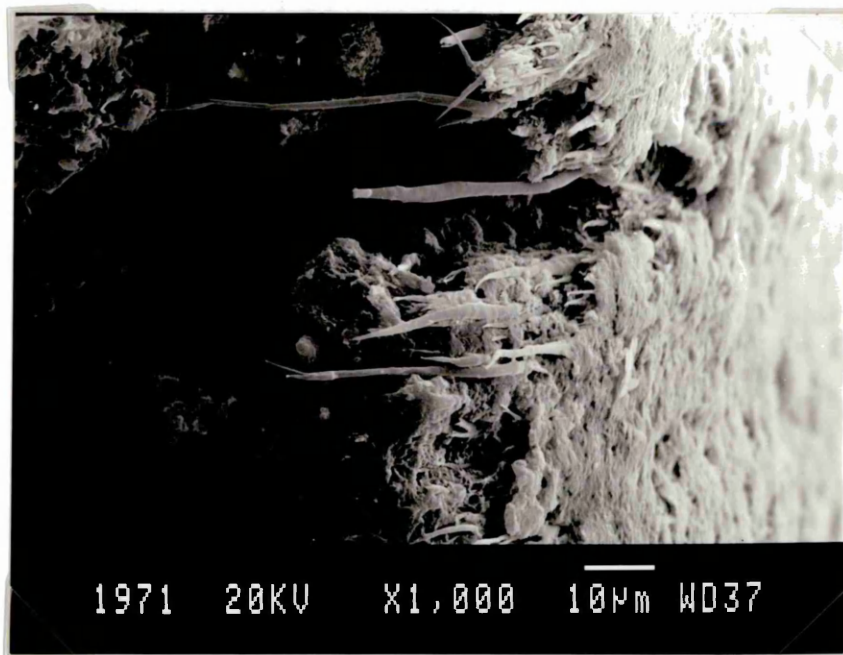


FIGURE 8.14 - Micrograph of 20% SRP1/PC processed at 280°C and a shear rate of  $\approx 9500\text{s}^{-1}$   
MAGNIFICATION x 1000

remaining section sandwiched between the two skin layers. The core can be split into two macro systems, Bands III and IV<sup>140</sup> or layers C and D<sup>80</sup>. The material in these regions is not orientated to the same degree as the skin and has lower values of modulus (in the flow direction).

Both Ophir and Ide<sup>80</sup> and Callear and Shortall<sup>140</sup> noticed that the outer core section exhibited 'flow arcs'. The cross-sectional samples produced in this study were polished to a 1µm diamond grit finish (no flow lines were observed as etchants were not used). Callear and Shortall<sup>140</sup> stated that the flow lines in the third region were caused by onset of solidification, during the filling of the mould by 'plug flow'. The subsequent increase in viscosity gave variations in crystallinity and thus flow contours which became visible on etching. It was also stated that the degree of orientation within the third region was much less than in the skin layers.

The final central core is the last space to be filled with material. It also has the longest time to relax being the most insulated. The material in this region is the most coarse and the least orientated (see figure 7.32). The average orientation in the outermost skin layers was reported to be within degrees of the flow direction (i.e very highly orientated). The orientation of the material along the centre line of the moulding has been discovered by some authors to be at 90° to the flow direction<sup>53</sup>.

Bearing in mind the orientation at the various points throughout the section, the tangent to the flow curve at any point gives an indication to the orientation at that point compared to the flow direction. This forms the basis of the mathematical model (orientation within the die) and will be discussed more fully later.

## 8.7 MIGRATION

Vinogradov et al<sup>147</sup> working with PE/PS blends discovered lateral migration. They noticed a layer of PE forming a 'jacket' (skin) on the extrudate surface. The authors stated that the migration was enhanced when processing through dies with a higher L/D ratio due to higher compressive forces exerted on the polymer in the die region. Early work by Collyer et al<sup>148</sup> sought migration in PES/PDMS blends but none was discovered using EDAX mapping for silicon. The results did not show any significant migration of the silicon rich phase as is observed by the work in this study (see figures 7.41). Polished sections of PC/LCP blends showed LCP in the outer section (see figure 8.11). This micrograph clearly demonstrates large regions of LCP confined to a band (macro-skin section) around the outside of the extrudate. This micrograph in itself does not prove migration, but it clearly demonstrates the spherodised morphology commonly adopted by the LCP.

Blizard and Baird<sup>95</sup> noticed migration in blends

containing liquid crystal polymer and polycarbonate. They discovered a higher concentration of LCP in the outermost skin regions. The authors stated that the reason for this was due to the lower viscosity of the LCP. Verhoogt et al<sup>149</sup> also noticed a similar effect in a blend containing LCP and SEBS (a thermoplastic rubber). They found a greater concentration of LCP in the skin layers and attributed this to the fact that the LCP had a lower viscosity. Weiss, Huh and Nicolais<sup>150</sup> worked with LCP and Polystyrene and found a higher concentration of LCP in the skin layers. Joseph, Wilkes and Baird<sup>73</sup> looked at the flow history of a pure LCP containing PET and HBA and found that the lower viscosity HBA was more plentiful in the skin regions.

Chaffey<sup>151</sup> showed that the lateral migration of deformed liquid drops in an elastic-viscous fluid is towards the tube axis; in shear thinning liquids an equilibrium position is set up between the tube axis and the wall. Gauthier et al<sup>152</sup> observed physical effects involving rigid/deformable spheres in Newtonian fluids. They found that spheres close to the die wall were subject to rotational forces, in agreement with Marrucci<sup>133</sup>. They found that the spheres migrated to the tube wall in pseudoplastic liquids and towards the tube axis for elasticoviscous systems and that deformable particles migrated towards the tube axis during flow at very low Reynolds numbers.

'Drops initially close to the tube axis migrated towards the wall and those initially close to the wall migrated towards the tube axis. The migration rates in both directions decreased with time until an equilibrium position was reached'.

Work by Mantia and Paci<sup>153</sup> stated that in blends of LCP (VECTRA B950) and Nylon-6 the LCP migrated in the die region towards the polymer-metal interface, decreasing the friction factor and resulting in an overall reduction of viscosity. They used examples of a reduction of torque and an increase in flow rate to substantiate this theory.

It is possible that the lower viscosity polymer (LCP) is 'squeezed' from the blend rather like water is pressed from a sponge, leaving the LCP free to act as a lubricant at the die wall and reducing the frictional forces to give a lower overall viscosity. Shih<sup>154</sup> attributed the lowering of viscosity to slip at the die wall where the dispersed LCP phase provides a large area over which slip can occur. The degree of slip increases at higher shear rates leading to a lower viscosity and shear thinning behaviour. The 'core' simply passed through the die in a plug type fashion lubricated by the low viscosity component; commonly seen in the extrusion of gun propellant cords. The higher the shear rate the more pronounced was the difference in the skin/core transition. Injection moulded samples and capillary extrudates processed at high shear rates had a

pronounced crack which ran laterally around the sample edge (figures 7.30, 7.31 and 8.7). Capillary samples produced at low shear rates did not suffer from this problem, but there was less orientation (along the flow direction).

The author found no real evidence to suggest that migration of the LCP to either the skin or core was taking place. Instead it is proposed that the LCP imposed a more aligned morphology on the matrix (see figures 7.41). The presence of the LCP improves barrier properties and gives a skin/core morphology in the processed specimens. The skin/core morphology accounts for the change in mechanical properties.

## 8.8 PHASE EQUILIBRIA

From results obtained over a range of shear rates all of the blends tested showed negative deviation behaviour from the log additive rule (see figures 7.17-7.20). The author is in agreement with the comments made by Utracki<sup>94</sup> and Shih<sup>154</sup> that the viscosity reduction of the blend is due to:-

- i) the entrance region of the capillary die; and
- ii) wall slippage (slip-stick effect)<sup>155</sup>.

Lack of adhesion between segregated domains of the two polymers resulted in slippage. To give the maximum effect it is necessary to maximise the area over which slip can occur. Total compatibility is therefore not desirable. The

region between the binodal and spinodal provides the best conditions for slip between the two phases.

### 8.9 MISCIBILITY

It is known that two polymers will co-exist on a molecular scale with no tendency to separate if the molecules of the two materials are compatible. A measure of this co-existence or compatibility is the Hildebrand solubility parameter, which is defined as follows :-

$$\delta = \left( \frac{L-RT}{M/D} \right)^{\frac{1}{2}}$$

where :-

- δ = solubility parameter
- L = latent heat of vaporisation
- R = gas constant
- T = absolute temperature
- M = the molecular weight
- D = the density

POLYMER	SOL <sup>y</sup> PARAMETER (MJ/m <sup>3</sup> ) <sup>1/2</sup>
PES	22.6
PC	19.4

TABLE 8.6 - Table of the solubility parameters for PES and PC.

It is possible to determine whether or not the two materials constituting the binary blend are compatible

using the solubility parameter. If the values for the solubility parameter overlap by within  $\approx 2 \text{ (MJ/m}^3)^{1/2}$  they should be compatible. Table 8.6 gives the solubility parameters for PES and PC.

The LCP's used in this study have much higher values of solubility parameter than PC and PES as calculated using Small's table<sup>98</sup>. The difference in solubility parameters meant that the LCP's and matrix polymers used in this study were not compatible as found by Lenz et al<sup>156</sup>. Solubility data are usually obtained by dissolving the two polymers in a common solvent and then drying them. The author is aware of the danger of using the results obtained in the laboratory to explain the miscibility of highly viscous polymer blends during processing. In support of this theory the SEM EDAX micrographs (see figures 7.41) demonstrate that the two phases were not compatible. This could also be seen in the optical microscopy results; polished extrudate samples of longitudinal sections revealed dark 'pits'. The pits were found to be regions where the LCP had fallen from the matrix during the polishing process (see figures 8.1 and 8.2)<sup>136</sup>. These figures show the poor degree of adhesion between the two phases for such samples. Transmission light microscopy of thin microtomed sections revealed poor compatibility between the LCP (especially VECTRA) and the matrix polymer (see figures 7.37 and 7.38). The two polymers were distinct and separate. It should be pointed out that SRP1 and PES 'appeared' to be partially miscible at low concentrations of SRP1 (the SRP1 adopted

a small dispersed morphology). This was evident (see figure 8.16) in the injection moulded samples 2% and 4% of SRP1 in PES, which were translucent. The blends containing VECTRA were not translucent and additions as small as 2% VECTRA resulted in an opaque moulding (the morphology of the VECTRA was less discrete with larger particles, possibly due to the hydrogen bonding of the amino-phenol component). This accounts for the superior mechanical properties of the SRP1/PES blends at low concentrations of SRP1.

#### 8.10 BINODAL/SPINODAL DECOMPOSITION

In systems with marginal miscibility (blends in the vicinity of binodal) there is a strong correlation between flow mechanics and thermodynamics. Their interaction is evident in that flow affects phase separation which in turn affects the rheological properties. Lipatov<sup>106</sup> stated that there was a limited miscibility at low concentrations (<10%). He studied blends of polyoxymethylene (POM) mixed with both celluloseacetatebutyrate (CAB) and polyethylene (PE). In the approximate position of the binodal/spinodal he discovered unusual rheological characteristics. The blend exhibited negative deviation behaviour in the propinquity of the binodal determined from a plot of heat of mixing vs concentration. From this he stated that the reason for the negative deviation behaviour was due to an expansion in the free volume.

In summary the author believes that the <sup>spinel.</sup> decomposition mechanism has a bearing on the morphology and thus the rheological characteristics of the blend. Further understanding of the interactions of the two materials would be necessary to model this behaviour. This is the reason that the author has attempted to model the behaviour of the 'macro' system in this study.

#### 8.11 MECHANICAL PROPERTIES

Malik et al<sup>123</sup> looked at the effect of shear rate on the Tensile modulus of polycarbonate blends. It was discovered that the modulus of polycarbonate mouldings were largely unaffected by the shear rate. The same results were obtained at increased processing temperatures giving the same modulus values. The values of modulus for the LCP (VECTRA) were different however; extrudates of LCP taken at relatively high shear rates formed filaments of high modulus suggesting a high level of fibre orientation. The samples were prepared containing 2.5%, 5%, 10%, 25%, 50% and 100% LCP in PC. They found that an addition of up to 10% LCP significantly improved the tensile behaviour compared with the unblended material. The authors went on to say:-

'It appears that there is a critical composition value beyond which the liquid crystalline polymer no longer acts as self-reinforcing species'.

VECTRA

SRP1

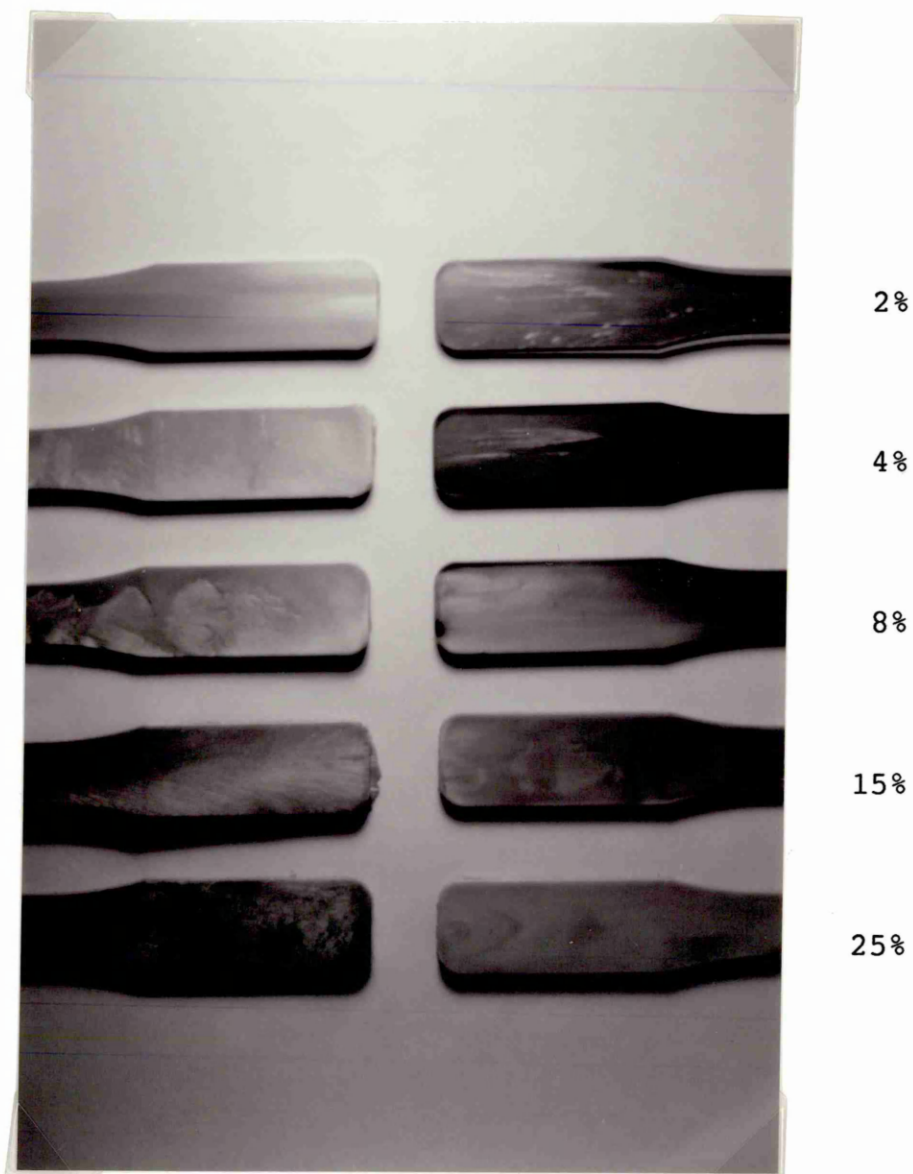


FIGURE 8.15 - Photograph showing tensile bars produced from blends of LCP/PES processed at 340°C and a shear rate of  $\approx 5000 \text{ s}^{-1}$   
MAGNIFICATION x 0.6

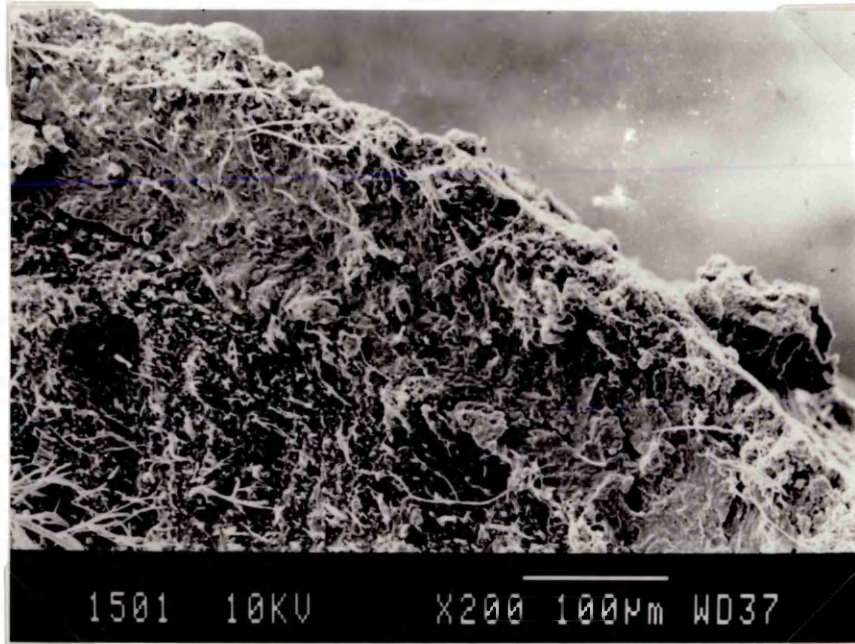


FIGURE 8.16 - Micrograph of 20% VECTRA/PC processed at 300°C and a shear rate of  $\approx 3200\text{s}^{-1}$   
MAGNIFICATION x 200

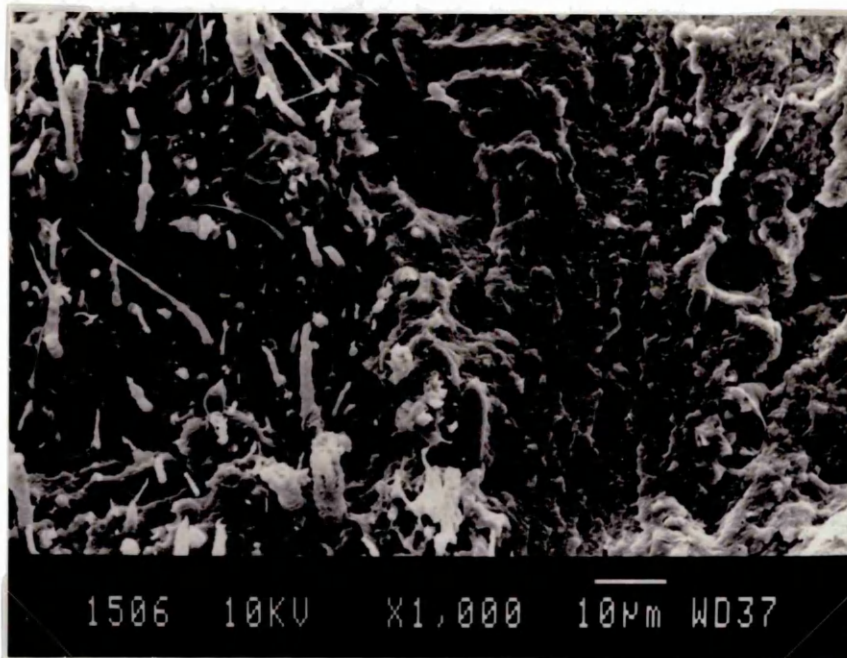


FIGURE 8.17 - Micrograph of 20% VECTRA/PC processed at 300°C and a shear rate of  $\approx 3200\text{s}^{-1}$   
MAGNIFICATION x 1000

The author believes the critical percentage to be around 8% LCP (from the current research). This was found to be the case for both VECTRA and SRP1. Above this concentration the rheological properties continue to change with no associated increase in mechanical properties. It was felt that either poor dispersion or poor adhesion between polymers was to blame. Isayev and Modic<sup>126</sup> stated that additions of LCP to PES/PC reduced the ductility giving a lower impact strength. They found that a small addition of LCP (10%) to PC gave a blend with superior strength than the pure LCP alone. The author does not agree with this (see figures 7.25 - 7.27). These figures show a gradual change from properties of PES/PC to LCP. The graph of load vs extension clearly demonstrates a gradual change from a ductile PES to a brittle LCP with intermediate compositions having intermediate properties, as found by Silverstein et al<sup>157</sup>. There was no evidence to support the theory of Isayev and Modic<sup>126</sup> from results of this study. The author does agree with the results of Blizard and Baird<sup>95</sup>, who showed that blends of Nylon-6,6/PC with a Liquid Crystal Polymer based on (HBA and PET) gave an almost linear relationship between LCP concentration and modulus values for both the PC and the Nylon blends.

Malik et al<sup>123</sup> observed higher values for modulus than predicted by the rule of mixing. This suggests that the two components were compatible at <10%. Above this concentration the experimental values were equal to the

values predicted by the rule. Above 10% the authors stated that in their opinion the blend then became partially miscible.

A range of tensile specimens (see figure 8.16) were produced containing varying amounts of LCP in PES. PES/SRP1 blends were translucent up to 4% LCP. Samples containing Vectra B950 in contrast were not translucent (2%). It appears that small additions of Vectra B950 has a more profound effect on both rheological and mechanical properties of both PC and PES.

#### 8.12 MATHEMATICAL MODELLING OF THE VELOCITY PROFILE

In several texts studied by the author<sup>160-162</sup> it became apparent that there was a correlation between the velocity profile and the orientation of the intransigent rod segments which constitute the backbone chain. The paper by Bright et al.<sup>158</sup> stated there was a relationship between the tangent to the velocity flow profile and the orientation of the polymer within the cross-section.

Bright et al.<sup>158</sup> demonstrated how the velocity profile is altered for different values of  $n$ . Newtonian fluids ( $n=1$ ) have a parabolic shaped profile, whereas shear thinning materials ( $n<1$ ) have a blunter shape with a flat profile (plug flow as  $n\rightarrow 0$ ), see figure 4.3 and equation 4.7.

From equation 4.7 it can be seen that the velocity profile is dependent on the material. The parabolic shaped arcs cited by Bright et al<sup>158</sup> have been witnessed in etched core sections of LCP blends<sup>80</sup>.

The tangent to the flow curve indicates the orientation of filler particles (intransigent rod sections of LCP) within the cross section. The paper by Weng et al<sup>53</sup> states that:-

'From WAXS data taken at several points along the lines of flow the preferred molecular orientation was found to be parallel to the pattern lines'.

In the case where ( $n \rightarrow 0$ ) and plug flow dominated, orientation at right angles to the flow direction (in the core region) would be expected. Both Weng et al<sup>53</sup> and Goettler<sup>159</sup> observed this effect due to the compressive forces, which build up in the entry region of the die. These forces lead to a deceleration of flow, giving a subsequent rotation in the reinforcing agent to varying degrees.

A model was developed which generated a flow profile for the material using the variables defined in equation 7.1. Appendix A shows the working of the model from first principles. Steps 13-19 incorporate the volumetric flow rate, so that it could be compared to equation 8.5 to see

if it correlated. Equation 19 from Appendix A is shown below :-

$$\bar{v} = \frac{Q \frac{n}{3n+1} R_o^{\frac{n+1}{n}}}{2\pi \frac{n}{n+1} \left( R_o^{\frac{n+1}{n}} \frac{R_o^2}{2} - \frac{n}{3n+1} R_o^{\frac{3n+1}{n}} \right)} \quad (8.4)$$

where :-

Q = volumetric flow rate ( $m^3s^{-1}$ )

n = shear thinning index

$R_o$  = radius of die (m)

The values obtained from figures 7.5-7.7 for n,  $R_o$  and Q were put into above equation for a series of different flow rates and temperatures. The average velocity of the extrudate was also calculated using a volumetric flow rate balance, see below :-

$$\bar{v} = \frac{A_p v_p}{A_E} \quad (8.5)$$

where :-

$A_p$  = area of piston ( $m^2$ )

$v_p$  = velocity of piston ( $ms^{-1}$ )

$A_E$  = area of die section ( $m^2$ )

The average velocity correlated for all calculations which indicated that there were no mathematical errors in the model. The profiles for PC, 25% VECTRA/PC and VECTRA

were drawn using equation 7.1. The mean velocity for VECTRA was drawn using equation 7.2.

The interface position for the blends ( $X_1-X_4$ ) occurred where the profile and the mean velocity for the LCP intersected (see figures 7.42-7.45) tabulated below:-

COMPOSITION	SHEAR THINNING INDEX	CONSISTENCY CONSTANT	INTERFACE POSITION
PC	0.65	1445	0.3620
4%	0.59	2137	0.3642
10%	0.57	2290	0.3651
15%	0.56	2290	0.3655
25%	0.47	4365	0.3700
LCP	0.71	467	0.3601

TABLE 8.7 - Table to show how the interface position changes with composition, processed at 320°C.

The modelled results for the blends assume that the shear thinning index and the consistency constant remained uniform across the flow. Figures 7.5-7.7 graphs of log shear stress vs log shear rate were virtually linear over all of the shear rates tested and it is therefore not unreasonable to model the flow using constant values for (n) and (K).

Table 8.7 demonstrates that the modelled interface position is dependent on the composition of the blend. The shear thinning index and consistency constants were used over a variety of shear rates and the interface positions

remained constant. The author feels that the interface position is therefore a function of the LCP concentration and not shear rate. The blend must be processed above the nematic transition temperature and a critical concentration of LCP, for the skin/core interface to occur, therefore this hypothesis is not unreasonable.

A temperature rise can have a very significant effect on the velocity profile (rheological properties) of the LCP and thus the resultant morphology of the extrudate. This effect becomes more pronounced at the nematic transition temperature of the LCP. From the work carried out there was little evidence of any shear heating. The viscosity and thus the morphology of the blends was affected at the specific softening temperature of the LCP as expected. For typical values of PES :-

$$\Delta P = 5 \text{ MPa}$$

$$C_p = 1150 \text{ Jkg}^{-1}\text{K}^{-1}$$

$$\rho = 1.37 \times 10^3 \text{ kgm}^{-3}$$

the shear heating was confined to  $\pm 1.5^\circ\text{C}$ . Using typical values for PC :-

$$\Delta P = 5 \text{ MPa}$$

$$C_p = 1750 \text{ Jkg}^{-1}\text{K}^{-1}$$

$$\rho = 1.2 \times 10^3 \text{ kgm}^{-3}$$

the shear heating was confined to  $\pm 1.1^\circ\text{C}$ . The calculated shear heating is therefore small. It is possible that if

the shear heating was concentrated locally at the polymer/metal interface, the temperature rise could be greater leading to a local slip-stick effect and an overall reduction in viscosity. The viscosity reduction could also be due to the extensional forces which orientate the LCP. Material between the die wall and the interface is subject to elongational forces in the entry region of the die. LCP's are easily aligned in such flows and the author feels that once elongated the LCP induces an imposed morphology on the matrix. On exit from the die the LCP retains its acicular morphology and does not allow the matrix to recoil. Once elongated the domains slide easily past one another possibly lubricating the outer region, leading to a viscosity reduction. The author feels that this mechanism could also account for the reduction in die swell. On exit from the die the long thin rods of LCP reinforce the extrudate in the flow direction and reduce the recoil.

If the lower viscosity polymer (LCP) migrated to the die wall and the interface appeared at the point between the two materials, the interface positions would be as follows :-

BLEND COMPOSITION	DISTANCE FROM CENTRE OF DIE (mm)
6%	0.4847
10%	0.4743
15%	0.4609
25%	0.4330

TABLE 8.8 - The calculated interface position if total migration of the LCP occurred.

Measurements from the micrographs of extrudates taken indicated that the interface position was  $\approx 0.4$  mm from the die centre. The interface position did not vary much (and was not dependent on shear rate), apart from one sample (see figure 8.11), which the author cannot explain within the confines of the current research. It can be seen that the actual interface position is closer to the die wall than the model predicts. This is because the author made certain assumptions (see page 54 i-v) in order to simplify the modelling. From the research carried out it is known that conditions (i) and (v) are incorrect. Local shear heating could be responsible for a local slip/stick effect which would reduce the frictional drag on the polymer. A decrease in this force would lead to a reduction of the shearing forces in the surface layers with a resultant shift in the interface position away from the die wall (as would domain lubrication).

### 8.13 GENERAL DISCUSSION

The pre-testing production is very important as the thermal history has a direct bearing on the final rheological properties and thus the morphology. The blend must contain sufficient LCP to confer the favourable properties and be processed above the nematic transition temperature of the LCP. If these constraints were met, extruded samples of the blends in this study, adopted a characteristic skin/core morphology. The morphology appeared to be independent of the shear rate and

temperature (dictated by the materials) and the interface position did not shift significantly as shown by the micrographs and predicted by the model.

There is no evidence that the LCP migrates either towards or away from the die wall although it is a possibility (cited by various other workers). Finally the LCP induces orientation in the blend and reinforces the matrix with a production of 'in-situ' fibres. At high shear rates the extensional forces are so great that the fibres break up and adopt a characteristic spherical morphology (usually in the surface layers).

## 9 CONCLUSIONS

- i) An addition of a small amount of LCP to conventional engineering polymers causes a significant improvement in processability. Blending with LCP's allows the polymer processor to utilise some of the desirable attributes of LCP's at a reduced cost.
  
- ii) The ease with which the LCP is elongated in extensional flows confers a fibrillar morphology which can be retained in the solid state. The resultant fibrillar structure of the dispersed phase (bounded by the die wall and the interface) induces the matrix to adopt a more orientated morphology. The fibrillar structure allows adjacent LCP domains to flow easily past one another lubricating the flow and causing an apparent reduction in viscosity of the blend. A viscosity minimum has been cited by other workers in this area, However the blend production and processing methods used in this study gave no such results. If long capillaries are used (or very high shear rates), the fibres can break up to form spherical particles.
  
- iii) The imposed morphology has a direct bearing on the tensile and shear fields in the entry region of the capillary die. This in turn has an affect on the velocity profile within the die. The shape and

distribution of the dispersed phase appears to be related to the viscosity ratio and interfacial adhesion of the phases. The surface area over which slip could occur is greater in the biphasic region (region of the binodal) giving a further reduction of viscosity.

iv) The melt viscosities of the LCP's and the matrices were similar which enabled a good dispersion of the LCP within the matrix. The rheology of blends containing liquid crystal polymers is similar to that of filled systems. Increasing additions of liquid crystal polymer to filled systems acts to reduce the viscosity whilst enhancing orientation (especially in the surface layers). As the orientation becomes more pronounced (higher concentrations of liquid crystal polymer and higher shear rates) the orientation perpendicular to the flow direction decreases. The high degree of orientation in the surface layers increases the barrier properties of the material by reducing the distance between adjacent molecules (this could be seen as exfoliation in the surface layers). By controlling the orientation in the surface layers it would be possible to control the barrier properties.

iv) The model predicted the position of the interface in extrudate samples. The interface can be seen in

various micrographs and remained a reasonably constant distance from the die wall over a range of shear rates (except one sample). The author feels that the position of the interface is affected by the concentration of LCP within the sample, rather than the shear rate.

- v) From the research it was noticed that the blend must contain a critical amount and be processed above the nematic transition temperature of the LCP for a skin-core morphology to occur. For blends containing SRP1 the amount was 8%, for blends containing VECTRA the amount was 6%.
  
- vi) The blends were found to be immiscible (see figure 7.41). The VECTRA was less miscible than the SRP1 with the particular base materials chosen. It is not essential for the LCP's to be miscible with the matrix, indeed the immiscibility could be the reason for the lowering of viscosity seen in this study. Poor interfacial adhesion would however limit the physical properties of the final blend. It was found that the physical properties could be tailored using varying amounts of LCP in the blends. If the amount of LCP in the blend was too high (>10%) the physical properties suffered. At concentrations lower than this there was a trade off between loss of physical properties and the reduction of the blend viscosity.

## 10 FURTHER WORK

- i) Further work will be necessary on PES/SRP1 blends at concentrations of less than 6% SRP1. At this concentration or less the resultant blends were 'similar' to PES (i.e. comparative tensile/impact properties) with the advantage of a lower processing viscosity.
  
- ii) It would be useful to know how the pre-testing history affected the rheological/morphological properties. If blends containing pre-determined compositions were blended using a variety of different processing techniques the resultant properties could be compared. This would allow production methods which gave a wide variance of data for consecutive test runs to be eliminated.
  
- iii) It will be necessary to carry out further research on how processing variables affect the fibre/droplet morphology and the dispersion of the LCP within the blend. The model used in this study goes some way in explaining how the extensional forces on the LCP cause the domains to elongate but does not explain the LCP dispersion within the extrudate.
  
- iv) The author found no evidence of migration in the current study. Further work using SIMS could be used

to determine the dispersion and position of the VECTRA in the matrix by locking in on the double benzene rings (in the VECTRA backbone).

## 11 REFERENCES

- 1) F. N. Cogswell, B. P. Griffin and J. B. Rose, USP 4,386,174, May 31, (1983).
- 2) F. Reinitzer, Monatsch , 9, 421, (1888).
- 3) L. Gattermann and A. Ritschke, Ber ., 23, 1738, (1890).
- 4) O. Lehmann, Z. Phys. Chem., 5, 427, (1890).
- 5) O. Lehmann, Engelmann, Leipzig, (1904).
- 6) R. Schenk, Engelmann, Leipzig, (1905).
- 7) D. Vorländer, Kristallinisch Flussige Substanzen, Enke, Stuttgart, (1908).
- 8) G. Friedel, Ann. Phys., 18, 273, (1922).
- 9) P. L. Flory, Proc. Roy. Soc., 73, A234, (1956).
- 10) S. G. Cottis, J. Economy and B. E. Nowak, U.S. Patent No. 3975486, (1973).
- 11) H. W. Hill, S. L. Kwolek, and W.Sweeny, U.S. Patent No. 3094511, (1963).
- 12) W. Sweeny, U. S. Patent No. 3287324, (1966).
- 13) S. L. Kwolek, P.W. Morgan and W. R. Sorenson, U.S. Patent No. 3063966, (1962).
- 14) S. L. Kwolek, U.S. Patent No. 3600350, (1971).
- 15) S. L. Kwolek, U.S. Pat 3671542, (1972).
- 16) P. W. Morgan, Macromolecules, 10, 1381, (1977).
- 17) S. L. Kwolek, P.W. Morgan, J. R. Schaeffgen, and L.W. Gulrich, Macromolecules, 10, 1390, (1977).
- 18) T. I. Bair, P. W. Morgan and F. L. Killian, Macromolecules, 10, 1396, (1977).
- 19) E. E. Magat, U. S. Pat. 2831834, (1958).

- 20) C. R. Payet, Ger. Offen. 2751653, (1978).
- 21) H. F. Kuhfuss and W. J. Jackson, U. S. Patent No. 3778410, (1973).
- 22) H. F. Kuhfuss and W. J. Jackson, U. S. Patent. No. 3804805, (1974).
- 23) W. J. Jackson, J. F. Kuhfuss and T. F. Gray 30th Annual Technical Conference Section 17, pg 1, (1974).
- 24) W. J. Jackson and H. F. Kuhfuss, J. Polym. Sci. Chem Ed., 14, 2043, (1976).
- 25) T. C. Pletcher, U. S. Patent. No. 3991014, (1976).
- 26) J. J. Kleinschuster, U. S. Patent No. 3991014, (1976).
- 27) J. R. Schaeffgen U. S. Patent. No. 4075262, (1978).
- 28) J. R. Schaeffgen U. S. Patent. No. 4118372, (1978).
- 29) G. W Calundann U. S. Patent. No. 4067852, (1978).
- 30) G. W Calundann U. S. Patent. No. 4130545, (1978).
- 31) G. W Calundann U. S. Patent. No. 4161470, (1979).
- 32) A. J. East and G. W. Calundann, U. S. Patent. No. 4318841, (1982).
- 33) A. J. East and G. W. Calundann, U. S. Patent. No. 4318842, (1982).

- 34) R. Daubeny, C. W. Bunn, and C. J. Brown, Proc. Roy. Soc. 226, 231, (1954).
- 35) R. S. Porter and J. F. Johnson, Rheology, Vol 4, F. R. Eirich Ed., Academic, New York, (1967).
- 36) W. J. Jackson, Br. Polym. J., 12, 154, (1980).
- 37) J. I. Jin, S. Antoun, C. Ober, and R. W Lenz, Br. Polym. J., 12, 132, (1980).
- 38) Japan Plastics Age, pg 19-25, Mar-Apr, (1986).
- 39) J. B. Russell, General Chemistry, Published by McGraw-Hill International Book Company, pg 30, (1980).
- 40) R. A. Higgins, Properties of Engineering Materials, Published by Hodder and Stoughton, pg 32, (1981).
- 41) J. L. White and S. Onagi, J. Appl. Poly. Sci., pg 70-73, Vol 41, (1985).
- 42) R. Lenz, Polymer Journal, Vol 17, No 1, pg 105-115, (1985).
- 43) W. Brostow, Kunststoffe German Plastics 78, pg 411-419, (1988)., TRANSLATED.
- 44) D. Clegg and A. A. Collyer, High performance plastics, Vol. 4, No. 1, pg 1-7, Nov., (1988).
- 45) A.A. Collyer, Private Communication
- 46) B. P. Griffin and M. K. Cox, Br. Polym. J., 12, 147, (1980).
- 47) G. Calundann, M. Jaffe, R.S. Jones and H. Yoon, 'Fibre Reinforcement for composite materials', Ed A. R. Bunsell, Elsevier, Amsterdam, Chapter 5, pg 211-248, (1988).

- 48) R. Chivers, J. Blackwell and G. A. Gutierrez,,  
Polymer, 25, 435, (1984).
- 49) S. G. Cottis, 'Aromatic polyesters as high  
performance engineer engineering plastics', 32nd  
SPE Tech Conf., pg 496, (1974).
- 50) J. B. Russell, General Chemistry, Published by  
McGraw-Hill International Book Company, pg 658,  
(1980).
- 51) D. J. Blundell et al, Polymer, Vol. 29, Pg 1459-  
1467, August, (1988).
- 52) T. I. Ablazova et al, J. Appl. Polym. Sci., Vol  
19, pg 1781, (1975).
- 53) T. Weng, A. Hiltner, E. Baer, J. Mat. Sci., 21,  
pg 744-750, (1986).
- 54) T.C.B. McLeish and R. C. Ball, J. Polym. Sci.,  
Part B, Vol. 24, pg 1735-1745, (1986).
- 55) T. C. B. McLeish, J. Polym. Sci., Part B., Vol.  
25, pg 2253-2264, (1987).
- 56) I.C.I plc, Private communication
- 57) H. A. Barnes, J. F. Hutton and K. Walters, 'An  
Introduction to Rheology', Elsevier, pg 4, (1989).
- 58) I. Newton, Principia, (1687).
- 59) J. A. Brydson, 'Flow properties of polymer melts', pg  
5, London Iliffe Books, (1981).
- 60) E. B. Bagley, J. Appl. Physics, Vol 28, No. 5,  
(1987).
- 61) S. Y. Hobbs and C. F. Pratt, J. Appl. Poly. Sci., Vol  
19, pg 1701-1722, (1975).

- 62) K. F. Wissbrun, *J. Rheol.*, Vol 25, pg 619, (1981).
- 63) S. Onogi and T. Asada, 'Rheology and rheo-optics of polymer liquid crystals', 8th International Congress of Rheology, pg 127-147, (1980).
- 64) J. M. Pochan, 'A Structural interpretation of the Rheo-optic properties of the cholesteric mesophase', *Liquid crystals*, F. D Saeva, Ed. Marcek-Dekker, New York, (1978).
- 65) F. N. Cogswell, *Rheology of thermotropic polymer liquid crystals*, Chapter 10, pg 165-175, 'Observations on the Rheology of Thermotropic Polymer Liquid Crystals', (1984).
- 66) L. Chapoy, B. Marcher and K. N. Rasmussen, 'Liquid Crystals', Vol 3, No. 12, pg 1611-1636, (1988).
- 67) M. Prasadarao, E. M. Pearce and C. D. Han, *J. Appl. Polym. Sci.*, Vol 27, pg 1343-1354, (1982).
- 68) F. N. Cogswell, 10th Anniversary Society of Rheology, Japan, July, (1983).
- 69) H. Sugiyama et al, *J. Appl. Polym. Sci.*, July, (1986).
- 70) A. D. Gotis and D. G. Baird, *Rheol. Acta*, 25, pg 275-286 (1986).
- 71) A. K. Yevseyev et al, *Polym. Sci. USSR*, Vol 29, No 3, pg 570-576, (1987). TRANSLATED
- 72) K. Shimamura, J. L. White, J. F. Fellers, *J. Appl. Sci.*, No 26, pg 2165, (1981).

- 73) E. G. Joseph, G. L. Wilkes and D. G. Baird, Polym. Eng. Sci., Vol. 25, No. 7, pg 377 - 387, May (1985).
- 74) M. G. Dobb, J. E. McIntyre, Advances in Polymer Science 60/61, pg 64, (1984).
- 75) R. E. Jerman and D. G. Baird, 'Rheological properties of copolyester liquid crystal polymer melts in capillary rheometry', J. Rheol, 25, pg 275-292, (1981).
- 76) K. F. Wissbrun, 'Observations on the melt rheology of thermotropic aromatic polyesters', Br. Polym. J., 12, pg 163-169, (1980).
- 77) Victrex SRP self reinforcing polymers, Properties and processing, ICI data sheet No. VR1
- 78) M. H. Naitove, Plastics Technology, pg 85, April, (1985).
- 79) A. S. Wood, Modern Plastics, pg 78, April, (1985).
- 80) Z. Ophir and Y. Ide, Polym. Eng. Sci., Vol 23, pg 792, (1983).
- 81) L. E. Nielsen, Mechanical Properties of Polymers and Composites, Vol. 2, Marcel Dekker, N. Y. (1974).
- 82) J. A. Manson and L. H. Sperling, Polymer Blends and Composites, pg 430-442, Plenum Press, N. Y. (1976).

- 83) C. D. Han, *Multiphase Flow in Polymer Processing*, Academic Press, New York, (1981).
- 84) W. Huh, R. A. Weiss and L. Nicolais, *Polym. Eng. Sci.*, Vol. 23, No. 14, pg 779-782, October (1983).
- 85) C. D. Han, *J. Appl. Polym. Sci.*, 18, Pg 821 (1974).
- 86) C. D. Han, *Rheology in Polymer Processing*, Chapter 7, pg 184, Academic Press, New York (1976).
- 87) J. L. White, J. Chan and Y. Onanagi, *J. Rheol.*, Vol. 22, pg 507 (1978).
- 88) J. L. White and V. M. Lobe, *Polym. Eng. Sci.* Vol. 19, pg 617 (1979).
- 89) J. L. White and H. Tanaka, *Polym. Eng. Sci.*, Vol. 20, pg 949 (1980).
- 90) A. Seigmann, A. Dagan, S. Kenig, *Polymer*, Vol. 26, pg 1325-1330, August (1985).
- 91) S. H. Jung, S. C. Kim, *Polymer*, Vol 20, No 1, (1988).
- 92) A. I. Isayev and M. Modic, *Polymer Composites*, Vol. 8, No. 3, June (1987).
- 93) T. Nishimura and H. Sakai, *Kobunshi Ronbunshu*, 5, 45, pg 401 - 408 (1988).
- 94) L. A. Utracki, *Polym. Eng. Sci.*, Vol. 23, No. 11, pg 602, August (1983).
- 95) K. G. Blizard and D. G. Baird, *Polym. Eng. Sci.*, Vol. 27, No. 9, pg 653 - 661, May (1987).

- 96) W. Brostow, T. S. Dziemianowicz, J. Romanski and W. Werber, *Polym. Eng. Sci.*, Vol 28, No. 12, 6, (1988).
- 97) M. Subramanian and V. Mehra, 'Laminar morphology in polymer blends structure and properties', ANTEC, pg 301-305, (1986).
- 98) J. A. Brydson, *Plastic Materials*, pg 74-89, Newnes Butterworth, (1990).
- 99) A. Dobry, F. Boyer-Kawenoki, *J. Polym. Sci.*, 2, 90 (1947).
- 100) L. Bohn, *Rubber Chem. Technol.*, 41, 495, (1968).
- 101) S. Krause, *J. Macromol. Sci. Rev. Macromol. Chem.*, C7, 251, (1972).
- 102) R. L. Scott, *J. Chem. Phys.*, 17, 279 (1949).
- 103) P. J. Flory, *J. Chem. Phys.*, 10, 51, (1942).
- 104) M. L. Huggins, *J. Phys. Chem.*, 46, 151, (1942).
- 105) S. M. Aharoni, 'Rigid backbone polymer XVII: Solution viscosity of polydisperse systems', *Polymer*, 21, pg 1413-1422, (1980).
- 106) Y. S. Lipatov, A. N. Shumskii, A. M. Gorbatenko and Geitmanchuk, *Fiz. Khim. Mekh. Disp. Struktur.*, pg 117, (1983).
- 107) C. Noel and J. Billard, *Mol. Cryst. Liq. Cryst. Lett.*, Vol 41, pg 269-274, (1978).
- 108) M. Ballauff, *Molec. Cryst. Liq. Cryst.*, 4, 15, (1986).
- 109) M. F. Achard, G. Sigaud, P. Keller and F. Hardouin, *Int. Conf. Liq. Cryst. Polym.*, Bordeaux, France, Paper 11P3, 7, (1987).

- 110) S. K. Sharma, A. Tendolkar and A. Misra. *Molec. Liq. Cryst.*, 157, 597, (1988).
- 111) M. Takayanagi, T. Ogata, M. Morikawa and T. Kai, *J. Macromol. Sci. Phys.*, B17, (4)., 591, (1980).
- 112) J. M. Starita, *Trans. Soc. Rheol*, 16, 2, pg 339-367, (1972).
- 113) A. Mehta and A. I. Isayev, *Polym. Eng. Sci.*, Mid-July, Vol. 31, No. 13, (1991).
- 114) D. Acierno, M. R. Nobile and G. Marino, *European Regional Meeting, PPS, September 15-18*, pg 151-152, Palermo ITALY, (1991).
- 115) J. B. Hull, M. Hawksworth and A. A. Collyer, *Irish Materials Forum, Limerick, 4-6 September*, Trans Tech Publications, *Key Engineering Materials Vols. 72-74*, pg 627-634, (1992). - SEE APPENDIX C.
- 116) A. A. Collyer, J. B. Hull and M. Hawksworth, 'The Rheology of Liquid Crystal Polymer Blends', Chemtec Publishing, *Processing and Properties of Liquid Crystalline Polymers and LCP based blends*, pg 65-87, (1993). - SEE APPENDIX C.
- 117) A. Kohli, N. Chung and R. A. Weiss, *Polym. Eng. Sci*, May, Vol. 29, No. 9, (1989).
- 118) P. K. Currie, *Rheol. Acta.*, 16, 205, (1977).
- 119) C. R. Gochanour and M. Weinberg, *J. Rheol.*, 30, 1, pg 101-124, (1986).
- 120) B. Lee, *SPE ANTEC, Tech Papers*, 34, 1088, (1988).
- 121) L. Lorenzo, S.K. Ahuja and H. Chang, *Am. Chem. Soc.*, *Div. Polym. Chem, Polym. Prep*, 29, 488, (1988).

- 122) La Mantia, A. Valenza, P. L. Magagnini, European Regional Meeting, PPS, September 15-18, pg 157-158, Palermo ITALY, (1991).
- 123) T. M. Malik, P. J. Carreau and N. Chapleau, Polym. Eng. Sci., May, Vol. 29, No. 9, (1989).
- 124) S. G. James, A. M. Donald and W. A. MacDonald, Molec. Cryst. Liq. Cryst, 153, 49, (1987).
- 125) M. R. Nobile, E. Amendola, L. Nicolais, D. Acierno and C. Carfagna, Polym. Eng. Sci. 29, 244, (1989).
- 126) A. I. Isayev and M. J. Modic, pg 573-579, ANTEC, (1986).
- 127) T. S. Chung, Plastics Engineering, October, pg 39-41, (1987).
- 128) D. Beery, A. Seigmann and S. Kenig, J. Mater. Sci. Lett., 7, pg 1071-1073, (1988).
- 129) A. B. Metzner and G. M. Prilutski, J. Rheol. 30, 3, pg 661-691, (1986).
- 130) J. L. Ericksen, Trans. Soc. Rheol, 13,9, (1969).
- 131) G. Kiss, Polym. Eng. Sci., March, Vol. 27, No. 6, (1987).
- 132) R. A. Weiss, W. Huh and L. Nicolais, Int. Conf. Liq. Cryst. Polym., Bordeaux, France, Paper 8P8, (1987).
- 133) G. Marrucci, Pure and Appl. Chem., Vol. 57, No. 11, pg 1545-1552, (1985).
- 134) D. Acierno, M. R. Nobile, L. Nicolais and L. Incarnato, J. Rheology, 34, 1181, (1990).
- 135) K. Min, J. L. White and J. F. Fellers, Polym. Eng. Sci., December, Vol. 24, No. 17, (1984).

- 136) W. G. Perkins, A. M. Marcelli and H. W. Frerking, J. Appl Polym. Sci., Vol. 43, pg 329-349, (1991).
- 137) M. V. Tsebrenko, M. N. Rezanova, and G. V. Vinogradov, Rheol. Polym., November, 11th Mater. Uses Simp. Rheol., 2, 136, (1982).
- 138) E. S. Clark, SPE Journal, July, PG 47-49, (1967).
- 139) D. McNally, Polym. Plast. Technol. Eng., 8, 101, (1977).
- 140) J. E. Callear and J. B. Shortall, J. Material Sci., 12, pg 141-152, (1977).
- 141) H. Thapar and M. Bevis, J. Mater. Sci. Lett., 2, pg 733-736, (1983).
- 142) M. T. Heino, J. V. Seppälä, J. Appl Polym. Sci., Vol. 44, pg 2185-2195, (1992).
- 143) Z. Tadmor, J. Appl. Polym. Sci., 18, 1753, (1974).
- 144) M. R. Kantz, Int. J. Polym. Mater., 3, 245, (1974).
- 145) L. C. Sawyer and M. Jaffe, J. Mater. Sci., 21, pg 1897-1913, (1986).
- 146) M. R. Kantz, H. D. Newman and F. H. Stigale, J. Appl. Polym. Sci. Vol. 16, pg 1249-1260, (1972).
- 147) G. V. Vinogradov, N. P. Krasnikova, V. E. Dreval, E. V. Kotova, E. P. Plotnikova and Z. Pelzbauer, Intern. J. Polymeric. Mater., Vol. 9, pg 187-200, (1982).
- 148) A. A. Collyer, D. W. Clegg, G. H. France, M. Morris, K. Blake, D. J. Groves and M. K. Cox, IXth Int. Congr. Rheol., Acapulco, Oct. 8-13, 3, 543-550, Elsevier Applied Science Publishers, London and New York, (1985).

- 149) H. Verhoogt, C. R. J. Willems, J van Dam and A. Posthuma de Boer, European Regional Meeting, PPS, September 15-18, pg 149-150, Palermo ITALY, (1991).
- 150) R. A. Weiss, W. Huh and L. Nicolais, Polym. Eng. Sci., May, Vol. 27, No. 9, (1987).
- 151) C. E. Chaffrey, H. Brenner and S. G. Manson, Rheol. Acta., 4, 64, (1965).
- 152) F. Gauthier, H. L. Goldsmith and S. G. Mason, Trans. Soc. Rheol., 15, 2, pg 297-330, (1971).
- 153) F. P. La Mantia, A. Valenza, P. L. Magagnini and M. Paci, J. Appl. Polym. Sci., Vol. 38, pg 583-589, (1989).
- 154) C. K. Shih, Polym. Eng. Sci., 16, 742, (1976).
- 155) T. Q. Jiang, A. C. Young and A. B. Metzner, Rheol. Acta 25, pg 397-404, (1986).
- 156) R. W. Lenz, A. K. Rao, C. R. Reddy, S. Bafna and S. Bhattacharya, J. Polym. Sci., Part B: Polymer Physics, Vol. 27, pg 2117-2130, (1989).
- 157) J. X. Li, M. S. Silverstein, A. Hiltner and E. Baer, J. Appl. Polym. Sci. Vol. 44, pg 1531-1542, (1992).
- 158) P. F. Bright, R. J. Crowson and M. J. Folkes, J. Mater. Sci., 13, pg 2497-2506, (1978).
- 159) L. A. Goettler, Modern Plastics, April, pg 140-146, (1970).
- 160) N. J. Alderman and M. R. Macklay, Faraday Discuss, Chem. Soc., 79, pg 149-160, (1985).
- 161) J. K. Hunter and M. Slemrod, Phys. Fluids, 26, 9, September, (1983).

$$\tau = k\dot{\gamma}^n = k \left( \frac{\partial v}{\partial r} \right)^n \quad (1)$$

$$-\frac{\partial P}{\partial l} + \frac{1}{r} \cdot \frac{\partial}{\partial r} \cdot (r \tau) = 0 \quad (2)$$

Equation 2 is Newtons Law; 1 and 2 combine to form :-

$$k \frac{\partial}{\partial r} \left[ r \left( \frac{\partial v}{\partial r} \right)^n \right] = r + \frac{\partial P}{\partial l} \quad (3)$$

$$\partial \left[ r \left( \frac{\partial v}{\partial r} \right)^n \right] = \left( \frac{\partial P}{\partial l} \right) r \cdot dr \quad (4)$$

$$r \left( \frac{\partial v}{\partial r} \right)^n = \left( \frac{\partial P}{\partial l} \right) \frac{r^2}{2} \quad (5)$$

$$\left( \frac{\partial v}{\partial r} \right)^n = \left( \frac{\partial P}{2k} \right) r \quad (6)$$

This is solved for solutions of  $n \geq 0$  and  $(\partial P/\partial l)/2k \geq 0$

$$\frac{\partial v}{\partial r} = \left( \frac{\partial P}{2k} \right)^{\frac{1}{n}} r^{\frac{1}{n}} \quad (7)$$

$$v_r = \left( \frac{\partial P}{2k} \right)^{\frac{1}{n}} \frac{n}{n+1} \left( R_o^{\frac{n+1}{n}} - r^{\frac{n+1}{n}} \right) \quad (9)$$

$$\int_0^v dv = \left( \frac{\partial P}{\partial l} \right)^{\frac{1}{n}} \frac{1}{2k} \int_0^{R_0} r^{\frac{1}{n}} dr \quad (8)$$

This gives  $v_r$  the radial velocity of the profile at a point  $0 \leq r \leq R_0$  within the die. The mean velocity ( $\bar{v}$ ) occurs at  $R_0/2$  as follows :-

$$\bar{v} = \left( \frac{\partial P}{\partial l} \right)^{\frac{1}{n}} \frac{n}{3n+1} R_0^{\frac{n+1}{n}} \quad (10)$$

The maximum velocity  $v_{MAX}$  occurs at the centre of the flow profile as follows :-

$$v_{MAX} = \left( \frac{\partial P}{\partial l} \right)^{\frac{1}{n}} \frac{n}{n+1} R_0^{\frac{n+1}{n}} \quad (11)$$

To simplify the expression  $\xi$  is defined as follows :-

$$\xi = \left( \frac{\partial P}{\partial l} \right)^{\frac{1}{n}} \quad (12)$$

The volume flow rate can be calculated as follows :-

$$Q = 2\pi \int_0^{R_0} v_r r \cdot dr \quad (13)$$

$$Q = 2\pi\xi \frac{n}{n+1} \int_0^{R_o} \left( R_o^{\frac{n+1}{n}} - r^{\frac{n+1}{n}} \right) r \cdot dr \quad (14)$$

$$Q = 2\pi\xi \frac{n}{n+1} \int_0^{R_o} R_o^{\frac{n+1}{n}} r - r^{\frac{2n+1}{n}} \cdot dr \quad (15)$$

$$Q = 2\pi\xi \frac{n}{n+1} \left[ R_o^{\frac{n+1}{n}} \frac{r^2}{2} - \frac{n}{3n+1} r^{\frac{3n+1}{n}} \right]_0^{R_o} \quad (16)$$

$$Q = 2\pi\xi \frac{n}{n+1} \left( R_o^{\frac{n+1}{n}} \frac{R_o^2}{2} - \frac{n}{3n+1} R_o^{\frac{3n+1}{n}} \right) \quad (17)$$

$$\xi = \frac{Q}{2\pi \frac{n}{n+1} \left( R_o^{\frac{n+1}{n}} \frac{R_o^2}{2} - \frac{n}{3n+1} R_o^{\frac{3n+1}{n}} \right)} \quad (18)$$

Substituting into equation 10 we have an expression for the mean velocity of the extrudate as follows :-

$$\bar{v} = \frac{Q \frac{n}{3n+1} R_o^{\frac{n+1}{n}}}{2\pi \frac{n}{n+1} \left( R_o^{\frac{n+1}{n}} \frac{R_o^2}{2} - \frac{n}{3n+1} R_o^{\frac{3n+1}{n}} \right)} \quad (19)$$

## CONTENTS

1) INTRODUCTION . . . . .	1
2) MATERIALS BACKGROUND . . . . .	2
3) PROPERTIES REQUIRED OF AEROSPACE MATERIALS . . .	2
3.1) COST REDUCTION . . . . .	3
3.2) THERMAL STABILITY . . . . .	4
3.3) WEIGHT . . . . .	4
4) ALUMINIUM ALLOYS IN AEROSPACE APPLICATIONS . . .	5
5) POLYMERIC MATERIALS IN AEROSPACE APPLICATIONS .	7
5.1) LIQUID CRYSTAL POLYMER AS A MICRO- COMPOSITE . . . . .	9
6) DESIGN CONSIDERATIONS FOR PLASTIC COMPONENTS . .	14
6.1) IMPROVED STIFFNESS . . . . .	14
6.2) REINFORCING RIBS . . . . .	16
6.3) REPAIR TECHNOLOGY . . . . .	17
6.4) FIXING METHODS . . . . .	17
7) RESULTS . . . . .	18
7.1) BENDING STIFFNESS . . . . .	18
8) CONCLUSIONS . . . . .	22
9) REFERENCES . . . . .	24

## 1) INTRODUCTION

For many years the polymeric industry has been continually developing its products, to the point where they can now replace metals in some of aerospace's more demanding applications. This case study looks at the ability of an Imperial Chemical Industries advanced polymeric material to replace a specific component, produced from an aluminium alloy from both a technical and economic viewpoint.

The argument that metal components can 'do the job', is not always satisfactory. In many cases, non-metallic materials can offer a unique combination of properties, which are at least equal, or superior to the metal. The main drawback to using polymers is the poor comparative stiffness, important because design in plastics is governed by this key factor. In spite of this, they may have greater impact resistance, a superior surface hardness and a lower thermal conductivity, coupled with a weight saving of around 15-40%.

The component looked at in this study, is an access door on an aircraft, constructed using two skins of aluminium over a honeycomb core, making the resulting structure both stiff and light, see figure 1. The design and calculations incorporate eight fixing holes used to hold the door in place.

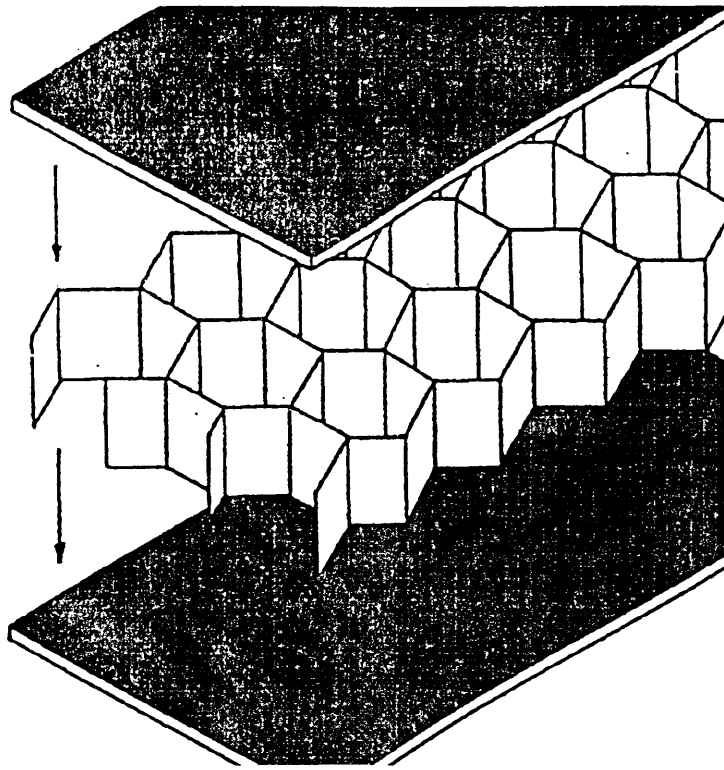


**Figure 1** - Diagram demonstrating the honeycomb core sandwiched between two aluminium skins.

## 2) MATERIALS BACKGROUND

The materials that will be examined are an Aluminium-Lithium alloy (2024) and a glass fibre reinforced liquid crystal polymer SRP1500GL30. It is the aspiration of the case study, to compare the two materials in question to see if it feasible to replace the aluminium component using a honeycomb centre, with either a solid injection moulding or a foamed moulding produced from the glass fibre reinforced liquid crystal polymer, having stiffness equivalent to the aluminium article.

## 3) PROPERTIES REQUIRED OF AEROSPACE MATERIALS

The materials used in aerospace applications must have

excellent mechanical properties while at the same time remain cost effective. It is only military aircraft that can waive the economic considerations to achieve superior efficacy. The three major aspirations for materials used in the aerospace industry are:-

- i) cost reduction;
- ii) thermal stability; and
- iii) weight.

### 3.1) COST REDUCTION

The major saving in this area can be achieved by the automation of a lot of simpler tasks. A large number of labour intensive tasks can be done by one machine, which can produce a wide variety of parts on either a large or small scale. Automation also has the added advantage that the apparatus can run for 24 hours without cost penalties (night shift bonuses etc.), despite their initial high capital cost.

The reuse of scrap is also a major consideration, it is possible to add ground sprues and runners to virgin material to allow for a more economical use of the polymer. The level of re-work will dependant almost entirely upon its quality. Contamination from oil, metal, other polymers and general dirt will have a deleterious effect upon the mechanical properties of the finished article. Information from ICI data sheets<sup>6</sup> suggests that there is little deterioration in properties if levels no greater than 30%

scrap are added. Scrap aluminium waste can be sold back to the suppliers, giving a reduction in production costs<sup>1</sup>.

### 3.2) THERMAL STABILITY

There is a need to find materials which have good thermal stability. The fact that aircraft are flying at higher and higher speeds, means that the resultant friction with the atmosphere leads to high external temperatures of the fuselage, especially on the leading edge of the wings and tails. Flying at a speed of Mach 2.2 gives an average surface temperature of 135°C, an increase in speed to Mach 2.4 would give a corresponding increase in operating temperatures of 175°C, see figure 2. The standard by which materials are judged is that their mechanical properties must not fall below 80% of their room temperature (23°C) performance, whilst operating at elevated temperatures. This is known as the point of unacceptability.

### 3.3) WEIGHT

The use of light materials, not only facilitates improved speed and manoeuvrability, but also reduced fuel consumption. This will allow military aircraft to fly faster and spend more time in the air, without refuelling.

Weight is by no means the only way of judging a material's performance, other factors such as low friction and wear; dimensional stability; improved environmental resistance; and good fatigue resistance.

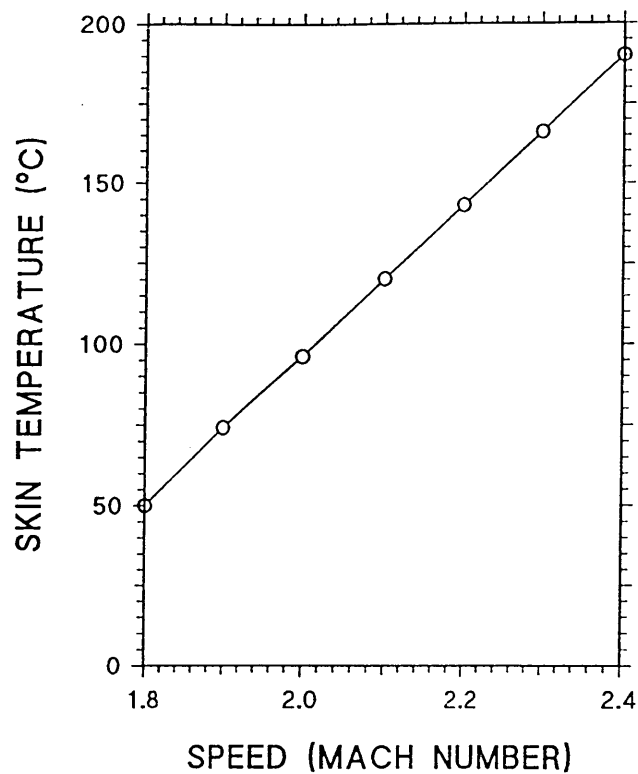


**Figure 2** - Graph to demonstrate the correlation between aircraft speed and external skin temperature.

#### 4) ALUMINIUM ALLOYS IN AEROSPACE APPLICATIONS

Aluminium-lithium alloys command the most research, than any other aerospace alloy. A primary reason for this development activity is the search for more fuel efficient aircraft in a climate of escalating fuel costs. The addition of lithium to aluminium simultaneously reduces the density and increases the elastic modulus of the resultant alloy. In aircraft produced in the early 1980's, 75% of the structure was produced using established high strength aluminium alloys. If the western world continues to produce aircraft at the current rate, i.e. 450 airliners per annum, this equates to 20,000 tonnes of aluminium being used in the aerospace industry every year. It has been estimated<sup>2</sup>

that about 4,400 airliners will have to be constructed between 1983 and 1995. If this usage pattern remained unchanged, 196,000 tonnes of aluminium will be required. In addition to this, there is military aircraft production, which will also increase the tonnage required. It is in this market that the aluminium-lithium based alloys are aimed, and success in development could result in substitution of virtually all of the conventional alloys, with lithium containing alloys. There have been several reviews in this area, Schmidt<sup>3</sup>, and more recently Peel<sup>4</sup>, have given excellent perspectives of the development story so far. A brief history of Al-Li development can be seen below, in Table 1

TABLE : 1

1921 - Al Mond - Metallgesellschaft - 'structural alloy'
1926 - P Assmann - Ludwigshafen - Al-Li-Zn and Al-Li-Cu
1931 - Nisimura - Furukawa Denki KK - Corrosion resistant alloy Al-Li (0.01-5%); Cu (0.1-5%); Cd (0.1-5%)
1942 - Le Baron - Alcoa - Al-Cu-Li-Cd
1957 - Alcoa - technical - commercial publicity for 2020 - higher operating temperatures, 3% weight savings, 8% stiffness
1968 - Fridlyander, Ambartsumyan, Shiryaeva and Gabidullin - USSR Alloy 01420
1983 - Royal Aircraft Establishment Patent Al-Li-Cu-Mg - DTD Draft Specification XXXA
1984 - Alcan patent - DTD Draft Specification XXXB

One of the most detailed studies available to the public sector in recent years was one carried out by engineers at the Lockheed-California Company for the US

National Aeronautics and Space Administration. The study demonstrates that considerable weight savings could be made by using Aluminium - Lithium alloys between 8 and 10%, but with re-sizing this could be between 10 and 16% for the larger aircraft. The report found that this represents more than a \$1 million saving per annum. The use of the Al-Li alloys means that smaller, more fuel efficient aircraft can be built. Aluminium based alloys are already being incorporated in limited quantities, into a number of experimental military aircraft. There are good grounds for supposing success in consistently producing material through the routine production system. Matching the quality of the best material produced from laboratory cast metal, will rapidly lead to much more widespread use of the alloys in aerospace applications. Indeed, recently Alcan have introduced the new Lital series A, B, and C, which are superior to the alloy used in this case study. Their use will be encouraged by the fact that the new lithium-containing alloys (alloyed with Copper, Magnesium, and Zirconium), can be treated in a manner that is virtually identical with that currently being used with established aircraft alloys.

##### 5) POLYMERIC MATERIALS IN AEROSPACE APPLICATIONS

The use of composites in aerospace is not a new concept, the Wright brothers used composite materials some 85 years ago. The main material they used was wood (nature's classic composite); modern composite materials

can trace their origins to about the turn of the century to Bakelite and Tufnol.

Composites consist of two or more physically distinct different materials which are combined in a controlled way to achieve a mixture having more useful properties than any of the constituents on their own. The more common case is where a polymer matrix is reinforced by a high strength and stiffness fibre, e.g. carbon or kevlar. These types of reinforcing agents are utilised to great effect in aerospace applications, because of the weight saving advantage over traditional materials e.g aluminium and titanium.

At the beginning of the second World War, France was occupied, and the use of the bauxite deposits were lost. Britain looked at the possibility of building aircraft from other materials and the first of these new 'plastic' reinforced composites was based on a phenolic matrix, filled with an untwisted flax, known as Gordon Aerolite. The spitfire was the first aircraft to utilise such materials in its production. Figure 3 shows a spitfire fuselage being constructed out of this material. It was not until the 1960's that the first fibre reinforced epoxies came onto the market. The material had specific stiffness characteristics and a very long fatigue life, making it excellent for helicopter blades. The next step was the development of carbon fibre which became the favourite

material for reinforcement. It can be produced in a number of forms :- unidirectional fibres, tapes and fabric. The carbon fibres composite or (CFC) has made major strides forward in recent years. Indeed the CFC has been put forward on numerous occasions as an alternative material to the aluminium lithium alloys. There would of course be a significant weight saving. The CFC system is a macro-composite, i.e. the fibres are placed in the matrix and are different in composition to the matrix. Liquid crystalline materials are micro-composites, the polymer is highly aligned in the flow direction which gives anisotropic properties, see figure 7. The reinforcing effect is caused by the high degree of alignment of molecular chains, within the article. The alignment can be disrupted by the addition of small glass fibres, giving more uniform properties. This gives improved toughness and stiffness to the liquid crystal polymer.

It has been predicted<sup>5</sup> that the use of advanced polymers in general, will increase annually. Figures 4 to 6, show the market sector use for advance polymers in 1984 and the predicted use in 1995, if current trends continue. It can clearly be seen that there is a huge potential market place in the aerospace industry.

#### 5.1) LIQUID CRYSTAL POLYMER AS A MICRO-COMPOSITE

The polymer SRP1500GL30 (Self Reinforcing Polymer), is a liquid crystal polymer which possesses a unique

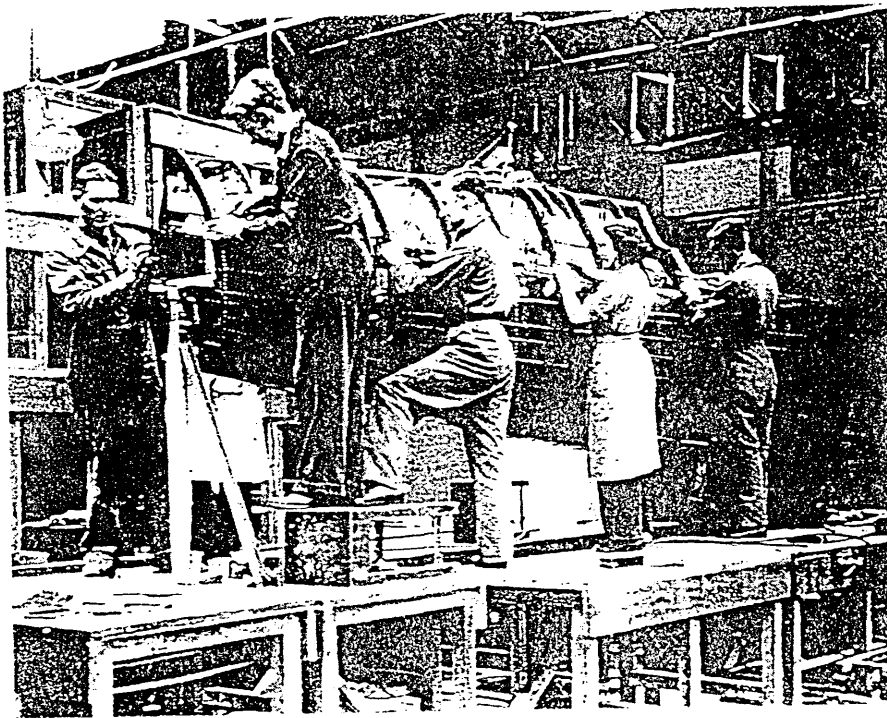
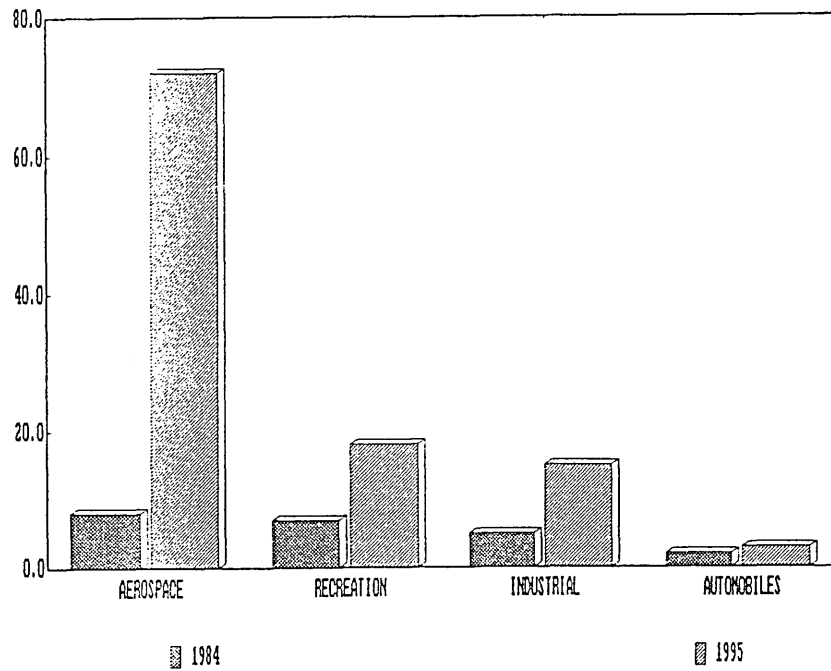


Figure 3 - Diagram showing a spitfire fuselage being constructed of polymeric materials.

molecular structure, which produces a unique property profile. The term Self Reinforcing Polymer describes the polymer, since the properties of unfilled liquid crystal polymer are similar to those of fibre reinforced conventional thermoplastics. Liquid crystal polymer molecules are rigid and rod like (unlike the flexible molecules of conventional thermoplastic polymers). Under shear, the rod-like molecules, which constitute the structure, stack up in propinquity to each other. On cooling an ordered solid is formed<sup>6</sup>, see figure 7. The SRP grades have very low melt viscosities under shear, enabling injection moulding of products with long or complex flow paths or thin sections. They also have fast cycle times and

## MARKET SEGMENT DEVELOPMENT



**Figure 4** - Bar graph to show the market areas which use polymers, along with future predicted trends.

need very little if any mould release agent. They can be moulded to tight tolerances to produce precision mouldings with low mould shrinkage, sinkage and warpage. The final article will have excellent stiffness and strength in flexure, tension and impact. All of the above factors are important when considering that the aircraft will be subject to fatigue. By their nature, molecular composites have several advantages over heterogeneous ones :-

- i) they can be processed using conventional thermoplastic processing equipment;
- ii) they exhibit unconventional viscosities at low shear rates; and

## USE OF ADVANCED POLYMERS - 1984

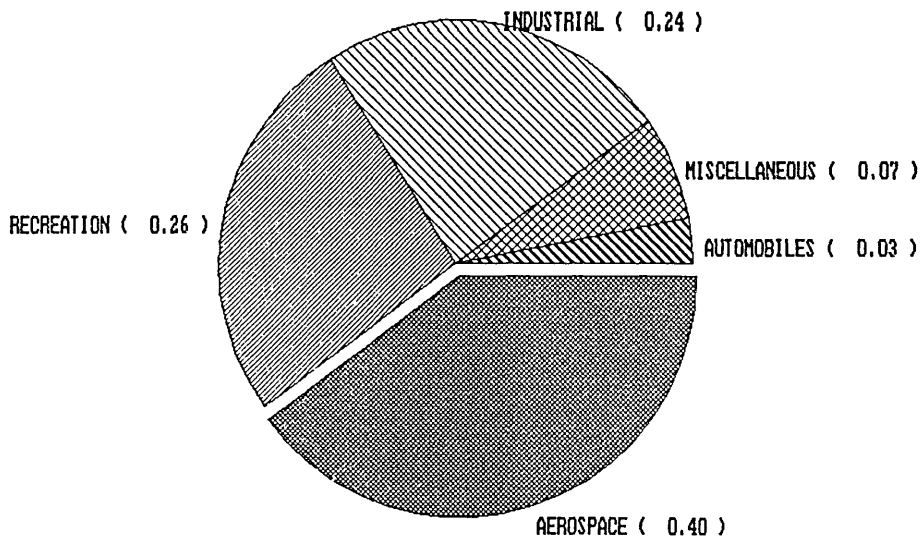
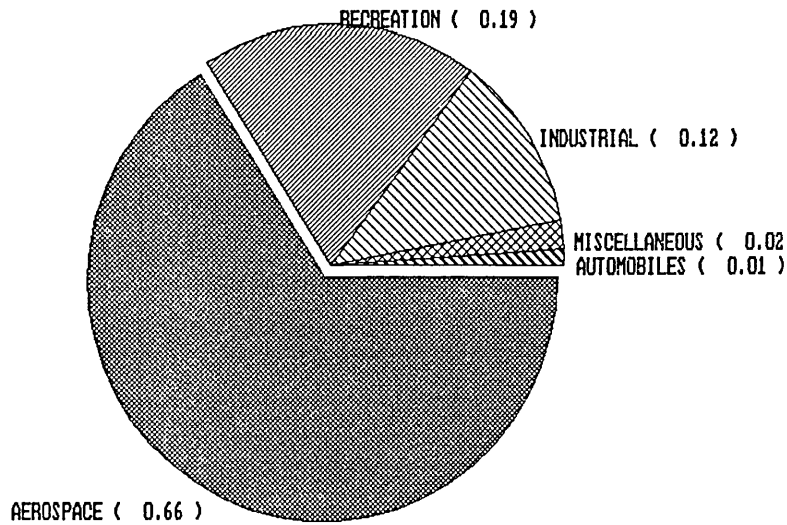


Figure 5 - Pie graph showing the market using advanced polymers in 1984.

iii) their mechanical properties are at least as good as those of heterogeneous composites.

The rate at which technology has developed over the past decade has meant that engineers have had to reconsider the materials used in, and the design of many different articles in use today. Articles produced from plastics and rubbers contribute strongly to the economy in general. They operate in a broad range of environments, and have good durability coupled with useful ranges of deformability. In addition to this polymers can often be readily transformed into usable products having complex shapes and reproducible dimensions. Finally it is interesting to note that the

## USE OF ADVANCED POLYMERS - 1995



**Figure 6** - Pie graph showing the predicted trends of markets using advanced polymers in 1995.

volume of polymers used in the Western economy already exceeds that of metals.

The polymer producers have been continually improving their products, to the point where they can now be used to replace metals in some of the more demanding applications. It has become fashionable over the past 15-20 years to try to replace existing materials with composite materials. There are certain applications, where the technology of polymers is insufficiently advanced for this to occur. The more demanding applications for polymers have been achieved using composites.

## 6) DESIGN CONSIDERATIONS FOR PLASTIC COMPONENTS

Polymers are widely used, in spite of their low moduli which normally lies in the range of  $1\text{MN/m}^2$  to a few  $\text{GN/m}^2$ . The design characteristics of a polymer is governed by stiffness rather than strength. If molecules become lined up during processing and are frozen in the lined up configuration (e.g. by shear in the mould filling, or by inflation of parisons or drawing of films), then the material becomes stiffer, along the direction of alignment and more flexible in the transverse direction. The following methods can be used to increase the stiffness of a polymer:-

- i) alter the molecular architecture;
- ii) encourage crystallinity;
- iii) crosslinking the polymer;
- iv) co-polymerisation;
- v) blending;
- vi) fibre reinforcement;
- vii) incorporation of liquid crystal units.

Without going into depth about the other methods, the system used to give improved stiffness in this case study is a combination of (vi) and (vii).

### 6.1) IMPROVED STIFFNESS

Ideally the finished article should have the optimum stiffness to unit cost ratio possible, while still being

able to perform the task required. If the polymer stiffness is increased by the addition of glass fibres, this might give a thinner wall with the added advantage of faster production rates, if the wall thickness is constant throughout the part. If bending is involved, the second moment can be exploited by using either an I, T or U section. This is the reason that many moulding bristle with ribs. But if the wall are too thin, webs and flanges may be prone to buckling instability. Panels can be stiffened (in bending) by the use of corrugation, ribs, curvature, or the production of a foam sandwich structure. Foamed plastics are much more flexible under direct or shear stress than their unfoamed counterparts. But in bending, the reduction in modulus is more than offset by the second moment of the area affects. This leads to foamed plastics being stiffer per unit weight than unfoamed plastics of the same polymer type. To replace a beam of modulus  $E$  and thickness  $h$  by a foam sandwich beam of the same breadth and bending stiffness, having a foam core of thickness  $h_f$  and modulus of  $E_f$  faced with two skins of thickness  $h_s$  and modulus  $E_s$  the criterion is :-

$$Eh^3 = E_s (h_f + 2h_s)^3 - E_s h_f^3 + E_f h^3 \quad (1)$$

The weight saving resulting from using a sandwich beam or panel rather than a solid panel can be readily calculated. This analysis assumes that the core has a uniform density and that there is a perfect bond between

skin and core; it also assumes that the core is not so deep that the failure by shear could occur. For long term loading, the appropriate creep modulus for the foamed and unfoamed polymers must be used in calculations of stiffness.

## 6.2) REINFORCING RIBS

As mentioned previously a polymer component often needs reinforcing ribs to strengthen the article. It has long been the standard procedure within the engineering industry to add reinforcing ribs to allow a reduction in section thickness without the equivalent reduction in section stiffness. In the specific case of military aircraft, external equipment cannot be compromised due to the necessity to maintain dimensional stability, impact resistance and high temperature resistance. Using reinforcing ribs around the perimeter of the component, the stiffness of the part in the two planar axes is only minimally affected, and the addition of the 'T' shaped reinforcing ribs in the centre will increase the flexural rigidity of the thinner sections. Even if ribs are not adopted for the purpose of reducing weight or enhancing performance, they may be necessary purely due to the components being significantly thinner than aluminium. This is particularly important in external applications where air turbulence should be considered.

### 6.3) REPAIR TECHNOLOGY

There are many benefits to using thermoplastics with facility for structural repair. These include the ability to repair rather than replace complex expensive parts resulting in more cost, and function effective operation. In most cases the damage is due to impaction by a small high velocity projectile, causing localised damage. This is a major drawback in using aluminium. A patch is usually glued or bolted into place, which after temporary repair must return from the field to have more permanent repairs carried out. The polymer component on the other hand can be repaired using a variety of techniques, having less harmful effects on the component's performance than in the case of aluminium. SRP1500GL30 has excellent solvent resistance, whilst aluminium is subject to oxidation leading to exfoliation of the surface layers<sup>1</sup>.

### 6.4) FIXING METHODS

The main methods of fixing within the aerospace industry is bolting, riveting or adhesion. Considering the specific application of the panel, it would be necessary for the door to be removed at regular intervals for inspection purposes. This means that adhesive and rivets cannot be used as a means of fixing. The bolts used must have a similar thermal expansion to that of the polymer to minimise damage to the polymer component.

## 7) RESULTS

The following calculations will now be used to compare the different designs and materials, maintaining a suitable stiffness.

### 7.1) BENDING STIFFNESS

The bending stiffness can be found by using equation [2] below :-

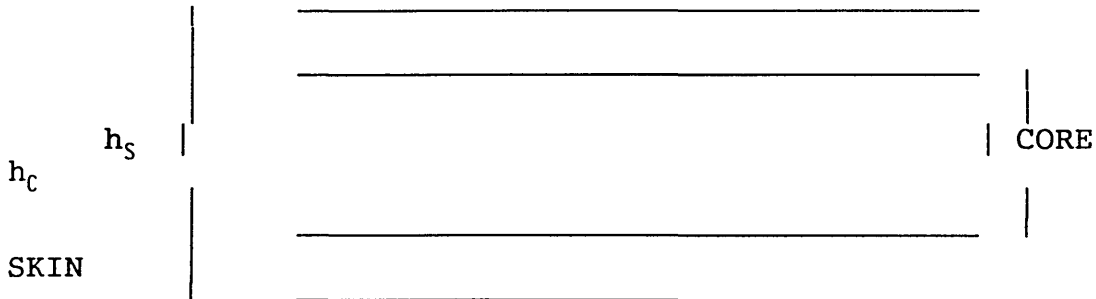
$$D = \frac{bh_s^3}{12} \cdot E_s \left(1 - \left[\frac{h_c}{h_s}\right]^3\right) \quad (2)$$

where

- D = bending stiffness
- b = breadth
- $h_s$  = total thickness of sheet
- $h_c$  = thickness of the core
- $E_s$  = tensile of modulus of the solid

materials

where :-



Equation [2] is used where there are two skins, with a core joining them together. The equation can be simplified below for a solid component.

$$D = \frac{bh^3}{12} \quad (3)$$

Equation 3 will be used for the solid injection moulded polymer component, and can be used to calculate the relative thickness of LCP needed to give an equivalent stiffness. Properties of the Aluminium alloy and the LCP can be seen below :-

TABLE : 2

MATERIAL	DENSITY(g/cm)	STRENGTH (MPa)	MODULUS (GPa)
Al - Li	2.68	100	73
SRP	1.6	230	16

For the purpose of the calculations a simplified hatch design was used. The door was assumed to have the following dimensions :-

Length - 1 m  
 Width - 0.5 m  
 Core thickness - 4 mm  
 Skin thickness - 1 mm  
 Total thickness - 6 mm

This stiffness of the Aluminium component can be calculated, by using this stiffness value it is possible to determine the amount of polymer necessary to give equivalent mechanical properties.

Stiffness of Aluminium component = 2.14043 Nm<sup>2</sup>

TABLE : 3

		VOLUME (m <sup>3</sup> )	
MATERIAL	COMPONENT	HOLES	TOTAL
Al - Li	SKIN	9.87 x 10 <sup>-7</sup>	0.000999
	CORE	1 x 10 <sup>-6</sup>	0.001998

TABLE : 4

		VOLUME (m <sup>3</sup> )	
MATERIAL	COMPONENT	HOLES	TOTAL
SRP1	0.006	2.96 x 10 <sup>-6</sup>	0.002997

TABLE : 5

		VOLUME (m <sup>3</sup> )	
MATERIAL	COMPONENT	HOLES	TOTAL
FOAMED SRP1	SKIN	1.51 x 10 <sup>-6</sup>	0.00153
	CORE	1.42 x 10 <sup>-3</sup>	0.00146

From the above tables it is possible to calculate the associated stiffness of the component. The solid injection moulded SRP1 has a stiffness far in excess needed to meet the Al-Li requirements. It was calculated that a component with a skin thickness of 1.537mm and a core thickness of 2.925mm would give an equivalent stiffness to the Aluminium component. The following table shows the weights and stiffnesses for the various methods of production :-

TABLE 6:

MATERIAL	STIFFNESS (Nm <sup>2</sup> )	WEIGHT (g)
Al-Li	2.14	3314.72
SRP1	18	4795.26
FOAMED SRP1	2.14	2924.61

From the above table it is possible to see that the solid polymeric component is more heavy than the Aluminium one, with a much greater stiffness.

## 8) CONCLUSIONS

The access hatch could indeed be produced from foamed SRP1. It might even be possible to produce sections using co-injection moulding techniques. The component would be lighter, cheaper and more easily repaired. Looking at the bad points, polymers are prone to creep to a much greater extent and the high temperature properties of the polymer are poor if the aircraft was to fly at high speeds, see figure 7, the mechanical properties of the polymer are reduced to a much greater extent than that of the aluminium, see figure 8.

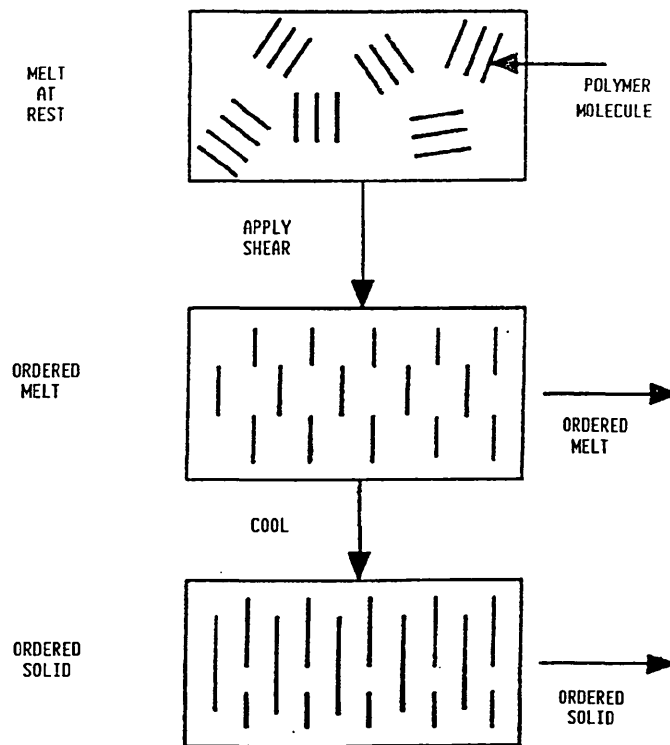


**Figure 7** - Diagram to demonstrate how anisotropic properties result in LCP's.

If it were possible to shield the polymer from an heating effects and give the component adequate support,

then it may be possible that the hatch could be produced from the foamed polymer, if not there would always be the possibility of macro-composite systems.

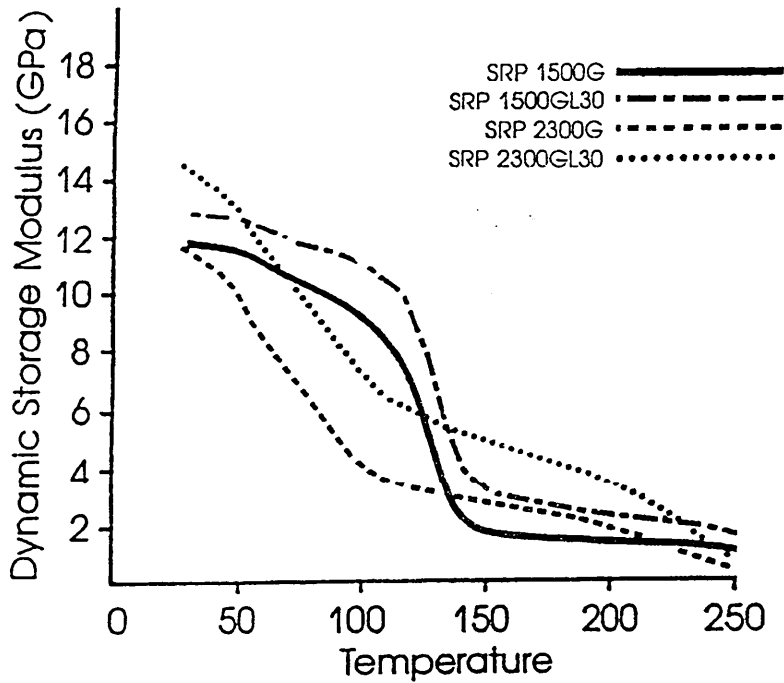


Figure 8 - Diagram to demonstrate how the modulus of four LCP's vary with temperature.

It may be possible to utilise the polymer in a missile, where the time of flight is very small and there would be insufficient time for the polymer to heat up, causing a reduction of mechanical properties.

## 9) REFERENCES

- 1) Lital data sheet, Publication Number 8602/3M/1.88
- 2) Nouvel Economiste, 6 June 1983.
- 3) Balmuth, E. S. and Schmidt, R. Aluminium - Lithium alloys; Sanders, T. H. and Starke, E. A. AIME, New York, 1981, 69
- 4) Peel, C. J., Evans, B., Baker, C., Bennett, D. A., Gregson, P. J. and Flowers, H. M.; Aluminium - Lithium alloys II; Sanders, T. H. and Starke, E. A. AIME, New York, 1983, 363
- 5) Final Year Degree Project, Reference A. A. Collyer
- 6) Victrex SRP, Properties and Processing data handbook Ref No VR1.

Key Engineering Materials Vols. 72-74 (1992)

# **Materials for Advanced Technology Applications**

Editors: M. Buggy and S. Hampshire

Trans Tech Publications

## RHEOLOGY OF LIQUID CRYSTAL POLYMER BLENDS

J.B. Hull (a), M. Hawksworth and A.A. Collyer (b)

(a) University of Bradford, UK  
(b) Sheffield City Polytechnic, UK

*Keywords: liquid crystal polymer, rheology, blend, VECTRA, polycarbonate, polyethersulphone*

### SYNOPSIS

Two binary blend systems, polycarbonate (PC) and polyethersulphone (PES), blended with VECTRA an aromatic LCP were prepared by extrusion melt blending. An investigation of the rheological behaviour of both blend systems, using a capillary extrusion rheometer, has shown that the apparent viscosity ( $\eta_A$ ) is strongly dependent on the shear stress ( $\tau$ ), the processing temperature and the blending ratio. At low shear rates ( $\dot{\gamma} < 40s^{-1}$ ), the behaviour of both PC and PES is shown to be Newtonian, becoming less Newtonian, with increasing shear rate ( $40s^{-1} < \dot{\gamma} < 400s^{-1}$ ). VECTRA exhibits marked non-Newtonian behaviour over the same decade of shear rate.

### ABSTRACT

Thermotropic liquid crystal polymers (LCP's) are easier to process than conventional thermoplastics. However, LCP's are relatively expensive materials, with limited commercial appeal. Hence, recent interest has focused on the production of hybrid blends of standard polymers with small amounts of LCP (< 10%) in order to enhance the processability and reduce the mould shrinkage of the base material. Two binary blend systems, polycarbonate (PC) and polyethersulphone (PES), blended with VECTRA an aromatic LCP were prepared by extrusion melt blending. An investigation of the rheological behaviour of both blend systems, using a capillary extrusion rheometer, has shown that the apparent viscosity ( $\eta_A$ ) is strongly dependent on the shear stress ( $\tau$ ), the processing temperature and the blending ratio. At low shear rates ( $\dot{\gamma} < 40s^{-1}$ ), the behaviour of both PC and PES is shown to be Newtonian, becoming less Newtonian, with increasing shear rate ( $40s^{-1} < \dot{\gamma} < 400s^{-1}$ ). VECTRA exhibits marked non-Newtonian behaviour over the same decade of shear rate. At compositions of > 25% LCP, the viscosity of a blend approaches that of the pure LCP. However, the toughness of blends with LCP content > 8% is significantly impaired. SEM studies have shown a pronounced skin/core effect of such blends with an increasing degree of surface layer exfoliation.

## INTRODUCTION

The idea of using a thermotropic liquid crystal main chain polymer, as a processing aid for isotropic thermoplastics, was patented by Cogswell et al in 1981<sup>(1)</sup>. They found that the addition of 10% liquid crystal polymer reduced the viscosity of the blend below that of the isotropic base material.

Siegmann et al (2) noted that for concentrations of LCP, around 5%, the blend viscosity could be lower than that of the individual components. This kind of behaviour has been observed before in immiscible blends, and may not necessarily be a property peculiar to LCP's. In addition, Siegmann et al observed that the tensile strength of blends was significantly improved with increasing LCP content. For example, LCP additions of 15%, to an amorphous polyamide, were equivalent to a 30% glass fibre reinforcement of the base material.

Electron optical studies have revealed that blends comprise of two phases, with the dispersed LCP phase changing from an ellipsoidal morphology to a fibrillar structure as the LCP blend content increases. The aim of the present work was to establish the rheological behaviour of blends of polycarbonate and polyethersulphone and VECTRA B 900 LCP produced by extrusion mixing at 330°C. The rheological characteristics of both blends and base materials were investigated at temperatures above and below the nematic transition temperature for VECTRA ( $T_N \approx 275^\circ\text{C}$ ), using a Davenport single capillary rheometer.

## EXPERIMENTAL PROCEDURE

The investigation was carried out on blends produced by adding the appropriate masses of two polymers together. The mixture was placed in the hopper of a single screw extruder and then processed, using the temperatures below.

HOPPER	REAR	CENTRE	FRONT	DIE
COOLED	310°C	320°C	330°C	330°C

It was considered that by using such temperatures both polycarbonate and polyethersulphone could be processed without too much difficulty. This would also standardise on the temperature at which the liquid crystal polymer was to be processed.

The resulting extrudate was granulated into fine 'chips', and subsequently re-chipped and re-processed through the extruder. The base polymers were also processed in this manner so that all of the polymers had the same thermal history. The blends had the following liquid crystal polymer contents:- 0%, 2%, 4%, 6%, 8%, 10%, 15%, 20%, 25% (mass%).

Once a blend had been produced using the two different polymers, it was necessary to pre-dry the material before experimentation could commence. The drying conditions of the liquid crystal polymer/polyethersulphone were similar. This made drying easy. However, this was not the case in the

polycarbonate VECTRA blends. The drying conditions for polycarbonate were too low to give adequate drying of the VECTRA. The drying conditions used for all the blends was 4 hours at 150°C. The blends were dried in mild steel trays with dimensions 40mm x 30mm x 2mm, and the polyblends were spread to a thickness of 1.5mm.

#### Capillary Rheometry

The pre-dried polyblend was placed in a heated barrel, of dimension 21.92 mm (internal bore) x 245.5 mm (long). The piston was then used to compress the loose chipped extrudate and the barrel was then topped up. A soak time of fifteen minutes was used to allow the polymer in the barrel to achieve a uniform temperature gradient (to within  $\pm 0.5^\circ\text{C}$ ). After this soak time, a BBC microcomputer was used to control the stepping speed of the piston, which forced the polymer out of die (with an L/D ratio of 20). The computer controlled the shear rate, and also measured the pressure at the entrance to the die by means of a 10,000 p.s.i. mercury transducer. The program sampled a burst of 100 readings per second, and when two sets of consecutive transducer data correlated within a set tolerance, the data was accepted and the program increased the speed for the piston. This approach was repeated until all of the data sets had been recorded.

The initial sets of experiments were carried out upon the variation of the mass% of liquid crystal polymer in the host polymer and seeing how this mass% affected the general flow characteristics of the engineering polymer under investigation. These experiments were carried out on both polycarbonate and polyethersulphone as the base. It was also necessary to see how the variation of temperature would affect the rheological characteristics. For this, a fixed composition of 20 mass% liquid crystal polymer to 80 mass% engineering polymer was used. The polyblend was produced and dried as before and again processed through the Davenport capillary rheometer. The extrudates were then collected for further investigation, using a sheet of paper to support the sample in order to avoid extensional effects due to gravity [3]. The extrudates were allowed to air cool, and some of the extrudates were then mounted in bakelite, ground and polished down to a 0.25 $\mu\text{m}$  finish. The polished samples were then looked at using electron microscopy.

#### RHEOLOGICAL ANALYSIS OF BLENDS

##### Capillary flow properties

Figures 1-3 show the relationship between the viscosity and the shear rate of all the base polymers under investigation. Figures 1 and 2 show that both Polycarbonate (PC) and Polyethersulphone (PES) are non-Newtonian. The behaviour is more Newtonian at lower shear rates ( $\dot{\gamma} \approx 40\text{S}^{-1}$ ). This is indicated by the formation of the plateau as the curve moves towards the ordinate axis. Figure 3 shows clearly that the viscosity of VECTRA decreases proportionally with an increasing shear rate ( $\dot{\gamma}$ ) at any temperature. Pronounced non-Newtonian behaviour of the liquid crystal polymer is thus indicated. Differential scanning Calorimetry has shown the nematic transition temperature for VECTRA is 275°C, (4). This is the temperature at which the particular LCP changes into the low viscosity 'non-isotropic' phase. The marked shift in the position of consecutive curves, above and below 275°C, can be observed. It can be noticed that the most significant change in the viscosity of two successive lines occurs at the nematic transition temperature.

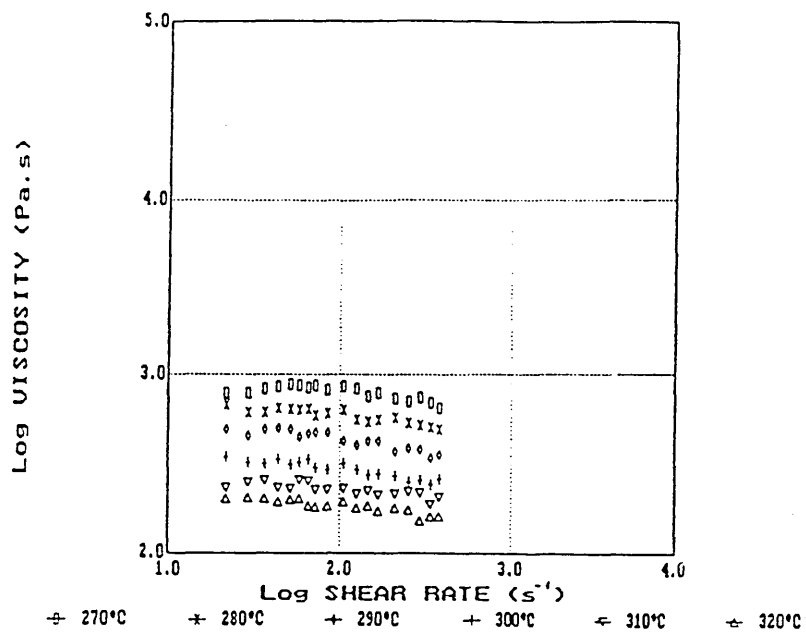


Figure 1: Log Viscosity vs Log Shear Rate for PC at 270°C to 320°C.

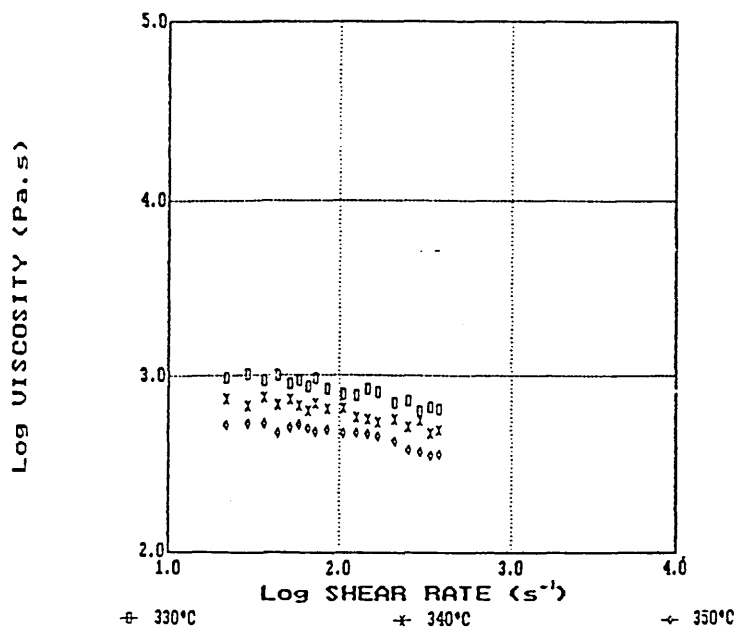


Figure 2: Log Viscosity vs Log Shear Rate for PES at 330°C to 350°C.

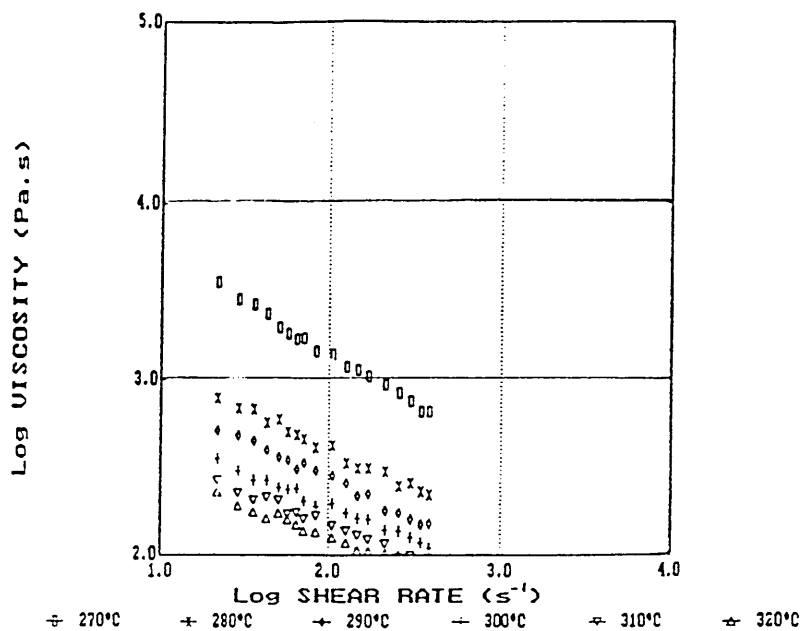


Figure 3: Log Viscosity vs Log Shear Rate For VECTRA at 270°C to 320°C.

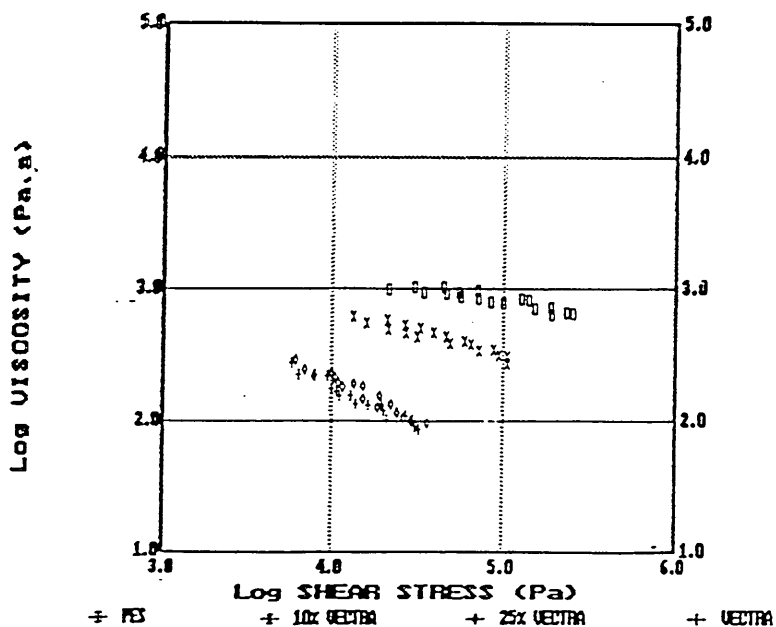


Figure 4: Log Viscosity vs Log Shear Stress for PES 10% & 25% VECTRA in PES; and VECTRA at 330°C.

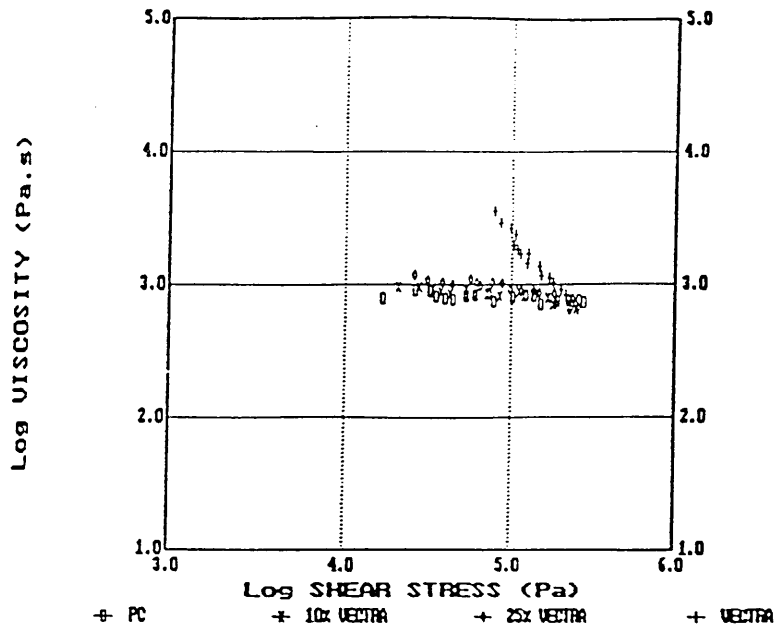


Figure 5: Log Viscosity vs Log Shear Stress for PC 10% & 25% VECTRA in PC; and VECTRA at 270°C.

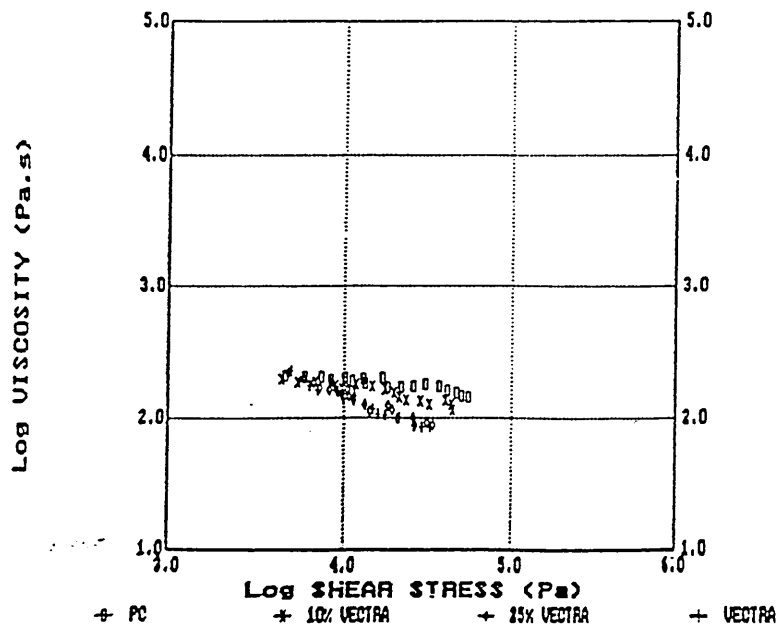


Figure 6: Log Viscosity vs Log Shear Stress for PC 10% & 25% VECTRA in PC; and VECTRA at 320°C.

There is no such transition for the PC and PES since they are amorphous and exhibit relatively little temperature dependence, as might be expected because of the difference in molecular structure from that of the LCP. Figures 4-6 show the relationship between the viscosity and shear stress for the blend systems at various temperatures. At 270°C, the viscosity of PC is lower than that of the LCP. The viscosity increases above that of PC with an increasing weight fraction of LCP in PC. At 25% LCP in PC the viscosity of the blend is still higher than the initial base polymer. This is attributable to the fact that the bulk of the LCP remains unmelted and that the viscosity of the blend is therefore largely governed by PC. Blends processed at temperatures above  $T_N$ , the melting point of the LCP, show a very different behaviour. This change in behaviour occurs because the viscosity of the LCP is lower than the base polymer. In this nematic state the LCP aligns very easily under extensional flow. At compositions of 25% VECTRA in PC it can be seen that the viscosity of the blend approaches viscosity of the pure LCP.

#### Limitations of Blending

Although blending of conventional thermoplastics with liquid crystal polymers results in both improved "flowability" during processing (5), and increased tensile strength of the product (2), there exist certain limitations which need to be addressed.

LCP additions of  $> 8\%$  to both PES and PC result in a significant impairment of the blend impact properties. A reduction in impact strength by 50% - 80% from that of the base materials (PES = 700 J/m VECTRA = 520 J/M) has been observed (4).

In addition, SEM studies have shown that high LCP contents result in a pronounced skin/core morphology of blends, which results from the complex flow/shear profiles developed in such materials during processing (5).

#### CONCLUSIONS

1. The viscosity of PES/LCP and PC/LCP blends, processed above  $T_N$ (LCP) show a strong dependence on shear stress.
2. Blending can be an aid to processing resulting in improved flow characteristics when processing occurs above  $T_N$ .
3. At temperatures below  $T_N$ , the rheological behaviour of the blend is dependent on the base polymer.
4. Blending should be limited to  $< 8\%$  LCP for both systems because the beneficial processing characteristics are offset by limitations in mechanical and physical properties.

---

REFERENCES

1. Cogswell F.N., Griffin B.P., and Rose J.B., Eur. Pat. Appl., 1981, No. 30417.
2. Siegmann A., Dagau A and Kenig S., Polymer, 1985, 26.
3. Jung S.H. and Kim S.C., Polymer, 1988, 20.
4. M. Hawsworth Ph.D. thesis 1991 (to be published).
5. Nishimura N. and Sakei T, Kobunshi Robunshu, 1988 45, No.5.
6. M. Hawsworth, J.B. Hull and A.A. Collyer, to be published.

Processing and Properties  
of  
Liquid Crystalline Polymers  
and  
LCP Based Blends

Domenico Acierno  
Francesco Paolo La Mantia  
Editors



**ChemTec Publishing**

# The Rheology of Liquid Crystal Polymer Blends

M. Hawksworth, J. B. Hull\* and A. A. Collyer\*\*

*School of Engineering Sheffield City Polytechnic, Pond Street,  
Sheffield S1 1WB, UK*

*\*Present address: Department of Mechanical and Manufacturing  
Engineering Richmond Building, Bradford University, Bradford, UK*

*\*\* School of Science (Applied Physics Division), Sheffield City Polytechnic,  
Pond Street, Sheffield S1 1WB, UK*

This paper reviews the rheological behavior of LCP/isotropic polymer blends in capillary flows with particular reference to the minimum viscosity turning point in viscosity-concentration graphs. This occurs at about 5% LCP in the blend. A model is proposed to account for the viscosity minimum based on the blend thermodynamic conditions lying between the binodal and spinodal to provide domains of large surface area over which slip can occur. On increasing the LCP concentration spontaneous two-phase separation takes place, reducing interfacial area and hence the area of the slip surface. The properties of LCPs make them ideal for obtaining highly deformed domains of large surface area required for a low blend viscosity.

## INTRODUCTION

It has been known for some time that a small addition (5%) of a main chain thermotropic liquid crystal polymer (LCP) to isotropic polymers leads to a viscosity reduction of the blends, and as such, LCPs may be regarded as processing aids. This was patented by Cogswell, Griffin, and Rose<sup>1</sup> in 1983. The blend viscosities exhibit negative deviation behavior (viscosities below those predicted by the log additive rule) and in some cases the viscosities of the blends are lower than those of the component melts.<sup>2</sup> This gives a minimum in the viscosity-concentration curve and the LCP acts as an excellent processing aid.

It would be of great benefit to polymer processors to understand the circumstances under which these viscosity minima occur and how the appropriate conditions can be generated in any isotropic polymer/LCP blend. In this review an analysis of some recent results is given, augmented with a few pertinent

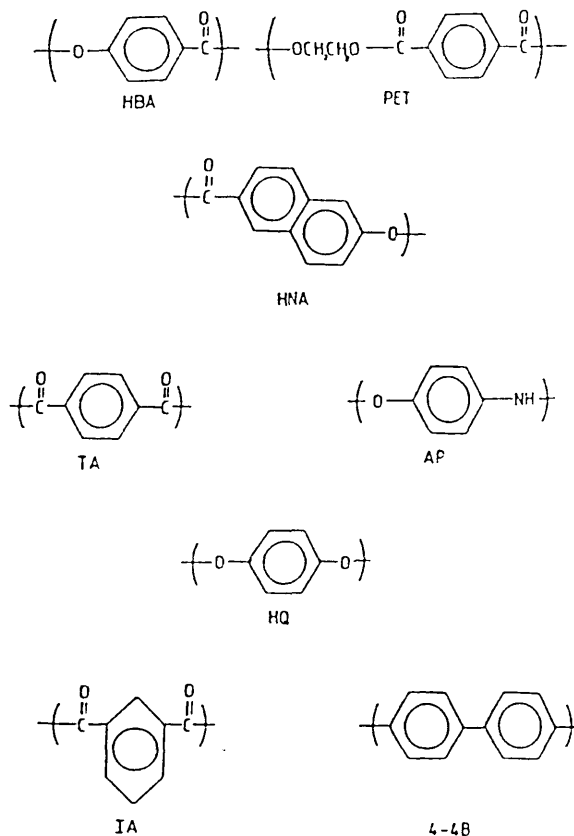


Figure 1. The structure of some commercial thermotropic liquid crystal polymers.

results of the authors, and a theory is given to explain the conditions favorable for viscosity minima based on the existence of a large interfacial area between the two phases (necessary) and an imposed, aligned morphology in the sheath region of a capillary flow (helpful). How this may be achieved in any specific flow of a given LCP/isotropic polymer pair will need further investigation.

Before describing and commenting on results obtained in the various LCP/isotropic polymer blends, it is instructive to examine the LCPs used in the various research programs.

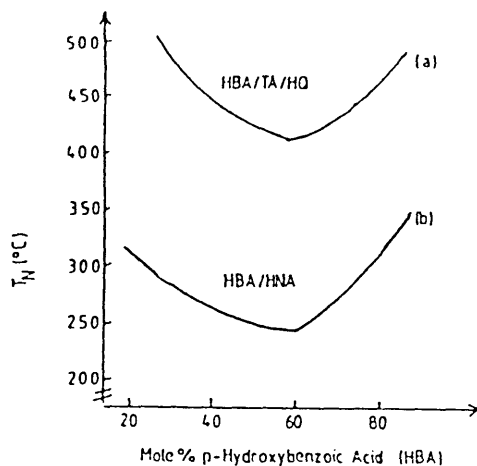


Figure 2. The variation of the nematic transition temperature with composition for two random copolyesters, involving hydroxybenzoic acid (HBA), terephthalic acid (TA), hydroquinone (HQ), and 6-hydroxy-2-naphthoic acid (HNA).<sup>6</sup>

## LCPs USED IN BLEND RESEARCH

Much of the early work was carried out with the Tennessee Eastman-Kodak X7G LCP. This consists of 40% polyethyleneterephthalate (PET) and 60% hydroxybenzoic acid (HBA), which is the mesogen. The PET acts as a flexible spacer for the stiff HBA mesogens and it enables the mesogens to align in elongational and shear fields. The use of such a spacer between the liquid crystal units in the main chain leads to a low nematic transition temperature and the intrinsic flexibility gives an LCP of lower modulus and tensile strength than an LCP without such spacers. The nematic transition temperature,  $T_N$ , is 200°C (DSC).<sup>3</sup> Such an LCP is suitable for use with engineering thermoplastics at temperatures below 300°C. The structure is shown in Figure 1.

The Hoechst-Celanese Vectra LCPs have also been popular, particularly A900 or A950, with a structure shown in Figure 1. The copolymerization of different structures breaks up chain regularity and frustrates chain packing needed to give a crystalline solid. Instead a nematic liquid crystal mesophase occurs, and in the cases of A900 and A950, one of the constituents is a particularly disruptive crankshaft unit, 6-hydroxy-2-naphthoic acid (HNA), which lowers  $T_N$  well below the decomposition temperature. For A950,  $T_N = 275^\circ\text{C}$ .<sup>4</sup> Figure 2 shows the effect

of copolymerization of different units on the nematic transition temperature. With the para-linked linear units HBA, terephthalic acid (TA) and hydroquinone (HQ), a smaller lowering of  $T_N$  occurs and if any one of the constituents predominates  $T_N$  is very high. This gives a very stiff molecule that has to be processed close to its decomposition temperature. The addition of HNA greatly reduces  $T_N$  but the molecule is less rigid.<sup>5</sup>

Isayev and Modic<sup>6</sup> used LCP-2000, a similar copolyester to A950, comprising 70% HBA/30% HNA, giving, from Figure 2, a  $T_N$  of 270°C.

Kohli *et al.*<sup>7</sup> used a different Hoechst-Celanese LCP, Vectra RD500, whose structure is shown in Figure 1. The  $T_N$  for this copolyester is 236°C.<sup>7</sup>

Hoechst-Celanese have commercialized a polyestheramide, Vectra B950. In addition to 60% HNA and 20% TA there is 20% aminophenol (AP). This produces some hydrogen bonding, but apart from this Figure 3 reveals little difference in  $T_N$  from a copolyester in which the AP is replaced by HQ.<sup>5</sup> The  $T_N$  for B950 is 285°C. Two interesting points to note about B950 are that there may be some interesting effects when blending small quantities with polyamides and it may be possible to map the position and shape of LCP droplets in a non-amide matrix by looking on to the NH stretching modes or to the NH structure.

The last LCP to be mentioned in this section is the Bayer K161, involving HBA/isophthalic acid (IA)/TA/HQ/4,4'-biphenol (4-4B). This has not been used as much as the others as it is intended for matrices of higher processing temperatures, such as polyetherimide (PEI).<sup>8</sup> The 4,4'-biphenol units would raise the  $T_N$  of this copolyester and give a very stiff molecule (Figure 1). Nobile *et al.*<sup>9</sup> found two solid mesophase transitions at 118 and 279°C, respectively, with isotropization at around 380°C.

## VISCOSITY REDUCTION WITH LCP ADDITIVES

In this section the observations described are used to formulate the necessary requirements for minima to be found in viscosity - LCP concentration graphs:

- often blend viscosities are intermediate between those of the individual components
- sometimes a large viscosity reduction occurs at a low concentration of LCP.

In all but rare cases, the blends show negative deviation behavior (NDB). The review is not exhaustive and will cover several isotropic polymer/LCP pairs.

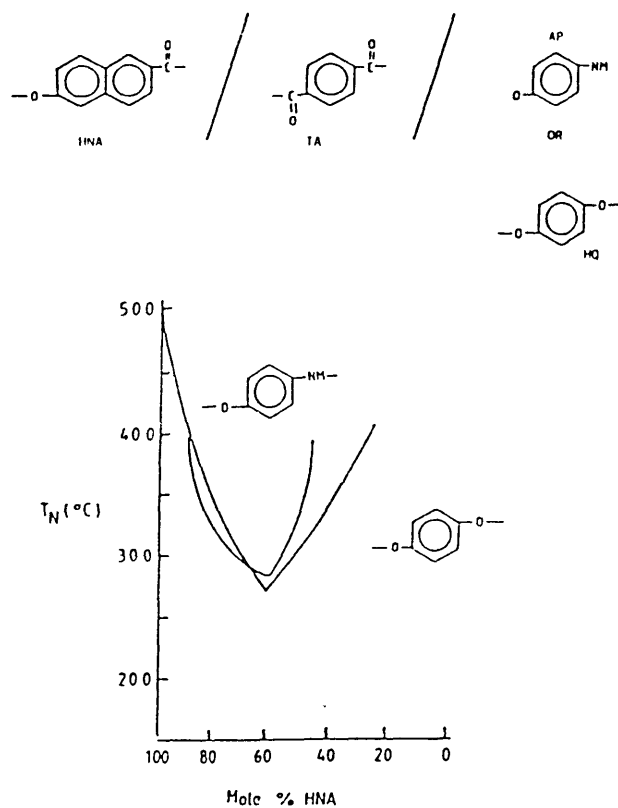


Figure 3. The variation of nematic transition temperature with concentration of HNA and the presence of aminophenol.

### Polystyrene/LCP

Weiss *et al.*<sup>10,11</sup> studied blends of polystyrene (PS) and an LCP synthesized by Professor Sirigu at the University of Naples, with a structure shown in Figure 4. X-ray diffraction and DSC revealed a nematic mesophase between 158 and 251°C. Parallel plate and capillary rheometer results were obtained for blends at 220°C. The die had a length to diameter (L/D) ratio of 57:1 and an entrance angle of 100°. At low shear rates the LCP domains were spherical and not deformed by the shear field; the blends viscosities were higher than that of the

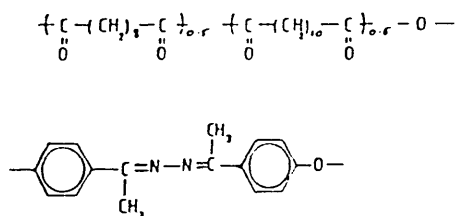


Figure 4. Structure of LCP synthesised by Sirigu.<sup>10,11</sup>

PS. These workers attributed the increase in viscosity to the dissipation of energy in the rotation and tumbling of the LCP domains.

At the higher shear rates in the capillary rheometer the blend viscosities were lower than that of PS, decreasing with increasing LCP concentration. A reduction in viscosity of 40% was obtained for 10 wt% LCP. The reduction in viscosity was attributed to the deformation and orientation of the LCP domains caused at the die entrance and the relatively long relaxation times of the LCP maintains deformation and alignment and provides slip surfaces to lubricate the flow.

This work highlights the different flow regimes involved in Couette flow, where a steady-state is reached, and in capillary flows, where entrance tensile fields elongate LCP domains, which provide large interfacial areas over which slip can occur.

### X7G/Polycarbonate Blends

In general, blends involving the X7G LCP do not show a minimum in the viscosity-LCP concentration curve, but Acierno *et al.*<sup>8</sup> indicated the presence of minima in results from blends of X7G/PC examined by Blizard and Baird,<sup>12</sup> but in the work of Acierno *et al.*<sup>13,14</sup> minima were absent with blend viscosities intermediate between those of the constituents. General observations made by Acierno *et al.*<sup>8</sup> were that as the  $L/D$  ratio of the die increases the morphology of the blends changes from fibers to droplets during the extrusion, but in the cone and plate rheometry only a droplet morphology is seen. In all systems the fibers lubricate the flow and their presence would seem to be a pre-requisite for viscosity minima for the reason suggested by Weiss *et al.*<sup>10,11</sup>

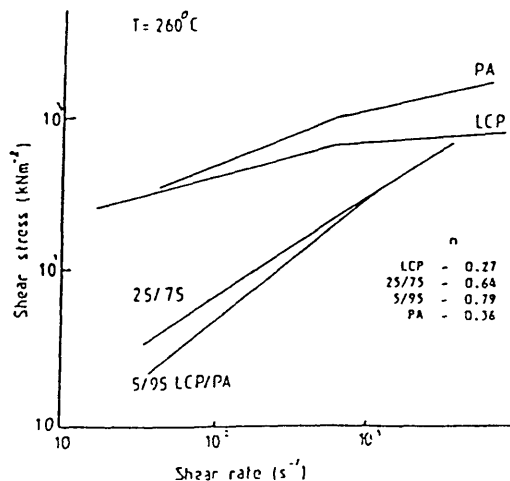


Figure 5. The variation of log shear stress with log shear rate for Vectra A900 and Trogamid T and two of their blends at 260°C using a capillary die of L/D = 33 (after Siegmán *et al.*<sup>2</sup>). The shear thinning index is given for each extrusion.

### Vectra/Trogamid T Blends<sup>2</sup>

The first blend system reported to give viscosity minima involved the amorphous polyamide traded under the name Trogamid T (Dynamit Nobel, Germany) and the Vectra A900. The experiments were carried out by Siegmán *et al.*<sup>2</sup> at 260°C, below the  $T_N$ ; the L/D ratio of the die was 33:1 and no entrance pressure correction was made. Figures 5 and 6 show the results. From Figure 5 it will be appreciated that for the component materials the shear stresses are high and the curves in these regions are flattened. The present authors feel that this is indicative of appreciable shear heating, which may raise the temperature in the sheath region of a blend above  $T_N$ . The estimate of shear heating was made as follows:<sup>15,16</sup>

$$\Delta T = \Delta p / \rho C_p$$

where  $\Delta T$  is the temperature increase due to the shear heating at a pressure difference between the ends of the die of  $\Delta p$  (there may be an overestimate here

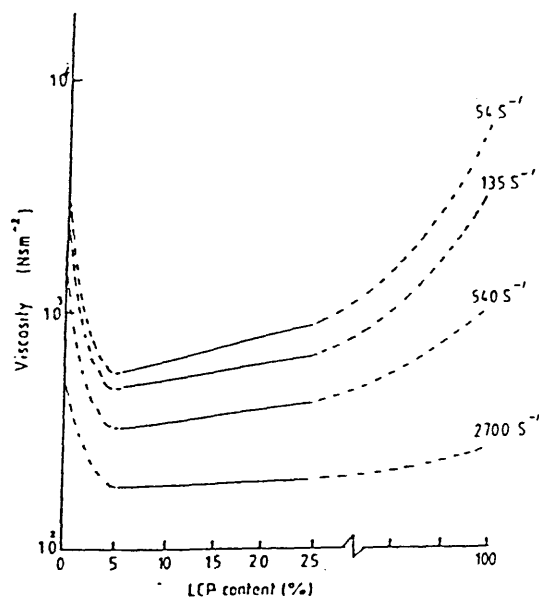


Figure 6. Composition dependence of the viscosity of Vectra A900/Trogamid T blends as a function of shear rate at 260°C (after Siegmann *et al.*<sup>2</sup>).

as no entrance pressure correction was made), a melt of density,  $\rho$ , and a specific heat capacity,  $C_p$ .

The shear stress  $\sigma$  is given by

$$\sigma = \Delta p / 4(1/d)$$

$$\Delta T = 4\sigma(1/d) / \rho C_p$$

For the purposes of calculation, it is assumed that  $C_p$  for Trogamid T is about  $2500 \text{ J} \cdot \text{kg}^{-1} \cdot \text{K}^{-1}$  similar to that of PA11 and PA12, with a density of  $1100 \text{ kg} \cdot \text{m}^{-3}$ .<sup>15</sup> For values of  $\sigma$  around  $5 \cdot 10^5 \text{ Nm}^{-2}$ ,  $\Delta T \approx 24^\circ\text{C}$ , which is quite sufficient to raise the blend temperatures above  $T_N$ . The shear stress values of Siegmann *et al.*<sup>2</sup> were higher than those of other workers using different blends. Siegmann *et al.*<sup>2</sup> observed elongated LCP domains of a few  $\mu\text{m}$  in diameter, implying that the

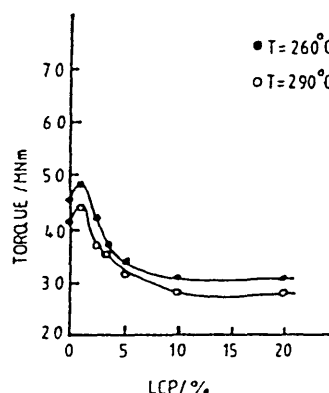


Figure 7. The variation of torque with LCP concentration in Vectra B950/PA6 blends (after La Mantia *et al.*<sup>17</sup>).

LCP had softened. A sheath/core morphology was present, with higher orientation in the sheath. Good interfacial adhesion was noted, but this was during mechanical tests and not at the extrusion temperature.

### Vectra A950/Polycarbonate

Isayev and Modic<sup>6</sup> used temperatures above  $T_N$  (280 and 310°C),  $L/D$  ratios of 30 and 40 and as such did not employ an entrance pressure correction. Minima in viscosity were noted at 310°C at high and low shear rates. They noted that as the  $L/D$  ratio is lessened the tensile strength of the extrudates increases and the uniformity and the number of fibers increase. At 5-10% LCP the extrudates peeled and they attributed this to the formation of nearly continuous fibers (2-5  $\mu\text{m}$  in diameter) randomly distributed across the extrudate.

Nishimura and Sakai<sup>4</sup> took measurements close to and below  $T_N$  (250, 260, 270, 280°C) with a die of  $L/D = 10$ ; there were no corrections for entrance pressure or to the apparent shear rate. There were minima at 50/50 mixtures. At 260°C the LCP domains were lumpy and irregular signifying that the LCP had not softened, whereas at 280°C the LCP domains were rod-shaped and of diameter 1-8  $\mu\text{m}$ .

Kohli *et al.*<sup>7</sup> used a different form of Vectra in PC, RD500. They conducted experiments above  $T_N$  and obtained minima at high shear rates in dies for 5-10%

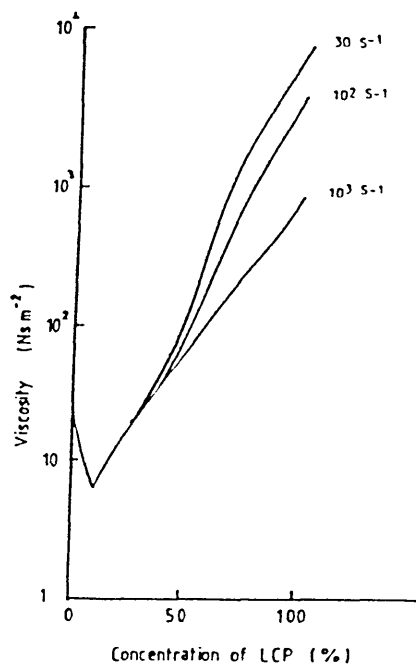


Figure 8. Viscosity versus LCP concentration in Vectra B950/polybutyleneterephthalate blends at 260°C (after La Mantia<sup>17b</sup>).

LCP. For cone and plate rheometry and for extrusion rheometry at low shear rates and large  $L/D$  ratios a droplet morphology occurred, whereas particles were elongated in capillary flows at high shear for dies of low  $L/D$  ratios.

### Vectra B950 in Polyamide 6 and Polybutyleneterephthalate

La Mantia et al.<sup>17</sup> extruded blends of Vectra B950/PA6 in a capillary viscometer, Rheoscope 1000, at 260 and 290°C using a die of  $L/D = 40$ . For Vectra B950  $T_N = 285^\circ\text{C}$  (Hawksworth). Figure 7 shows the variation in torque with LCP concentration.

An interesting feature of this graph, the maximum at about 1% LCP, will be discussed later, but at higher concentrations the viscosity drops and remains low from between 10-20% LCP. These investigators noted that even when extruding LCP below  $T_N$  there may be fibers formed on passing through a die of

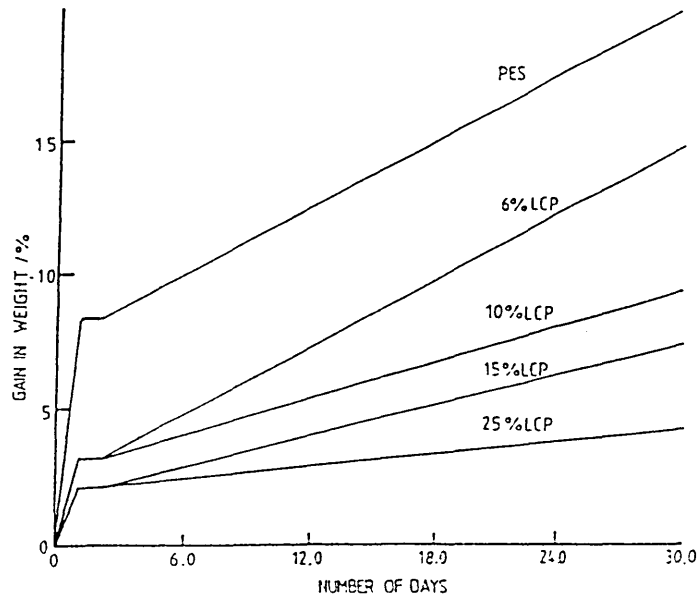


Figure 9. Water absorption versus time for Vectra B950/polyethersulphone blends: 0%, 10%, 15%, and 25% LCP in PES.

$L/D=0$  and a conical inlet at  $\dot{\gamma} = 1200 \text{ s}^{-1}$ . They stated that the fiber formation and interfacial slip caused the viscosity minimum. This could be assisted by migration of the LCP to the high shear rate regions.

The same authors blended B950 with polybutyleneterephthalate and obtained the viscosity minima shown in Figure 8. These were not preceded by the maximum as for PA6 blends.

### Vectra B950/Polycarbonate and with Polyethersulfone

The present authors found no minima when working with B950/PC blends with a die of  $L/D = 20:1$  at extrusion temperatures of 270 and 320°C or with blends involving PES at 330°C. In both cases the LCP domains were elongated and aligned along the streamlines, but the  $L/D$  ratio of the domain was about 10:1. Therefore it was surmised that the elongation was insufficient to provide sufficient interface for slip to give minima. Migration of the LCP to the sheath region was not noted. An explanation for the absence of viscosity minima is that

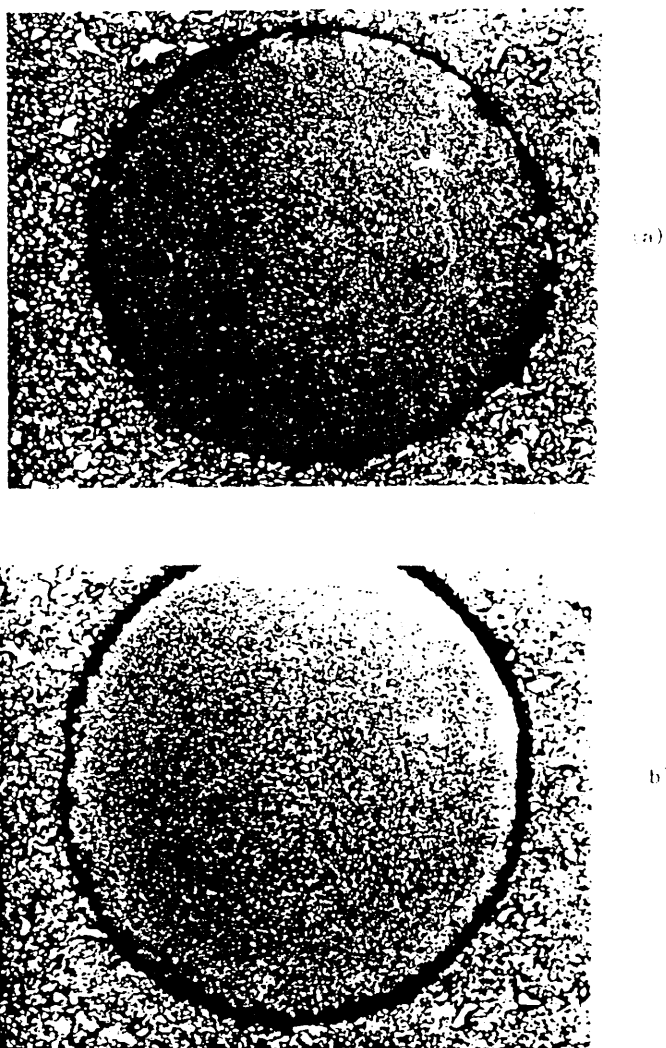


Figure 10. The position of the sheath/core interface in Vectra B950/polyethersulfone 25/75 blend. (a) below  $T_N$ , 290°C, (b) above  $T_N$ , 310°C. Note pale sheath region in (b).

the hydrogen bonding in the polyesteramide is sufficient to make B950 so incompatible with PC or PES that it is difficult to generate a large interface. This was not the case with PA6 and PBT.<sup>17</sup>

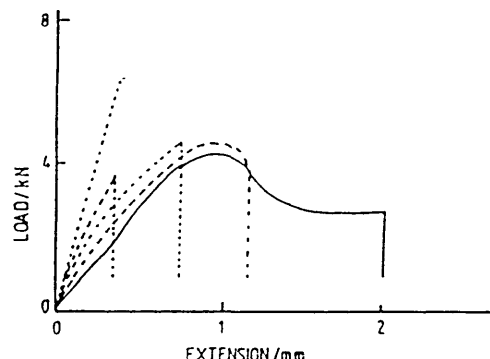


Figure 11. Tensile test results on Vectra B950/polyethersulfone blends, showing increased brittleness and pure LCP response to stress as the LCP concentration increases.

Some work was carried out by the present authors on the sheath/core morphology. This was achieved firstly by investigating the barrier properties of B950/PES extrudates to the ingress of water.

Although the uptake of water in PES is not great, there was a vast reduction of this on the addition of small amounts of B950, as shown in Figure 9; as little as 6% LCP caused at least a halving of the water uptake. This could suggest a migration of LCP to the sheath region, although no morphological evidence was found for this.

The second investigation concerned the ease by which the sheath region of an extrudate readily peels away<sup>2,4,6,14,18,19</sup> as for pure LCP extrudates, and some injection moldings showed a crack at the sheath/core interface. As little as 7% B950 in PES or in PC will produce this effect and Figure 10 shows the lighter sheath region surrounding the core in Figure 10b. Note that for extrusions below the  $T_N$  there was no evidence for a sheath/core interface. Measurements showed that 16% of the blend lies outside this interface for a 25% LCP concentration. For 20% B950/PC blends there was a large variation in results with an average value of 19% lying in the sheath region, with an SD of 2.5%. The results indicate migration that is almost complete, but the present authors are doubtful of this.

Isayev and Modic<sup>6</sup> noted that the TS of extrudates increased when  $L/D$  ratio of the extruding die was decreased. The current authors carried out mechanical tests on blends to investigate a different aspect, namely the LCP concentration effect, in the hope of substantiating the findings on the sheath/core interface.

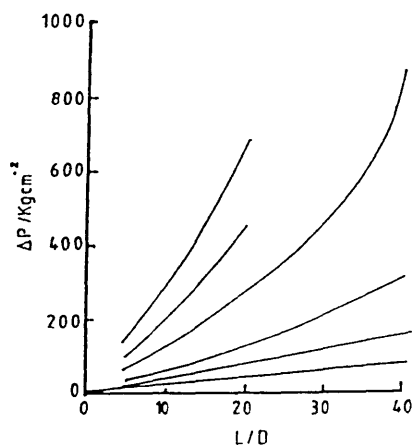


Figure 12. Bagley plots for polyetherimide at 330°C (after Nobile *et al.*<sup>20</sup>).

Figure 11 shows results of tensile tests of B950/PES tensile specimens. There is a shift towards brittle behavior, characteristic of pure LCP specimens, as the LCP concentration is increased. Again, as little as 15% LCP produced a marked departure from the ductile behavior of PES. This could be attributed to the increase in size of the sheath region of more oriented particles, which may be due to the migration of LCP.

An explanation given by the current authors<sup>18</sup> is that migration of LCP is not needed to produce the above effects and that the LCP imposes a more aligned morphology on the isotropic polymer matrix by virtue of its presence. Migration would assist this but would not be necessary. Such an imposed morphology would improve barrier properties, would give a sheath/core morphology and would account for the observed mechanical properties.

#### K161/Polyetherimide<sup>8,9,20,21</sup>

K161 is one of a few LCPs suitable for use with specialty polymers such as PEI. Acierno *et al.*<sup>8,9,20,21</sup> made rheological studies at 315, 330, and 350°C. With additions of about 5% LCP a drop of 30% occurs in viscosity at the high shear rates. For both 5 and 10% LCP blends the morphology contains spheroidal LCP domains of about 0.5  $\mu\text{m}$ . For 30% LCP blends the initial LCP domains are of about 3  $\mu\text{m}$  in size and these deform on extrusion at the higher shear rates into

long thread-like fibrils, well aligned to the flow direction. These results were for a die of  $L/D = 10$ ,  $\dot{\gamma} = 800 \text{ s}^{-1}$  at  $330^\circ\text{C}$ . No viscosity minima were reported. One problem associated with the PEI blend at low concentration of K161 was that the Bagley plots were non-linear, as shown in Figure 12. These show that the viscosity of PEI is sensitive to hydrostatic pressure, which makes an accurate correction for entrance pressure difficult. In fact, the entrance pressures are negative. Similar results have been obtained for isotropic melts.<sup>22-25</sup>

Acierno *et al.* corrected for entrance pressure using dies of  $L/D = 5$  and  $10$  and later found that the entrance pressure for the die of  $L/D = 10$  was only about 10% the total pressure drop, and results were similar to cone and plate values. A summary of the agreement between the previous authors must include the following points:

- LCP/isotropic polymer blends are negative deviation blends, except for Vectra B950/PA6.
- Some, but not all, blends give viscosity minima.
- A sheath/core morphology is present even for low concentration of LCP.
- A fibrillar LCP structure is much more likely for low values of die  $L/D$  ratio.
- Elongation of the LCP dispersed phase is necessary for enhanced viscosity reductions, giving a minimum in the viscosity-concentration curve.
- The minimum viscosity may be due to interfacial slip coupled with migration of the LCP to the regions of high shear rate.

## MODELS TO EXPLAIN VISCOSITY MINIMA

As mentioned in the introduction, viscosity minima are not restricted to blends involving LCPs, and below are discussed four reasons that have been proposed to explain their occurrence.

### Phase Equilibria

Lipatov<sup>26</sup> explained the variation of viscosity with concentration of polyoxymethylene (POM) in cellulose acetate butyrate (CAB) in terms of thermodynamic equilibrium by considering the heat of mixing  $\Delta G$ . Figure 13 shows how both  $\Delta G$  and viscosity  $\eta$  vary with the concentration of POM. On adding a small amount of POM to CAB, the heat of mixing decreases showing compatibility between the two species and a binodal composition; the viscosity rises. As the concentration of POM is increased  $\Delta G$  increases and thermodynamic conditions are meta-stable in the region between the binodal and spinodal. The two

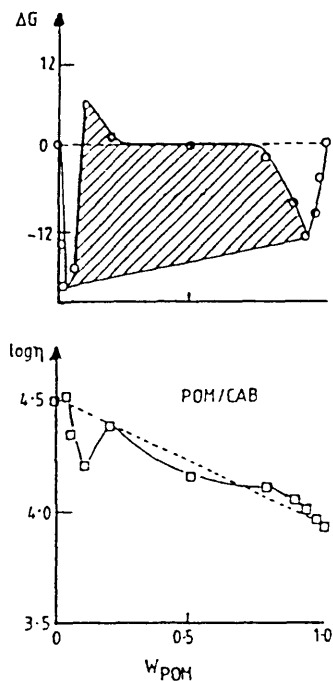


Figure 13. Variation of heat of mixing,  $\Delta G$ , and the viscosity with weight fraction of polyoxymethylene (POM) in cellulose acetate butyrate (CAB). The shaded area represents the region of immiscibility (after Lipatov *et al.*<sup>20</sup>).

species are not particularly compatible and the viscosity falls. Any further increase in POM concentration causes an increase in particle size due to nucleation and growth, which is controlled by local perturbations in particle density. The overall interfacial area may decrease, giving less interfacial slip and an increase in viscosity. Further increases in POM concentration causes spontaneous phase separation as the spinodal regime is reached. From Figure 13 the blend viscosity hovers around the log additive value.

A similar explanation can be used to account for the behavior of the Vectra B950/PA6 blends used by La Mantia.<sup>17</sup> Wisniewski *et al.*<sup>27</sup> observed a limited compatibility between polystyrene (PS) and polycarbonate (PC) at low concentrations of PS (<5%). At these low concentrations the  $T_g$  of the PC in the blend

was depressed by 10°C and an intermediate transition at 120°C appeared. At a concentration of about 5% PS, spontaneous phase separation occurred, the  $T_g$  of PC reverted to 149°C and the intermediate transition disappeared. From these kinds of considerations the thermodynamics of the blend system must be suitable to provide a large interfacial area between the two phases, an area over which slip can occur. Compatibility is therefore, undesirable and the meta-stable region between the binodal and spinodal may provide the best conditions for large slip surfaces.

### Droplet Breakup

The occurrence of viscosity minima is assisted by the elongation of the dispersed phase, and Plochocki<sup>28</sup> noted minima in polyethylene (PE)/polypropylene (PP) blends for a die of  $L/D = 33$  but not for  $L/D = 66$  in which some of the droplet elongation was lost.

Similar results have been noted with LCP blends,<sup>6,8</sup> and their ability to form fibers, and hence a large interface, and maintain them during the relaxation of the tensile forces as capillary flow continues, would account for their ability to cause permanent viscosity minima under the optimum conditions. The conditions that determine whether fibers or ellipsoidal dispersions occur are determined by  $\lambda$ , the ratio of viscosities of the dispersed to the matrix phases and  $\lambda_N$ , the ratio of the first normal stress differences of the dispersed to the matrix phases. Originally it was believed that if  $\lambda \leq 1$  a fibrillar structure would occur, but this condition is not now believed sufficient.<sup>29,30</sup> The formation of fibrillar morphologies has been widely investigated by Ablazova *et al.*<sup>31</sup> and Tsebrenko *et al.*<sup>32-34</sup> The optimum viscosity ratio range was  $0.76 \leq \lambda \leq 0.91$ , although some observers<sup>2</sup> believed that  $\lambda = 1$  gave the optimum condition. Values of  $\lambda \ll 1$  will be favorable for the formation of fibers, but break-up will occur in the capillary. More recent research suggests that  $\lambda_N$  is important and that it influences the driving force for domain deformation; for fiber formation  $\lambda \ll 1$ . This situation is very likely in LCP blends as the LCPs alone show small first normal stress differences. More detailed coverage of this area is given by Utracki.<sup>35</sup>

### Migration

The migration of the lower viscosity component to the die wall or to the high shear rate regions close to the wall is a distinct possibility. Collyer *et al.*<sup>36-38</sup> working with blends of polydimethylsiloxane (PDMS) in polyethersulfone

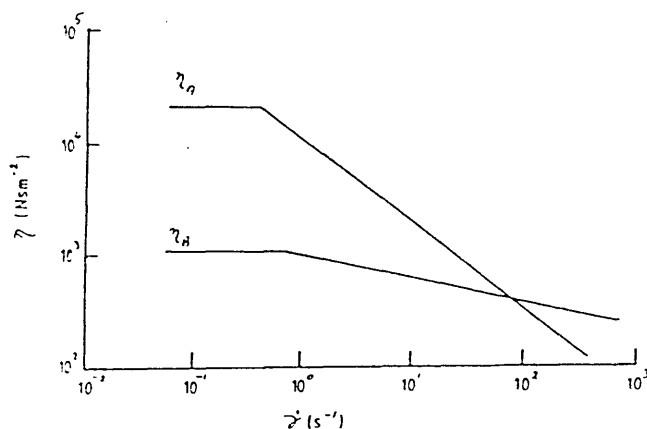


Figure 14. Viscosity versus shear rate for two fluids whose viscosities cross over at a particular shear rate (after Han<sup>33</sup>).

(PES), investigated the migration of PDMS to the edges of extrudates. The PDMS particles were mapped by EDX, following the silicon in the PDMS. Migration of PDMS did not seem to occur. Verhoogt *et al.*<sup>39</sup> worked with blends of Vectra A900 in Kraton G1650 (Shell), which is a styrene/ethylene-butylene/styrene block copolymer elastomer. They observed partial migration of the LCP to the sheath region and the LCP fibers were much longer in the sheath region than in the core. Han<sup>40</sup> discussed two mechanisms leading to a complete migration of one phase in a long capillary. Migration of the less viscous phase to the wall occurs for  $\lambda < 1$  and  $\lambda_N = 1$ . For  $\lambda = 1$  and  $\lambda_N < 1$ , the more elastic phase will migrate to the wall. In LCP blends  $\lambda_N$  may be much less than 1, providing the best conditions for the migration of the LCP phase. This migration could be conducive to viscosity minima as follows from Han.<sup>40</sup> Consider a coextruded flow in which the variation of viscosity with shear rate is given in Figure 14 for both components. The important feature is the crossover point, after which material A becomes less viscous than material B. If it can be arranged that material A can occupy the high shear rate regimes, where  $\eta_A$  is lower than  $\eta_B$  and material B the lower shear rate regimes ( $\eta_A < \eta_B$ ) a viscosity minimum is possible. This is shown in Figure 15, a plot of pressure gradient against concentration of material A. The shear rate close to the wall must be

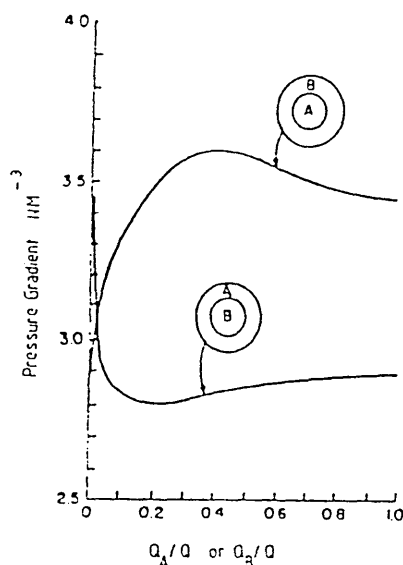


Figure 15. Theoretically predicted pressure gradient versus volumetric flow rate for two fluids in Figure 14 (after Han<sup>33</sup>).

greater than the shear rate at the crossover point. The minimum would be much deeper if interfacial slip occurred.

The other observation of Verhoogt *et al.*<sup>39</sup> that the LCP fibers were longer in the sheath region, was explained by Alderman and Mackley.<sup>41</sup> They stated that outside a certain radius there is an acceleration of the flow so that the parabolic profile in the die can change to the plane velocity profile in the free flow outside. This acceleration would lead to extensional forces that would elongate the LCP domains. Inside this radius the molecules could suffer a deceleration, which would discourage alignment. The simple theory they developed from this model was not successful in the prediction the position of the sheath/core interface in pure LCP extrudates, but nevertheless the present authors believe that the basic model is correct.

Migration of the lower viscosity component may not be important in the production of viscosity minima because, whereas the larger  $L/D$  ratio would give more scope for migration, it is the dies of lower  $L/D$  ratio that favour viscosity minima. Nevertheless, the extruded flow above can be used to develop a model to account for these minima.

## Slip at the Interface

Several observers have attributed the viscosity minima to interfacial slip or slip at the die wall.<sup>8,13,14,42-48</sup> Dispersed phases that maintain large elongations would provide large surface areas over which slip can occur, and should partial migration take place this would increase slip in the higher shear rate regions. Migration would also assist slip at the die wall, in which a plug flow of high viscosity fluid is lubricated by a low viscosity component; this often occurs in the extrusion of gun propellant cords.<sup>43-48</sup> In this process nitrocellulose is extruded in the presence of some solvent (acetone) and nitroglycerine, which acts as a plasticizer. In experiments where the nitroglycerine has been replaced by a poorer plasticizer for nitrocellulose, or in model experiments involving cellulose acetate/acetone/dibutyl phthalate, the high hydrostatic pressure during extrusion and the poor compatibility between the solid and liquid components allow phase separation, such that liquid is observed running out of the die with the solid cord. Under these circumstances slip is considerable. The present authors believe that interfacial slip is the main cause of the viscosity minima. Lyngaae-Jørgensen *et al.*<sup>49</sup> demonstrated interlayer slip in polystyrene/polymethyl-methacrylate multi-layer samples and calculated the interphase viscosity; it was at least ten times smaller than that of the lower viscosity component. Such conditions would certainly give viscosity minima.

## CONCLUDING REMARKS

There are various phenomena occurring that could assist in giving a minimum turning point in the viscosity-concentration curves for LCP blends at low LCP concentration. These phenomena are similar to those in blends of isotropic polymers, but LCP behavior is more conducive to producing minima and this is confirmed by experiment.

## Induced Morphology

The elongation and alignment of the dispersed LCP phase is believed by the authors to force a more oriented morphology on the isotropic matrix in the sheath region of the capillary flow. This would cause the viscosity of the matrix phase to be lower than in the absence of the ordering LCP phase. This would assist in causing a viscosity minimum but is not adjudged to be the main contributing factor.

## Migration

With values of  $\lambda_N$  and  $\lambda$  of less than unity, and in the case of  $\lambda$  a great deal less, the migration of the LCP phase to the die wall would be expected. For this to take place, the die L/D ratio should be large, but this is conducive to droplet break-up, which has the greater influence on the appearance of viscosity minima.

## Domain Elongation and Interfacial Slip

The two factors that are crucial to obtaining viscosity minima at low concentration of LCP in blends are the presence of elongated domains with interfacial slip. LCP molecules like to align and have high tensile strength. This assists in producing elongated domains, which cause a large surface area of interface, over which slip may occur under the right conditions. With LCPs in blends with isotropic polymers  $\lambda_N < 1$  and in addition, it is possible to obtain the optimum viscosity conditions for fiber production, namely  $0.76 \leq \lambda \leq 0.91$ .

The authors suggest that the optimum thermodynamic conditions require non-compatibility between the LCP and isotropic polymer phases and yet without spontaneous phase separation. Such conditions prevail between the binodal and spinodal.

On increasing the LCP content spontaneous phase separation will occur, with an attendant reduction in interfacial area and slip and a rise in the blend viscosity.

With this in mind, it is tempting to analyze the thermodynamics of possible LCP/isotropic polymer pairs, but the thermodynamic functions are derived in static conditions and the influence of the flow on phase separation as well as the influence of phase separation on the resulting flow are not well understood. It is, therefore, impossible at present to be certain of achieving viscosity minima and hence excellent processing aids for high viscosity polymers, with a given LCP/isotropic polymer pair. The authors hope that this paper may assist in achieving this seemingly distant goal.

## ACKNOWLEDGMENTS

One of the authors (MH) would like to thank SERC for a grant to pursue LCP research, of which a very small part is mentioned here. We should also thank ICI Materials for a fruitful collaboration and Mr. M. Furniss for provision of the Figures.

## REFERENCES

1. F. N. Cogswell, B. P. Griffin, and J. B. Rose, *USP* **4,386,174**, May 31 (1983).
2. A. Siegmann, A. Dagan, and S. Kenig, *Polymer*, **26**, 1330 (1985).
3. S. H. Jung and S. C. Kim, *Polym. J.*, **20**, 73 (1988).
4. T. Nishimura and H. Sakai, *Kobunshi Ronbunshu*, **45**, 401 (1988).
5. G. Calundann, M. Jaffe, R. S. Jones, and H. Yoon, in *Fibre Reinforcements For Composite Materials*, Ed. A. R. Bunsell, *Elsevier*, Amsterdam, Ch5, 211-248 (1988).
6. A. F. Isayev and M. Modic, *Polym. Composites*, **8**, 158 (1987).
7. A. Kohli, N. Chung, and R. A. Weiss, *Polym. Eng. Sci.*, **29**, 273 (1989).
8. D. Acierno, M. R. Nobile, L. Nicolais, and L. Incarnato, in *Polymer Rheology and Processing*, Eds. A. A. Collyer and L. A. Utracki, *Elsevier Applied Science Publishers*, London and New York, Ch4., (1990).
9. M. R. Nobile, D. Acierno, L. Incarnato, E. Amendola, L. Nicolais, and C. Carfagna, *J. Appl. Polym. Sci.*, in press.
10. R. A. Weiss, Wansoo Huh, and L. Nicolais, *Polym. Eng. Sci.*, **27**, 684 (1987).
11. R. A. Weiss, Wansoo Huh, and L. Nicolais, in *High Modulus Polymers*, *Marcel Dekker Inc. Publishers*, New York, 145, (1988).
12. K. G. Blizard and D. G. Baird, *Polym. News*, **12**, 44 (1986); *ANTEC* 311 (1986); *Polym. News*, **12**, 173 (1987); *Polym. Eng. Sci.*, **27**, 653 (1987).
13. D. Acierno, E. Amendola, C. Carfagna, L. Nicolais, and M. R. Nobile, *Mol. Cryst. Liq. Cryst.*, **153**, 553 (1987).
14. M. R. Nobile, E. Amendola, L. Nicolais, D. Acierno, and C. Carfagna, *Polym. Eng. Sci.*, **29**, 244 (1989).
15. J. A. Brydson, *Flow Properties of Polymer Melts*, *Iliffe* (1980).
16. F. N. Cogswell, *Polymer Melt Rheology*, *George Goodwin Ltd* (1980).
17. F. P. La Mantia, A. Valenza, M. Paci, and P. L. Magagnini, *Rheol. Acta*, **28**, 417 (1989); *Polym. Eng. Sci.*, **30**, 7 (1990).
18. J. B. Hull, M. Hawksorth, and A. A. Collyer, *Irish Materials Forum*, Limerick, 4-6 Sept. (1991).
19. A. A. Collyer, *PPS European Regional Meeting*, Palermo, 15-18 Sept., Paper 5.01kn, 145 (1991).
20. M. R. Nobile, D. Acierno, L. Incarnato, and L. Nicolais, *J. Rheology*, **34**, 1181 (1990).
21. D. Acierno, M. R. Nobile, and G. Marino, *PPS European Regional Meeting*, Palermo, Italy, 15-18 Sept., Paper 5.03 (1991).
22. R. C. Penwell and R. S. Porter, *J. Polym. Sci.*, **A2**, **9**, 463 (1971).
23. G. A. Toelke, C. G. Gogos, and J. A. Biesenberger, *SPE 13th ANTEC*, 98 (1967).
24. A. Casale, R. C. Penwell, and R. S. Porter, *Rheol. Acta*, **10**, 412 (1971).
25. R. J. Crowson, M. J. Folkes, and P. F. Bright, *Polym. Eng. Sci.*, **20**, 925 (1980).
26. Yu. S. Lipatov, A. N. Shumskii, A. M. Gorbatenko, and Geitmanchuk, *Fiz. Khim. Mekh. Disp. Struktur.*, 117 (1983).
27. C. Wisniewski, G. Marin, and Ph. Monge, *Eur. Polym. J.*, **21**(5)479 (1985).
28. A. P. Plochocki, in *Polymer Blends*, Eds. D. R. Paul and S. Newman, *Academic Press*, New York, Ch2 (1972).

29. J. Lyngaae-Jørgensen and A. Valenza, *Makromol. Chem., Macromol. Symp.*, **38**, 43-60 (1990).
30. J. Lyngaae-Jørgensen, L. A. Utracki, A. Valenza, and K. Sondergaard, *PPS European Regional Meeting*, Palermo, Italy, 15-18 Sept., P5.06, 159 (1991).
31. T. I. Ablazova, M. V. Tsebrenko, A. V. Yudin, G. V. Vinogradov, and B. V. Yarlykov, *J. Appl. Polym. Sci.*, **19**, 1781 (1975).
32. M. V. Tsebrenko, A. V. Yudin, T. I. Ablazova, and G. V. Vinogradov, *Polymer*, **17**, 831 (1976).
33. M. V. Tsebrenko, A. I. Benzar, A. V. Yudin, and G. V. Vinogradov, *Vysokomol. Soed.*, **A21**, 830 (1979).
34. M. V. Tsebrenko, M. N. Rezanova, and G. V. Vinogradov, *Nov. Reol. Polim., 11th Mater. Vses. Simp. Reol.*, **2**, 136 (1982).
35. L. A. Utracki, in *Polymer Alloys and Blends*, Hanser Publishers, Munich, Vienna, New York (1990).
36. A. A. Collyer, D. W. Clegg, G. H. France, M. Morris, K. Blake, D. J. Groves, and M. K. Cox, *IXth Int. Congr. on Rheology*, Acapulco, 8-13 Oct., **3**, 543-550, (1984); Elsevier Applied Science Publishers, London and New York, (1985).
37. G. H. France, A. A. Collyer, D. L. Blackmore, K. Blake, D. W. Clegg, M. Morris, D. J. Groves, J. P. C. Bootsma, and J. H. Kampschreur, *Proc. Xth Int. Congr. on Rheol.*, Sydney, 14-19 Aug., **1**, 324-6, (1988).
38. A. A. Collyer, G. H. France, K. Bott, D. W. Clegg, M. Morris, S. Edney, and D. J. Groves, *The 1989 Int. Chem. Conf. of the Pacific Basin Countries*, Honolulu, Hawaii, USA, 17-22 Dec., Paper O7J-98 (1989).
39. H. Verhoogt, C. R. J. Willems, J. Van Dam, and A. Posthuma de Boer, *PPS European Regional Meeting*, Palermo, Italy, 15-18 Sept., P5.02, 149-150, (1991).
40. C. D. Han, in *Multiphase Flows in Polymer Processing*, Academic Press, New York, 348-352 and 386-394 (1981).
41. N. J. Alderman and M. R. Mackley, *Faraday Discussions, Chem. Soc.*, **79**, 149-160 (1985).
42. R. Kann and M. T. Shaw, *52nd Ann. Meeting of Soc. Rheol.*, Williamsburgh, Virginia, USA, 23-28 Feb., Paper D8 (1981).
43. F. S. Baker, R. E. Carter, and R. C. Warren, *Rheology*, Plenum Press, New York, Vol.3, 591 (1980).
44. F. S. Baker and R. E. Carter, *Propellants, Explosives and Pyros.*, **7**, 139 (1982).
45. F. S. Baker and G. J. Privett, *Polymer*, **28**, 1121, (1987).
46. A. A. Collyer, C. N. Tsang, D. W. Clegg, F. S. Baker, and G. J. Privett, *Proc. Xth Congr. on Rheology*, Sydney, Australia, 14-19 Aug., 282, (1988).
47. A. A. Collyer, C. N. Tsang, D. W. Clegg, and F. S. Baker, *The 1989 Int. Chem. Congr. of Pacific Basin Countries*, Honolulu, Hawaii, 17-22 Dec., Paper 075, 354, (1989).
48. A. A. Collyer, D. W. Clegg, C. N. Tsang, and R. Abram, *PPS Seventh Ann. Meeting*, Hamilton, Ontario, 21-24 April, 52-53 (1991).
49. J. Lyngaae-Jørgensen, L. Dahl Thomsen, K. Rasmussen, K. Sondergaard, and F. E. Andersen, *Intl. Polym. Proc.*, **2**, 123 (1988).